

"SOME GEOCHRONOLOGICAL APPLICATIONS OF  $^{210}\text{Pb}$  IN  
THE COASTAL MARINE AND FRESHWATER ENVIRONMENTS"

A thesis submitted to  
the University of Glasgow  
in fulfilment of the requirements  
for the degree of  
Doctor of Philosophy

by

DAVID SAMUEL SWAN

October 1978

Department of Chemistry,  
University of Glasgow,  
Glasgow G12 8QQ

ProQuest Number: 13804169

All rights reserved

INFORMATION TO ALL USERS

The quality of this reproduction is dependent upon the quality of the copy submitted.

In the unlikely event that the author did not send a complete manuscript and there are missing pages, these will be noted. Also, if material had to be removed, a note will indicate the deletion.



ProQuest 13804169

Published by ProQuest LLC (2018). Copyright of the Dissertation is held by the Author.

All rights reserved.

This work is protected against unauthorized copying under Title 17, United States Code  
Microform Edition © ProQuest LLC.

ProQuest LLC.  
789 East Eisenhower Parkway  
P.O. Box 1346  
Ann Arbor, MI 48106 – 1346

# C O N T E N T S

	<u>Page</u>
List of figures	
List of tables	
List of plates	
Acknowledgements	
 Abstract	
 <u>CHAPTER 1 - INTRODUCTION</u>	
1.1 Sediments : Composition and Properties	1
1.2 Geochronology of recent sediments;	10
History and theory of $^{210}\text{Pb}$ dating;	13
Application of the dating method;	20
Complementary radiometric dating techniques	29
1.3 Background to the areas under study	36
Clyde Sea Area	36
Loch Lomond	56
Cilicia Basin (Eastern Mediterranean)	61
1.4 Aims of Research	64
 <u>CHAPTER 2 - EXPERIMENTAL</u>	
2.1 Introduction : General outline of experimental investigations.	65
2.2 Sample collection and handling;	72
Clyde Sea Area sediments;	72
Loch Lomond sediment;	77
Eastern Mediterranean Sea sediment	79

<u>CHAPTER 2 (cont'd)</u>	<u>Page</u>
2.3 Sample preparation and subsidiary analyses	80
Sample preparation	80
Subsidiary analyses	80
Trace metal analysis	80
Calcium carbonate analysis	81
Particle density determination	82
2.4 Sample dissolution and radiochemical analyses	84
Sample dissolution	84
<sup>210</sup> Pb analysis	87
Nuclear counting technique - $\alpha$ spectrometry	98
<sup>226</sup> Ra analysis and nuclear counting technique	105
Radiocaesium analysis and nuclear counting technique	112
2.5 Reproducibility	114
 <u>CHAPTER 3 - RESULTS AND DISCUSSION</u>	
3.1 General approach	120
3.2 Eastern Mediterranean	136
3.3 Loch Lomond	152
3.4 Clyde sea-loch sediments : Gareloch and Loch Goil	175
Gareloch	175
Loch Goil	182
Station 1	204
Station 2	215
3.5 Summary and General Conclusions	268

	<u>Page</u>
<u>APPENDIX 1</u>	
Particle size analysis	279
<u>APPENDIX 2</u>	
Sample calculations and computer programmes	284
Calculation of $^{210}\text{Pb}$ activity in sediment	284
Calculation of $^{226}\text{Ra}$ activity in sediment	287
<u>REFERENCES</u>	291

-----oo0oo-----

## LIST OF FIGURES

<u>Figure</u>		<u>Page</u>
1	Annual transfer of erosion products to the ocean.	2
	Figures are in units of $10^{14}$ g. Figures in parentheses refer to dissolved products.	
2	Exchange of matter in an idealised estuarine system	7
3	The $^{238}\text{U}$ , $^{235}\text{U}$ and $^{232}\text{Th}$ natural decay series; vertical arrows denote alpha decay and slanted arrows beta decay; the number beneath each symbol of the isotopes denotes the half-life	14
4	Water content of Loch Goil sediment	22
5	The Clyde Sea Area	37
6	Variation of dissolved oxygen in bottom water of Loch Goil during 1974.	44
7	Surface sediments in the northern region of the Clyde Sea Area	47
8	Gareloch; lateral sections and section along axis of greatest depth	54
9	Loch Goil; lateral sections and section along axis of greatest depth	55
10	The Cilicia Basin, Eastern Mediterranean	62
11	Flow diagram of radioanalytical separations	68
12	Typical $\alpha$ -spectrum	69
13	Typical $\gamma$ -spectrum	70
14	Sections of Craib and gravity corers	73

<u>Figure</u>	<u>Page</u>
15 Freezer/transporter for gravity cores	76
16 Section of Mackereth mini-corer	78
17 Polonium plating cell	92
18 Schematics of alpha surface barrier detector and alpha source/detector assembly	99
19 Block diagram of $\alpha$ -spectrometer	103
20 $^{222}\text{Rn}$ emanation system	106
21 $^{222}\text{Rn}$ detector/photomultiplier assembly	108
22 Graph of decay of $^{222}\text{Rn}$	111
23 Depth profiles of uncorrected total $^{210}\text{Pb}$ and salt corrected total $^{210}\text{Pb}$ activities for Loch Goil gravity core LGG5.	127
24 Total $^{210}\text{Pb}$ and $^{226}\text{Ra}$ profiles for the Eastern Mediterranean Core	146
25 a Porosity profile for the Eastern Mediterranean core,	
b Curve of age (calendar date) versus depth for the Eastern Mediterranean core,	147
26 Depth profile of excess $^{210}\text{Pb}$ for the Eastern Mediterranean core	148
27 Cilicia Basin sampling station	149
28 Loch Lomond sampling station	165
29 Depth profiles of total $^{210}\text{Pb}$ and $^{226}\text{Ra}$ for Loch Lomond mini-Mackereth core LLRPM1	166
30 $^{137}\text{Cs}$ profile for Loch Lomond mini-Mackereth core LLRPM1	167
31 Porosity profile for Loch Lomond mini-Mackereth core LLRPM1	168
32 Depth profile of excess $^{210}\text{Pb}$ for L. Lomond mini-Mackereth core LLRPM1	169

<u>Figure</u>	<u>Page</u>
33 Curve of age (calendar date) against depth for Loch Lomond core LLRPM1, based on sedimentation rate of $22 \text{ mg.cm}^{-2}\text{y}^{-1}$	170
34 Magnetic measurements on Loch Lomond mini-Mackereth core LLRPM1	171
34a Curve of age (calendar date) against depth for Loch Lomond core LLRPM1 based on sedimentation rates of $22 \text{ mg.cm}^{-2}\text{y}^{-1}$ to a depth of 8 cms, and $63 \text{ mg.cm}^{-2}\text{y}^{-1}$ at greater depths	172
35 $^{14}\text{C}$ ages for Loch Lomond Mackereth core LLRDM1	173
36 Lead profile for Loch Lomond mini-Mackereth core LLRPM1	174
37 Gareloch sampling station	183
38 Depth profiles of total $^{210}\text{Pb}$ and $^{226}\text{Ra}$ for Gareloch gravity core GLG2	189
39 Radiocaesium profile for Gareloch gravity core GLG2	190
40 Porosity profile for Gareloch gravity core GLG2	191
41 Lead profile for Gareloch gravity core GLG2	192
42 Depth profile of excess $^{210}\text{Pb}$ for Gareloch gravity core GLG2	193
43 Age/depth curve for Gareloch gravity core GLG2	194
44 Depth profiles of total $^{210}\text{Pb}$ and $^{226}\text{Ra}$ for Gareloch Craib core GLC3	198

<u>Figure</u>	<u>Page</u>
45 Radiocaesium profile for Gareloch Craib core GLC3	199
46 Porosity profile for Gareloch Craib core GLC3	200
47 Depth profile of excess $^{210}\text{Pb}$ for Gareloch Craib core GLC3	201
48 Porosity profile for Gareloch Craib core GLC2	200
49 Curve of age (calendar date) versus depth for Gareloch Craib core GLC3	202
50 Lead profile for Gareloch Craib core GLC2	203
51 Loch Goil sampling stations	221
52 Depth profiles of total $^{210}\text{Pb}$ and $^{226}\text{Ra}$ for Loch Goil gravity core LGG5	227
53 Radiocaesium profile for Loch Goil gravity core LGG5	228
54 Porosity profile for Loch Goil gravity core LGG5	229
55 Depth profile of excess $^{210}\text{Pb}$ for Loch Goil gravity core LGG5	230
56 Curve of age (calendar date) versus depth for Loch Goil gravity core LGG5	231
57 Lead profile for Loch Goil gravity core LGG5	232
58 Depth profiles of total $^{210}\text{Pb}$ and $^{226}\text{Ra}$ for Loch Goil Craib core LGC2	236
59 Radiocaesium profile for Loch Goil Craib core LGC2	237

<u>Figure</u>	<u>Page</u>
60 Depth profiles of total $^{210}\text{Pb}$ and $^{226}\text{Ra}$ for Loch Goil Craib core LGC9	241
61 Radiocaesium profile for Loch Goil Craib core LGC9	242
62 a Porosity profile for Loch Goil Craib core LGC9	243
b Porosity profile for Loch Goil Craib core LGC2	
63 Depth profile of excess $^{210}\text{Pb}$ for Loch Goil Craib core LGC9	244
64 Curve of age (calendar date) versus depth for Loch Goil Craib core LGC9	245
65 Lead profile for Loch Goil Craib core LGC9	246
66 Depth profile of total $^{210}\text{Pb}$ and $^{226}\text{Ra}$ for Loch Goil Craib core LGC4	250
67 Porosity profile for Loch Goil Craib core LGC4	251
68 Radiocaesium profile for Loch Goil Craib core LGC4	252
69 Depth profile of excess $^{210}\text{Pb}$ for Loch Goil Craib core LGC4	253
70 Curve of age (calendar date) against depth for Loch Goil Craib core LGC4	254
71 Lead profile for Loch Goil Craib core LGC4	255

LIST OF TABLES

<u>Table</u>		<u>Page</u>
1	Physical dimensions of the Clyde Sea Area	38
2	Some major pollutant inputs to the Clyde Sea Area	40
3	Physical dimensions of Loch Lomond	57
4	Partial decay schemes for $^{134}\text{Cs}$ and $^{137}\text{Cs}$ (Lederer et al., 1967) showing the $\gamma$ -rays diagnostic of the radiocaesium isotopes	67
5	$^{210}\text{Pb}$ , $^{226}\text{Ra}$ and $^{137}\text{Cs}$ concentrations in fractional dissolution of sediment from Loch Goil core LGC1 (8.4.75)	85
6	Reanalysis of $^{210}\text{Pb}$ in solutions originally exhaustively stripped of polonium isotopes and stored to allow regrowth of $^{210}\text{Po}$	94
7	Repeat determination of $^{210}\text{Pb}$ in samples (6N in HCl) stored in glass containers for prolonged periods.	96
8	$\alpha$ -spectrometry; detector backgrounds and silver disc blanks	97
9	$^{222}\text{Rn}$ detector backgrounds and efficiencies	110
10	Results of $^{210}\text{Pb}$ replicate measurements	115
11	a Results of $^{226}\text{Ra}$ replicate analyses	116
	b Results of repeat analyses for $^{226}\text{Ra}$ on one sample solution	116
12	Results of $^{210}\text{Pb}$ duplicate analyses	117

<u>Table</u>	<u>Page</u>	
13	Results of $^{226}\text{Ra}$ duplicate analyses	118
14	Comparison of porosity corrected and uncorrected sedimentation rates for some cores analysed in this study	124
15	Age/depth relationships for Loch Lomond core LLRPM1 derived from porosity corrected and uncorrected sedimentation rates	125
16	Comparison of $^{226}\text{Ra}$ and 'at-depth' $^{210}\text{Pb}$ activities for Gareloch gravity core GLG2	129
17	Comparison of $^{210}\text{Pb}$ measurements in Gareloch gravity core GLG2 by Harwell and Glasgow laboratories	131
18	Comparison of mean $^{226}\text{Ra}$ activities and mean $^{210}\text{Pb}$ activities measured at depth in 'long' cores	133
19	Background information for Cilicia Basin gravity core 188	143
20	Chemical and mineralogical analyses of grab samples from station 188	144
21	Cilicia Basin gravity core 188; results of analytical investigations	145
22	Geographical variation of mean annual flux of $^{210}\text{Pb}$ in precipitation	150
23	Chemical analyses on Cilicia Basin core 1092	151
24	Background information on Loch Lomond core LLRPM1	161
25	Loch Lomond mini-Mackereth core, LLRPM1; results of analytical investigations	162/164

<u>Table</u>	<u>Page</u>
26 Background information for Gareloch gravity core GLG2	184
27 Gareloch gravity core GLG2; results of analytical investigations	185/188
28 Background information for Gareloch Craib core GLC3	195
29 Gareloch Craib core GLC3; results of analytical investigations	196/197
30 Background information for Loch Goil gravity core LGG5	222
31 Loch Goil gravity core LGG5; results of analytical investigations	223/226
32 Background information for Loch Goil Craib core LGC2	233
33 Loch Goil Craib core LGC2; results of analytical investigations	234/235
34 Background information for Loch Goil Craib core LGC9	238
35 Loch Goil Craib core LGC9; results of analytical investigations	239/240
36 Background information for Loch Goil Craib core LGC4	247
37 Loch Goil Craib core LGC4; results of analytical investigations	248/249
38 Loch Goil Craib core LGC8; station 1: Particle size distribution (%)	260
39 Loch Goil Craib core LGC8; station 1: Clay mineral composition (%) by X-ray diffractometry	260

TablePage

- |    |   |         |
|----|---|---------|
| 40 | Settling times for clay (equivalent settling diameter $< 1.4 \mu\text{m}$ and $< 20 \mu\text{m}$ ) at 10 cms. depth | 281     |
| 41 | Programme in Fortran IV for the calculation of $^{210}\text{Pb}$ activity in sediment                               | 286     |
| 42 | Programme in Fortran IV for the calculation of $^{226}\text{Ra}$ activity in sediment                               | 289/290 |

LIST OF PLATES

		<u>Page</u>
PLATE 1	X-radiograph of Craib core LGC9 from Loch Goil station 1	211
PLATE 2	X-radiograph of a Craib core from Loch Goil station 2	217

## ACKNOWLEDGEMENTS

I am indebted to many people both directly and indirectly. In particular, however, I express my sincere gratitude to my supervisor, Dr. M.S. Baxter, for guidance, encouragement and invaluable advice given throughout.

My thanks are also due to many of the staff of the Clyde River Purification Board for ready provision of sampling facilities and for practical expertise, enthusiasm and good humour during sampling surveys, often in adverse conditions; in particular I thank J. Curtis, W. Ingram, T. Jickells, G. Latona, Dr. T. Leatherland, D. MacKay, E. McBride and Dr. A. Newton.

Included in this thesis are results of colleagues involved in complementary sediment studies. Special thanks go to Dr. A.B. MacKenzie and I.G. McKinley for radiocaesium data and to Dr. J.G. Farmer for stable lead data. Thanks are also due to Dr. W. Jack for provision of facilities for sediment core X-radiography and for helpful general advice, to T. Aitchison for the weighted linear regression analysis programme, and to Dr. A.B. MacKenzie for permission to reproduce several diagrams from his Ph.D. thesis. In addition, I thank K. MacKay for invaluable technical assistance and calcium carbonate analyses and the staff of the vital glassblowing, mechanical and electrical workshops of the Chemistry Department.

Amongst others, Dr. H.M. Blauer, J. Smith-Briggs, Dr. J.A. Campbell, R. Crawford, J. Docherty, Dr. N. Drndarski, Dr. A.E. Fallick, Dr. J.G. Farmer, D. Lennie, Dr. T.D.B. Lyon, K. MacKay, A. Mackie, I.G. McKinley, A. Saad and Dr. M.J. Stenhouse formed a very special group of friends who provided stimulating conversation and discussion of both a scientific and social nature, at work and at play.

I am indebted to Mrs. J. Whitelaw for excellent typing, to Mrs. J. Rodgers for many excellent illustrations and to R. Munro for prints. I acknowledge with gratitude the financial support of the S.R.C.

Finally, I warmly thank my parents and close family for support and continuous encouragement during this study.

## ABSTRACT

Radioanalytical techniques for  $^{210}\text{Pb}$  dating of sediments have been established.  $^{210}\text{Pb}$  is measured indirectly via  $\alpha$ -spectrometric determination of its  $\alpha$ -emitting grand-daughter  $^{210}\text{Po}$ .  $^{226}\text{Ra}$  is quantified indirectly via separation and gas-phase  $\alpha$ -scintillation counting of its radioactive rare-gas daughter,  $^{222}\text{Rn}$ . Sediment cores recovered from the Cilicia Basin in the Eastern Mediterranean, Loch Lomond, a freshwater loch in west central Scotland, and Loch Goil and Gareloch, two fjord-like sea-lochs of the Clyde Sea Area, have been examined for their  $^{210}\text{Pb}$  and  $^{226}\text{Ra}$  distributions. Where appropriate  $^{210}\text{Pb}$  chronologies covering the last 100 to 150y have been developed. Complementary studies include radio-caesium and stable lead analyses.

In interpreting  $^{210}\text{Pb}$  chronologies, the importance of correcting data for a number of sediment properties has been emphasised. Thus, (1)  $^{226}\text{Ra}$  concentrations should be measured throughout the length of cores before making correction for supported  $^{210}\text{Pb}$  contributions, (2) it is essential to correct  $^{210}\text{Pb}$  specific activities for variable water contents produced in surficial deposits by compaction processes, and (3) in the case of marine sediments, variable salt-residues from interstitial waters must be quantified and allowed for in  $^{210}\text{Pb}$  activity calculation.

Based on the exponential decrease of excess  $^{210}\text{Pb}$  with depth, a sedimentation rate of around  $16 \text{ mg.cm}^{-2}\text{y}^{-1}$  ( $0.34\text{mm.y}^{-1}$ ) is estimated for the Cilicia Basin; this may, however, best be

regarded as a lower limit estimate of the accumulation rate since there is considerable evidence to suggest that the sediment surface was not recovered during sampling.

For Loch Lomond, a sediment accumulation rate of  $22 \text{ mg.cm}^{-2} \text{ y}^{-1}$  ( $1.0 \text{ mm.y}^{-1}$ ) is estimated. The presence of  $^{137}\text{Cs}$  in this core, largely confined to the upper 2 to 3 cms. of the deposit, is consistent both with the  $^{210}\text{Pb}$ -derived time-scale and with recovery of surface material.

In the principal area of study, the Clyde Sea Area,  $^{210}\text{Pb}$  is shown to be in sufficient excess over that required for secular equilibrium with  $^{226}\text{Ra}$  to permit its use as a geochronological indicator in the region. In Gareloch and Loch Goil, considerable differences are apparent in the patterns and rates of recent sediment accumulation. For example, in Gareloch, a  $^{210}\text{Pb}$ -based sedimentation rate of  $540 \text{ mg.cm}^{-2} \text{ y}^{-1}$  ( $1.5 \text{ cm.y}^{-1}$ ) is derived, while values of  $200 \text{ mg.cm}^{-2} \text{ y}^{-1}$  ( $6 \text{ mm.y}^{-1}$ ) and  $123 \text{ mg.cm}^{-2} \text{ y}^{-1}$  ( $3.5 \text{ mm.y}^{-1}$ ) are similarly estimated for two stations in Loch Goil. Sedimentation rates estimated from radiocaesium ( $^{134}\text{Cs}$  and  $^{137}\text{Cs}$ ) distributions are in generally good agreement to those based on  $^{210}\text{Pb}$ . The major source of  $^{210}\text{Pb}$  to the deposits is shown to involve river and stream particulate inputs. Modern fluxes of stable lead to the deposits are considerably greater than those of pre-industrial times. Both radionuclide evidence and X-radiographs of frozen cores indicate Loch Goil sediments to be homogeneously reworked by bioturbation to depths of 4 to 6 cms. Of particular interest,  $^{226}\text{Ra}$  concentrations are considerably greater in the upper few centimetres of Loch Goil sediments than those at depth. This 'excess'  $^{226}\text{Ra}$  is attributed to its enrichment in siliceous marine organisms, the remains of which are subsequently

incorporated into bottom deposits.

Sediment cores analysed in this study have been collected by a variety of coring devices, viz. conventional small-diameter gravity corers, mini-Mackereth and Craib corers, the latter two samplers being specifically designed to collect undisturbed samples of surface sediment. One of the major features of this study is the comparison of results from both Craib and gravity cores of Clyde Sea Area sediments. Highly significant differences in the vertical distribution of tracer species are evident in cores collected with these different samplers at identical locations. As a result, the applicability of conventional small-diameter gravity coring for collection of sediments is questioned, particularly in studies, such as  $^{210}\text{Pb}$  dating, to which recovery of vertically undisturbed material is critical.

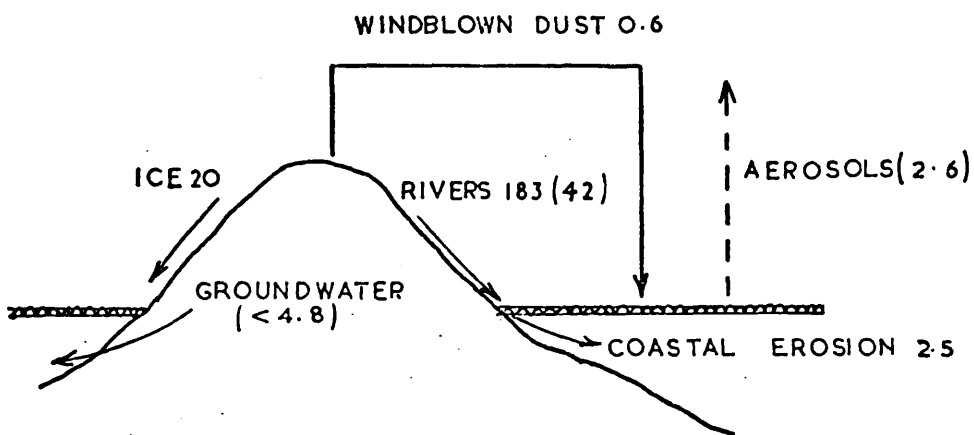
CHAPTER 1

INTRODUCTION

1.1 Sediments: Composition and Properties

Sediments have been the subject of intensive investigation by oceanographers and marine geologists for many years. Indeed, much of our present knowledge of chemical processes occurring within the sea has derived from studies on underlying sediment deposits. Although the sediment matrix is highly variable, with a wide variety of materials contributing to the overall chemical composition, four major sedimentary components can be recognised - namely, detrital, authigenic, biogenic and cosmogenic fractions. Detrital or lithogenous material is that which derives from the land and comprises particulates which result from the mechanical weathering of rocks and minerals exposed at the earth's surface. Rivers are by far the largest transporters of detrital material to the major water bodies (fig. 1) and in addition, carry many species introduced in solution through chemical weathering. In the open ocean, a further significant source of lithogenous sediment arises from submarine volcanic activity. (Terrestrial volcanic eruptions can also contribute to sedimentation, e.g. through ash falls). Authigenic materials are solid phases which form in-situ through precipitation, adsorption and diagenetic reactions. Examples are barite, zeolites (phillipsite), iron oxides and the much studied manganese nodules. The biogenic component of sediment derives from the biological activity of the overlying waters and consists of the skeletal (mainly opal and calcite)

FIGURE 1 Annual transfer of erosion products to the ocean. Figures are in units of  $10^{14}$ g. Figures in parentheses refer to dissolved products (Based on Garrels and MacKenzie, 1971) (From Davies and Gorsline, 1976)



and organic remains of organisms and plants. The cosmogenic fraction comprises material derived from outside the earth's atmosphere and, although quantitatively insignificant in comparison to the other components, is present to some extent in all sediments. Such material includes micrometeorites and tektites..

The relative composition of any particular sediment depends very much on its environment of deposition. However, in all environments, sediments appear to exert an important influence on the composition of the overlying waters due to the remarkable ability of their constituents to efficiently remove many substances from solution.

Under ideal circumstances, sediments are deposited in a layered sequence, each layer being representative of the particular environmental conditions pertaining at the time of deposition. Consequently, if a vertical column of undisturbed sediment is recovered from the sea-floor, subsequent chemical, physical and biological examination of its various strata can disclose a record of past geological/chemical environments. Occasionally, however, this record is to some extent blurred due to partial homogenisation of the upper layers of the deposit through physical/biological disturbance. Interruption of the steady accumulation of material can also arise through episodic surges of sediment supply, e.g. turbidites in the deep-sea (Ericson and Wollin, 1968) and slumping, or the effects of violent climatic events in inshore or loch areas. Meade (1973) concluded that periodic flooding of some rivers through hurricane activity can produce in one week an amount of detritus equivalent to that normally supplied by the same river in several years.

For many years, deep-sea sediments, recovered by gravity or piston corers, have been carefully examined and much evidence of changing climatic and geologic conditions on time scales extending to millions of years has been gathered. Recently, however, investigational emphasis has turned to study of coastal marine, estuarine and loch sediments. This change in priorities has been induced by rising concern over the increasing volume of non-degradable materials (petroleum, heavy metals, artificial radionuclides, aliphatic hydrocarbons) entering the hydrosphere from man's cultural activities over the last 200 years. For instance, some metals are now being introduced to the atmosphere and hydrosphere in concentrations equivalent to and in some cases exceeding those mobilised naturally in the major sedimentary cycle (Goldberg 1971, Patterson 1971). While the precise nature of the removal processes involved is still poorly understood, general trends are apparent; a significant fraction of discharged wastes, including many heavy-metals and man-made radionuclides, exhibit non-conservative behaviour (i.e. are chemically/biologically reactive) in the hydrosphere, are concentrated by sedimentary material (through a combination of ion-exchange, adsorption and absorption reactions on to Mn/Fe oxides, living and dissolved organic material and clay minerals) and are rapidly transferred to sediments. Estuarine and loch systems (traditional sites for human settlement) adjacent to local centres of dense population and industrial development face the greatest burden of anthropogenic discharge and are also often subject to high concentrations of the above reactive particulate materials. As a result, marked increases in the concentration of many heavy metals in the upper layers of

sediment deposits from such environments (and normally attributed to human activities) are regularly observed (Presley et al., 1972; Bortleson and Lee, 1972; Aston et al., 1973; Chow et al., 1973; Thomson et al., 1975; Edgington and Robbins, 1976; Matsumoto and Wong, 1977; Goldberg et al., 1977); surface concentrations are often many times greater than natural levels found at depth in the sediment. Many artificial fallout radionuclides encountered globally due to nuclear weapon detonations and locally due to their controlled release as wastes from nuclear power and fuel reprocessing plants are also found concentrated in surface sediments. (United Nations, 1972; Miller and Stannard, 1975; National Academy of Sciences, 1971; Mitchell, 1975).

The extent to which sediments can be regarded as permanent traps or sinks for deposited materials remains to be established, however, since remobilisation of certain species can occur within the sediment column in response to diagenetic changes induced by changing pH or redox potential. At present this topic represents a major field of geochemical investigation.

Estuarine sediments are generally chemically reducing below a relatively thin aerated upper layer and species undergoing removal processes on to particulate phases, under oxidising conditions in overlying waters, can become chemically unstable after burial, when the environment becomes reducing. For example, redissolution of some species (e.g. Fe/Mn) into interstitial waters of sediments can occur, followed by upward migration towards the sediment/water interface where a concentration gradient exists. Such diffusing species can subsequently reassociate with solid materials encountered in the oxygenated surface layer of the deposit or diffuse out of

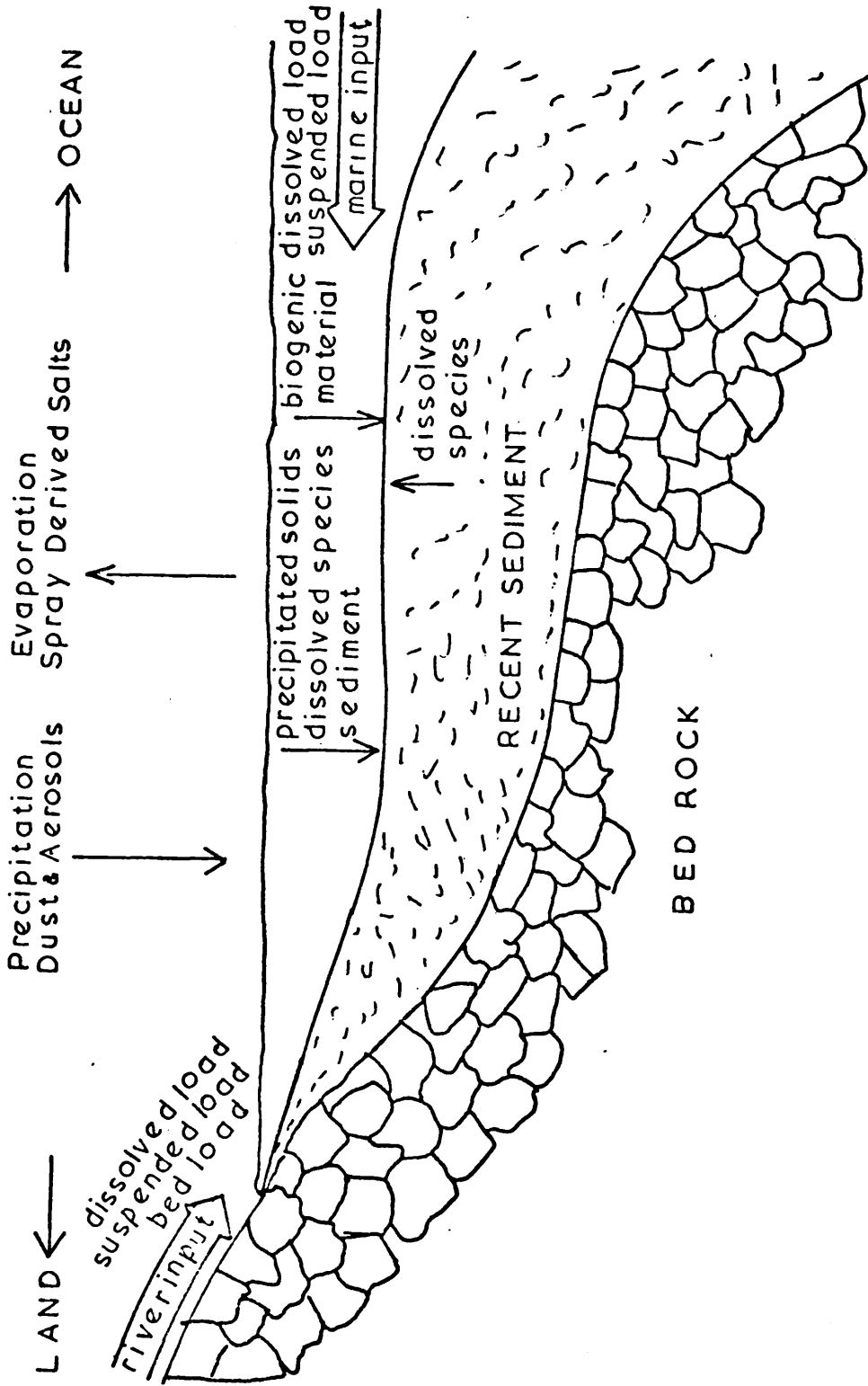
the sediment in response to the concentration gradient. (The possible importance of trace-metal, metal-organic interactions in stabilising dissolved metals in pore waters has been emphasised in recent years, (Singer, 1972; Elderfield and Hepworth, 1975; Yen, 1977). Sediments can therefore under some circumstances be regarded as a source of materials to overlying waters, rather than as a repository for them. Turekian (1977), however, has suggested that the failure thus far to obtain direct evidence for the existence of anthropogenic changes in the open ocean concentration of heavy metals is largely a result of their previous entrainment in estuarine and coastal marine environments. While there may be movement of some heavy metals into and out of solution, the dominant cycle remains internal to the estuary and little material escapes to the open sea (see for example Evans et al (1977) describing the internal cycle of Mn in an estuarine situation, and Benninger et al (1975) outlining a budget for  $^{210}\text{Pb}$  in Long Island Sound and indicating that all of the  $^{210}\text{Pb}$  input can be accounted for within the sediment).

Clearly then, the estuarine environment, even without the superposition of inputs arising from the activities of man, is a particularly complex one because of the variety of sources from which chemical and material inputs are received and the diversity of biogeochemical/biogeophysical interactions. (Burton and Liss, 1976; Church, 1975; Riley and Chester, 1977). Figure 2 summarises the major exchanges of material occurring within the estuarine system.

The enrichment of heavy metals/radionuclides in sediments and sediment pore waters also has implications regarding their uptake by organisms and therefore their potentially dangerous

FIGURE 2 Exchange of matter in an idealised estuarine system

(from Bricker and Troup, 1975)



return to man through the food chains. Although sediment, by removing considerable fractions of heavy metals/radionuclides from solution, can reduce their availability to many marine organisms (phytoplankton, free-swimmers), association with particulate material may increase the possibility of uptake by benthic fauna. (Templeton and Preston, 1966; Duursma and Gross, 1971). Thus some of the highest concentration factors for trace elements in marine organisms have been reported for benthic filter feeders (Duursma and Gross, 1971). Oysters have been reported to concentrate  $^{65}\text{Zn}$  up to 250,000 times the amounts present in water (Chapman et al., 1958; Preston, 1966). Studies of the distribution of plutonium between water, biota and sediments in the Great Lakes have shown that phytoplankton strongly concentrate plutonium from solution with a concentration factor of x5000; however, the benthic food chain exhibits even higher concentration factors due to the relatively high concentration of plutonium in the sediments (Edgington et al., 1975). Sediments, by retaining trace elements/radionuclides can make these species available to organisms for longer periods of time than if they had remained in solution or were suspended in water.

Thus sediments, due to their pre- and post-depositional reactions, exert a dominant influence over marine geochemical processes in general. A basic knowledge of the geochemical processes occurring within estuarine, coastal marine and loch systems in addition to being of immediate importance with regard to study of anthropogenic pollutant effects is also essential to the overall future understanding of oceanographic problems. To quantify and evaluate the record of man's involvement in the sedimentary cycle, to differentiate this from diagenetic

processes occurring within the sediment and to measure the residence time and fluxes of materials into and out of sediments, a reliable chronology is required for such deposits. For this reason, considerable research effort has been focussed on the investigation of patterns and rates of recent sediment accumulation in coastal marine and loch environments.

## 1.2 Geochronology of Recent Sediments

The rate of sediment accumulation in the deep sea is in the order of  $\text{mm } 10^{-3}\text{y}$ . Absolute chronologies for such deposits have been provided by radiometric dating techniques using isotopes with relatively long half-lives such as  $^{14}\text{C}$  ( $t_{1/2} = 5,730\text{y}$ ),  $^{230}\text{Th}$  ( $t_{1/2} = 75,200\text{y}$ ) and  $^{231}\text{Pa}$  ( $t_{1/2} = 32,500\text{y}$ ) from the natural decay series, and  $^{40}\text{K}$ - $^{40}\text{Ar}$  ( $t_{1/2} = 1.24 \times 10^9\text{y}$ ) (references in Thomson and Walton, 1972). Palaeomagnetic, palaeontological and chemical stratigraphic marker techniques have also been applied. The palaeomagnetic sequence of polarity reversals of the earth's magnetic field at various times in the past has been particularly useful in this respect; the timings of these reversals on the continents have been established by  $^{40}\text{K}$ - $^{40}\text{Ar}$  dating and the discovery of equivalent reversals in deep-sea sediments has allowed precise correlation over the past 5 million years. (Harrison and Funnell, 1964; Opdyke et al., 1966; Cox, 1969). While these methods have been of considerable value in dating over extensive periods of time, they are not applicable to coastal marine and loch deposits where rates of accumulation are several orders of magnitude greater ( $\text{mm.y}^{-1}$  to  $\text{cm.y}^{-1}$ ). Interest in these sediments lies in the detailed investigation of patterns and rates of sedimentation in the last 100 to 200 years.

Before the development of suitable radiometric techniques for dating recent sediments, chronology had been based largely on stratigraphic and palynologic methods applicable over this time range. For instance, the unique observation of exotic materials such as cereal or pollen, of known time introduction, at a specific horizon in the sediment has been used to introduce calendar dates to sediments. (Wright, 1971; Davis, 1968;

Davis et al., 1973; Bradbury and Waddington, 1973). Magnetic studies have also been of some value. Recent investigations of freshwater sediments from northwest England (Mackereth, 1971; Pennington, 1973) and Northern Ireland (Batterbee, 1973) have shown that lake sediments can record past changes in the geomagnetic field. The magnetic parameters of use in investigating loch deposits are declination, inclination and intensity of the natural remanent magnetisation. In particular, variations in declination (the horizontal component of magnetic remanence) with depth, can be used to date sediments through comparison of observed measurements in sediments with recorded observatory and archaeomagnetic results over the past 400y. The last westerly maximum in declination occurred early in the 19th century (ca. 1820) and the depth in sediment of this turning point can be used to assign an approximate calendar date to the sediment. (Mackereth, 1971). (The dating range of this method can be extended to 10,000 years if a constant periodicity in declination of 2,700 years is accepted. On this basis good agreement has been observed with  $^{14}\text{C}$  derived ages in Windermere sediment (Mackereth, 1971)). The presence in certain deposits of annual laminae or varves (alternating bands of light and dark material due to seasonal changes in the major component of sediment input) has also been of some use in investigation of the recent sedimentary record. However, varving is retained only in deposits which are not subject to physical or biological disturbance such as low-energy anoxic basins and fjords where bottom currents are weak and the population of benthic fauna low.

Application of these stratigraphic methods, however, is of limited usefulness only, for two reasons,

- (1) the number of sediment deposits in which these datable horizons exist is limited.
- (2) at best, such horizons (varves excluded) can give only historical averages of sediment accumulation rates over the last 100 to 200 years, and they therefore lack the necessary precision and detail; such averages may not accurately reflect rates of accumulation in the upper layers of deposits (where, for example, water content often increases sharply).

A variety of direct methods of determining sedimentation rates have also been established, viz, through introduction of a distinctive layer of material to the sediment surface (Bloom, 1966) or the positioning of stakes as markers against which the rise in sediment can be observed (Runwell, 1964). Sediment traps suspended in the overlying water column have also been used. However, these techniques are appropriate only for long term studies and are subject to error such as washout of marker horizons or atypical deposition in the region of the sediment trap/stake caused by the device itself.

Clearly then there has been a distinct lack of a reliable and rapid method of general applicability for introducing a time parameter of the required accuracy to detailed investigations of recent sedimentation processes such as exchanges occurring at the sediment/water interface or sediment composition changes resulting from anthropogenic effects. To a large extent this difficulty has now been overcome through the development and application of the  $^{210}\text{Pb}$  radiometric dating technique.

## History and Theory of $^{210}\text{Pb}$ Dating

Three natural radioactive decay series (fig 3), each of which has a parent of very long half-life, have remained in existence since the time of nucleosynthesis. During geological time, the three parent nuclides have continuously generated their shorter-lived daughter isotopes through radioactive decay and in a closed system (i.e. where there has been no transfer of matter to or from the system), the condition known as 'secular equilibrium' has been attained such that a steady state exists for each nuclide in the series, i.e. production rate equals radioactive decay rate. Thus in an undisturbed geochemical system, the activities of each nuclide in any one series are equal.

The secular equilibrium steady state condition is, however, frequently not encountered in sediments. The various members of the radioactive decay series have widely differing physical and chemical properties. Thus their dissimilar responses to the natural processes of weathering, solution and precipitation, which ultimately give rise to sediment deposits, result in the separation of parent/daughter pairs within the series; natural series dating techniques result from the subsequent growth (or decay) of these isotopes back to secular equilibrium. In other words, natural series dating of sediments depends upon the disequilibrium which exists between the various members of the decay series in sediments, and the geochronological methods are essentially of two kinds,

- (1) where a time scale is provided by the extent of decay of an unsupported nuclide, and
- (2) where a time scale is provided by the growth of a daughter towards equilibrium with its parent in

FIGURE 3 The  $^{238}\text{U}$ ,  $^{235}\text{U}$  and  $^{232}\text{Th}$  decay series:  
vertical arrows denote alpha decay and  
slanted arrows, beta decay: The numbers  
beneath each symbol of the isotopes  
denotes the half-life



a material in which originally there was an insignificant (or known) concentration of the daughter,  $^{210}\text{Pb}$  is a member of the  $^{238}\text{U}$  natural decay series (fig. 3) and has a half-life of 22.26y (Höhndorf, 1969). The dating technique is of the general form outlined in (1) above and its application is discussed in detail in a later section. The isotope is brought into the major sedimentary cycle in the following way. The radioactive rare gas isotope  $^{222}\text{Rn}$ , which has a half-life of 3.825d (Tobailem, 1955) is a precursor of  $^{210}\text{Pb}$  in the  $^{238}\text{U}$  natural decay series.  $^{222}\text{Rn}$  is released from surface rocks and soils into the atmosphere. There, because it is unreactive and gaseous and therefore has a long atmospheric residence time relative to its half-life, it decays through a series of short-lived daughters to produce  $^{210}\text{Pb}$ . Radon daughters, however, are chemically reactive in the atmosphere and are quickly adsorbed on to atmospheric dust particles (Feely and Seitz, 1970). The  $^{210}\text{Pb}$  is then returned to the earth's surface either in precipitation or in dry fallout. Its residence time in the lower levels of the atmosphere (troposphere), based on disequilibrium measurements of  $^{210}\text{Pb}$  and its daughters in aerosols and precipitation, has been calculated to be of the order of days or weeks (Burton and Stewart, 1960; Peirson et al., 1966; Francis et al., 1970; Moore et al., 1973; Poet et al., 1972).

A further source of atmospherically derived  $^{210}\text{Pb}$  is that due to its possible production in nuclear weapon detonations. This, however, is an unresolved question. Peirson et al (1966) and Jaworowski (1969, 1970) have indicated that  $^{210}\text{Pb}$  may be produced in nuclear explosions through the reaction  $^{208}\text{Pb}(2n, \gamma)^{210}\text{Pb}$ , while Beasley (1969) and Feely and Seitz (1970)

concluded from their respective measurements of  $^{210}\text{Pb}$  in soil samples at test-sites, and in the atmosphere immediately following tests, that  $^{210}\text{Pb}$  is not produced by this mechanism.

The use of atmospherically derived  $^{210}\text{Pb}$  as a geochronological tool was first proposed by Goldberg (1963), who applied the technique to permanently accumulating snowfields. From the observed  $^{210}\text{Pb}$  distribution in Greenland glaciers a mean accumulation rate, in good agreement with that derived from stratigraphic markers, was obtained. This result suggested that both the flux of excess  $^{210}\text{Pb}$  and the rate of ice accumulation had been fairly constant over the time interval dated. Subsequently the technique was applied to the Antarctic ice sheet by Crozaz et al (1964). The  $^{210}\text{Pb}$  activity was again found to decrease exponentially with depth and the annual rates of water accumulation derived from the decay curve were again in good agreement with independently derived dates. Windom (1969) applied the technique to a group of Alpine glaciers and, although in this case some difficulty in establishing a time scale was encountered due to a high dust contribution of  $^{226}\text{Ra}$  supported  $^{210}\text{Pb}$ , the general reliability of the technique was established.

Following this success in dating ice-sheets, the applicability of the method to lake and marine sediments was examined. Krishnaswami et al (1971) found an excess  $^{210}\text{Pb}$  over and above that required for equilibrium with its parent in cores from various European lakes and an Indian lake. With the initial assumption that the rate of deposition of  $^{210}\text{Pb}$  was uniform with time for a given lake, the results were in reasonable agreement with those obtained by other methods. Koide et al (1972) derived a mean sedimentation rate of  $6.0 \text{ mm y}^{-1}$  on the

basis of  $^{210}\text{Pb}$  measurements for a lake Mendota core which was in good agreement to that previously derived by Bortleson and Lee (1972) for the same lake based on pollen analysis.

While early profiles of  $^{210}\text{Pb}$  in lake sediments had shown exponential decrease in  $^{210}\text{Pb}$  activity from surface to depth consistent with the assumptions of Krishnaswami et al (1971), some later profiles exhibited reduced or constant activity within a zone of varying thickness at the sediment/water interface. Rates of sediment accumulation in Lake Superior deposits investigated by ragweed pollen and  $^{210}\text{Pb}$  techniques were consistent if a small depth of physical/biological mixing was considered, (Bruland et al., 1975). Robbins and Edgington (1975) found mainly classical  $^{210}\text{Pb}$  profiles in a study of a suite of cores from L. Michigan. However, certain samples exhibited constant  $^{210}\text{Pb}$  activity in their surface strata which again could best be explained by considering a model in which a zone at the top of the sedimentary column was assumed to be completely homogeneous as a result of rapid physical/biological reworking. Robbins et al (1977) compared the depth distribution of  $^{210}\text{Pb}$  with that of the benthic macroinvertebrates in L. Huron sediments and found a high degree of correlation, >90% of the invertebrate population being found within the zone of constant  $^{210}\text{Pb}$  activity. Robbins and Edgington (1975) and Robbins et al (1977) concluded from their evidence that many sedimentary deposits were subject to rapid reworking by burrowing organisms and that the observed depth distribution of  $^{210}\text{Pb}$  (and other radionuclides) was a useful indicator of the extent of this mixing. A sedimentation rate could be derived from the  $^{210}\text{Pb}$  profile below the depth of active burrowing and mathematical models were developed which included the effects of biological

disturbance, and which satisfactorily explained the  $^{210}\text{Pb}$  and  $^{137}\text{Cs}$  radionuclide profiles.

The earliest attempts to determine the applicability of the  $^{210}\text{Pb}$  dating technique to coastal marine sediments were performed on the varved anaerobic deposits of the Santa Barbara Basin (Koide et al., 1972, 1973). Annual layers were readily separable in these deposits and provided excellent standards against which to first test the reliability of the method in the coastal environment. The mean rate of sediment accumulation derived from the  $^{210}\text{Pb}$  data was  $0.39 \text{ cm y}^{-1}$ , in good agreement with that estimated from the mean varve thickness of  $0.4 \text{ cm y}^{-1}$ . Koide et al (1973) extended the geochronology from varved to unvarved anoxic marine deposits and concluded that the method was valid for dating over periods of a century or more. Since then the dating technique has enjoyed widespread application to provide a reliable time-scale against which anthropogenic inputs to, and diagenetic changes within, recent sediments could be assessed. A limited number of studies have now been conducted on oxic marine sediments. (Thomson et al., 1975; Koide et al., 1975; Goldberg et al., 1977; Farrington et al., 1977; Matsumoto et al., 1977). The technique has also found some application in determination of rates of accumulation in estuarine marsh environments (Armentano and Woodwell, 1975) and to peat bogs (Eakins, 1977, personal communication).

The excess  $^{210}\text{Pb}$  observed in the surface sediment of marine and loch systems has two sources. In addition to that derived from atmospheric fallout,  $^{210}\text{Pb}$  produced in-situ by decay of  $^{226}\text{Ra}$  present in the waters overlying the deposit, also contributes to a varying degree. While  $^{226}\text{Ra}$  is highly soluble, it is apparent from every study to date, that the  $^{210}\text{Pb}$

produced from decay of  $^{226}\text{Ra}$  in solution, together with that derived from atmospheric deposition, is rapidly scavenged by particulate/biological mechanisms and transferred to the underlying sediments in a time which is very short relative to its half-life. Schell (1977) estimates the residence time of  $^{210}\text{Pb}$  in inshore and coastal waters of Washington State to be around 60 to 160 days, depending on distance from coast and water depth. Goldberg (1963) and Klein and Goldberg (1970) have also demonstrated the short residence time of  $^{210}\text{Pb}$  in natural waters.

In addition to the unsupported  $^{210}\text{Pb}$  in marine and lacustrine sediments, there also exists a background supported  $^{210}\text{Pb}$  activity due to the presence of  $^{226}\text{Ra}$  in the sedimentary materials. This  $^{210}\text{Pb}$  is in secular equilibrium with its parent  $^{226}\text{Ra}$  and its activity is often low relative to that of excess  $^{210}\text{Pb}$ . Since the dating technique depends upon the decrease in excess  $^{210}\text{Pb}$  activity with depth in the sediment column it is necessary to correct for supported  $^{210}\text{Pb}$ . This is particularly important at depth in the core where excess  $^{210}\text{Pb}$  and supported  $^{210}\text{Pb}$  are of similar magnitude. The difference between the total  $^{210}\text{Pb}$  and the supported  $^{210}\text{Pb}$  effectively limits the period over which the dating technique is applicable and the accuracy with which the sedimentation rate can be determined. By correcting for supported  $^{210}\text{Pb}$ , the effective range of the method can normally be extended from ca. 100 years to around 150 years (assuming reasonably high analytical precision in experimental determination of total  $^{210}\text{Pb}$  and supported  $^{210}\text{Pb}$ ).

### Application of the Dating Method

The dating method depends upon the measurement of two quantities in the sediment, (1) the total  $^{210}\text{Pb}$  and (2) the supported  $^{210}\text{Pb}$ . The difference between these quantities gives a measure of the excess  $^{210}\text{Pb}$ , the exponential decrease of which with depth due to radioactive decay is the basis of the dating technique. For the purposes of evaluating excess  $^{210}\text{Pb}$ , supported  $^{210}\text{Pb}$  is normally assumed to be in secular equilibrium with  $^{226}\text{Ra}$ , thus

$$A_{^{210}\text{Pb}_{\text{XS}}} = A_{^{210}\text{Pb}_{\text{TOT}}} - A_{^{226}\text{Ra}} \quad (1)$$

where, the  $A_{^{210}\text{Pb}_{\text{TOT}}}$  and the  $A_{^{226}\text{Ra}}$  are the measured values of the total  $^{210}\text{Pb}$  and  $^{226}\text{Ra}$  in the sediment, respectively. The activity of  $^{226}\text{Ra}$ -supported  $^{210}\text{Pb}$  is determined either independently or from the measured values of  $^{210}\text{Pb}$  at depths in the core sufficient for all excess  $^{210}\text{Pb}$  to have decayed.

In its simplest form, the model involves four assumptions, as outlined in Robbins and Edgington (1975),

- (1) that there has been a constant flux of  $^{210}\text{Pb}$  to the sediment,
- (2) that there has been a constant rate of sediment accumulation,
- (3) that there has been no post-depositional migration of  $^{210}\text{Pb}$  within the sediment,
- (4) that the supported  $^{210}\text{Pb}$  activity is constant with depth.

Under these conditions, in ideal (unmixed) sediments experiencing no compaction, the profile of  $^{210}\text{Pb}$  should show exponential decrease with depth and,

$$A\left(^{210}\text{Pb}_{\text{XS}}\right)_t = A\left(^{210}\text{Pb}_{\text{XS}}\right)_{t=0} e^{-\lambda t}, \quad \text{and } t = \frac{z}{s} \quad (2)$$

where,

$A(^{210}\text{Pb}_{\text{XS}})_t$  and  $A(^{210}\text{Pb}_{\text{XS}})_{t=0}$  are the measured activities of excess  $^{210}\text{Pb}$  at time  $t$  (or depth  $z$  cm.) and time zero (or depth zero) respectively, and  $s$  is the sedimentation rate in  $\text{cm.y}^{-1}$ . A plot of  $\log. A_{^{210}\text{Pb}_{\text{XS}}}$  against depth should yield a straight line in which the slope corresponds to  $-\frac{\lambda}{s}$ , from which a value of  $s$  in  $\text{cm.y}^{-1}$  can be derived.

However, most rapidly accumulating coastal marine and loch sediments exhibit very high water content in their upper strata (up to ca. 85% by weight). The percentage weight loss upon drying and porosity (water volume fraction) are presented for a typical core in fig. 4. The porosity often exhibits exponential decrease in the upper layers of the deposit, in which case a constant sedimentation rate described in terms of  $\text{cm.y}^{-1}$  is inappropriate since the thickness corresponding to one year's increment is rapidly decreasing with depth of burial due to compaction; this despite constant rate of accumulation of solid materials. Consequently it is preferable to measure the rate of sediment accumulation in terms of the weight of dry material depositing per  $\text{cm}^2$  per unit time. The accumulation rate  $\omega$  ( $\text{mg.cm}^{-2}\text{y}^{-1}$ ) is related to the sedimentation rate  $s$  ( $\text{cm.y}^{-1}$ ) by the expression

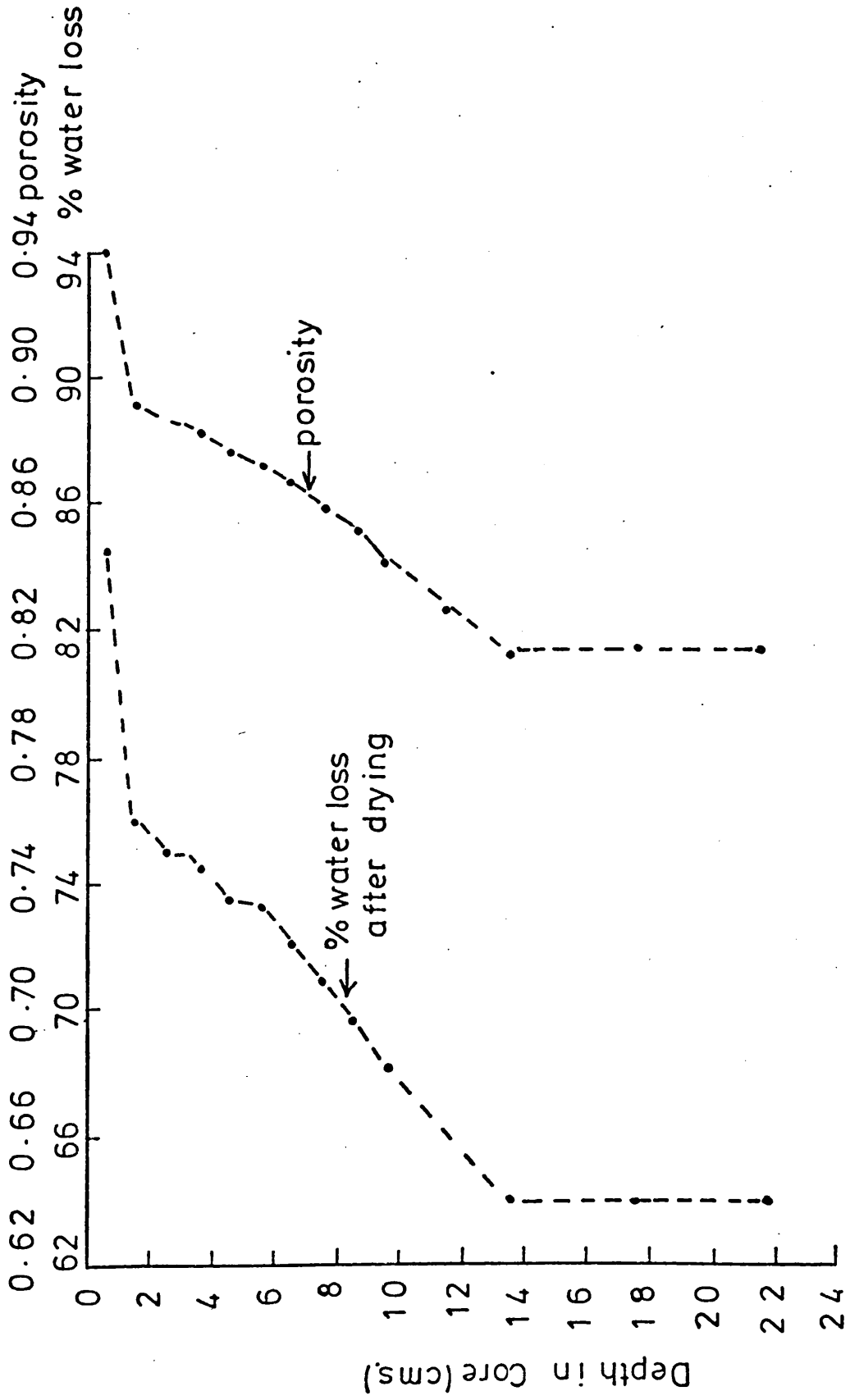
$$\omega = \rho s, \text{ where,}$$

$\rho$  ( $\text{g.cm}^{-3}$ ) is the in-situ density of the sediment (i.e. weight of dry sediment per  $\text{cm}^3$  of deposit), corresponding to  $s$ . The in-situ density  $\rho$  is also related to the porosity by the expression

$$\rho = \bar{\rho} (1-\gamma), \text{ where,}$$

$\bar{\rho}$  is the measured density of the dried solids, and  $\gamma$  is the

FIGURE 4 Water content of Loch Goil sediment



appropriate porosity.

In areas where sediments are rapidly compacting (i.e. the sedimentation rate in  $\text{cm.y.}^{-1}$  is rapidly changing with depth), a mean value for the sedimentation rate can nonetheless be evaluated from equation (2). However, for some purposes this may not be of sufficient accuracy and it is preferable therefore to correct for compaction in some way. One method is to measure the rate of sediment accumulation directly in terms of weight of dry sediment deposited per  $\text{cm}^2$  per unit time as defined above, thereby, in effect, normalising to zero water content throughout the length of the column. Thus equation (2) is applicable in rapidly compacting sediments if  $z$  is expressed in units of  $\text{mg. cm.}^{-2}$  from which a sedimentation rate in  $\text{mg. cm.}^{-2}\text{y.}^{-1}$  is evaluated.

Correction for compaction has been performed in other ways, viz, by normalising  $^{210}\text{Pb}$  activity against the concentration of a second component of the sediment assumed not to be subject to variable input (i.e. its concentration per unit volume in the absence of other effects would be constant); for example, Goldberg et al (1974) normalised  $^{210}\text{Pb}$  activity against aluminium in Santa Barbara coastal sediments. (In the case of marine sediments this method has the advantage of correcting for salt dilution of sediment material). Pennington et al (1976) evaluated a mean rate of sediment accumulation from structured  $^{137}\text{Cs}$  profiles in deposits of Blelham Tarn. Subsequently they corrected for increasing water content towards the sediment/water interface by normalising to a constant annual input of potassium and hence obtained a more accurate estimate of the thickness of each annual increment. An alternative approach is to normalise the observed depth

to a corrected depth which would have been the true depth in the absence of compaction (Matsumoto 1975, 1977). Robbins and Edgington (1975) developed an explicit function relating depth to age in homogeneous compacting sediments and described a rigorous mathematical expression applicable to the analysis of  $^{210}\text{Pb}$  profiles in rapidly compacting but otherwise undisturbed sediments.

A complication can arise in the interpretation of  $^{210}\text{Pb}$  profiles in coastal marine and loch sediments due to physical/biological post-depositional disturbance of the surface layers. As described previously, this can result in the observation of a constant activity of  $^{210}\text{Pb}$  (or other radionuclide) with depth in surface sediment. In these cases the rate of sediment accumulation can usually be determined from the excess  $^{210}\text{Pb}$  profile below the zone of active mixing. The effect of mixing in the upper layers of deep-sea deposits on the profiles of long-lived ( $^{230}\text{Th}/^{232}\text{Th}$ ) radioactive and stable species has been discussed by Goldberg and Koide (1962) and Berger and Heath (1968). Recently a number of models have been developed to relate the effects of biological mixing in recent coastal and lacustrine sediments on the distribution of the relatively short-lived radionuclides such as  $^{210}\text{Pb}$  and  $^{137}\text{Cs}$ .

---

Robbins and Edgington (1975) developed a steady-state mixing model with the basic assumption of complete

redistribution of particles entering the mixing zone in a time short with respect to further input of material (i.e. rapid and complete homogenisation), and showed that this would account for measured distributions of  $^{210}\text{Pb}$  in sediments from L. Michigan. Robbins et al (1977) further showed that the quantitative effect on the distribution of  $^{210}\text{Pb}$  of a mixing process with the above assumption could be determined from considerations of mass balance alone (i.e. flux of  $^{210}\text{Pb}$  to the sediment, decay within the mixed zone and the flux of  $^{210}\text{Pb}$  through the bottom of the mixed zone). They derived the expression,

$$A_m = A_s / (1 + \frac{\lambda d}{w}) \quad (3)$$

where  $A_m$  = activity of excess  $^{210}\text{Pb}$  in the mixed zone  
 $A_s$  = activity of excess  $^{210}\text{Pb}$  added to the sediment surface.

$d$  = depth of the mixed zone

The distribution of excess  $^{210}\text{Pb}$  activity,  $A$ , within the sediment is

$$\begin{aligned} A &= A_m \text{ within the mixed zone, and} \\ A &= A_m e^{-\lambda(z-d)/w} \text{ below the mixed zone} \end{aligned} \quad (4)$$

(from which the rate of sediment accumulation can be determined). In deriving this expression they showed that the effect of mixing was to reduce the activity of  $^{210}\text{Pb}$  in the mixed layer from that which would have occurred in undisturbed sediments by the factor  $(1 + \frac{\lambda d}{w})$ .

An alternative approach is to treat mixing as a diffusive process brought about by the burrowing activities of bottom-dwelling organisms and hence to evaluate a biological mixing or diffusion coefficient for the sediment. Modelling on these lines has met with some success (Goldberg and Koide, 1962; Bruland, 1974; Robbins, et al., 1977; Guinasso and Schink, 1975). Such

treatments involved the use of the general diagenetic equation and Fick's laws of diffusion to derive an expression which describes the distribution of  $^{210}\text{Pb}$  (or other radionuclide) with depth. The general expression (Berner, 1971; Bruland, 1974) is of the form

$$\frac{dA}{dt} = \frac{d}{dz} (K_b \frac{dA}{dz}) - s \frac{dA}{dz} - \lambda A \quad (5)$$

where,  $A$  = concentration of excess  $^{210}\text{Pb}$  in  $\text{dpm.g}^{-1}$   
 $K_b$  = biological mixing coefficient in  $\text{cm}^2\text{y}^{-1}$   
 $s$  = sedimentation rate in  $\text{cm.y}^{-1}$   
 $\lambda$  = decay constant for  $^{210}\text{Pb}$  in  $\text{y}^{-1}$   
 $z$  = depth in sediment in  $\text{cm}$ ,

This expression shows that the concentration of  $^{210}\text{Pb}$  at any depth in the sediment is dependent upon (a) the biological mixing of the surface sediments, (b) the sedimentation rate and (c) radioactive decay. Solutions to this equation under various limiting conditions have for the sake of "convenience and sanity" (Guinasso and Schink, 1975) retained the concept of a constant biological mixing rate within a well defined thickness of sediment (i.e. below the mixed zone  $K_b = 0$ ). Both steady-state ( $\frac{dA}{dt} = 0$ ) solutions and alternatives with time-dependent influx of materials to the sediment have been presented (Guinasso and Schink, 1975; Robbins et al., 1977). For  $^{210}\text{Pb}$ ,  $\frac{dA}{dt}$  is assumed to be zero, in which case the above expression reduces to

$$K_b \frac{d^2A}{dz^2} - s \frac{dA}{dz} - \lambda A = 0 - \text{within the mixed zone} \quad (6)$$

$$\text{and } -s \frac{dA}{dz} - \lambda A = 0 - \text{below the mixed zone} \quad (7)$$

As  $K_b \rightarrow \infty$  (i.e. rapid and complete biological mixing) the solution to the former equation is identical to that of Robbins et al (1977) (i.e. equation 4) The solution to the

latter equation is simply  $A_t = A_0 e^{-\lambda t}$ , i.e. equation 2.

Fundamental to the general approach to  $^{210}\text{Pb}$  dating described so far, is the assumption of a constant initial concentration of excess  $^{210}\text{Pb}$  per unit dry weight of material in each section of the sediment; in other words both a constant flux of  $^{210}\text{Pb}$  to the sediment and a constant rate of deposition of solid material are assumed. While this general approach to  $^{210}\text{Pb}$  dating has met with considerable success, Oldfield et al (1978), in recent studies of deposits from the New Guinea Highlands and Loch Erne, N. Ireland, observed  $^{210}\text{Pb}$  profiles which were incompatible with a deposition model based on these assumptions. In these studies evidence was found for the apparent dilution of excess  $^{210}\text{Pb}$  due to an increased rate of sediment deposition towards the sediment surface. By adopting an alternative approach to  $^{210}\text{Pb}$  dating which allowed for a changing rate of sediment accumulation, Oldfield et al (1978) derived  $^{210}\text{Pb}$  dates from these profiles which were both internally consistent and compatible with external evidence. Details of the development and application of the method are described in Appleby and Oldfield (1978). This approach, originally proposed by Goldberg (1963) for dating Greenland glaciers and Sackett (1965) for  $^{231}\text{Pa}$  and  $^{230}\text{Th}$  dating of pelagic sediments, assumes that while the flux of excess  $^{210}\text{Pb}$  to the sediment in unit time has been constant, the quantity of dry material depositing in unit time may have varied. The age of any horizon can then be found from the expression

$$\Sigma A_{(210\text{Pb}_{\text{xs}})_z} = \Sigma A_{(210\text{Pb}_{\text{xs}})_{\text{TOT}}} e^{-\lambda t} \quad (8)$$

$$\text{and, } t = \frac{-2.303}{\lambda} \log \frac{\Sigma A_{(210\text{Pb}_{\text{xs}})_z}}{\Sigma A_{(210\text{Pb}_{\text{xs}})_{\text{TOT}}}}$$

where,  $\Sigma A_{(210\text{Pb}_{\text{xs}})_{\text{TOT}}}$  = the total integrated excess  $^{210}\text{Pb}$  activity in dpm,  $\text{cm}^{-2}$  in the sediment column,

$\Sigma A_{(210\text{Pb}_{\text{xs}})_z}$  = the total integrated excess  $^{210}\text{Pb}$  activity in dpm,  $\text{cm}^{-2}$  below depth  $z$  cm,

and  $t$  = the age of horizon  $z$ .

This approach has the advantage that where the rate of sediment accumulation has been constant, both the constant initial concentration (C.I.C.) and the constant rate of supply (C.R.S.) models (Oldfield et al (1978)) will yield identical results. If the deposition rate has fluctuated over a long period of time however the C.I.C. model (in contrast to the C.R.S. model) cannot be used to derive accumulation rates or date horizons. Strictly speaking, however, the C.R.S. model requires determination of the in-situ density and excess  $^{210}\text{Pb}$  activities throughout the length of the column.

### Complementary Radiometric Dating Techniques

In general then,  $^{210}\text{Pb}$  has been shown to be a reliable indicator in investigations of patterns and rates of recent sediment accumulation, with a dating range of around 100 to 150 years. Complementary radioisotope techniques also exist which have been of some value in sediment studies over periods of ca 0 - 10 years and 0 - 30 years. These arise from two sources, (1) two further short-lived members of the natural decay series,  $^{228}\text{Th}$  ( $t_{1/2} = 1.9\text{y}$ ) and  $^{234}\text{Th}$  ( $t_{1/2} = 24.1\text{ d.}$ ); and (2) artificial nuclides.

In the aquatic environment, thorium isotopes tend to behave chemically in like manner to those of lead, i.e. thorium isotopes present in solution are highly insoluble and are rapidly removed to the sediment by adsorption on to settling particulates. Their use in studies of sedimentary processes therefore arises in a similar fashion to that of  $^{210}\text{Pb}$ . Koide et al (1973, 1975) found an excess of  $^{228}\text{Th}$  over and above that supported by its parent  $^{232}\text{Th}$  (and  $^{228}\text{Ra}$ ) in surface layers of Santa Barbara and Baya California sediments and made use of a decreasing  $^{228}\text{Th}/^{232}\text{Th}$  activity ratio with depth to date over a time period of a decade. Similarly, Aller and Cochran (1976) found an excess of  $^{234}\text{Th}$  above that expected for radioactive equilibrium with its parent  $^{238}\text{U}$  in the upper strata of sediments from Long Island Sound. They utilised this unsupported  $^{234}\text{Th}$  to obtain information on short-term (seasonal) sediment reworking and rapid diagenetic changes occurring within the upper few cms. of the deposit. In addition to their potential use as short-term chronometers, the presence of an excess of either isotope in the upper layers of a core can provide permissible evidence that an undisturbed core has been retrieved

and sampled without loss of surface material (Koide et al., 1973).

The use of artificial nuclides in dating sediments is essentially a form of stratigraphic marker which covers the last 20 to 30 years. These nuclides made their first significant appearance in the environment in the late 1940's due to their production in nuclear weapon detonations and their controlled release from nuclear power and fuel reprocessing plants. Following the Castle Test in 1954, in the Pacific, the concentrations of fission nuclides in the atmosphere exceeded those of their natural counterparts. In the early 1960's production of man-made nuclides in weapon tests reached a significant maximum and atmospheric fallout in the northern troposphere peaked in 1963. The entry of radionuclides from fallout into natural waters has thus resulted in uptake by lake and marine sediments, and this 1963 peak, when recorded in sediments, can be used as a horizon for dating the sediment layer accumulated during 1963-64. Furthermore, the maximum sediment depth at which artificial radionuclides are found can be regarded as an indication of the 1954 horizon.

Krishnaswami et al (1971, 1973) found a distinct peaked distribution for  $^{55}\text{Fe}$  in recent Santa Barbara basin cores. By attributing this peak to maximum atmospheric fallout in 1963, excellent correlation was observed between  $^{55}\text{Fe}$  derived sedimentation rates and rates based both on annual varves and  $^{210}\text{Pb}$  methods. Krishnaswami therefore concluded that  $^{55}\text{Fe}$  showed promise in dating coastal sediments deposited during the last 20 years.

In comparison, records of fallout plutonium in marine sediments have shown quite different trends. Both Koide

et al (1975) and Goldberg et al (1977) failed to observe a plutonium peak in studies of anaerobic, biologically undisturbed coastal sediments. In contrast, a continuously increasing concentration of plutonium-239 and -240 from depth to near the sediment/water interface was found, although in both instances the first appearance of plutonium was observed in strata corresponding to 1954 on  $^{210}\text{Pb}$  radiometric evidence, consistent with that expected from the onset of nuclear testing. However, Koide et al (1975) did observe a maximum  $^{238}\text{Pu}$  activity at a depth in their cores which (again from  $^{210}\text{Pb}$  data) corresponded to the burnup in 1964 of the American System for Auxiliary Power (SNAP) 9A Satellite. From this evidence they concluded that there could have been no significant migration of plutonium in the anoxic sediments and that the unexpected profile could best be rationalised by invoking the wind or river-borne transport of material, containing sorbed plutonium, which had been eroded from the continents. However, Noshkin (1972) detected both  $^{239}\text{Pu}$  and  $^{137}\text{Cs}$  at depths in cores from Buzzards Bay far in excess of those expected from the known sedimentation rate in the deposits. Redistribution of plutonium within the deposit either through molecular diffusion or bioturbation or a combination of both had apparently occurred. Recently, Livingston and Bowen (1975) have claimed evidence of the upward migration of plutonium in Buzzards Bay sediments. In contrast, Edgington et al (1975) determined the vertical distribution of plutonium and  $^{137}\text{Cs}$  isotopes in a suite of cores from L. Michigan and found not only correspondence of the  $^{137}\text{Cs}$  and plutonium profiles but excellent agreement between sedimentation rates calculated from the positions of

the early 1950's and 1963 horizons and those determined radiometrically with  $^{210}\text{Pb}$ . Clearly there exists some confusion regarding the geochemical behaviour of plutonium in the aquatic environment which to some extent limits its usefulness in dating sediments.

$^{137}\text{Cs}$  has also been used fairly extensively in sediment studies. However, once again, conflicting results have been obtained. Goldberg and Bruland (1974), in quoting a significant value of  $10^{-9}$  to  $10^{-8}$   $\text{cm}^2\text{s}^{-1}$  for the diffusion coefficient of  $^{137}\text{Cs}$  in sediments, argued that the distribution of the isotope could be markedly altered by post-depositional diffusion processes. Thus they concluded that  $^{137}\text{Cs}$  migration represents a major obstacle to its use as a geochronological tool even in sediments accumulating at a rate of several  $\text{cm.y}^{-1}$ . This mobility of  $^{137}\text{Cs}$  in sediments has been extensively investigated (Duursma and Bosch, 1971; Lietzke et al., 1973; Lerman and Lietzke, 1975) and it has been widely accepted that its utility in determination of sedimentation rates is limited. For instance, Lerman and Lietzke (1975) measured the concentration of  $^{137}\text{Cs}$  in lakes Erie and Ontario sediments and found them to increase continuously from depth to the sediment-water interface. This they attributed to a combination of  $^{137}\text{Cs}$  diffusion and integrative effects in the overlying water column smoothing the time-dependent input of the nuclide. Nevertheless, in certain instances, the observed depth distribution pattern of  $^{137}\text{Cs}$  has corresponded closely to that expected from atmospheric fallout and it has been suggested by some that the isotope can be regarded as a reliable chronometer for dating sediments over 20-30 years. (Pennington et al., 1973;

Ritchie et al., 1973; Pennington et al., 1976; Batterbee et al., 1976). In these cases, consistent results were obtained when sedimentation rates based on  $^{137}\text{Cs}$  maxima were compared with those derived from other dating techniques (Pennington et al., 1973, stratigraphic marker; Pennington et al and Batterbee et al., 1976,  $^{210}\text{Pb}$  dating). These results suggested a low diffusional mobility of  $^{137}\text{Cs}$  in sediments. In any case, as Krishnaswami et al (1971) have observed, the effect of diffusion would merely be to broaden the peak rather than to alter its position. Moreover, Robbins and Edgington (1975) determined  $^{137}\text{Cs}$  distributions in L. Michigan cores and found the profiles to be in generally good agreement with time-scales based on  $^{210}\text{Pb}$  measurements. In some cases, however, they observed a downward displacement of  $^{137}\text{Cs}$  peak activity relative to that expected on the basis of  $^{210}\text{Pb}$  dating, and agreed with the conclusion of Krishnaswami et al (1973) that an apparent downward displacement of peak activity must arise as a result of physical or biological mixing. As outlined previously, a mathematical model was developed which, including a surface mixing depth of  $\sim 4\text{cms}$ , satisfactorily accounted for the observed  $^{137}\text{Cs}$  profiles, while giving consistent results with  $^{210}\text{Pb}$  chronologies.

It would seem therefore that the use of man-made radio-nuclides as definitive indicators of rates of sediment accumulation is questionable and appears to depend upon the particular geochemical environment of the area under study. Their reliability as geochronological tools is dependent upon the time-dependent atmospheric flux of the nuclides being faithfully recorded within the sediment column, which appears to depend upon the following;

- (1) the rate of sediment accumulation; this must be sufficiently high to be compatible with the inherent sampling resolution. If the total activity of the nuclide is contained within the upper few cms. of the deposit it would be impossible to derive a meaningful sedimentation rate;
- (2) the chemical nature of the sediment; this will effectively control the post-depositional mobility of the nuclides;
- (3) the extent of physical/biological mixing; this will control the depth at which the peak activity is observed;
- (4) the delay between atmospheric rainout on to both the waters overlying the deposit and the surface soils of the catchment area and incorporation of the nuclide into the sediment; this must be short for the pattern of atmospheric fallout to be duplicated in the sediment.

Despite these reservations, man-made nuclides together with  $^{228}\text{Th}$  and  $^{234}\text{Th}$ , are clearly of considerable value when used in conjunction with  $^{210}\text{Pb}$  to investigate recent sedimentary processes. Even in the absence of distinctive marker horizons with which to introduce time-scales, their presence and distribution in the upper layers of the sediment are useful in indicating the recovery of the topmost layers of the deposit and in establishing the extent to which the sample has been subject to physical/biological disturbance. Artificial nuclides released locally from nuclear fuel reprocessing plants and reactors can also be of considerable value in this context. Temporal variations in output are normally well documented and

since effluents generally contain a range of radiochemical species of widely differing marine behaviour and radioactive half-life (e.g.  $^{134}\text{Cs}$ ,  $t_{\frac{1}{2}} = 2.1\text{y}$ ;  $^{60}\text{Co}$ ,  $t_{\frac{1}{2}} = 5.26\text{y}$ ) these can be useful as tracers of both water movement and sediment processes.

### 1.3 Background to the Areas under Study

The main aim of this research project is a preliminary investigation of sedimentation processes in sea-lochs of the northern region of the Clyde Sea Area using the  $^{210}\text{Pb}$  dating technique. During the project it became possible to expand the study to include analysis of sediment cores both from the nearby freshwater loch, Loch Lomond and from an inshore marine basin (the Cilicia Basin) on the south coast of Turkey. The following sections describe background information on these environments with detail roughly in proportion to the amount of time afforded to each study. While certain aspects of this information may not seem of immediate relevance to the major objectives of the project, they are nevertheless included since they firstly ensure a fairly comprehensive review of each area of study and secondly may well be of a more general interest.

#### Clyde Sea Area

##### General

The Clyde Sea Area (fig. 5), situated on the west coast of Scotland, consists of three distinct regions; an upper shallow drowned estuary, a broad outer firth to the south, and a series of seven narrow fjord-like sea-lochs which run northwards into the highlands of Argyll. These water bodies lie to the north of a line (lat.  $55^{\circ}15'$ ) which joins the tip of the Mull of Kintyre to Girvan on the Ayrshire coast and together constitute an area of greater than  $2,500 \text{ km}^2$ . The physical dimensions of the various water bodies are presented in table 1. The hinterlands of the estuary and mainland firth support a highly developed industrial and urban community with a total population of well over  $2\frac{1}{2}$  million

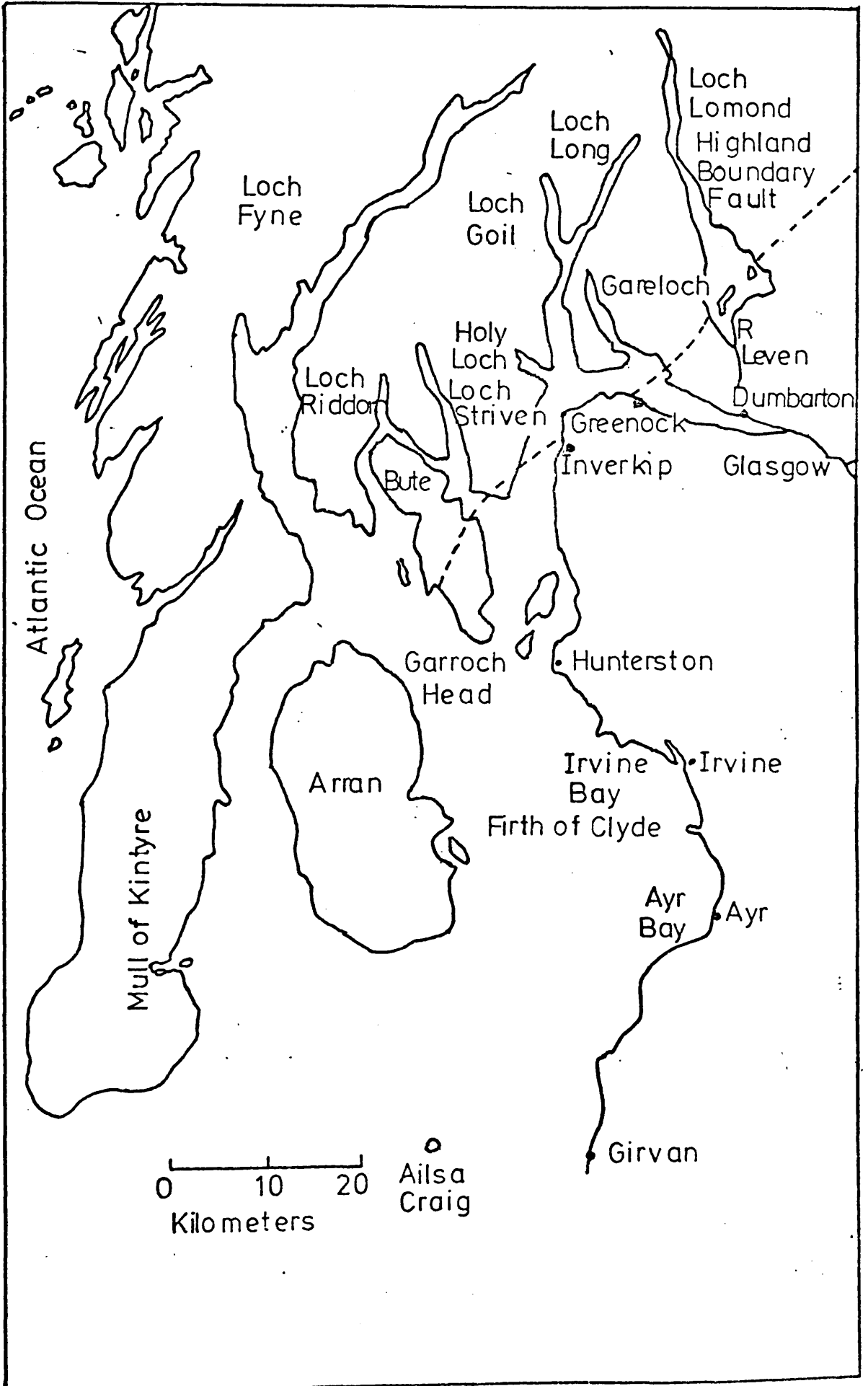


TABLE 1                      PHYSICAL DIMENSIONS OF THE  
CLYDE SEA AREA

Section	Coastline (km)	Area (km <sup>2</sup> )	Volume (km <sup>3</sup> )
Total Clyde Sea Area		2,500.0*	165.0**
Estuary	170.0	69.0	0.9
Inner Firth		185.0	7.8
Gareloch	33.0	20.5	0.21
Loch Long	57.0	36.2	1.3
Loch Goil		9.0	0.31
Holy Loch	11.0	4.9	0.07
Loch Striven	33.0	15.0	0.5
Loch Riddon/ Kyles of Bute	67.0	44.5	1.27
Loch Fyne	183.0	210.0	13.3

\* Natural Environment Research Council, 1974

\*\* Cambray et al., 1975.

All other information from Clyde River Purification  
Board baseline data; Leatherland, 1976.

(around half the population of Scotland). The firth is the main shipping channel into western Scotland, serving in part the industrial and commercial needs of the region, and in addition, together with the sea-lochs, constitutes one of the major recreational areas of the country. The region also supports a very valuable commercial fishing industry, the main catches being herring, white fish, shell-fish and salmon.

Since the initial work of Mill (1892) the Clyde Sea Area has been the subject of considerable interdisciplinary scientific investigation. Information from these studies has been collected and presented in review form in a report by the Clyde Study Group (Natural Environment Research Council [N.E.R.C.], 1974) which in addition to summarising existing knowledge identified areas where future research effort might be most advantageously concentrated. Some of the basic information from this report and other sources is presented in table 2.

### Geological Setting

The Clyde Sea Area cuts across the Highland Boundary Fault, a major dislocation in the earth's crust which forms a natural boundary between the Scottish Highlands and the Midland Valley. Rocks belonging to the three main divisions, igneous, metamorphic and sedimentary, occur in the region. Ancient, resistant, metamorphic rocks are confined to the north of the Fault and form part of the great Dalradian sequence which occurs throughout the south-west Highlands. These rocks, which have a thin peaty soil covering, are predominantly composed of quartzose micaschists with subordinate grits, slates, quartzites and limestones (Johnstone et al., 1966). In contrast, thick sequences of younger, more easily eroded

TABLE 2

## SOME MAJOR POLLUTANT INPUTS TO THE CLYDE SEA AREA

\*Sewage:

Section	Estimated input ( $\text{m}^3 \text{ day}^{-1}$ )
Upper Estuary	$10^6$
Lower Estuary	$0.045 \times 10^6$
Firth	$0.059 \times 10^6$

\*\*Metals:

Metal	Input from River Clyde ( $\text{tonnes y}^{-1}$ )	Sewage sludge deposits ( $\text{tonnes y}^{-1}$ )	Input from Irish Sea ( $\text{tonnes y}^{-1}$ )	Freshwater input from run off ( $\text{tonnes y}^{-1}$ )	Input by rainwater ( $\text{tonnes y}^{-1}$ )
Cu	10.0	25.0	43.0	10.0	50.0
Zn	45.0	60.0	270.0	50.0	250.0
Cd	0.4	0.25	4.0	0.6	1.7
Pb	20.0	25.0	8.0	35.0	60.0

\* Natural Environment Research Council, 1974

\*\* Cambray et al, 1975

sedimentary rocks are confined mainly to the area south east of the Highland Boundary Fault (i.e. the Midland Valley). These rocks are composed in the main of Upper Palaeozoic Lavas, Upper and Lower Old Red Sandstone and Carboniferous sequences; thick coal seams are present and surface covering is of peat, sand, gravel moraines and boulder clay (MacGregor and MacGregor, 1948). Intrusive igneous rocks (e.g. granite and appinite) occur as outcrops in parts of the Highland region.

During the Pleistocene, the Clyde Sea Area was covered by an extensive ice sheet, and the present bathymetry of the region is largely a result of the differing response of the various rock-types to the erosive action of the retreating glaciers.

#### Drainage

The Clyde catchment, total area around 8,265 km<sup>2</sup> can be subdivided into three major basins, two of which drain directly into the upper Clyde estuary. The first of these and the largest single catchment is that of the Clyde Basin (2,600 km<sup>2</sup>), which, in addition to the River Clyde itself, draining the plateaux of south and east Lanarkshire, includes two further major tributaries, the Kelvin and the Carts, which drain respectively the Campsie Fells and the Renfrewshire hills. The second major catchment emptying into the Clyde estuary is that of L. Lomond (785 km<sup>2</sup>) which drains a mountainous region to the north and the Campsie Fells and Fintry hills to the east, before discharging into the upper estuary via the R. Leven. The third major catchment is that of Ayrshire which is approximately 2,850 km<sup>2</sup> in area and is drained

by short fast-flowing rivers. The Highlands of Argyll are drained by a large number of short mountain streams and together with direct run-off from the hills, this represents the major freshwater input to the various sea-lochs. (N.E.R.C., 1974).

### Water Circulation

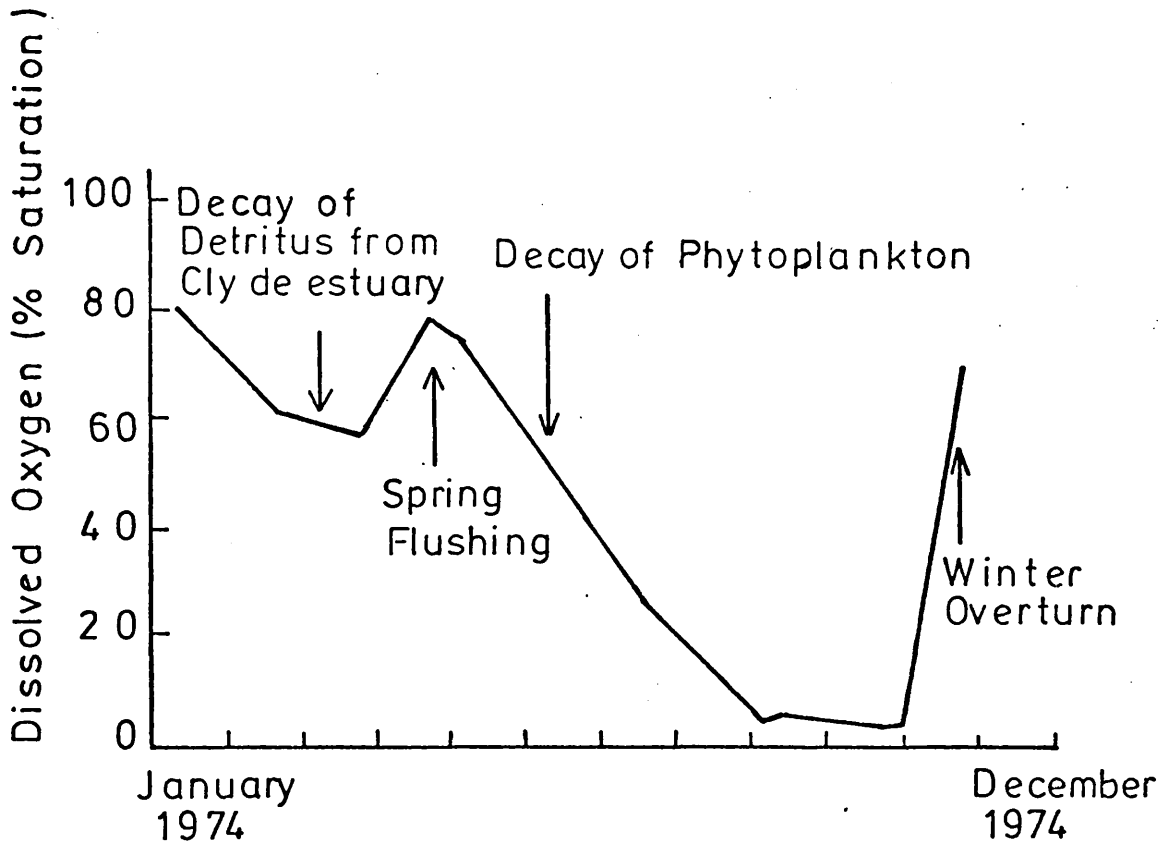
The tidal characteristics of the Clyde Sea Area have been investigated since the mid-1800's and tidal ranges have been shown to be small in comparison to other estuaries of the United Kingdom (Milne, 1974; Collar, 1974). Measurements of salinity and temperature have also been performed for many years. In the firth, horizontal and vertical profiles of temperature and salinity exhibit only very gradual variations, indicating a system which is relatively stable and unlikely to be subject to density induced currents (Johnston et al., 1974). Near-shore water movement is predominantly wind-controlled, while circulation in offshore waters is more complex and depends upon a number of factors including winds, tides and estuarine circulation (Dooley and Steele, 1969; Johnston, 1974; Clyde River Purification Board (C.R.P.B.), 1973). Tidal patterns and water circulation in the upper estuary have been particularly well characterised and hydraulic models of the system have been developed by Thom (1949) and Thomson (1969). Vertical profiles of salinity indicate the estuary to be intermediate in nature between a partly-mixed and a well-mixed system.

Until recently estimates of water residence times in the area had been limited. Mill (1892) and Craig (1959), using salinity and freshwater input data, estimated replacement

times of around nine days and nine months for the waters of Loch Fyne and the Firth of Clyde respectively, while the C.R.P.B. have inferred relatively long residence times for water in some sea-lochs based on monthly surveys of temperature, salinity and dissolved oxygen. In these latter surveys, evidence was obtained for an annual cycle in which large gradients developed in the vertical profiles of these parameters during the summer months (C.R.P.B., 1974a). This was particularly true of dissolved oxygen content in Loch Goil where virtually anoxic conditions have been observed in bottom water in late summer, followed by a rapid increase in oxygen levels in early winter (fig. 6). These results have been interpreted in terms of water stratification during the summer months, with entrainment of bottom water and very little vertical mixing, followed by rapid winter 'overturn'; this phenomenon has been used as evidence of relatively long residence times for water in the sea-lochs. (C.R.P.B., 1974b). However, the definitive studies of MacKenzie (1977) and McKinley (1978), based on the measurement of the radiocaesium isotopes,  $^{134}\text{Cs}$  and  $^{137}\text{Cs}$  in Clyde Sea Area waters, have placed estimates of water renewal times, water mixing processes and water transit times in the area on a much firmer basis.

$^{137}\text{Cs}$  ( $t_{\frac{1}{2}} = 30\text{y}$ ) and  $^{134}\text{Cs}$  ( $t_{\frac{1}{2}} = 2.1\text{y}$ ) are present in the Clyde Sea Area due to their controlled release in waste from the nuclear power and fuel reprocessing plant at Windscale in Cumbria. ( $^{137}\text{Cs}$  is also present in the marine environment as a result of its production in nuclear explosions; however, in the Clyde Sea Area, output from Windscale is by far the dominant source). Caesium isotopes behave essentially conservatively in sea-water and following their discharge from

FIGURE 6 Variation of dissolved oxygen in the  
bottom water of Loch Goil during 1974.  
(Clyde River Purification Board, 1974a)



Windscale, a significant proportion of these isotopes are transported northwards through the North Channel and around the west coast of Scotland. Their 'point-source' release and the halving-time of around 2.2y for the  $^{134}\text{Cs}/^{137}\text{Cs}$  ratio make these isotopes ideal tracers of inshore water movement processes. Moreover, a small proportion of the radiocaesium isotopes passing through the Clyde Sea Area are incorporated into surface sediments and this is of considerable value in sediment studies of the area.

The levels of radiocaesium discharge from Windscale show considerable variation with time and by 'pulse matching' of Windscale output data with observed radiocaesium concentrations in the North Channel and in the Clyde Sea Area, mean water transit times of around 6 months from Windscale to the North Channel and about 2 months from the North Channel to the northern parts of the Clyde Sea Area have been derived (MacKenzie et al., 1978; Baxter et al., 1978). A value of 4.5 months has been obtained for the mean residence time of water in the area based on radiocaesium mass budget calculations. Furthermore, the observation of homogeneous vertical profiles of radiocaesium in the area has shown the system to be rapidly mixed vertically with the exception of Loch Goil and Loch Fyne where radiocaesium profiles indicate the presence of summer stratification resulting in relatively long residence times for deep water (in agreement with the results of the C.R.P.B.) due to the formation of a strong pycnocline. MacKenzie (1977) also determined the concentrations of  $^{226}\text{Ra}$  and  $^{228}\text{Ra}$  in Clyde Sea Area water and, while the rather more complex behaviour of radium isotopes in the area

limited their effective use in water mixing studies, the radium distribution reflects water residence times consistent with those derived from radiocaesium data.

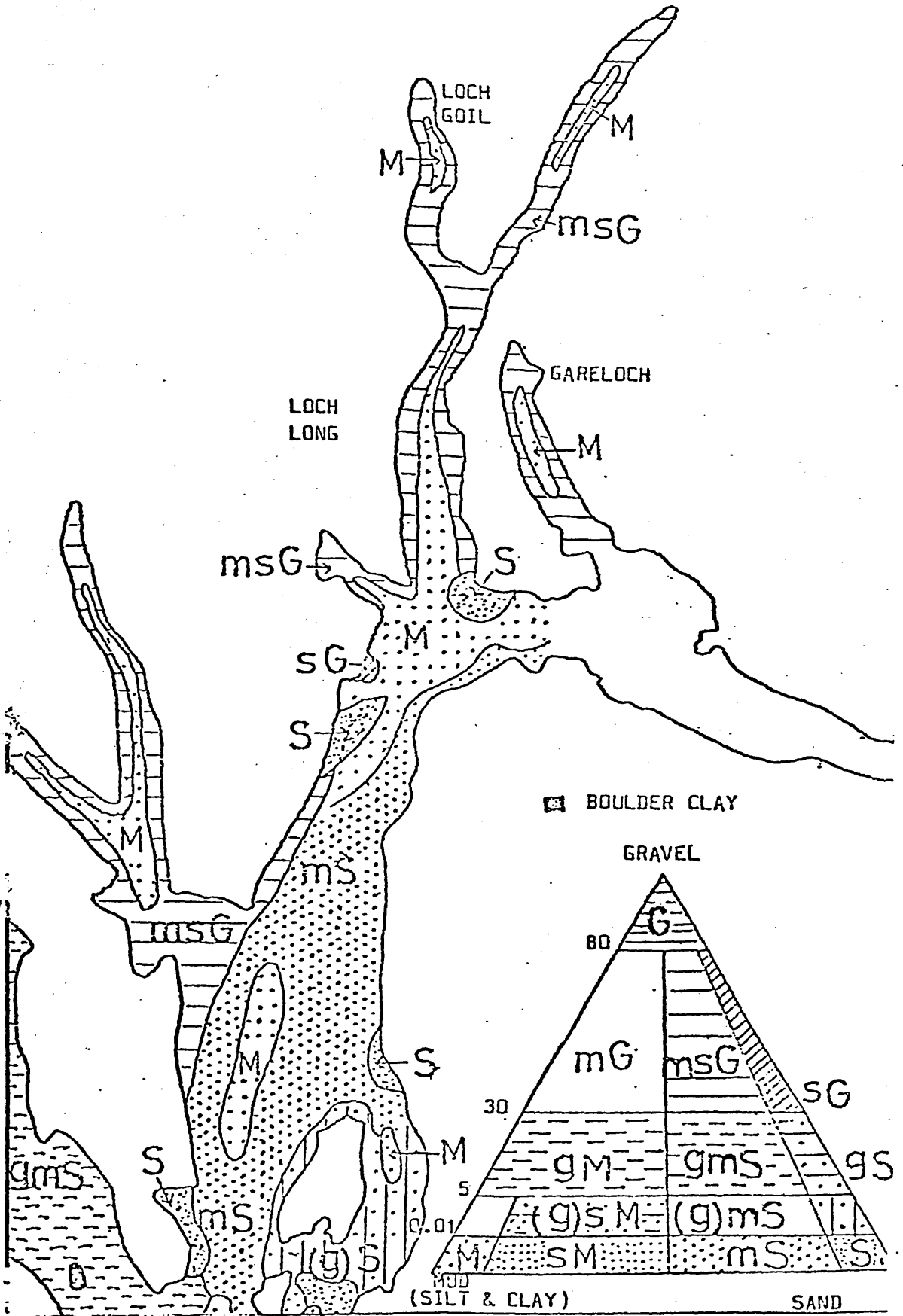
The waters of the Clyde Sea Area can exchange with those of the Atlantic Ocean and the Irish Sea via the North Channel. Radiocaesium measurements have indicated that around 90% of water in the area is of Irish Sea origin, while the Atlantic Ocean contributes around 9% and freshwater 1%. (McKinley, 1978; Baxter et al., 1978). This is consistent with the data of Topping (1974) and Cambray et al (1975) for trace metal input to the Clyde Sea Area which suggested a large Irish Sea contribution.

### Sediments

In a detailed study of the distribution of the superficial sediment deposits of the Clyde Sea Area, Deegan (1973) recognised three major sedimentary facies (coarse littoral, transitional and deep silty-clay), the distribution of which is largely controlled by bathymetry (fig. 7).

The coarse littoral facies (S; (g)S; (g)mS; gms; msG, in fig 7), include clean sands and sediments with a significant gravel fraction (~80% of the material being coarser than 62.5  $\mu\text{m}$ ). Grain size and mineralogy are highly variable and since these facies are normally confined to water depths of less than 40 m their distribution is restricted for the most part to a narrow strip close to shore.

The transitional facies (mS and Sm) bear more resemblance to the deep silty-clay facies than to the coarse littoral facies, the dominant component being a mud which includes variable quantities of sand and shell debris. Areal distribution is again limited, in most parts the coarse



littoral facies tending to merge directly into the deep silty-clay facies.

The deep silty-clay facies (M) is the most abundant and widely distributed sediment in the region, occurring in all the deeper water areas of the firth and in the central deeps of the sea-lochs where it results from infilling of low energy glacially scoured hollows. This sediment is a very fine grained brown to grey mud and lithologically is the most invariant facies in the region, the included sand fraction normally comprising less than 1%.

There is considerable variation in the thickness of surface sediments associated with the three sediment types. While those of the coarse littoral facies vary from zero to a few tens of cms., the surficial sediments of the deep silty-clay facies are much thicker, often merging without any noticeable lithological break into the Flandrian clays which lie beneath large areas of the firth.

The sources of sediments in the area have received very little investigation with the exception of those of the Clyde estuary which have been studied by Gair (1967) and Fleming (1969). The general conclusions from these studies indicated that little or no material is supplied to the estuary from the open waters of the firth and that the majority of sediment entering at the head of the estuary from the Clyde catchment is deposited within the estuary itself. It would seem therefore that new sediment material depositing in the Firth of Clyde is derived from that carried down to the various sea lochs by mountain streams or direct run-off and from rivers draining the Ayrshire Basin, since there is little evidence to suggest that sediment is supplied to the area to any great

extent from the open sea.

Patterns of sediment accumulation in some regions of the Clyde Sea Area have been considerably influenced by man's activities over the last century. This is particularly true of the upper estuary where dredging operations are continuously carried out to keep shipping channels open. The material from this operation, some 300,000 tonnes of sediment per year, is dumped near the mouth of L. Long. The deep water south of Garroch Head (100 m) has been used by Glasgow Corporation for over seventy years as a site for the disposal of sewage and industrial sludge at a present annual rate of around 1M tonnes. As a result of this practice, an area of sediment of some 20 km<sup>2</sup> is now highly contaminated to a depth of 50-60 cm. (Mackay et al., 1972; Halcrow et al., 1973; Baxter and Harkness, 1975).

Information on the rates of sediment accumulation in the area is sparse. Baxter and Harkness (1975) used <sup>14</sup>C/<sup>12</sup>C ratios to derive an 'artificial' sedimentation rate of ~0.75 cm.y<sup>-1</sup> for the Garroch Head dumping ground and a 'natural' sedimentation rate of around 0.3 to 0.6 mm.y<sup>-1</sup> for this and nearby areas. The only other quantitative estimate of sedimentation rates in the region was that of Moore (1931) who made use of sediment traps suspended at various depths in the water column and, in so doing, discovered seasonal fluctuations which were attributed to periodic diatom blooms; delicate banding (attributed to the seasonal diatom bloom) observed in sediment cores from Loch Striven indicated a sedimentation rate of ~0.5 cm.y<sup>-1</sup> for this locale. Indirect evidence for a generally slow rate of sediment accumulation throughout the area is suggested by the widespread distribution of manganese

nodules (Buchanan 1891; Calvert and Price, 1970; Ku and Glasby, 1972). Abundant Fe/Mn is present in the Clyde area (cf. a value of 4.4% for manganese in a nodule free sediment in lower L. Fyne), and manganese oxide minerals have in fact been found in all of the Clyde sea-lochs except the Gareloch, the Holy Loch and Loch Riddon. However, finds have been concentrated along the length of L. Fyne with smaller localised accumulations elsewhere. The scattered occurrence of the nodules in the sea-lochs and in the north-west of the Clyde have prompted Murray and Irvine (1894) and Allen (1960) to suggest that the source of the manganese might be the mountain streams draining Highland rock types. It is interesting to note that some of the nodules exhibit remarkably high concentrations of minor elements, e.g. 1500 ppm of Zn, and 800 ppm of Pb have been recorded (Deegan, 1973).

### Biology

Biologically, the Clyde Sea Area is highly productive and much is known of the occurrence and distribution of both micro- and macro-organisms (references in N.E.R.C., 1974). Long-term studies by the Scottish Marine Biological Association (S.M.B.A.) at Millport have established the periodicity of the planktonic outbreaks in the area. The firth and sea-lochs are subject to an annual spring "outburst" of phytoplankton, the precise time and size of which varies from year to year, secondary and usually smaller blooms occurring throughout the summer months. The benthic fauna, particularly those species inhabiting the sandy and rocky substrates of the Firth of Clyde have been well characterised; in general, however, less is known about the benthic communities living in muddy deposits. The sediments

of the upper estuary and the Garroch Head dumping ground have received detailed investigations by the C.R.P.B. to assess the effects of pollution on the fauna of the mud bottom. Mackay et al (1972) have reported a change from a molluscan/echinoderm community outside the dumping ground to a polychaete community within the dumping zone. In the estuary itself, both the diversity of species and numbers of flora and fauna are relatively restricted because of the effects of pollution.

### Pollution

The major pollution problem in the Clyde Sea Area is organic in nature, organic material being introduced to the system from three main sources:

- (1) the direct discharge of domestic and industrial sewage,
- (2) the dumping of sewage and industrial sludge off Garroch Head, and
- (3) the release of nitrate rich effluent into the Irvine Bay area from industries in Ayrshire (Annual Reports of the C.R.P.B., 1972, 1973, 1974; Mackay and Topping, 1970, Mackay et al., 1972).

Additional sources of organic pollutants are polychlorinated biphenyls and trace organic substances discharged from a variety of industrial sources and oil pollution which is a potentially serious hazard, Finnart on Loch Long serving as a major deep-water oil terminal for 300,000 ton tankers. Non-organic pollutants include toxic heavy metals (lead, copper, zinc, cadmium, mercury) released from industrial concerns. In addition, the area receives thermal pollution from the discharge of heated water from coal and oil-fired power stations. Radioactive materials are released from several sources. The Holy

Loch and Gareloch serve as bases for the American and British nuclear submarine fleets respectively, and radioactive contamination can occur due to accidental or controlled releases (Best, 1970). The Clyde Sea Area also receives radioactive isotopes discharged from the nuclear fuel reprocessing plant at Windscale as outlined previously and from the Hunterston reactors on the Ayrshire coast. Further sources of pollution in the region are contaminants present in rainfall and in Irish Sea water entering the area (Cambray et al., 1975). The most highly polluted area is the upper estuary which receives around  $10^6 \text{ m}^3\text{d}^{-1}$  of sewage, having undergone various degrees of treatment. In addition, the lower estuary receives an estimated  $0.045 \times 10^6 \text{ m}^3\text{d}^{-1}$  of partially treated and untreated sewage. During periods of low fresh water input during the summer the estuary can become anaerobic for a length of some 20 km below the tidal weir in Glasgow. This is a serious problem since it threatens the valuable salmon fisheries of the L. Lomond catchment and the R. Leven. Because of the relatively restricted environment, the ability of some of the sea-lochs to cope with any high degree of pollution, particularly organic, is questionable (C.R.P.B., 1974).

#### Areas of Study

Particular areas of interest in this study have been the sea-lochs, Gareloch and Loch Goil, and background descriptions to these lochs are given below.

Gareloch is 8 km in length and has an average breadth of 1.6 km. It forms an arm of the Clyde Estuary and runs in a north north-west direction. The total surface area of the loch is just under  $11 \text{ km}^2$  about three times smaller than the area of its drainage basin. Along its centre the loch has an average

depth of about 33 m. The entrance to the loch is both shallow (a sill which extends across its mouth has a depth of only 9 m at low water) and narrow (a sandyspits extends from the eastern shore narrowing the entrance to less than 0.3 km). The loch is shown in vertical profile in fig. 8. Although no major freshwater input occurs at the head of the loch, many large burns discharge directly along both banks. The major source of sediments is likely to be input of particulates carried in from the Clyde Estuary. Waters are well-mixed throughout the year and as a result are well oxygenated.

Loch Goil forms a north-west trending fork which branches roughly halfway to the head of Long Long. The loch is 8 km in length and has an average breadth of about 1.2 km. Its surface area is  $8.5 \text{ km}^2$ , roughly ten times less than the area of its catchment. The entrance to the loch is relatively narrow ( $\sim 0.6 \text{ km}$ ) and is protected by a shallow sill of depth just under 13 m. The loch in vertical profile is shown in fig. 9. A deep basin of  $>80$  metres depth is situated roughly three-quarters of the way to the loch-head. The major fresh-water inputs are those from the River Goil and Lettermay Burn which enter at the head of the loch. However, numerous fast flowing streams descend the steep slopes of the surrounding hills to discharge in several places along both shores. Such river run-off from the catchment is almost certainly the chief source of sediment since, as indicated previously relatively little sediment appears to be supplied to the northern areas of the Clyde Sea Area from marine sources. The waters of the loch become stratified during summer and, as a result, bottom waters are depleted in oxygen by autumn.

FIGURE 8

Gareloch : lateral sections and section along axis of greatest depth.

Horizontal scale 1:50,000; vertical exaggeration X 25 (Based on

Admiralty Chart 2000, Hall 1973)

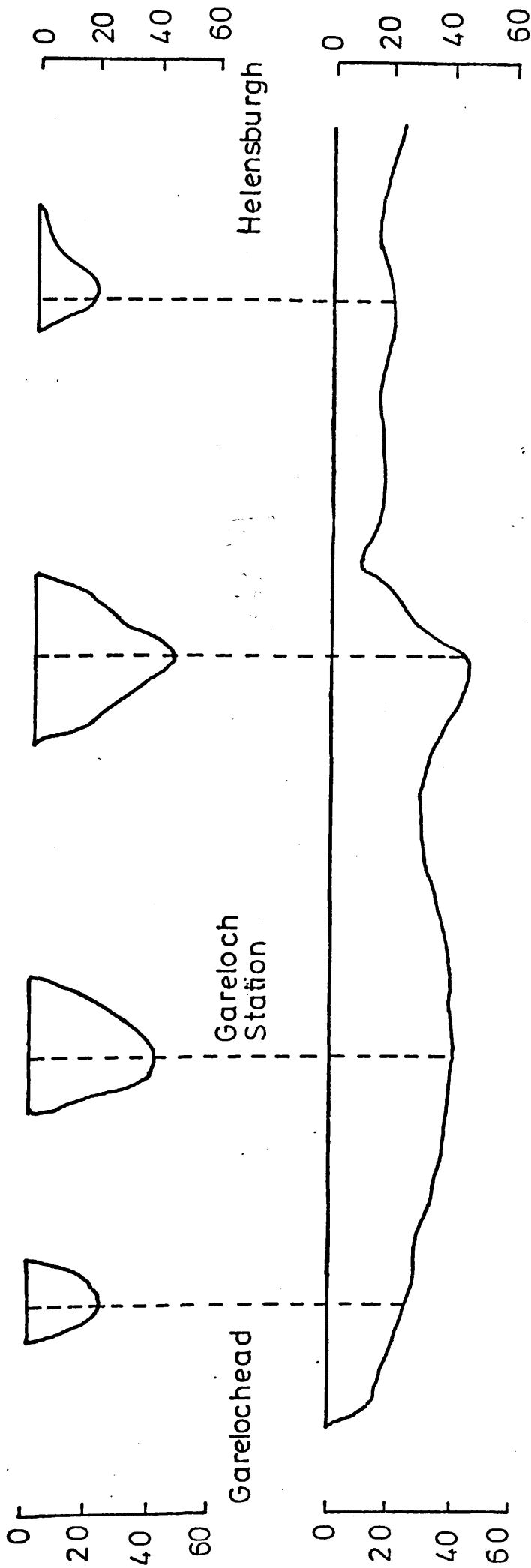
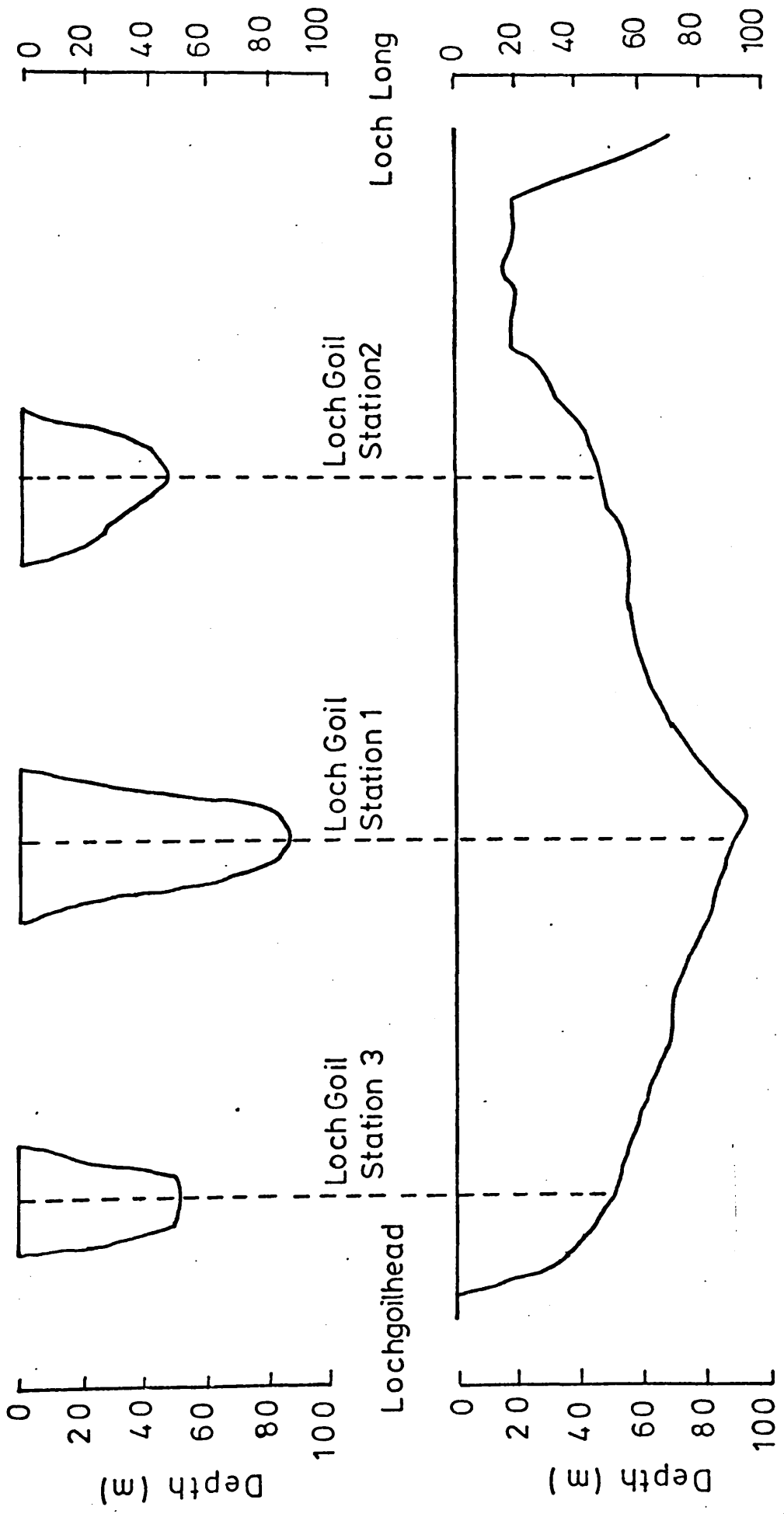


FIGURE 9  
Loch Goil: Lateral sections and section along axis of greatest depth.  
Horizontal scale 1: 50,000; vertical exaggeration X 25 (Based on  
Admiralty Chart 3746, Haslam 1975).



### Loch Lomond

Geographically and geologically Loch Lomond (fig. 5) can be regarded as a modern day freshwater extension of the Clyde Sea Area. The loch is the largest in the United Kingdom and runs north-south between latitudes  $55^{\circ}57'$  and  $56^{\circ}16'$  in the counties of Dumbarton and Stirling. It stands at a height of only 8 m above present day sea-level. Like the Clyde Sea Area, Loch Lomond cuts across the Highland Boundary Fault. The loch can be conveniently divided into two distinct halves, each of which exhibit very different topographies. To the north, at a point not far from the line of the Highland Boundary Fault, the loch closely resembles the fjord-like sea-lochs of the Clyde Sea Area, being long, narrow, deep and steep-sided and is tightly enclosed by high mountains. Here the bedrock is predominantly of mica-schist and schistose grit. To the south, the loch is shallow and wide and the bedrock is largely of Old Red Sandstone and Carboniferous sandstones, marls and basalts. The narrow fjord-like northern region is characterised by very few islands while in the south a series of large densely wooded islands extends across the basin (Tippett, 1974; Dickson, 1978). The physical dimensions of Loch Lomond are presented in table 3. The drainage area of Loch Lomond is around ten times as extensive as the water surface, the most important single source of water flowing into the loch being the Falloch Water which drains the rugged land of the Highland zone and enters at the northern tip. The major river input in the south is the Endrick Water which, after draining a large catchment including much of the Kilpatrick Hills and the Campsie Fells, flows into the south east corner. Although the area of land drained by the Falloch Water is about half of that drained by the Endrick,

TABLE 3PHYSICAL DIMENSIONS OF LOCH LOMOND

	<u>TOTAL SURFACE AREA</u>	<u>TOTAL CATCHMENT</u>
	72 km <sup>2</sup>	684 km <sup>2</sup>
	<u>NORTHERN REGION</u>	<u>SOUTHERN REGION</u>
Length	18 km	11 km
Max. Width	1.5 km	7 km
Max. Depth	200 m	18 m

the former supplies more than 75% of the freshwater input to the loch due to the much greater rainfall in the mountainous Highland region. A number of smaller rivers drain into the loch on its western shores. The entire outflow from Loch Lomond is at Balloch in the south-west where the R. Leven flows 9 km through the Vale of Leven to enter the Clyde Estuary at Dumbarton (Tippett, 1974).

L. Lomond was formed by glacial erosion during the ice-ages of the Pleistocene and emerged in its present form at the end of the L. Lomond readvance which, on the basis of  $^{14}\text{C}$  dates from Late-glacial marine shells in Loch Lomond, occurred between 11,700 - 10,500  $^{14}\text{C}$  years B.P. (Sissons, 1966, 1967). The Late-glacial period was characterised by very large fluctuations in sea-level and there is considerable evidence (in the form of marine clayey silts, shoreline land forms and the presence of marine plankton and absence of freshwater plants at depth in sediments) to suggest that during periods of relatively high sea-level, Loch Lomond was in fact a sea-loch, having a direct connection with the Firth of Clyde (McDonald, 1974; Dickson et al., 1978). One such marine incursion, when sea-level reached a maximum elevation of  $\sim 33$  m.O.D. is believed to have occurred around 12,500  $^{14}\text{C}$  years B.P. (just prior to the L. Lomond readvance), when the southern part of the loch was ice-free. During the L. Lomond readvance, the Loch Lomond glacier extended as far south as Alexandria in the Vale of Leven where a moraine ridge was formed which acted as a temporary barrier between the loch and the Clyde estuary; in so doing, this ridge controlled both the level of the freshwater loch and the extent to which sea-level was required to rise in order that salt-water could re-enter the basin. Recent studies of deep-

water cores from the southern basin of Loch Lomond have produced evidence that the loch did in fact experience a more recent marine incursion which  $^{14}\text{C}$  dating has shown to have lasted some 1450 years from 6900 to 5450 B.P. (Dickson et al., 1978).

Loch Lomond is a warm monomictic lake. During the summer, the south basin of the loch (with a maximum water depth of <20 m) remains well-mixed; however, from June to October, the deep northern basin is thermally stratified, three distinct layers of water developing with little or no vertical mixing. The surface layer extending to a depth of about 20 m is effectively heated by the sun and well-mixed by wind and current action, while the bulk of the underlying water remains unheated throughout the summer. In late autumn, the thermocline breaks down due to cooling of surface waters and thorough mixing of water follows (Tippett, 1974).

Biologically, the loch is not considered highly productive, although the area is subject to a spring plankton bloom. By far the greater proportion of nutrients are delivered to the loch by the Endrick Water which enters in the south after flowing over soft rocks and rich, well-fertilised farmland; hence the water is relatively rich in dissolved mineral nutrients and thus the southern basin is the least oligotrophic region. On the other hand, the Falloch Water and other streams and rivers draining the Highland zone flow over poor agricultural land and hard resistant rocks with the result that relatively few minerals are brought to the loch. In addition, large areas of the northern region of the south basin are devoid of any significant covering of surficial sediments suggesting either low detrital input or deposition in the region, or active re-erosion (Stewart, 1977, personal communication). Benthic flora and fauna are

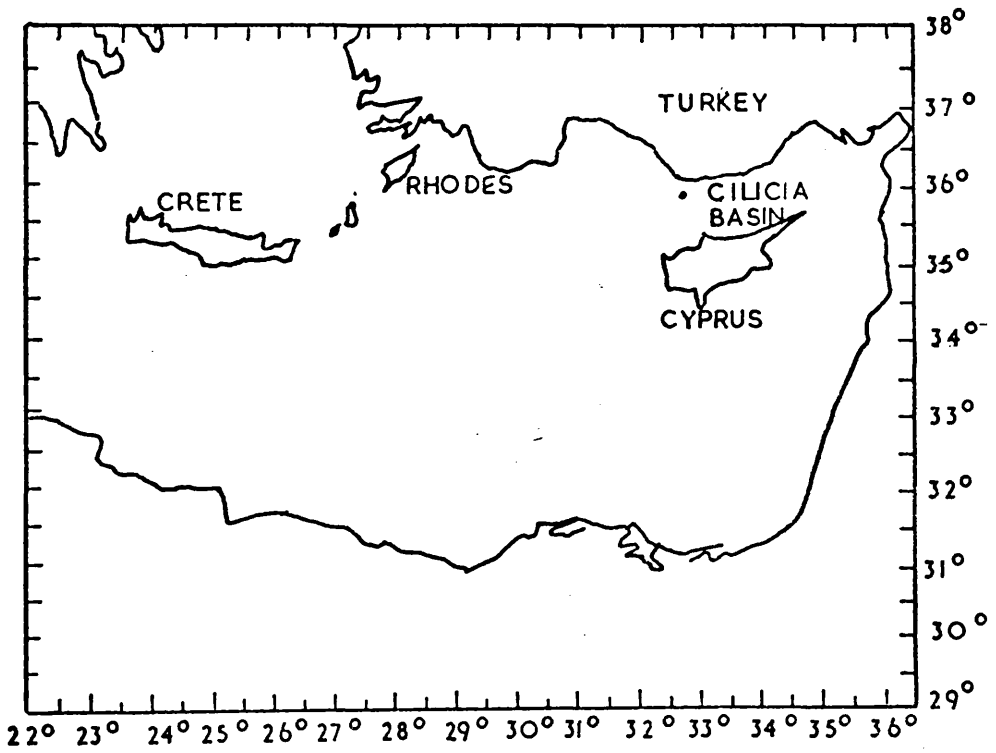
poorly represented even in the more productive area of the south and indeed are almost non-existent in the deeper northern region of the loch. Little biological reworking of the sediment is therefore to be expected. The loch supports a variety of fish, including the commercially valuable salmon and sea-trout, migratory fish, which use Loch Lomond and its associated rivers and streams as breeding grounds.

### Cilicia Basin (Eastern Mediterranean)

The Cilicia Basin is a deep marine basin (maximum depth 1500 m) which lies between Cyprus and the southern coast of Turkey in the north eastern Mediterranean (fig 10 ). The southern Turkish coastal area from the mainland opposite Rhodes in the west to the Syrian border in the east is a highly mountainous region with a coastline dominated by cliffs. Along the length of the coast the mountains are drained both by numerous long perennial rivers which stretch far inland and have extensive catchments, and by many shorter seasonal rivers which flow in winter and spring when rainfall is relatively heavy (70 - 150 cms. per year). The large perennial rivers discharge massive quantities of detrital material to the coast and further appreciable amounts of sediment are thought to derive from material transported by the short seasonal rivers draining the Turkish and Cypriot coasts and from windborne dust (silt and clays) blown during the summer from the arid lands bordering the eastern Mediterranean. While large quantities of this material are thought to deposit on the narrow inner shelf slopes, a significant fraction is believed transported to the adjacent deeper waters of the basin between Turkey and Cyprus (Evans, 1971).

During the last few years the sediments of the basin have been intensively investigated by the Geology Department of Imperial College London, who hope to construct a general model of sedimentation for such a basin adjacent to a high mountainous landmass from which a large burden of detrital sediment is derived. While preliminary investigations of the nature and distribution of the sediments in the basin and along the south Turkish coast have been completed (Shaw, 1978; Shaw and Bush, 1978), one

FIGURE 10    The Cilicia Basin, Eastern Mediterranean



outstanding problem which remains concerns the patterns and rates of sediment accumulation in the area, about which nothing quantitative is known.

#### 1.4 Aims of Research

This research involves a preliminary investigation of the patterns and rates of recent sediment accumulation in the northern region of the Clyde Sea Area by the  $^{210}\text{Pb}$  dating technique. The study forms part of a continuing research programme, the ultimate objectives of which are to gain insight into geochemical, sedimentation and water-mixing processes in the area, and to evaluate the impact of anthropogenic effects on the system.

The main aims of the project were therefore; to perform an initial survey of the distribution of  $^{210}\text{Pb}$  within the sediments of the area and to evaluate the applicability of  $^{210}\text{Pb}$  as a dating tool in this marine environment; to evaluate alternative experimental procedures for  $^{210}\text{Pb}$  assay and develop and apply the most appropriate method; to estimate rates of sediment accumulation and derive depth/time scales with which to examine both natural sedimentary processes and changes in sediment composition arising from anthropogenic factors.

During the project an opportunity arose to study a core from the nearby freshwater loch, Loch Lomond, for which, as for the Clyde Sea Area, little information is available on modern rates of sediment accumulation. A core from the south coast of Turkey was also examined to evaluate the potential of  $^{210}\text{Pb}$  in studies of sedimentation in this environment.

This specific project, specific to  $^{210}\text{Pb}$  dating and geochemistry in each area, was not performed in isolation but in parallel with complementary studies of other species in sediments and waters. Thus the overall objective involved assessment of  $^{210}\text{Pb}$  data in conjunction with additional results, obtained by collaborators, on other relevant parameters, such as palaeomagnetism, heavy metals and artificial radionuclides.

## CHAPTER 2

### EXPERIMENTAL

#### 2.1 Introduction: General outline of experimental investigations

This chapter is largely concerned with detailed descriptions of the techniques of sample collection and handling, and of radiochemical analysis developed in this and complementary studies for the  $^{238}\text{U}$  decay series nuclides,  $^{210}\text{Pb}$  and  $^{226}\text{Ra}$ , and for the artificial radiocaesium isotopes  $^{134}\text{Cs}$  and  $^{137}\text{Cs}$ , the radionuclides of principal interest in this work.

Sediment samples have been collected by a variety of coring methods, viz by a small diameter gravity corer, and by Craib and Mackereth corers, the latter two samplers being specifically designed to recover undisturbed cores of surface sediment. A description of the design and operation of these corers is presented in the following section.

Radiochemical analyses of the radionuclides indicated above are performed on measured aliquots of totally dissolved sediment samples. Complete dissolution of sediment is achieved by successive digestion with a variety of concentrated acids, intermediate leaching with hot 6N HCl dissolving around 99% of original material.

$^{210}\text{Pb}$  assay is by  $\alpha$ -spectrometric determination of its  $\alpha$ -emitting grand-daughter  $^{210}\text{Po}$  ( $\alpha$ ,  $t_{1/2}=138.4\text{d}$ ;  $E_{\alpha}=5.305\text{MeV}$ ), initially assumed and subsequently shown to be in secular equilibrium with its parent  $^{210}\text{Pb}$  in the sediment.  $^{208}\text{Po}$  ( $\alpha$ ,  $t_{1/2}=2.93\text{y}$ ;  $E_{\alpha}=5.11\text{MeV}$ ) spike is added to the sample prior to

dissolution and acts as chemical yield tracer for the analytical procedure. Polonium isotopes are spontaneously deposited on to silver discs from a dilute solution of HCl, providing a thin source suitable for high resolution  $\alpha$ -spectrometry.

$^{226}\text{Ra}$  analysis is performed indirectly by determination of the activity of its radioactive rare gas daughter  $^{222}\text{Rn}$  ( $\alpha$ ,  $t_{1/2} = 3.825\text{d}$ ;  $E_{\alpha} = 5.49\text{MeV}$ ), isolated from a further known volume of the sample solution assayed for  $^{210}\text{Pb}$ . Radioactivity measurement of the collected gas is by gas-phase  $\alpha$ -scintillation counting using ZnS(Ag) phosphor coated detector chambers, coupled to a photomultiplier tube and scaler.

Radiocaesium analysis was initially performed on the remaining fraction of the completely dissolved sample by passing the acid solution through the inorganic ion exchanger K.C.F.C. (potassium hexacyano cobalt (II) ferrate (II)), when caesium exchanges quantitatively for potassium. Radioactivity determination was by  $\gamma$ -spectroscopy of the exchanged resin using a 3 inch NaI(Tl) scintillation counter. The main decay modes of  $^{134}\text{Cs}$  and  $^{137}\text{Cs}$  are presented in table 4. In the latter stages of the study, caesium isotope assay has been performed using a 100cc GeLi detector by direct counting of a known weight of dried/homogenised sediment prior to dissolution and subsequent  $^{210}\text{Pb}$  and  $^{226}\text{Ra}$  analyses as outlined above.

A flow diagram of the above separation scheme is shown in fig 11. Typical  $\alpha$  and  $\gamma$  spectra are shown in figs 12 and 13 respectively.

Trace metal analyses are performed by atomic absorption spectrophotometry using an IL151 single beam spectrometer, incorporating a hydrogen lamp for background correction.

In the latter stages of the study, cores have been X-ray photographed prior to analysis to identify stratigraphic

TABLE 4 Partial decay schemes for  $^{134}\text{Cs}$  and  $^{137}\text{Cs}$  (Lederer et al, 1967) showing the  $\gamma$ -rays diagnostic of the radiocaesium isotopes.

$$\frac{^{137}\text{Cs}(t_{1/2}=30.0\text{y}) + ^{137\text{m}}\text{Ba}(t_{1/2}=2.55\text{min})}{}$$

<u>DECAY MODE</u>	<u>ENERGY (MeV)</u>	<u>INTENSITY (%)</u>
$\beta^-$	0.514	93.5
$\beta^-$	1.176	6.5
$\gamma$	0.6616	93.5

$$\frac{^{134}\text{Cs}(t_{1/2}=2.05\text{y})}{}$$

<u>DECAY MODE</u>	<u>ENERGY (MeV)</u>	<u>INTENSITY (%)</u>
$\beta^-$	0.662	71.0
$\beta^-$	0.089	38.0
$\gamma$	0.5692	14.0
$\gamma$	0.6046	98.0
$\gamma$	0.7958	88.0

FIGURE 11 Flow diagram of radioanalytical separations

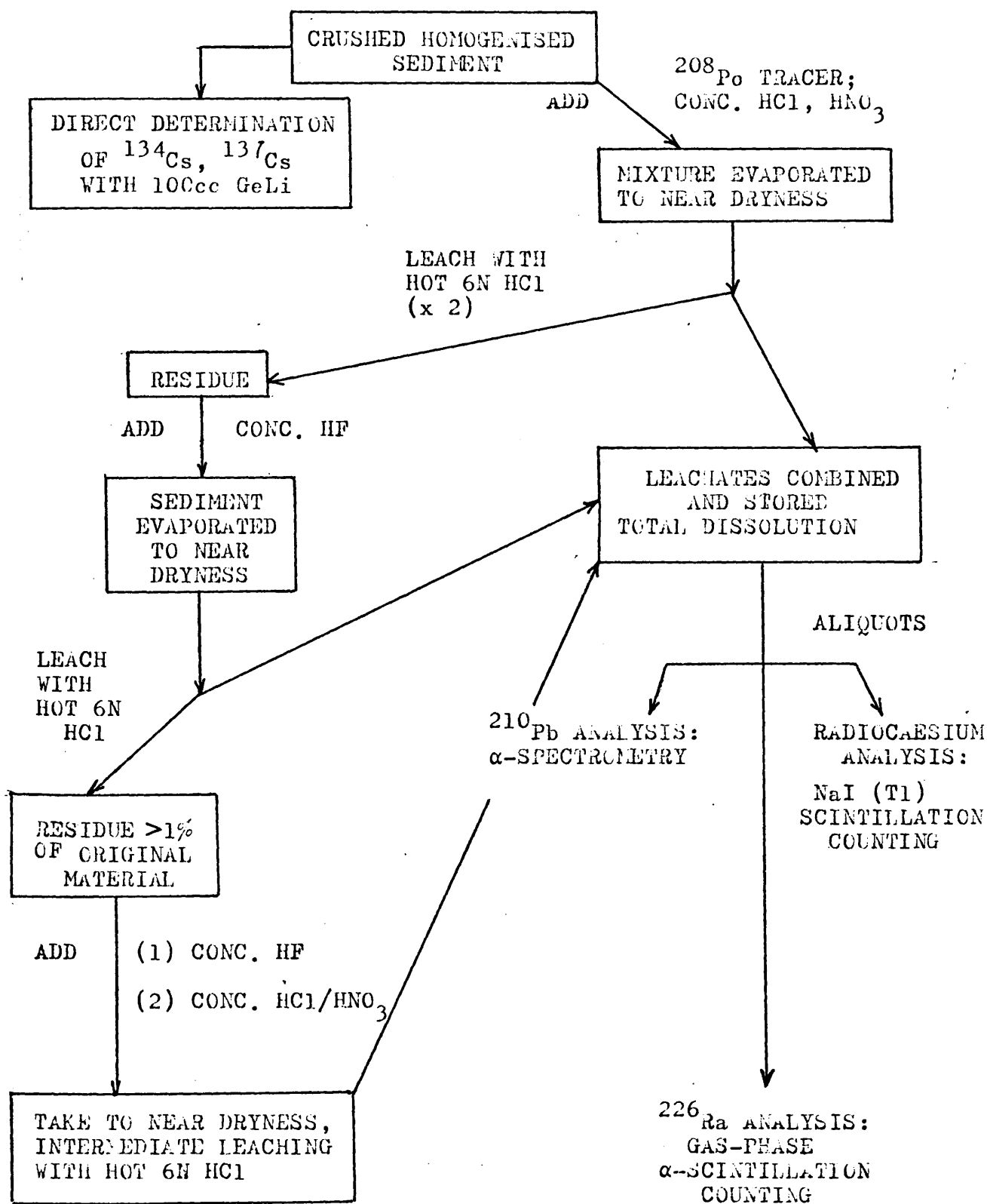


FIGURE 12

Typical  $\alpha$ -spectrum

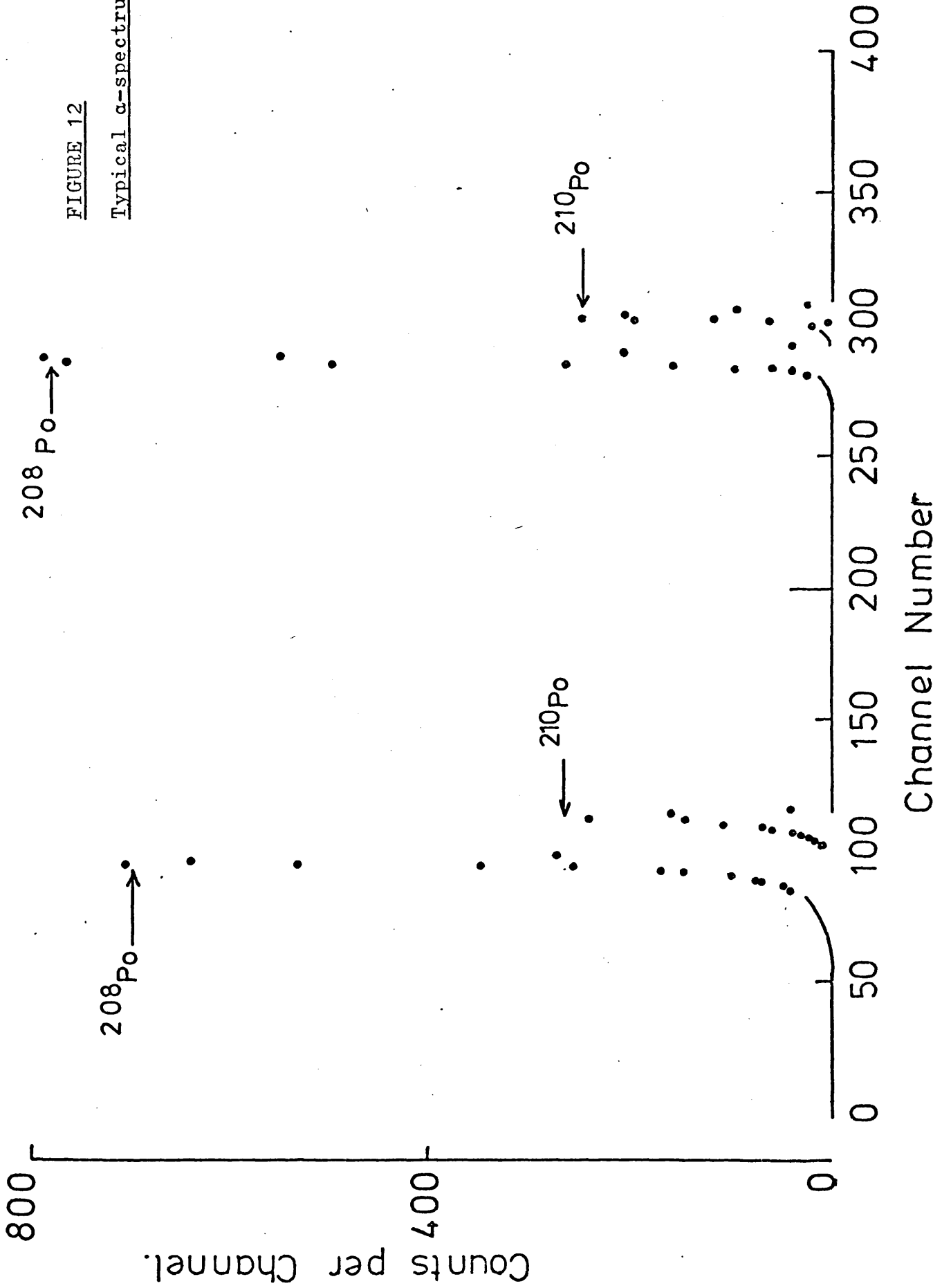
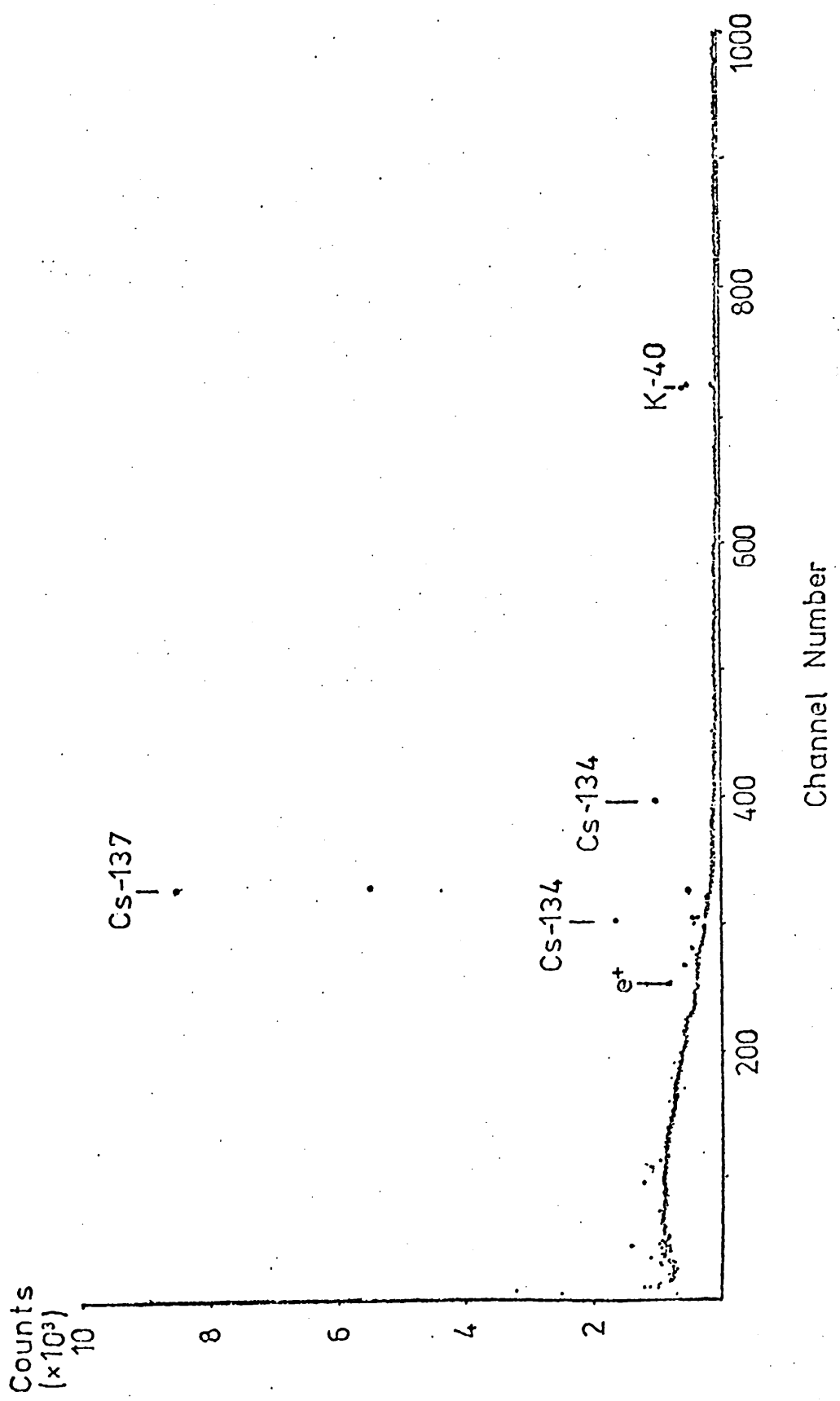


FIGURE 13      Typical  $\gamma$ -spectrum



discontinuities and/or bioturbative disturbance in the samples. A standard medical diagnostic X-ray unit operating at its peak voltage of 95kV and a tube current of 40mA is used, with exposure times of around 10 seconds.

To give an indication of the overall composition of the sediments, subsidiary analyses are performed for  $\text{CaCO}_3$  and C, H and N (performed routinely as a departmental service on a Perkin-Elmer 240 analyser.). Particle density, particle size distribution and clay mineral analyses have been effected on a small number of key samples; brief descriptions of the methods used for particle size and clay mineral analyses are presented in appendix 1. Palaeomagnetic measurements are available for the Loch Lomond core.

All reagents used in the radioanalytical and chemical procedures outlined above are wherever possible of Analar grade. The following decontamination procedure is applied to chemical apparatus between analyses. The apparatus is first rinsed with 6N HCl, scrubbed in a strong solution of Pyroneg and left to steep for a minimum of 24 hours in a 5% solution of Decon 90. The apparatus is further rinsed with 6N HCl and distilled water.

Due to the known tendency of polonium and bismuth isotopes to adsorb on to container walls, the following special precautions are adopted to ensure decontamination of glass/teflon apparatus used in  $^{210}\text{Pb}$  analysis. The apparatus is boiled in 8N  $\text{HNO}_3$  to which 20mg of bismuth (as  $\text{Bi}(\text{NO}_3)_2$ ) has been added, reboiled in 8N  $\text{HNO}_3$  and finally rinsed with 6N HCl and distilled water.

## 2.2 Sample collection and handling

Of major importance in the investigation of patterns and rates of recent sediment accumulation is the recovery of cores of undisturbed sediment in which, preferably, the flocculent surface layer of the deposit is retained. In addition, the core should be representative of the area under study.

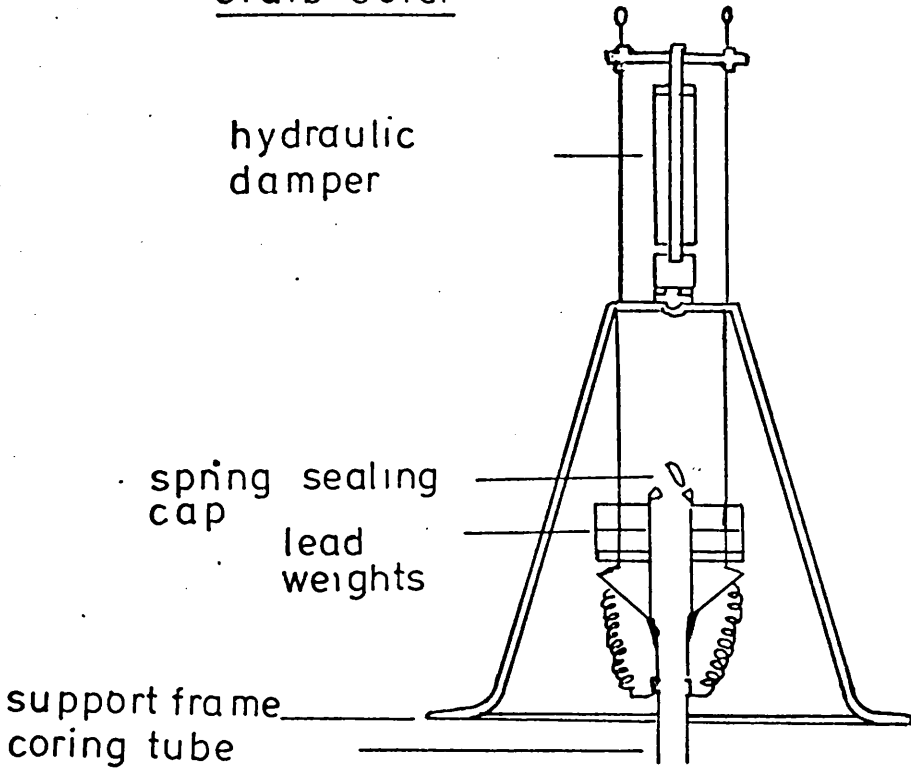
Ideally, the sampling site would be visually examined by divers or underwater photographic equipment both before and during the sampling operation. This would help minimise to a large extent the element of uncertainty which arises when samples are obtained 'blind'. Unfortunately, such facilities are not yet commonly available and could not be obtained during this study. However, the majority of cores examined in this work were collected by coring methods specifically designed to recover sediment samples which are stratigraphically undisturbed.

### Clyde Sea Area Sediments

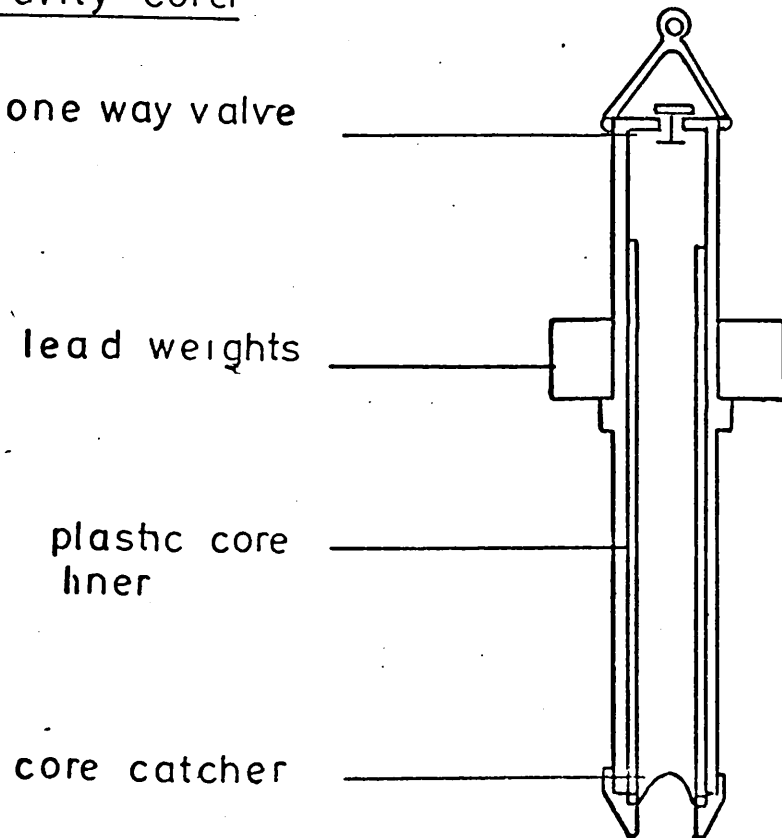
Bottom sampling of Clyde Sea Area sediments is performed by gravity and Craib corers operated from the survey vessel 'ENDRICK II' of the Clyde River Purification Board.

Gravity cores are collected using a conventional small-diameter sampler, the design of which is shown in fig. 14. It consists essentially of a metal barrel enclosing an exchangeable plastic liner. A dome-shaped core catcher consisting of a number of flexible metal fingers is positioned at the base of the plastic liner, above the cutting edge of the barrel. This unit is bolted on to the upper weighted assembly, attached to a winch. In operation, the corer is lowered to within a few metres of the sea floor where it is released and allowed to free-fall to be driven into the sediment by the heavy lead weights. The valve at the top of the barrel opens as the corer descends,

Craib Corer



Gravity Corer



allowing escape of water. Sediment enters the barrel through the fingers of the core-catcher, opened upon contact with the topmost layers of the deposit. On withdrawal from the sediment, the one-way valve closes and the fingers of the core retainer shut, preventing disturbance to and loss of sediment as the corer returns to the surface. Aboard ship, the barrel is released and maintained upright while the plastic liner enclosing the sediment is removed vertically from the tube. A core barrel of length 90cm is used to collect cores of diameter 6cm and length up to 80cm.

The disadvantage of this coring method lies in its tendency to physically disturb or lose the uppermost layers of sediment (which are relatively unconsolidated, containing about 90% water by volume), due to a combination of the pressure wave which travels in front of the barrel and the force of impact. Some disturbance to or loss of sediment was therefore expected using this device.

Recovery of undisturbed surface sediment, considered essential for this work, is achieved with the Craib corer, which is specifically designed to retain intact the light superficial layer of sediment (Craib, 1965).

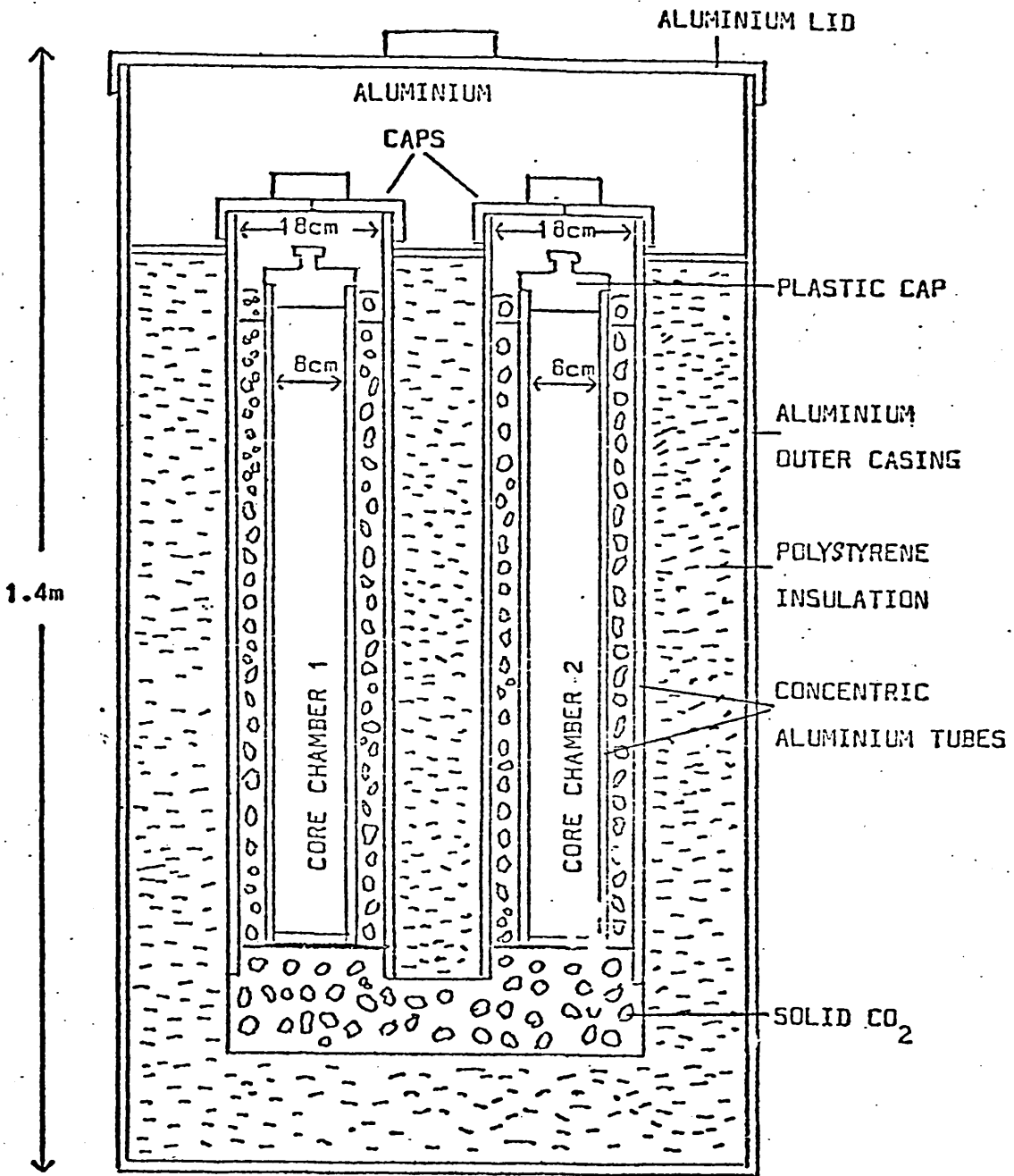
The construction of the Craib corer is shown in fig. 14. This sampler incorporates a hydraulic damper to ensure a slow approach and penetration of the sediment. In operation, the base frame is soft-landed on the sea bed, the impact being sufficient to release the weighted corer assembly which sinks at a slow speed predetermined by the rate at which water can escape from the hydraulic damper. As the corer is withdrawn from the sediment, operation of an automatic ball-closing device results in insertion of a rubber ball into the mouth of the coring tube, thus ensuring retention of the sample. Closure of

the hinged sealing cover prevents disturbance of the sediment as the sampler is returned to the surface. On deck, the closing ball is replaced by a similar ball and the coring tube, containing the sample, withdrawn downwards from the housing. The instrument recovers cores of 5.7cm diameter and in practice up to 18cm in length.

Since Craib cores are relatively short, a 'continuous' undisturbed profile of sediment from depth to the sediment/sea water interface can in theory be obtained by collecting gravity and Craib cores at each station and matching the lower end of the Craib core to the upper end of the gravity core.

On deck, gravity and Craib cores are carefully inspected for any visible signs of physical disturbance. If the water overlying the sediment is at all cloudy (due to the presence of suspended particulates) the core is rejected. If the overlying water is clear, and in the case of gravity cores, there is no indication of channelling between core-liner and sediment (this sometimes occurs due to the tearing action of the sharp fingers of the core retainer as sediment enters the barrel), the samples are accepted as undisturbed and the following steps taken to prevent subsequent disturbance of the sediment during transport to the laboratory.

After noting the length of each core, the supernatant water is removed by syringe, taking care not to suspend and withdraw fines. Cores are then quick-frozen in a deep freeze or placed directly into a specially designed freezer-transporter unit (using solid  $\text{CO}_2$  as refrigerant) for return to the laboratory. The construction of the chest for gravity cores is shown in fig 15; that for Craib cores is identical in form, but with a capacity for 6 cores. In the laboratory, cores are stored frozen in a deep-freeze prior to analysis.

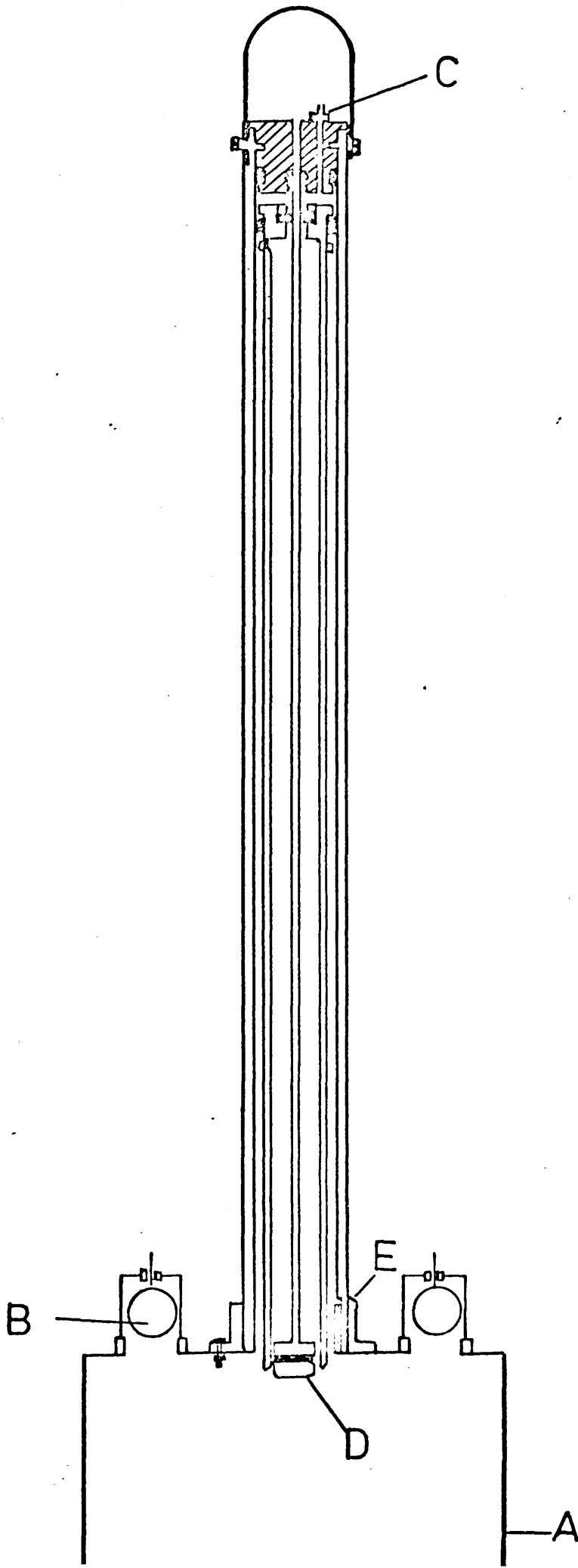


### Loch Lomond Sediment

The core from Loch Lomond was collected using a pneumatically driven mini-Mackereth corer (Mackereth, 1969), designed to collect undisturbed sediment samples. The main features of the corer are shown in fig 16. The core was one of a series recovered by Dr. R. Thompson of the Department of Geophysics, University of Edinburgh, and was received as 1cm thick sections of 'wet' sediment.

In operation, the apparatus is lowered until the base of the 'anchor' chamber (A) comes into contact with the sediment. As the anchor chamber sinks into the sediment, the 4 ball valves (B - 2 shown) lift, allowing water to escape freely from the chamber. With the anchor chamber at rest, embedded in the sediment, the ball valves close, preventing water from re-entering. Compressed air is then fed through the tube C, the resultant pressure driving the moving piston and coring tube downwards into the deposit, until the lower end of the piston is stopped by a flange on the upper plate of the anchor chamber. Meanwhile, the stationary inner piston D, ensures entry of sediment into the tube due to the external hydrostatic pressure. When the driving piston passes the point E, the compressed air flows into the anchor chamber, lifting the ball valves (which releases the anchor chamber), and escapes. The apparatus is then raised to the water surface by pulling on the attached line.

The core, retained in the plastic liner, is held vertically for return to the laboratory, where it is hydraulically extruded and cut into 1cm thick sections. A 1 metre perspex tube of internal diameter 5.40cms collected a sample of length 96cms.



### Eastern Mediterranean Sea Sediment

The core from the Eastern Mediterranean was collected from the coast of southern Turkey by conventional small-diameter (5.3cm) gravity corer, similar in design and operation to that used for the recovery of Clyde Sea Area cores. The sample was one of a series obtained during the summers of 1972 and 1974 by Drs. Evans, Shaw and Bush, all of the Department of Geology, Imperial College of Science and Technology, London, during cruises with the N.E.R.C. research vessel R.R.S. Shackleton. After sampling the core was stored at approximately 4°C prior to extrusion and cutting into 1cm thick sections. Samples were obtained as dry sediment in labelled polythene containers.

## 2.3 Sample Preparation and Subsidiary Analyses

### Sample Preparation

Clyde Sea Area cores are stored frozen in the laboratory. After X-radiography the cores are sliced into 1cm thick sections with a band-saw. In the case of gravity cores, the sediment is cut while frozen inside the plastic liner. In contrast, as Craib core liners are an integral part of the sampler and are therefore reused, it is necessary in their case, to extrude the sediment from the liner before sectioning. The tubes are wrapped in a double layer of polythene and completely immersed in boiled water for sufficient time to cause partial thawing of the outermost edge of the sediment; after withdrawal from the water, the polythene covering is removed and the sediment extruded by means of a snugly fitting piston lubricated with silicone grease.

Sediment sections are weighed wet, and oven-dried at 90°C to constant weight (24 to 48 hours). Material for analysis is selectively removed from the central portions of sections to prevent possible contamination of sediment from different depths, due to frictional smearing of the deposit along the core tube as the liner penetrates the sediment.

### Subsidiary Analyses

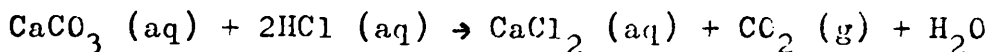
#### Trace Metal Analysis

Elemental analysis is performed by Dr. J.G. Farmer, Department of Forensic Medicine, University of Glasgow, according to the following procedure. A known weight (ca 0.5g) of sediment is sub-sampled from each section of the original ground homogenised core material. Chemical leaching is based on the method of Presley et al (1972), and involves an initial leach with a solution of 25% glacial acetic acid, 0.25M in  $\text{OHNH}_2\text{-HCl}$ , which

is found to extract around 95% of anthropogenically derived metals. The leachate, centrifuged and acidified with 5mls  $\text{HNO}_3$ , is heated slowly to dryness and redissolved in 100mls of 1M HCl, prior to determination of elemental concentrations by atomic absorption spectrophotometry using an IL151 spectrometer. Replicate analyses indicate an overall analytical precision of 5% ( $\pm 1\sigma$  error) on the measurement.

#### Calcium Carbonate Analysis

Calcium carbonate analysis is performed according to Ku's (1966) modification of Turekian's (1956) method for acid-soluble alkaline earths. About 0.1g of dried sediment, determined to 0.0001g, is weighed into a 50ml beaker. 5 mls of 0.5M acetic acid is added and the mixture evaporated to dryness on a hotplate. After cooling, 20 drops of 0.5N acetic acid and 10mls of distilled water are added and the solution filtered into a 100ml wide-necked conical flask, washing with distilled water. The solution is made up to 50mls with distilled water. 5mls of  $\text{NH}_4\text{Cl}$  buffer (pH 10) and 2mls of 2% KCN masking agent are added along with 10 drops of eriochrome Black-T indicator. The solution is titrated with 0.01M EDTA standard to a deep blue colour. The end point is a change from wine red to deep blue. The indicator is a coloured dye which has the property of forming a soluble complex with calcium ions - the resultant colour of which is distinctly different from the dye itself. The calcium ion - dye complex (wine red) is less stable than the calcium ion - EDTA complex. On addition of EDTA, the EDTA combines with calcium ions to form a 6 co-ordinated colourless complex, and the dye is released to its free form imparting a blue colour to the solution. Equations for the reactions are



Replicate analyses on homogenised sediment indicate a 1  $\sigma$  replicate error of  $\pm 1.6\%$  on the measurement.

#### Particle Density Determination

The particle density of a sediment sample is determined by water volume displacement of a known mass of sediment material, as described by Blake (1965). About 25g of sediment (weighed to 0.0001g) are added to a preweighed volumetric flask (50ml). The volumetric flask, and contents, are weighed and the flask half-filled with distilled water, taking care to wash down any sediment adhering to the inside of the neck. Entrapped air is removed by gentle heating of the water for a few minutes, with shaking. The flask and contents are cooled to room temperature and the mixture made up to the mark with boiled, cooled distilled water at room temperature. The flask, including stopper, is weighed and the temperature of the contents determined. The sediment is removed and the flask filled to the mark with boiled, cooled, distilled water at the same temperature as before. The flask and contents are weighed. Care is taken before each measurement to ensure that the outside of the flask is thoroughly clean and dry and the calibration mark on the flask is checked before and after each analysis by repeated weighings with distilled water.

The particle density is calculated as follows,

$$D_p = \frac{d_w (W_s - W_a)}{(W_s - W_a) - (W_{sw} - W_w)} \quad \text{where,}$$

$d_w$  = density of water in  $\text{g cm}^{-3}$  at temperature observed.

$W_s$  = weight in g of volumetric flask plus sediment sample.

$W_a$  = weight in g of volumetric flask filled with air.

$W_{sw}$  = weight in g of volumetric flask filled with sediment and water, and

$W_w$  = weight in g of volumetric flask filled with water at temperature observed.

## 2.4 Sample Dissolution and Radiochemical Analyses

### Sample Dissolution

In selecting an analytical separation route for  $^{210}\text{Pb}$  and  $^{226}\text{Ra}$  it is first necessary to decide whether (1) to dissolve the sample completely, releasing all  $^{210}\text{Pb}$  and  $^{226}\text{Ra}$  present in the sediment or (2) to leach the sediment sample and thereby dissolve only a fraction of the total  $^{210}\text{Pb}$  and  $^{226}\text{Ra}$ .

Exploratory tests with sediment samples from Clyde sea-lochs indicated that while 100% of caesium isotopes are solubilised after repeated boiling with 6N HCl (MacKenzie, 1977), around 10% of  $^{210}\text{Pb}$  and  $^{226}\text{Ra}$  activities remain in the residue following an acid leach process (table 5). These results are not unexpected since all caesium and most  $^{210}\text{Pb}$  present in the sediment are likely to exist as species surface adsorbed to clay minerals or hydrous oxides or be associated with organic phases; radionuclides bound in this fashion should chemically be relatively labile and therefore more readily susceptible to attack with 6N HCl. The residual  $^{210}\text{Pb}$  fraction is almost certainly that held within the lattice matrix of the minerals present in the sediment, and would therefore be more resistant to chemical attack. Similar reasoning applies to  $^{226}\text{Ra}$ , although in this case the labile  $^{226}\text{Ra}$  fraction is probably associated with siliceous organic remains; the  $^{226}\text{Ra}$  which is chemically resistant will again be that fraction held as an intrinsic part of the mineral matrix due to inclusion of natural decay series nuclides. Moreover, that fraction of  $^{210}\text{Pb}$  which derives from decay of  $^{226}\text{Ra}$  (and intermediate nuclides) contained within the lattice matrix is, in all probability, held in sites which are comparatively more acid-labile than those occupied by parent ( $^{226}\text{Ra}$ ) atoms; an acid leach process could therefore adversely affect results

TABLE 5  $^{210}\text{Pb}$ ,  $^{226}\text{Ra}$  and  $^{137}\text{Cs}$  concentrations in fractional dissolution of sediment from Loch Goil core L.G.C.1. (8.4.75). ( $^{226}\text{Ra}$  and  $^{137}\text{Cs}$  data after MacKenzie, 1977).

LEACH	$^{210}\text{Pb}$ CONTENT (dpm)	$^{226}\text{Ra}$ CONTENT (dpm)	$^{137}\text{Cs}$ CONTENT (dpm)
Post hot 6N HCl	11.3	9.0	87
Post conc HCl/HNO <sub>3</sub> digestion	0.5	0.5	
Post HF digestion	0.6	0.3	0
Post HClO <sub>4</sub> digestion <sup>4</sup>	0.4	0.2	0

at depth in the sediment where  $^{210}\text{Pb}$  is in secular equilibrium with  $^{226}\text{Ra}$ .

Two main factors resulted in the adoption of total dissolution as the more appropriate technique for the present study, (a) Preliminary experiments established the relatively low magnitude of excess  $^{210}\text{Pb}$  in Clyde sediment (approximately 6dpm/g at the sediment-water interface).

(b) In addition these early analyses indicated an unusually high and variant concentration of  $^{226}\text{Ra}$  in a core from Loch Goil. Concentrations of  $^{226}\text{Ra}$  in coastal sediments are normally around 1-4dpm/g and remain relatively constant with depth. In contrast, this station exhibited a  $^{226}\text{Ra}$  profile which decreased by a factor of 5 in the upper 10cm of the deposit.

An acid leach process, by introducing an additional uncertainty into the analytical results through possible variability in  $^{210}\text{Pb}$  and  $^{226}\text{Ra}$  extraction efficiencies, is considered unacceptable in view of these results, and of the obvious need for accurate and absolute concentration data.

The size of sample removed for dissolution depends upon the expected  $^{210}\text{Pb}$  activity but, wherever possible, 5 to 10g of homogenised sediment are weighed to better than 0.0001g in a 250ml teflon beaker. The sediment is moistened with a few drops of distilled water and an appropriate amount of  $^{208}\text{Po}$  tracer (an activity equivalent to at least twice that of  $^{210}\text{Po}$  expected in the sample) added by Eppendorf pipette. 50mls each of conc.  $\text{HNO}_3$  and conc.  $\text{HCl}$  are added slowly, and the mixture warmed gently on a hotplate; care is required to prevent loss of material through effervescence. When foaming has ceased, the mixture is heated more strongly and taken to near dryness (this ensures as far as possible equilibration of tracer and sample isotopes on

which all spike methods depend). Evaporation of the sample to dryness is carefully avoided since loss of polonium isotopes, as the highly volatile tetrachloride can occur when dry samples are heated above 150°C (Smith et al, 1955; Eakins and Morrison, 1977). The residue is leached with 80mls 6N HCl for 2 hours at 80°C, the cool solution filtered and the leachate stored in a 500ml stoppering flask. After oven-drying at 90°C the sediment is transferred to the original teflon beaker, and releached as above. Leachates are combined and the oven-dried sediment again returned to the original teflon beaker.

To effect dissolution of the silicates which remain the residue is evaporated to small volume with 2 x 25ml portions of conc. HF (40% w/v), leaching with hot 6N HCl after each digestion. If the residual solid comprises greater than 1% by weight of the original sample, it is again transferred to the teflon beaker and digested with further 25ml quantities of conc. HF, conc. HCl/HNO<sub>3</sub>, with intermediate leachings with 6N HCl. This process is continued to total dissolution (ca. 1% by weight of starting material undissolved). The residue, a very fine black powder, resembles coal-dust and comprises ca. 60% by weight of carbon.

The total combined leachates (350 to 400mls) are made up to volume and measured aliquots assayed for <sup>210</sup>Pb, <sup>226</sup>Ra and radiocaesium isotopes.

#### <sup>210</sup>Pb Analysis

Direct measurement of the very weak β-particle emitted by <sup>210</sup>Pb ( $E_{\max} = 0.061\text{MeV}$ ) has been performed by internal gas counting (Kulp, 1953) but the sophisticated techniques required render it difficult and time-consuming. More recent direct determinations

of the isotope were achieved by Gojkovic et al (1963) and Gaggeler et al (1976) by detection of the emission of a  $\gamma$ -ray of energy 46.52 KeV. However, consideration of the  $\gamma$ - $\beta$  branching ratio (4.1%) and the half-life of the isotope (22.26y) excludes  $\gamma$ -counting in most cases. As a result, it has become standard practice to evaluate the concentration of  $^{210}\text{Pb}$  indirectly by detection of either its  $\beta$ -emitting daughter  $^{210}\text{Bi}$  ( $E_{\text{max}} = 1.16\text{MeV}$ ) or its  $\alpha$ -emitting grand-daughter  $^{210}\text{Po}$ .

Determination of  $^{210}\text{Pb}$  activity by  $^{210}\text{Bi}$  (Rama et al, 1962; Krishnaswami et al, 1971; Koide et al, 1972; Petit, 1974) involves isolation of the nuclide by anion exchange, precipitation as sulphate or chromate, and subsequent measurement of the growth of its daughter  $^{210}\text{Bi}$  ( $t_{1/2}=5.01$  days) to secular equilibrium by low-level  $\beta$ -counting over a period of some 30 to 40 days, according to the relationship,

$$A_D = A_0(1 - e^{-\lambda_D t}), \quad \text{EQTN. 9.}$$

where,  $A_D$  = the activity of the daughter nuclide at time  $t$

$A_0$  = the activity of the parent nuclide at  $t = 0$ ,

and  $\lambda_D$  = the decay constant of the daughter nuclide.

Chemical yield is determined gravimetrically.

Disadvantages of the method include (a) the relatively long counting time required, (b) the possible presence of indistinguishable  $\beta$ -emitting contaminants in the source and (c) susceptibility to impurities in the lead salt resulting in erroneous chemical yield calculation.

On the other hand, indirect measurement of  $^{210}\text{Pb}$  activity by  $\alpha$ -spectrometric determination of  $^{210}\text{Po}$  has several distinct advantages:-

- 1)  $\alpha$ -spectrometry is inherently a more sensitive and more specific technique -  $\alpha$ -emission is monoenergetic, each nuclide having its own characteristic  $\alpha$ -energy (ies) (whereas

$\beta$ -emission involves continuous energy spectra); multi-channel pulse height analysis therefore gives unambiguous identification of  $^{210}\text{Po}$ . In addition, modern surface barrier detectors have relatively high detection efficiencies and very low backgrounds.

- 2)  $^{208}\text{Po}$  spike can be used as an internal yield tracer.
- 3) The deposited source can be counted immediately.
- 4) Chemical separation of polonium is a relatively straightforward and convenient process.

Furthermore, although the dating technique generally involves the assumption of secular equilibrium between  $^{210}\text{Po}$  and  $^{210}\text{Pb}$  within the sediment, if the original plating solution contains lead as well as polonium, a second plating after a period of a few months deposits  $^{210}\text{Po}$  which has grown in from its grand-parent. Thus the above assumption can either be verified or the degree of equilibrium which existed between  $^{210}\text{Po}$  and  $^{210}\text{Pb}$  in the sample evaluated.

The analytical method on which this work is based is that of Flynn (1968) who reviewed existing methods for the determination of low levels of  $^{210}\text{Po}$  in environmental materials and concluded that the most effective technique was the deposition of polonium on to silver from weakly acidic solution. Polonium will undergo chemical deposition on a number of other less noble metals (eg Cu, Ni), but contamination to a varying degree with RaE ( $^{210}\text{Bi}$ ) and/or RaD ( $^{210}\text{Pb}$ ) often occurs. (Bagnall, 1957; NAS, pub NS3037 - 1961).

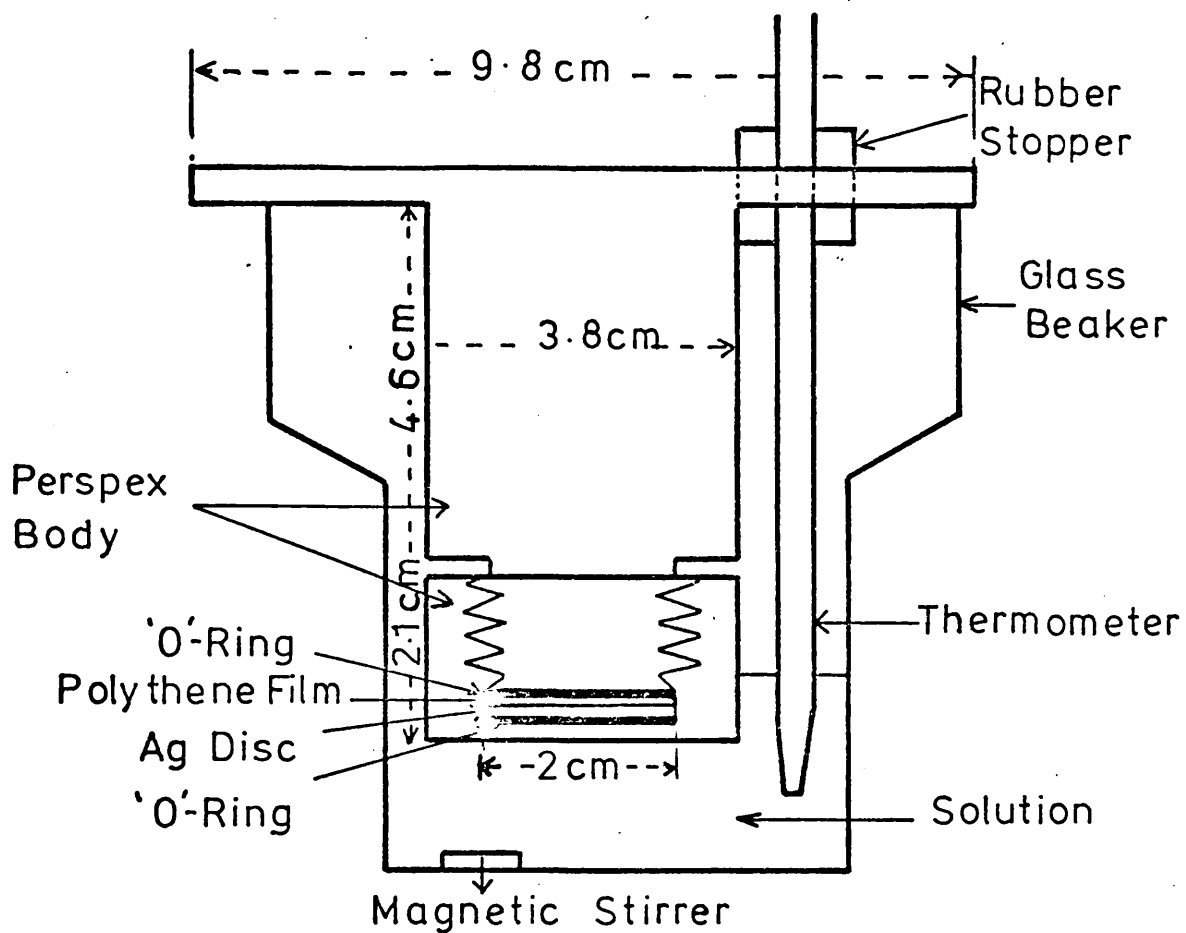
An aliquot of the dissolved sample in a teflon beaker is evaporated on a hotplate to a volume of ca. 30mls. After transfer, together with several hot 6N HCl washings, to a glass plating vessel, the volume of solution is further reduced by

heating, to ca. 10mls, and the walls of the glass beaker rinsed with 6N HCl. In preliminary experiments, 5mls of 30% w/v hydroxylamine hydrochloride were added to the sample (this reduces any  $\text{Fe}^{3+}$ ,  $\text{Cr}^{6+}$  or other oxidants which, if present, would interfere with deposition) along with 2mls of 25% sodium citrate and 10mg of bismuth hold-back carrier (to prevent co-deposition of bismuth on silver) as described by Flynn (1968). Subsequent analyses, however, showed that inclusion of sodium citrate in the plating medium appeared to have no advantageous effect on chemical yield and  $\beta$ -counting of deposited sources on a low background gas-flow ICN Tracerlab Geiger counter showed no  $\beta$ -activity compatible with the 5.01 day half-life of  $^{210}\text{Bi}$ . Consequently, the addition of sodium citrate and bismuth prior to deposition was discontinued. Addition of conc.  $\text{NH}_3$  raises the pH of the solution to 2 and the solution is heated at 85° to 90°C for 1 hour (the beaker is covered with a watch glass to prevent excessive evaporation) with stirring (magnetic paddle). Formation of a fawn gelatinous precipitate often occurs at this point. (Precipitation at this relatively low pH probably occurs as a result of the very high ionic strength of the medium - ca. 5g of sediment dissolved in <50mls of weakly acidic solution. Formation of a similar precipitate during whole rock and sediment analysis has been observed by others (Blauer, 1976; Murray, 1976; personal communications); the precipitate may be a mixture of hydroxides of Si and Al). If a precipitate forms, the solution is filtered, the sample returned to the plating vessel and re-heated to 85° to 90°C for 30 minutes. The volume of the final solution is maintained below 50mls, elevated temperature and low solution volume favouring efficient deposition.

Plating is performed in cells of the design shown in fig 17. The perspex holder restricts polonium deposition to one side of the 1" diameter silver discs (a diameter of 2cms of silver is exposed to solution), maximising counting sensitivity and at the same time minimising evaporative loss during plating. The holder with silver disc (rinsed and degreased with distilled water and chloroform before insertion) is placed in the solution. Air bubbles, occasionally trapped beneath the silver disc, are periodically removed by manipulation of the plating cell/beaker assembly. Plating is continued for 4 hours at 85° to 90°C with stirring (to maximise plating efficiency), following which the silver disc is removed from the holder, rinsed with distilled water and chloroform and left to air-dry prior to  $\alpha$ -spectrometric determination of the deposited polonium activity. Sill and Olson (1970) have indicated the possibility of detector contamination due to a 'pseudo' recoil effect of polonium, attributed to its own inherent volatility. While less marked for polonium deposited on silver, this spontaneous volatility tends to decrease with time possibly due to formation of a relatively involatile surface oxide. Silver discs are normally left overnight before counting and, while some increase in detector background has been observed during the study, this may have been reduced by the above procedure.

After counting, the overall efficiency (combined chemical yield and detection efficiency) for  $^{210}\text{Po}$  is corrected for via the observed count rate from the known activity of  $^{208}\text{Po}$  spike initially added, and the concentration of  $^{210}\text{Po}$  ( $^{210}\text{Pb}$ ) in the sediment then evaluated. The mean chemical yield using the above analytical procedure is 85% (although yields have ranged between 50% and 100%). The  $^{208}\text{Po}$  tracer used in the study was calibrated against a  $^{210}\text{Pb}$  standard, (obtained from J.D. Eakins,

FIGURE 17 Polonium Plating Cell



Harwell), which had  $^{210}\text{Po}$  in secular equilibrium with its grandparent. The  $^{210}\text{Pb}$  standard had a quoted activity of  $20.7 \pm 0.4$  dpm/ml (1 $\sigma$  error) on 10/11/75. Both solutions are stored in plastic containers to prevent adsorption of polonium and bismuth which can occur on glass vessels (Flynn, 1968) and tracer calibration is checked periodically during the project.

Silver discs are used many times, the surface deposit of polonium being readily removed by etching with conc.  $\text{HNO}_3$  and rubbing vigorously with fine emery paper. Sadauskis (1958, 1960) has demonstrated that the nature of the surface upon which source material is deposited significantly influences the resultant resolution. With this in mind, the silver disc, free of contamination, is polished (Swansdown mop/rouge) to a mirror finish surface suitable for subsequent high resolution  $\alpha$ -source preparation.

To check the validity of the assumption of secular equilibrium between  $^{210}\text{Po}$  and  $^{210}\text{Pb}$  in the sediment, several solutions, originally exhaustively stripped of polonium isotopes by successive plating with three silver discs (the last silver disc normally shows no  $\alpha$ -activity above background) have been reanalysed after varying periods of time. These solutions, following initial plating, are transferred with 6N HCl and 8N  $\text{HNO}_3$  washings to plastic containers, respiked with  $^{208}\text{Po}$  and after the addition of 20mg of hold-back carrier, stored to allow growth of  $^{210}\text{Po}$  from  $^{210}\text{Pb}$ . Prior to plating, the solutions are evaporated to near dryness with 2 x 25ml portions of conc. HCl to remove nitric acid which can interfere with polonium deposition. Results are given in table 6. Agreement between analyses is good within 1 $\sigma$  counting statistics for all samples except (2), which is consistent within a 2 $\sigma$  counting error, confirming that there is

TABLE 6 Reanalysis of  $^{210}\text{Pb}$  in solutions originally exhaustively stripped of polonium isotopes and stored to allow regrowth of  $^{210}\text{Po}$ .

SAMPLE	ORIGINAL DETERMINATION (dpm/g $\pm 1 \sigma$ COUNT)	REPEAT DETERMINATION (dpm/g $\pm 1 \sigma$ COUNT)
GLC3:14	6.53 $\pm$ 0.20	6.37 $\pm$ 0.16
LGC2: 3	11.85 $\pm$ 0.46	13.12 $\pm$ 0.33
LGC2: 6	11.39 $\pm$ 0.44	11.35 $\pm$ 0.28
LGC2: 8	11.68 $\pm$ 0.31	11.40 $\pm$ 0.29
LGC2:10	8.93 $\pm$ 0.29	9.27 $\pm$ 0.23
GLG1: 3	6.65 $\pm$ 0.32	6.59 $\pm$ 0.16
GLG1: 7	4.88 $\pm$ 0.23	4.72 $\pm$ 0.12
GLG1:20	2.18 $\pm$ 0.07	2.17 $\pm$ 0.05
L.LOM:2	19.64 $\pm$ 0.37	20.16 $\pm$ 0.50
L.LOM:3	14.25 $\pm$ 0.30	14.52 $\pm$ 0.36

apparently no increased mobility of polonium relative to lead in the sediment and that initial plating of  $^{210}\text{Po}$  can be used as an indicator of  $^{210}\text{Pb}$  concentration.

In addition, the results of repeat analysis on fresh aliquots of several solutions stored in glass containers following total dissolution are presented in table 7. The typical chemical yields observed indicate that no significant adsorption of polonium isotopes on to glass from solutions of this acid strength (6N) has occurred. Agreement between repeat measurements is again good.

In analytical procedures of this kind a major threat to accuracy/reproducibility of analyses is the introduction of radioactive contamination. In  $^{210}\text{Pb}$  analysis such contamination could arise from 2 distinct sources.

- (1) imperfectly cleaned silver discs.
- (2) contaminated reagents or glass/teflon apparatus.

Experiments are regularly performed to assess the magnitude of the contribution from these sources as follows,

- (1) Decontaminated silver discs are counted before reuse. 'Blanks' have been found to be essentially identical to backgrounds observed for the two Ortec surface barrier detectors used in the study. Table 8.
- (2) Blank determinations for  $^{210}\text{Po}$  and  $^{208}\text{Po}$  are performed on apparatus which has been used in many cycles of sample analyses. To blank solutions consisting of 6N HCl and Fe, Al and Bi carrier, aliquots of  $^{208}\text{Po}$  and  $^{210}\text{Po}$  tracer are added alternately and the blanks treated alongside sediment samples with the same quantities

TABLE 7 Repeat determination of  $^{210}\text{Pb}$  in samples (6N in HCl), stored in glass containers for prolonged periods.

<u>Sample</u>	<u>Original Determination</u> (dpm/g $\pm$ 1 $\sigma$ count)	<u>Repeat Determination</u> (dpm/g $\pm$ 1 $\sigma$ count)	<u>Storage Period</u> (months)	<u>Chemical Yield (%)</u>
GLC3:14	6.53 $\pm$ 0.20	6.64 $\pm$ 0.16	11	78
GLG1: 3	6.65 $\pm$ 0.32	6.73 $\pm$ 0.17	15	75
GLG1: 5	5.59 $\pm$ 0.22	5.68 $\pm$ 0.14	11	82
GLG1:7	4.88 $\pm$ 0.23	4.66 $\pm$ 0.12	13	83
GLG1:11	3.31 $\pm$ 0.15	3.28 $\pm$ 0.08	11	61
GLG1:20	2.18 $\pm$ 0.07	2.18 $\pm$ 0.05	12	86

TABLE 8    Detector Backgrounds

<u>Detector</u>	<u>Start of project</u>		<u>End of project</u>	
	<u>Mean activity</u> <u><sup>208</sup>Po peak region</u>	<u>Mean activity</u> <u><sup>210</sup>Po peak region</u>	<u>Mean activity</u> <u><sup>208</sup>Po peak region</u>	<u>Mean activity</u> <u><sup>210</sup>Po peak region</u>
14/744D	0.66 ± 0.06 c.p.h.	0.66 ± 0.06 c.p.h.	1.62 ± 0.20 c.p.h.	0.96 ± 0.12 c.p.h.
16/133B	0.18 ± 0.02 c.p.h.	0.18 ± 0.02 c.p.h.	0.78 ± 0.12 c.p.h.	0.84 ± 0.12 c.p.h.

TABLE 8    Silver Disc Blanks

<u>Detector</u>	<u>Mean activity</u> <u><sup>208</sup>Po peak region</u>	<u>Mean activity</u> <u><sup>210</sup>Po peak region</u>
14/744D	0.48 ± 0.18 c.p.h.	0.48 ± 0.18 c.p.h.
16/133B	0.17 ± 0.03 c.p.h.	0.14 ± 0.02 c.p.h.

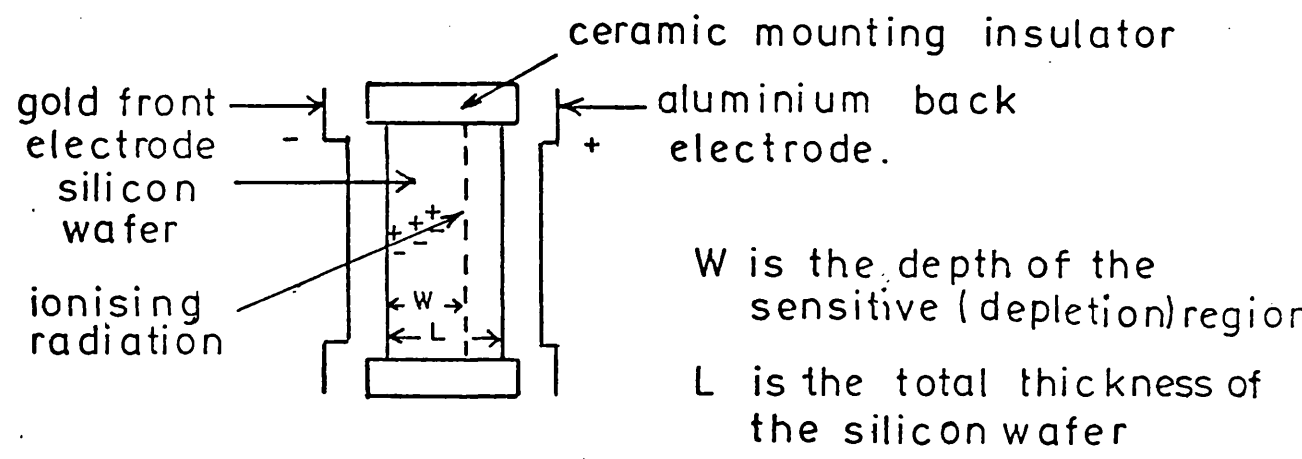
of reagents. Blanks are also run with no spike present. From numerous blanks, silver disc sources, with typical tracer yields, showed alpha activity significantly above that of silver disc 'blanks' on only one occasion. For the purposes of calculation, system blanks have therefore been taken as silver disc 'blanks'.

### Nuclear Counting Technique - $\alpha$ spectrometry

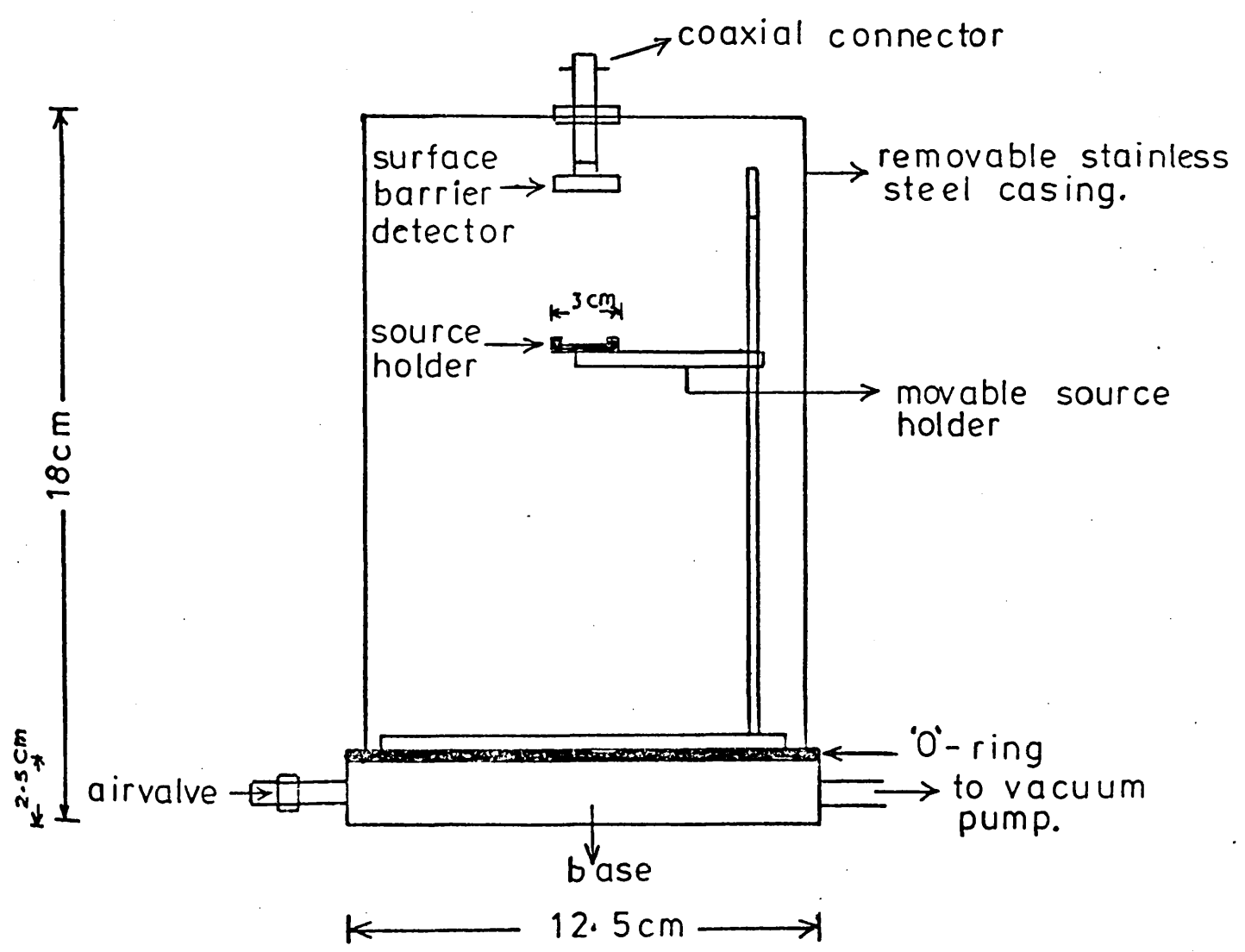
Determination of the  $\alpha$ -radioactivity of the deposited silver discs is by surface barrier (S.B.) detector. The conventional silicon S.B. detector is a large area diode consisting of an extremely thin ( $<1\mu$  thick) p-type layer on the sensitive face of a high purity, n-type silicon wafer. A uniform thin gold film ( $40 \mu\text{g}/\text{cm}^2$ ) is vacuum-deposited on the p-type surface to provide electrical contact, while that for the rear n-type silicon is provided by a thin layer of aluminium (fig 18), (Goulding and Stone, 1970; Dearnley and Northrup, 1966). When a reverse bias is applied, a depletion layer,  $w$ , containing almost no free electrons and holes is formed between the negative n and positive p regions. Under these conditions, current flow through the device is highly limited since neither the n or p regions can supply carriers of appropriate sign.

When a charged particle enters a semi-conductor detector it creates electron-hole pairs by losing energy at a rate of  $3.6\text{eV}/$  electron hole pair formed in silicon (cf.  $30\text{eV}/$ ion pair formed in a gas). Since both electrons and holes have large mobilities and since collection distances are short, it is possible to induce collection times as low as a few nano-seconds. Provided that the sensitive depth of the detector exceeds the range of the particles and that the electric field in the sensitive region

FIGURE 18      Schematics of  $\alpha$ -surface barrier  
detector and  $\alpha$ -source/detector assembly



Typical Surface Barrier Detector



$\alpha$ -Source / Detector Assembly

is sufficiently large to separate charge carriers before they recombine, the number of electron-hole pairs produced in the depletion layer is proportional to the energy of the incident radiation. These pairs are swept apart by the electric field, their collection producing a charge which is converted to a shaped voltage pulse (still directly proportional to the energy of the incident particle) for transmission to a multi-channel analyser.

The analyser sorts the incoming pulses according to their amplitude, assigning each pulse to a channel in the memory corresponding to a particular voltage increment. During counting, the analyser accumulates a spectrum of the number of particles of a particular energy measured (channel contents) versus the particle energy (channel number). Integration yields a quantitative estimate of the relative abundance of particles with different energies.

Good source preparation is essential to accurate  $\alpha$ -spectrometry because of the very high energy loss per unit length of  $\alpha$  track. Absorption seriously affects peak resolution and so it is particularly important that the source be very thin, of the order of a few tens of  $\mu\text{g}/\text{cm}^2$  (ideally a monomolecular layer) to minimise attenuation of  $\alpha$ -particle energy as it emerges from the source. (Techniques for source preparation have been reviewed by Yaffe (1962), and a general procedure for electrodeposition is described in Talvitie (1972)). Furthermore, the detector-source assembly must be operated under low pressure to eliminate appreciable degradation of the  $\alpha$ -particle energy by interaction with air between source and detector. In addition, a critical requirement in  $\alpha$ -spectrometry of natural radionuclides, in view of the low count rates normally

observed ( of the order of a few counts/minute), is excellent stability and reproducibility of the electronic system. Counting times are normally 24 hours or longer and significant 'drift' during this period due to electronic fluctuations can result in merging of individual  $\alpha$ -peaks, in severe cases to an extent which necessitates rejection of data. During the first half of this project, considerable difficulty was in fact experienced due to such electronic instability. While the original  $\alpha$ -spectrometry system (consisting of Nuclear Enterprises electronics) was capable, under optimum conditions, of a resolution of ca. 65KeV at full width half maximum (f.w.h.m.), serious intermittent drift was encountered during counting, resulting in the rejection of data. This situation continued for a considerable length of time. High resolution (dependent upon good electronic stability) is of particular importance in this study due to the relatively small difference in  $\alpha$ -particle energies of tracer ( $^{208}\text{Po}$ ;  $E_{\alpha} = 5.11\text{MeV}$ ) and sample ( $^{210}\text{Po}$ ;  $E_{\alpha} = 5.305\text{MeV}$ ) isotopes.

However, new  $\alpha$ -spectroscopic electronic equipment was subsequently obtained from Ortec electronics mid-way through the project and this proved highly stable, providing excellent resolution throughout the remainder of the study.

Thus, in this work, twin Ortec silicon/gold surface barrier detectors of active area  $300\text{mm}^2$  and sensitive depth  $100\mu\text{g}$  are used for  $\alpha$ -spectroscopic measurement, permitting simultaneous counting of two samples. Bias voltage is applied to the detectors via dual high voltage supplies (Ortec model 428) and detector output signals are fed through duplicate electronic systems consisting of low noise charge sensitive preamplifiers (Ortec model 125), pulse shaping main amplifiers (Ortec model 471) and bias amplifiers (Ortec model 408A). Bias amplifier outputs

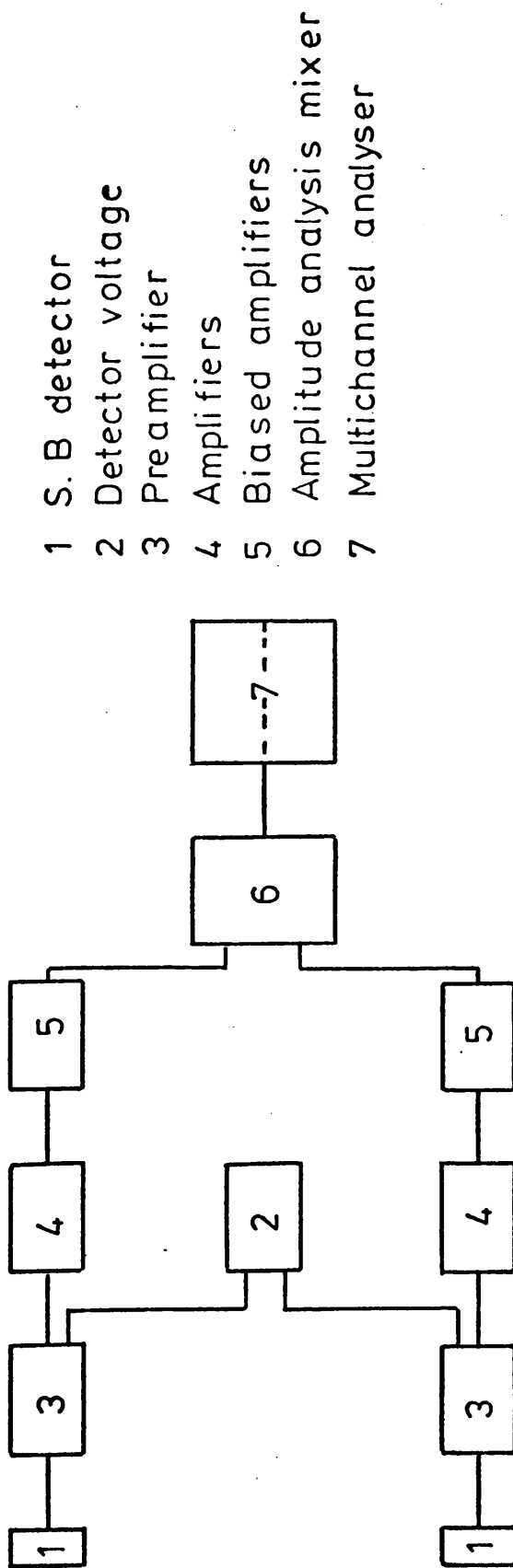
are transmitted to a Laben 400 channel pulse height analyser via a Laben M400 mixer which enables the outputs to be recorded simultaneously in two, 200 channel sub-groups of the analyser memory. A block diagram of the system is shown in fig 19.

Perspex spacers are used to provide constant geometry between source and detector (fig 18) and chambers are evacuated to better than  $10^{-2}$  torr, when H.V. is applied, and maintained there throughout the duration of the count. The detectors are protected by a splash bulb and liquid nitrogen trap from the oil pump, vapours from which could give rise to trapping centres in the detectors, seriously reducing resolution.

Detector counting efficiencies measured against a calibrated source (Radiochemical Centre, Amersham, code AMR22) containing electrodeposited  $^{241}\text{Am}$  (deposit diameter 2mm) with a certified rate of emergence of  $1.53 \times 10^4$   $\alpha$ -particles/min from the front surface ( $\pm 2\%$ ,  $3\sigma$  error) are 34.5% (detector 16/133B) and 33% (detector 14/744D) respectively. Efficiencies for silver discs, where the deposited activity is spread over a 2cm diameter face, are 26.5% and 24.5% respectively.

The system is calibrated and resolution maximised using a 3 nuclide source (Radiochemical Centre, Amersham, code AMR33) containing  $^{239}\text{Pu}$  ( $E_{\alpha} = 5.15\text{MeV}$ ),  $^{241}\text{Am}$  ( $E_{\alpha} = 5.48\text{MeV}$ ) and  $^{244}\text{Cm}$  ( $E_{\alpha} = 5.80\text{MeV}$ ) guaranteed capable of resolution to 20KeV at f.w.h.m. The total system resolution found for sample sources is 40 to 45 KeV (f.w.h.m.); standard sources are marginally better at 35 to 40KeV (f.w.h.m.). This compares with quoted detector resolution values of 20.2KeV (f.w.h.m.) and 18.4KeV (f.w.h.m.) for detectors 14/744D and 16/133B respectively. No significant spectrometer drift has been experienced throughout the period of study with Ortec equipment; the above discrepancy

FIGURE 19      Block diagram of alpha spectrometer



between observed and theoretical resolution is probably due to slight non-uniformity in source deposits. The resolution is sufficient to allow almost total separation of  $^{208}\text{Po}$  ( $E_{\alpha} = 5.11$  MeV) and  $^{210}\text{Po}$  ( $E_{\alpha} = 5.305$  MeV). A typical  $\alpha$ -spectrum is shown in fig 12.

Both peaks are integrated over 25 channels and a small correction for peak overlap made as follows. The last 16 channels of the 25 channel envelope comprising the  $^{210}\text{Po}$  peak are free of any contribution from  $^{208}\text{Po}$ . Similarly, the first 9 channels of the  $^{208}\text{Po}$  peak have insignificant contribution from  $^{210}\text{Po}$  decay events. The following ratio is therefore used to estimate the number of counts observed under the  $^{208}\text{Po}$  peak which are in fact due to  $^{210}\text{Po}$  disintegrations:-

$$\frac{\text{No of counts in last 16 channels of } ^{210}\text{Po peak}}{\text{No of counts in last 16 channels of } ^{208}\text{Po peak}} \times \text{No of counts in first 9 channels of } ^{208}\text{Po peak}.$$

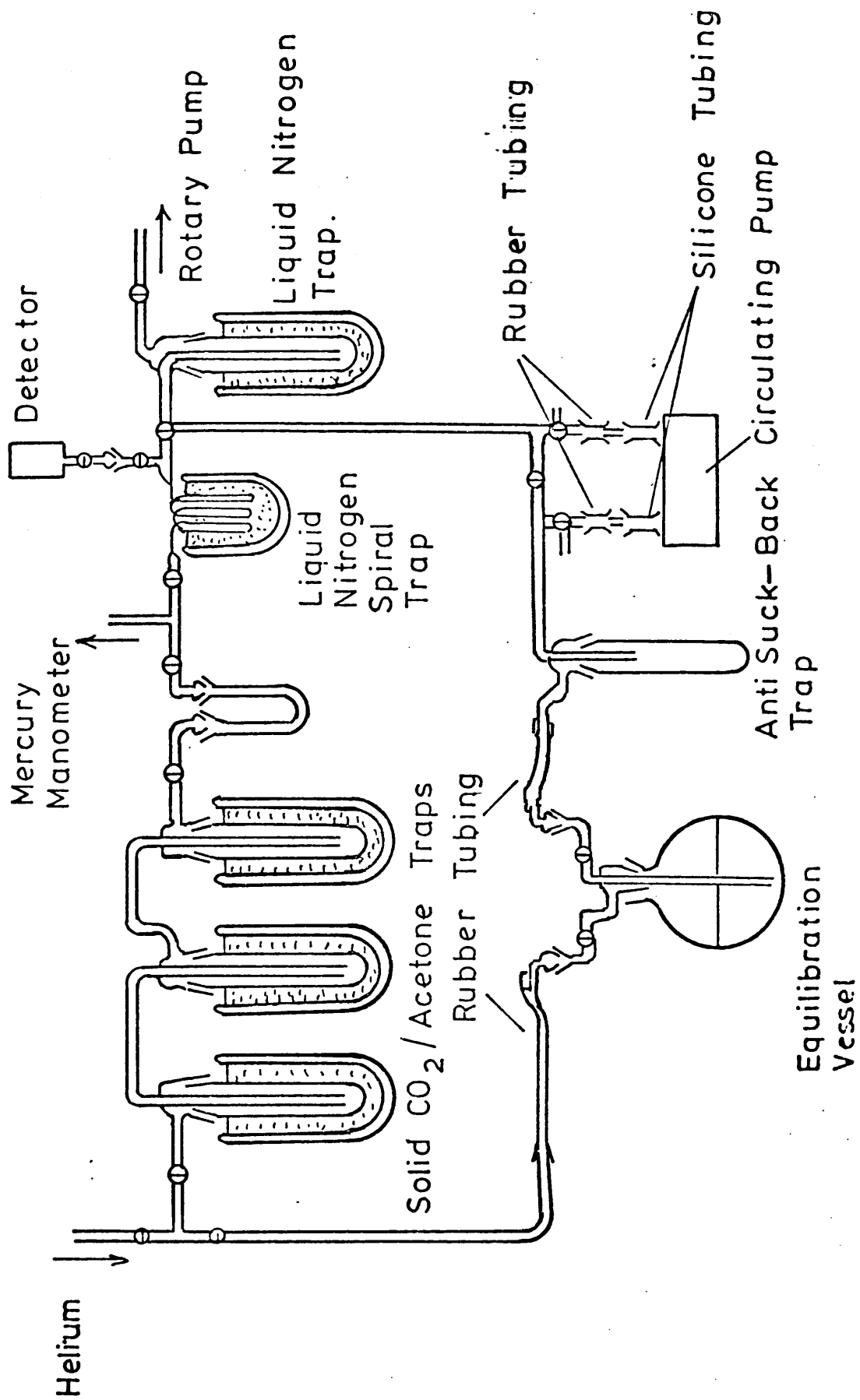
Since at least twice as much  $^{208}\text{Po}$  spike is used as  $^{210}\text{Po}$  activity in the sample, the effect of the overlap contribution on the above ratio is negligible. A description of the method used in sample calculation is given in appendix 2.

$^{226}\text{Ra}$  Analysis and Nuclear Counting Technique

The system used in this work for  $^{226}\text{Ra}$  analysis was described in detail by MacKenzie (1977). The method involves emanation, collection and  $\alpha$ -scintillation counting of  $^{222}\text{Rn}$ , the gaseous daughter product of  $^{226}\text{Ra}$  using the extraction system shown in fig 20.

The aliquot of the dissolved sample removed for  $^{226}\text{Ra}$  analysis is made up to 500mls with distilled water and transferred to a 1 litre glass equilibration vessel. Following a preliminary extraction to remove all  $^{222}\text{Rn}$  initially present, the equilibration vessel is sealed and the date and time noted. This preliminary stripping of  $^{222}\text{Rn}$  is performed by a flushing procedure identical to that described in the analytical procedure below, except that the emanated  $^{222}\text{Rn}$  is not collected at this time. The sealed sample is stored for a known period of time during which  $^{222}\text{Rn}$  activity grows in from its parent  $^{226}\text{Ra}$ , following equation (9) page 88, from which the percentage build up of  $^{222}\text{Rn}$  towards secular equilibrium with  $^{226}\text{Ra}$  can be calculated. Samples are normally stored for more than 12 days (corresponding to 88.7% equilibrium) prior to analysis. After this time, the sealed equilibration vessel is attached to the vacuum line as shown, but without the liquid nitrogen trap. The system (excluding the pump) is evacuated, the detector sealed, and the line filled twice to 1 atm pressure with helium, and then evacuated to remove impurities from the inlet system. The line is again filled to 1 atmosphere with helium and then closed off from the helium supply. The peristaltic circulating pump (Wab Pumps Ltd., Bournemouth, England) is flushed with helium for a few minutes and then opened to the rest of the

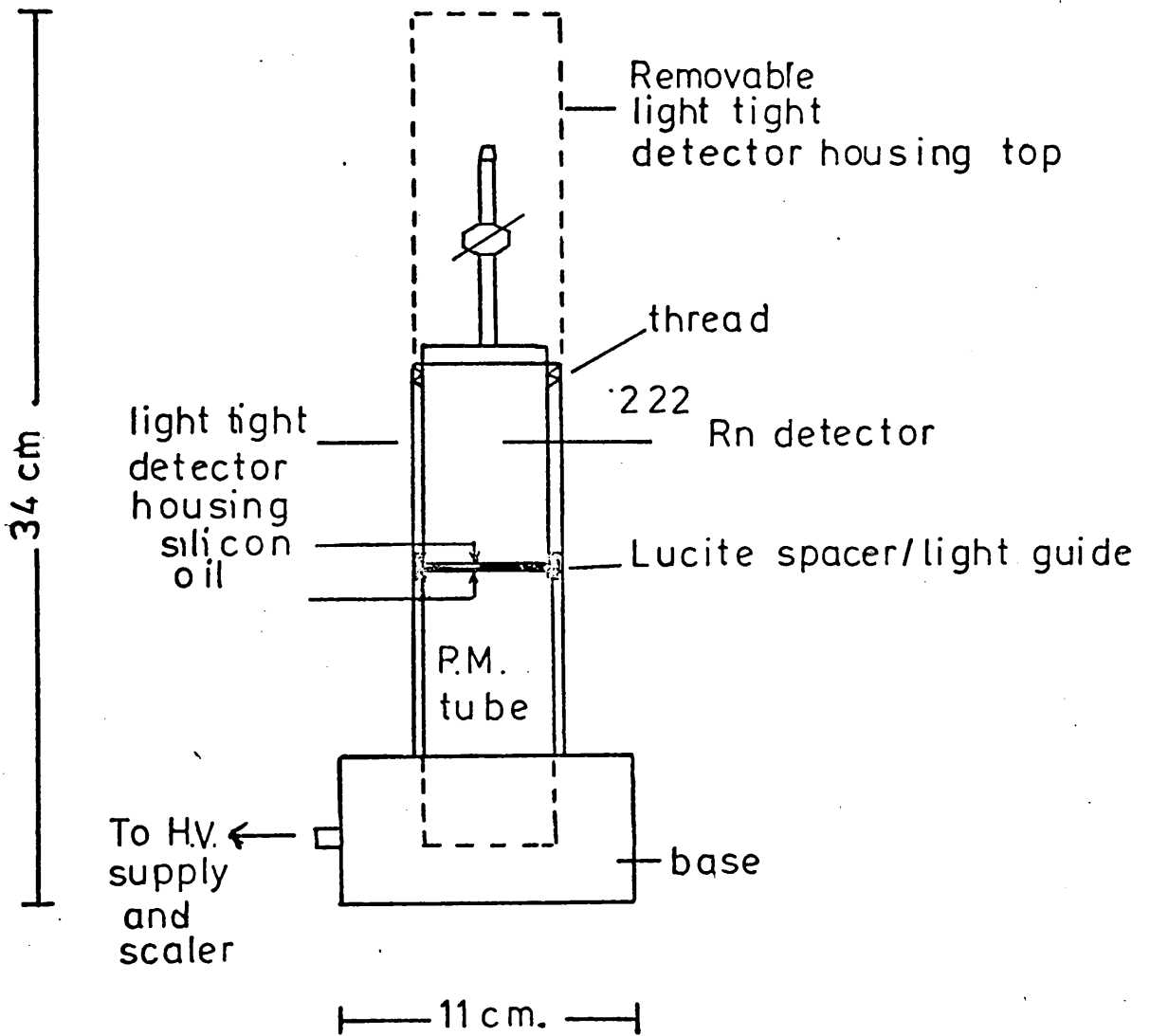
FIGURE 20  $^{222}\text{Rn}$  emanation system



line (the silicon rubber tubing of the pump is not sufficiently rigid to withstand evacuation). The equilibration vessel is opened to the rest of the system, and the peristaltic pump cycles the helium and  $^{222}\text{Rn}$  around the line, at a flow rate of 4 litres/min. The liquid nitrogen trap is filled and  $^{222}\text{Rn}$  frozen down in the spiral trap. Water vapour is removed by the solid  $\text{CO}_2$ /acetone traps. A flushing time of 45 minutes is sufficient to give total removal of  $^{222}\text{Rn}$  from 500ml samples. After completion of the flushing process, the equilibration vessel is again sealed and the time noted. With the liquid nitrogen trap still in position, the spiral trap and detector are isolated from the rest of the line and evacuated, leaving the condensed radon. The combined detector/ spiral trap is isolated from the rest of the line and the liquid nitrogen trap removed, vapourisation of the radon being accelerated by warming the trap with a hot-air blower. The radon distributed between the detector (volume approximately 50mls) and spiral trap (volume approximately 10mls) is transferred virtually quantitatively to the detector, by allowing a pulse of helium at one atmosphere pressure to enter the spiral trap from the vacuum line and immediately afterwards sealing the detector. The sample is then stored for repeat analysis after ingrowth of  $^{222}\text{Rn}$ , and the detector is removed for radioactivity measurement on the collected gas.

For radioactivity measurement the detector (based on a design by Ferrante et al (1964) which was a development from the original chamber of Damon et al (1952) and Lucas (1957)) is coupled to the face of a photomultiplier tube which is sealed in a light tight unit (fig 21) and connected to a scaler. A perspex spacer is placed between the photomultiplier face and

FIGURE 21  $^{222}\text{Rn}$  detector/photomultiplier assembly



the detector to provide constant geometry and silicone fluid applied to provide a good light path.  $\alpha$ -particles striking the ZnS (Ag) phosphor produce light pulses which are converted to current pulses and amplified before being fed as a voltage pulse to a scaler. Each  $^{222}\text{Rn}$  decay gives rise to two further  $\alpha$ -decays from its daughters  $^{218}\text{Po}$  and  $^{214}\text{Po}$ , which grow rapidly into secular equilibrium with their  $^{222}\text{Rn}$  parent. Detectors are left for 5 hours before counting to ensure secular equilibrium between  $^{222}\text{Rn}$  and those short-lived daughters so that  $3\alpha$ -decay events are assumed to occur for each  $^{222}\text{Rn}$  decay. Detectors are however transferred to photomultiplier/scaler assemblies at least 1 hour before counting commences to avoid interference from a slight photomultiplier memory effect which occurs after exposure to light. Samples are normally counted for 500 minutes, giving counting errors of less than 2%. A small correction for decay during counting is applied following the method of Hoffmann and Van Camerik (1967) which defines a correction factor based on the ratio of count time to half-life. Two photomultiplier/scaler systems, each having a working voltage of 1300V, are used in conjunction with four scintillation detectors. Backgrounds and efficiencies for the detectors are presented in table 9. System blanks are performed on equilibration vessels containing 500mls of 6N HCl and give a mean value of  $2.20 \pm 0.13$ cpm.

The efficiency for collection and counting of  $^{222}\text{Rn}$  is determined by analysis of a standardised  $^{226}\text{Ra}$  solution obtained from the U.S. National Bureau of Standards. Electronic stability is monitored throughout the project by periodic counting of  $^{222}\text{Rn}$  isolated from active  $^{226}\text{Ra}$  solutions. The decay plot also serves to characterise the observed radioactivity (fig 22).

Table 9  $^{222}\text{Rn}$  Detector Backgrounds and Efficiencies

<u>Detector</u>	<u>Efficiency %</u>	<u>Background (cpm <math>\pm 1\sigma</math>)</u>
1	74.0	0.60 $\pm$ 0.02
2	86.5	0.21 $\pm$ 0.02
3	71.5	0.10 $\pm$ 0.01
4	68.0	0.10 $\pm$ 0.01

Radiocaesium Analysis and Nuclear Counting Techniques

In the early stages of the work, radiocaesium analysis was performed by passing aliquots of totally dissolved sediment (ca. 6N in HCl) through columns of the inorganic ion exchanger K.C.F.C. (4cm x 1cm columns of 30-80 mesh K.C.F.C. contained in disposable plastic tubes), when caesium exchanges quantitatively for potassium. The  $\gamma$ -activity of the exchanged resin was subsequently determined using a 3" NaI (Tl) scintillation counter, the counting geometry of the K.C.F.C. plugs being defined by means of a perspex holder. As radiocaesium activity is confined to the top 1cm of the column, maximum counting efficiency and reproducibility were achieved by positioning this part of the source centrally over the detector face. Samples were normally counted for 800 minutes. A resolution of 9.3% at f.w.h.m. was sufficient to resolve the 0.662MeV and 0.796/0.802 MeV photopeaks associated with  $^{137}\text{Cs}$  and  $^{134}\text{Cs}$  decay respectively. Overall efficiencies of 5.6% and 4.8% were obtained for  $^{137}\text{Cs}$  and  $^{134}\text{Cs}$  respectively as determined from standard solutions obtained from the Radiochemical Centre, Amersham. Background count rates were 13.5cpm and 7.8cpm in the  $^{137}\text{Cs}$  and  $^{134}\text{Cs}$  photopeak regions, and the blank contribution from the K.C.F.C. resin was 0.3cpm in both regions.

Radiocaesium analysis was subsequently performed by direct counting of dried homogenised sediment contained in small plastic vials using a 100cc GeLi detector. The higher resolution of the GeLi system (1.8KeV f.w.h.m. for the 0.662 MeV  $^{137}\text{Cs}$  photopeak) allows complete separation of  $^{134}\text{Cs}$  and  $^{137}\text{Cs}$  photopeaks from peaks due to other nuclides present in the sediment, such as  $^{208}\text{Tl}$  (0.58MeV),  $^{214}\text{Bi}$  (0.61MeV) and  $^{95}\text{Zr}$  (0.72MeV)/ $^{95}\text{Nb}$  (0.77MeV). (The NaI detector is unable to resolve peaks associated with these

isotopes from photopeaks due to  $^{137}\text{Cs}$  and  $^{134}\text{Cs}$ , hence direct counting of sediment is not applicable in that case). Sample counting geometry is again specified by means of a perspex holder and samples are in general counted for 800 minutes. The detection efficiency for  $^{137}\text{Cs}$  is 1.88% with a background in the  $^{137}\text{Cs}$  peak region of 0.4cpm. Detailed information on these systems can be obtained in theses by Mackenzie (1977) and McKinley (1978).

## 2.5 Reproducibility

The ultimate test of any analytical procedure is the degree of reproducibility obtained from the repeated analysis of the same material throughout the period of study. With this in mind, a sediment core was ground, homogenised and repeatedly analysed for both  $^{210}\text{Pb}$  and  $^{226}\text{Ra}$  alongside authentic samples and blanks. The results of these replicate measurements are presented in tables 10 and 11a.

Furthermore, several samples were assayed in duplicate for  $^{210}\text{Pb}$  (table 12) and for  $^{226}\text{Ra}$  (table 13) and one repeatedly analysed for  $^{226}\text{Ra}$  activity (table 11b).

In the case of  $^{210}\text{Pb}$  determination, replicate analyses indicate an overall  $1\sigma$  error on the measurement of 2.41%, where the standard deviation,  $\sigma_{\text{REP}}$ , is defined as,

$$\sigma_{\text{REP}} = \sqrt{\frac{\sum (x - \bar{x})^2}{n - 1}}, \text{ where}$$

$x$  is the value obtained in an individual measurement, and  $\bar{x}$  is the mean of  $n$  observations.

The error associated with replicate measurements,  $\sigma_{\text{REP}}$ , can in fact be regarded as a combined or total error,  $\sigma_{\text{TOT}}$ , divisible into 2 distinct components: Component (1) is a statistical error,  $\sigma_{\text{c}}$ , arising from the observed number of counts, where the standard deviation,  $\sigma_{\text{c}}$ , on a count is defined as

$$\sigma_{\text{c}} = \sqrt{N} \text{ where } N \text{ is the observed number of counts.}$$

Component (2) is a non-counting error arising from inaccuracies in for example weighing of sample or use of the pipette in dispensing tracer. Moreover, a further source of non-counting 'error' can be recognised in this case as possible inhomogeneity of the replicate sample. Arguably this contribution is not an error in the true

Table 10 Results of  $^{210}\text{Pb}$  replicate measurements

$^{210}\text{Pb}$  Activity (dpm/g  $\pm 1\sigma$  count error)

4.81  $\pm$  0.11

4.80  $\pm$  0.10

4.64  $\pm$  0.11

4.76  $\pm$  0.09

4.85  $\pm$  0.11

4.60  $\pm$  0.08

4.56  $\pm$  0.10

4.66  $\pm$  0.10

4.77  $\pm$  0.11

4.96  $\pm$  0.10

4.92  $\pm$  0.10

4.77  $\pm$  0.09

4.64  $\pm$  0.08

4.69  $\pm$  0.09

4.63  $\pm$  0.10

4.76  $\pm$  0.11

Mean = 4.74 dpm/g

Standard deviation = 0.11 dpm/g

% error = 2.41

Table 11a Results of  $^{226}\text{Ra}$  replicate analyses $^{226}\text{Ra}$  Activity (dpm/g  $\pm 1\sigma$  count error)1.39  $\pm$  0.021.56  $\pm$  0.031.28  $\pm$  0.021.49  $\pm$  0.021.36  $\pm$  0.021.36  $\pm$  0.021.26  $\pm$  0.021.38  $\pm$  0.021.31  $\pm$  0.021.53  $\pm$  0.02

Mean = 1.39 dpm/g

Standard deviation = 0.10 dpm/g

% error = 7.4

Table 11b Results of repeat analyses for  $^{226}\text{Ra}$  on one sample solution $^{226}\text{Ra}$  Activity (dpm/g  $\pm 1\sigma$  count error)1.39  $\pm$  0.021.34  $\pm$  0.021.56  $\pm$  0.031.45  $\pm$  0.02

Mean = 1.44 dpm/g

Standard deviation = 0.10 dpm/g

% error = 6.9

Table 12      Results of  $^{210}\text{Pb}$  duplicate analyses

<u>Sample</u>	<u><math>^{210}\text{Pb}</math> Activity</u> (dpm/g $\pm$ 1 $\sigma$ count error)
GLC3:6	8.54 $\pm$ 0.17
	8.24 $\pm$ 0.17
GLC3:14	6.53 $\pm$ 0.20
	6.77 $\pm$ 0.20
L.LOM:3	14.52 $\pm$ 0.36
	14.00 $\pm$ 0.29
LGC9:8	9.90 $\pm$ 0.15
	9.74 $\pm$ 0.16

Table 13      Results of  $^{226}\text{Ra}$  duplicate analyses

<u>Sample</u>	<u><math>^{226}\text{Ra}</math> Activity (dpm/g <math>\pm 1 \sigma</math> count error)</u>
LGC9:5	5.68 $\pm$ 0.06
	5.99 $\pm$ 0.06
LGC4:1	2.49 $\pm$ 0.06
	2.47 $\pm$ 0.06
LGC4:2	2.68 $\pm$ 0.05
	2.55 $\pm$ 0.05
LGG5:2	4.16 $\pm$ 0.07
	4.19 $\pm$ 0.07
LGG5:7	3.80 $\pm$ 0.04
	3.55 $\pm$ 0.04
L.LOM:1	3.49 $\pm$ 0.06
	3.07 $\pm$ 0.07
L.LOM:3	2.89 $\pm$ 0.07
	2.66 $\pm$ 0.06
L.LOM:10	2.14 $\pm$ 0.04
	2.06 $\pm$ 0.04
L.LOM:20	1.75 $\pm$ 0.03
	1.43 $\pm$ 0.03

sense and as it is non-quantifiable, the total error terms,  $\sigma_{TOT}$  represent maximum values of the experimental uncertainty.

With

$$\sigma_{TOT} = \sigma_{REP} = \sqrt{\sigma_{COUNT}^2 + \sigma_{NON-COUNT}^2} \quad (A)$$

it is possible to determine a mean value for  $\sigma_{NON-COUNT}$  from the known values of  $\sigma_{REP}$  and  $\sigma_{COUNT}$ . In this way a value of 1.06% is obtained for the non-counting relative error. Counting errors associated with  $^{210}\text{Pb}$  determination are in general of the order of 2% to 3%. For this reason, errors quoted on  $^{210}\text{Pb}$  results are total 1 $\sigma$  errors recalculated from equation (A) by substitution of the value of  $\sigma_{NON-COUNT}$ .

However, in  $^{226}\text{Ra}$  determination, counting errors are in the range 1% to 2%, while replicate analyses define an overall 1 $\sigma$  error on the measurement of 7.4%; since this is so much larger than the counting error (in this case the non-counting error renders the counting error relatively insignificant), the latter is the value quoted on results.

Finally, the error quoted on a radiocaesium result is a total error comprising counting and non-counting contributions derived in a similar manner to those applied to  $^{210}\text{Pb}$  measurements.

## CHAPTER 3

### RESULTS AND DISCUSSION

This chapter presents the results of the radiochemical, chemical and physical analyses performed on sediment cores recovered from the three areas of study (a) the Cilicia Basin, (b) Loch Lomond and (c) the Clyde sea-lochs, Loch Goil and Gareloch, together with their interpretation. In the interests of clarity, a preliminary description of the general principles applied in developing a  $^{210}\text{Pb}$  chronology for the samples is followed by presentation and discussion of the results for each region in turn.

#### 3.1 General Approach

In Chapter 1, section 1.2, the principal assumptions involved in the alternative approaches to  $^{210}\text{Pb}$  dating were introduced. Briefly, the approaches differ in the following important respect; while the traditional "constant initial concentration" (C.I.C.) model assumes both a constant rate of sediment accumulation and a constant flux of excess  $^{210}\text{Pb}$  to the sediment, the recently developed "constant rate of supply" (C.R.S.) model assumes only a constant time flux of excess  $^{210}\text{Pb}$  to the deposit and can be applied if this condition is met even in environments experiencing a continuously varying rate of sediment accumulation (The C.I.C. method can cope with a changing rate of sediment accumulation only when the change is induced by a single-event [i.e. has occurred in a period of time very short relative to the half-life of  $^{210}\text{Pb}$ ] and in addition if pre- and post-event sedimentation rates were constant; in this special situation, a semi-log plot of excess  $^{210}\text{Pb}$  versus depth would ideally

exhibit intersecting straight lines of different gradient, the point of intersection corresponding to the age/depth at which the pattern of sedimentation altered). The C.R.S. method therefore has the advantage of potentially successful application under conditions where the C.I.C. model cannot be used, while yielding identical results in circumstances when the C.I.C. model is applicable. Nonetheless, the C.R.S. model, as noted previously, has the practical disadvantage that, because it is based upon the cumulative activity of excess  $^{210}\text{Pb}$  in the core it critically requires measurement of excess  $^{210}\text{Pb}$  activity throughout the length of the column. In this study, the C.I.C. approach has by necessity been adopted for the following reasons;

(1) Craib cores recovered from Clyde sea-loch sediments are not of sufficient length for all excess  $^{210}\text{Pb}$  to have decayed and it is therefore impossible to estimate the total cumulative excess  $^{210}\text{Pb}$  activity in these samples

and

(2) in cores which are of suitable age (length) for  $^{210}\text{Pb}$  to have attained equilibrium with  $^{226}\text{Ra}$ ,  $^{210}\text{Pb}$  assay has not been performed on every section. Estimation of excess  $^{210}\text{Pb}$  values in non-analysed sections would therefore be most reasonably achieved only by assuming exponential decrease between measured values in adjacent sections. Such interpolation would clearly deny the fundamental difference between the approaches of the C.R.S. and C.I.C. models. Thus a cumulative excess  $^{210}\text{Pb}$  activity could not be derived. In any event, for the two gravity cores which come into this category, very good approximations to exponential decrease of

excess  $^{210}\text{Pb}$  with depth were observed and thus differences between the C.R.S. and C.I.C. approaches would be minimal and comparison of the two methods unrevealing.

In applying the C.I.C. model to age determination special consideration has been centred on porosity, salt dilution and supported  $^{210}\text{Pb}$  activities, as discussed below.

(1) Profiles of porosity (water volume fraction) for each core have been calculated from

$$\varphi = \frac{V_{\text{water}}}{V_{\text{water}} + V_{\text{solids}}} = \frac{\frac{M_{\text{water}}}{D_{\text{water}}}}{\frac{M_{\text{water}}}{D_{\text{water}}} + \frac{M_{\text{solids}}}{D_{\text{solids}}}}$$

where  $\varphi$  = porosity

$V$  = volume

$M_{\text{water}}$  = mass of water loss upon drying

$D_{\text{water}}$  = density of interstitial water (for  
marine cores taken as  $1.025\text{g.cm}^{-3}$ )

$M_{\text{solids}}$  = mass of dried solids (salt-corrected,  
see below)

$D_{\text{solids}}$  = measured density of sediment solids

(The porosity is commonly converted to a percentage basis by multiplying by 100).

With the exception of the Cilicia Basin core, porosities are both very high and exhibit rapid decrease as a function of depth, consistent with compressional loss of water from the sediment. This is particularly apparent in the upper layers of the deposits which contain the profiles of excess  $^{210}\text{Pb}$  useful in dating. Since the thickness of sediment which represents an annual layer is therefore decreasing as a function of depth through compaction, accurate age/depth curves are critically dependent on correction for this depth-dependency

of water content. In this work, such correction has been performed by expressing the depth in sediment in terms of cumulative weight of dry sediment deposited per  $\text{cm}^2$ , thus effectively normalising the water content to zero throughout the column length. From a semi-log plot of excess  $^{210}\text{Pb}$  activity versus depth in core ( $\text{mg}\cdot\text{cm}^{-2}$ ), an estimate of the rate of sediment accumulation in terms of dry sediment deposited per  $\text{cm}^2$  per year ( $\text{mg}\cdot\text{cm}^{-2}\cdot\text{y}^{-1}$ ) is derived. The age of any particular layer of sediment (in the absence of mixing) is then obtained simply by division of the cumulative weight of solids ( $\text{mg}\cdot\text{cm}^{-2}$ ) by the estimated rate of sediment accumulation ( $\text{mg}\cdot\text{cm}^{-2}\cdot\text{y}^{-1}$ ). Since the cumulative weight of sediment corresponds to a known depth in the column an estimate of the mean sedimentation rate in the more easily visualised units of  $\text{cm}\cdot\text{y}^{-1}$  can then be determined for a defined depth interval. For example, in theory, an estimate of the surface rate of sedimentation in  $\text{cm}\cdot\text{y}^{-1}$  can be obtained from the reciprocal of the age of the upper 1cm. section. Table 14 presents average sedimentation rates (column 1) for various cores derived from semi-log plots of excess  $^{210}\text{Pb}$  versus depth, measured in centimetres (i.e. with no porosity correction), and porosity corrected surface sedimentation rates (column 2); table 15 compares age/depth relationships for Loch Lomond core LLRPM1 based on the sedimentation rates of table 14 and illustrates the overestimate of horizon age which results for the upper layers of a deposit if sediment compaction is disregarded. The importance of correcting for compaction is clearly seen.

In marine sediments of very high water content (e.g.  $> 90\%$  porosity or  $> 80\%$  water by weight) the apparent weight of dry sediment material in any section of a core can be appreciably

TABLE 14                      COMPARISON OF POROSITY CORRECTED (COL. 2)  
AND UNCORRECTED SEDIMENTATION RATES FOR  
SOME CORES ANALYSED IN THIS STUDY

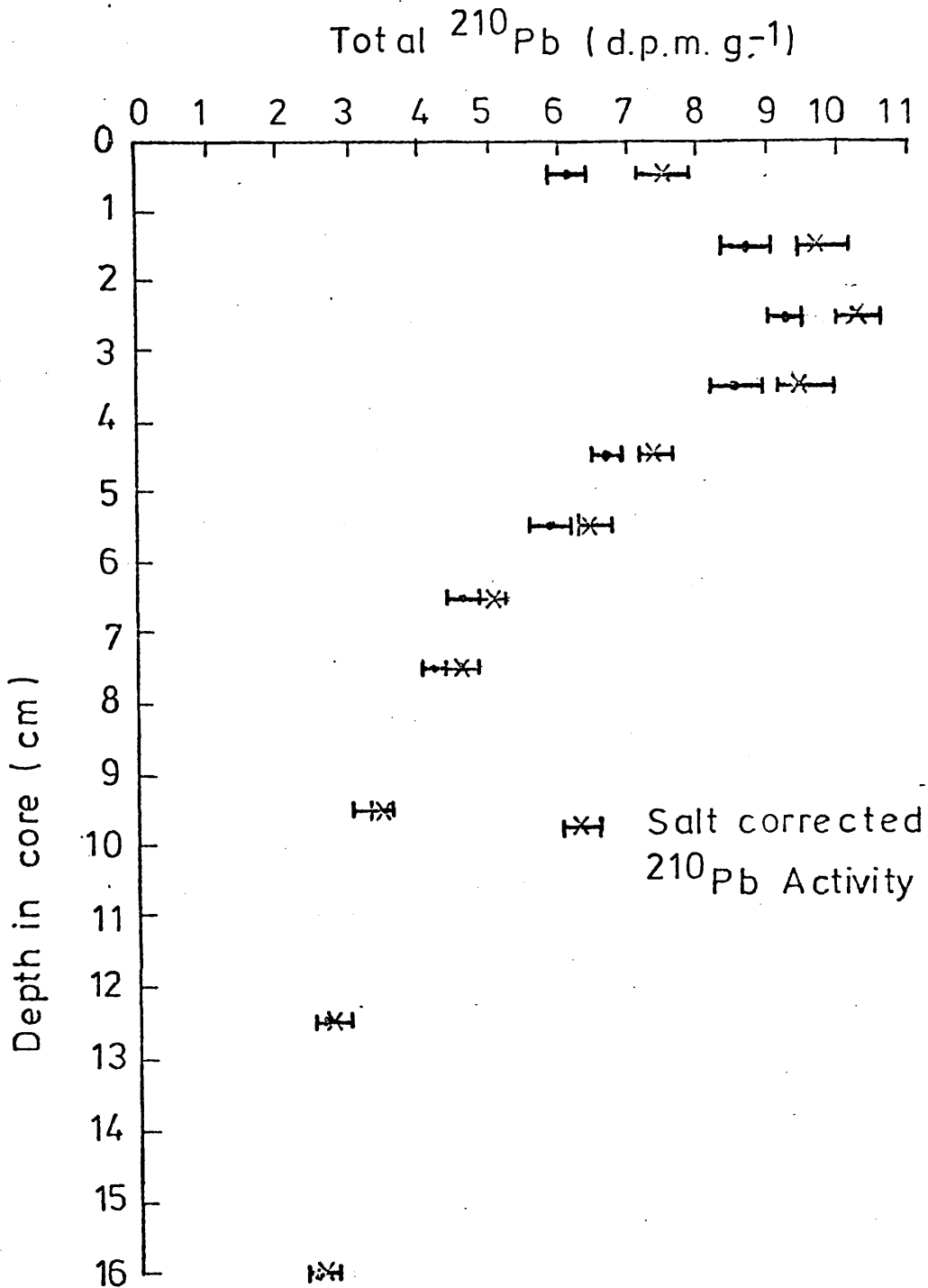
<u>CORE</u>	<u>COLUMN 1</u> <u>(mm.y<sup>-1</sup>)</u>	<u>COLUMN 2</u> <u>(mm.y<sup>-1</sup>)</u>
LLRPM1	0.6	0.9
MED. CORE	0.4	0.5
GLG2	1.6	2.1
LGG5	1.1	2.3
LGC9	5.5	9.0
LGC4	3.0	5.0

Column 1 presents mean sedimentation rates (mm.y<sup>-1</sup>) evaluated without porosity correction. Column 2 presents equivalent 'surface' sedimentation rates (mm.y<sup>-1</sup>) evaluated from compaction - corrected accumulation rates. (Because of the difficulty in defining precisely the centimetre section immediately beneath the sediment/water interface, these results are derived from the second centimetre section below the mud surface and are therefore slightly lower than the 'true' present rate of sediment accumulation).

TABLE 15                      AGE/DEPTH RELATIONSHIPS FOR  
LOCH LOMOND CORE LLRPM1 DERIVED  
FROM POROSITY CORRECTED (COL. 2)  
AND UNCORRECTED SEDIMENTATION RATES

<u>Section</u> <u>(cm)</u>	<u>Column 1</u> <u>(Age : years)</u>	<u>Column 2</u> <u>(Age ; years)</u>
0 - 1	17	9
1 - 2	34	20
2 - 3	50	31
3 - 4	67	43
4 - 5	84	55
5 - 6	100	69
6 - 7	117	84
7 - 8	134	96
8 - 9	150	110
9 - 10	167	126

overestimated because of the salt deposited from interstitial waters upon drying. The extent of this contamination effect must clearly vary with depth, being dependent upon the volume of interstitial water in each segment. The percentage salt dilution to the sediment material can be as much as 31% in the upper layers of high porosity deposits (e.g. 90% water by weight) which underlie saline (35<sup>0</sup>/oo) waters. The cores recovered from the Clyde sea-lochs and the Cilicia Basin fall within this category. In these cores, the salt contribution to the total dried weight of sediment was estimated, assuming a salinity for interstitial waters equivalent to the mean salinity of the water overlying the deposits (32.8<sup>0</sup>/oo in Loch Goil, 31.8<sup>0</sup>/oo in Gareloch and 39<sup>0</sup>/oo in the Eastern Mediterranean). Salinities were also assumed to be constant within each core profile; justification for this assumption arises from the work of Emery (1960) and Grill (1978) who found the chlorinities of the interstitial waters of fresh sediment cores to be almost identical to those of the overlying waters. In these sediments, salt dilution varied from ca. 5% at depth to >20% in surface strata. Fig.23 illustrates the effects of salt correction on total <sup>210</sup>Pb activities in gravity core LGG5 from Loch Goil. Correction for salt dilution has significant effects on two sediment parameters; (1) the specific activity of <sup>210</sup>Pb (or any other radionuclide) per unit weight of solids is both increased and normalised; thus an apparent change in species concentration in the upper strata of a deposit is not in part or in total due to non-uniform salt-dilution (e.g. the depression of <sup>210</sup>Pb activities in the surficial layers of marine sediments commonly observed),



and  
 (2) the weight of 'real' sediment material per section  
 (and therefore per cm.<sup>2</sup>) is reduced.

The overall result of salt correction is therefore to increase nonlinearly the specific activities of total  $^{210}\text{Pb}$  in the core, and consequently to reduce the estimated rate of sediment deposition. Thus for Loch Goil, core LGG5, correction for salt residues reduces the sedimentation rate by  $\sim 10\%$ , and increases by  $\sim 13\%$  the estimate of excess  $^{210}\text{Pb}$  at the sediment/water interface.

All radionuclide and lead results given in this chapter are salt-corrected and sedimentation rates are based on salt-free weights of depositing solids. Errors quoted on results are  $\pm 1\sigma$ , and all concentrations are expressed on a dry weight basis.

In this study, difficulties have arisen, for two reasons; in the estimation of excess  $^{210}\text{Pb}$  activities.

(1) A small experimental discrepancy exists between  $^{226}\text{Ra}$  concentrations measured directly via  $^{222}\text{Rn}$  emanation and values of total  $^{210}\text{Pb}$  determined at sufficient depths for all excess  $^{210}\text{Pb}$  to have decayed. This is illustrated in table 16 for the Gareloch gravity core GLG2. While the respective mean values agree within  $\pm 2\sigma$  error limits,  $^{226}\text{Ra}$  measurements are consistently slightly lower than corresponding  $^{210}\text{Pb}$  activities, indicating a systematic difference between the two. The data for this particular core tend to illustrate the discrepancy at its worst; nonetheless, the consistency with which  $^{226}\text{Ra}$  concentrations were found to be lower than supported  $^{210}\text{Pb}$  activities,

TABLE 16                      COMPARISON OF  $^{226}\text{Ra}$  AND  $^{210}\text{Pb}$  ACTIVITIES  
FOR GARDELOCH GRAVITY CORE GLG2

<u>Section</u> <u>(cm)</u>	<u><math>^{226}\text{Ra}</math> Activity</u> <u>(dpm g<sup>-1</sup>)</u>	<u><math>^{210}\text{Pb}</math> Activity</u> <u>(dpm g<sup>-1</sup>)</u>
1 - 2	1.76 ± 0.13	
5 - 6	1.79 ± 0.14	
7 - 8	1.67 ± 0.13	
13 - 14	1.54 ± 0.12	
22 - 23		2.18 ± 0.10
26 - 27	1.87 ± 0.14	2.14 ± 0.11
32 - 33	1.62 ± 0.13	2.17 ± 0.09
Mean	1.71 ± 0.13	Mean 2.16 ± 0.10

suggests that the difference is real. Similar effects have been found by other workers (e.g. Thompson, 1975; Robbins and Edgington, 1975). The cause of this discrepancy must lie either in a minor calibration error in the  $^{208}\text{Po}$  or  $^{226}\text{Ra}$  standard solutions used in the study, or in an overestimated blank in the case of  $^{226}\text{Ra}$  analysis or the reverse in  $^{210}\text{Po}$  measurement. Since the standards employed are from reliable sources (A.E.R.E. Harwell, the National Bureau of Standards, Washington and the Radiochemical Centre, Amersham) the more likely explanation involves a blank effect. Confirmatory evidence for this is outlined below. The results of  $^{210}\text{Pb}$  analyses, via  $^{210}\text{Po}$ , by Eakins (A.E.R.E. Harwell) on subsections of ground homogenised sediment (supplied by the author) from Gareloch gravity core GLG2, also analysed independently in this work, are presented in table 17 (Eakins, 1976). ( $^{210}\text{Pb}$  results are not salt-corrected in this case since such correction is not performed by the A.E.R.E. Harwell dating service). Clearly, both sets of results should be identical within error. The data indicate close agreement in the upper 'high' activity sections of the core (where a small blank error would be negligible). However, as the  $^{210}\text{Pb}$  activity decreases with depth, an increasing discrepancy is observed between the respective measurements of  $^{210}\text{Pb}$ , the Glasgow results being systematically higher than those obtained at Harwell. This is therefore good evidence that the analytical discrepancy reflects an undetected blank in this work. Using the last three co-analysed data

TABLE 17      COMPARISON OF  $^{210}\text{Pb}$  MEASUREMENTS IN  
GARELOCH GRAVITY CORE GLG2 BY HARWELL  
AND GLASGOW LABORATORIES

<u>Section (cm)</u>	<u>TOTAL <math>^{210}\text{Pb}</math> (dpm. g<sup>-1</sup>)</u>	
	<u>Harwell</u>	<u>Glasgow</u>
0 - 1	6.71 ± 0.44	6.63 ± 0.28
1 - 2	6.38 ± 0.40	6.31 ± 0.23
2 - 3	6.27 ± 0.44	6.65 ± 0.33
3 - 4		6.28 ± 0.20
4 - 5	5.40 ± 0.40	5.59 ± 0.23
5 - 6		5.40 ± 0.23
6 - 7		4.88 ± 0.24
7 - 8	3.80 ± 0.35	
8 - 9		3.95 ± 0.13
10 - 11		3.31 ± 0.16
12 - 13	2.46 ± 0.22	
13 - 14		2.63 ± 0.09
15 - 16	1.87 ± 0.14	
16 - 17		2.25 ± 0.17
19 - 20		2.18 ± 0.07
22 - 23	1.78 ± 0.13	2.08 ± 0.10
25 - 26	1.54 ± 0.13	
26 - 27		2.06 ± 0.11
32 - 33	1.50 ± 0.13	2.09 ± 0.09

points for each profile, the apparent magnitude of this blank is estimated at  $0.5 \pm 0.2$  dpm.g<sup>-1</sup>. Table 18 presents the mean results of the measurements of total <sup>210</sup>Pb at depth in long cores from the Cilicia Basin, Loch Lomond, Gareloch and Loch Goil, together with their respective mean <sup>226</sup>Ra concentrations. From these data a mean discrepancy of  $0.4 \pm 0.1$  dpm.g<sup>-1</sup> between <sup>210</sup>Pb and <sup>226</sup>Ra is apparent, in good agreement with the above estimate. Despite the frequent blank analyses performed during this work, as described in chapter 2, the source of this contamination effect remains at present unresolved. In this study, therefore, to bring measurements of supported <sup>210</sup>Pb into agreement with <sup>226</sup>Ra concentrations, all <sup>210</sup>Pb activities have been reduced by a value of  $0.4 \pm 0.1$  dpm.g<sup>-1</sup>.

(2) Direct measurements of <sup>226</sup>Ra have shown that concentrations vary considerably and systematically with depth, significantly higher values being recorded in surface layers of some cores relative to deeper sections (see for example, fig 60). At their most marked, these vertical variations in <sup>226</sup>Ra concentration may reflect changing conditions of sedimentation in recent years and thus may invalidate some of the basic assumptions of the dating method; at the very least, they give rise to difficulties in estimation of an appropriate mean value in correcting total <sup>210</sup>Pb for its supported component.

The problem outlined above has resulted in alternative approaches being adopted to estimate supported <sup>210</sup>Pb activities in some cores. Thus, in cores exhibiting <sup>226</sup>Ra concentrations which increase towards maximum activity at or near the sediment/water interface, three alternatives present themselves.

TABLE 18

COMPARISON OF MEAN  $^{226}\text{Ra}$  ACTIVITIES AND  
MEAN  $^{210}\text{Pb}$  ACTIVITIES MEASURED AT DEPTH IN  
'LONG' CORES

<u>Core</u>	<u>Mean <math>^{226}\text{Ra}</math> Activity(dpm.g<sup>-1</sup>)</u>	<u>Mean <math>^{210}\text{Pb}</math> Activity(dpm.g<sup>-1</sup>)</u>
E. Mediterranean	1.20	1.67
Loch Lomond	1.81	2.06
Gareloch	1.70	2.16
Loch Goil	1.73	2.10

In each section,

- (a) supported  $^{210}\text{Pb}$  is equivalent to that measured at depth,
  - (b) supported  $^{210}\text{Pb}$  is equivalent to measured  $^{226}\text{Ra}$
- or
- (c) supported  $^{210}\text{Pb}$  takes some value intermediate between (a) and (b) above.

Options (a) and (b) are relatively straightforward. In applying (c) the following initial assumption is made; the difference between measured supported  $^{210}\text{Pb}$  activities at depth (i.e.  $^{226}\text{Ra}$  values at depth) and surface values is due to excess surficial  $^{226}\text{Ra}$  which has been deposited from overlying waters by some as yet undefined process and has not arisen through upward migration from deep in the core. On this basis, a preliminary estimate of the rate of sediment accumulation is made using option (a), from which an initial age/depth curve is derived. An estimate of  $^{210}\text{Pb}$  growth from 'excess  $^{226}\text{Ra}$ ' for each section is then made on the basis of this curve and an iterative technique applied to derive the optimal estimate of sedimentation rate and supported  $^{210}\text{Pb}$ . The method of correction for supported  $^{210}\text{Pb}$  and the reasons for its choice are indicated for each core.

In profiles of excess  $^{210}\text{Pb}$ , error values associated with individual data points are not constant with depth but increase as the magnitude of total  $^{210}\text{Pb}$  approaches that of supported  $^{210}\text{Pb}$ . Simple linear regression analysis, on log of excess  $^{210}\text{Pb}$  against depth, could therefore be a biased estimator of sedimentation rates by placing equal reliance on all data and ignoring associated errors. In this study, errors are accounted for via a weighted linear regression analysis programme, with weighting proportional to the square of the

percentage error on individual excess  $^{210}\text{Pb}$  values. For example, for Loch Lomond core LLRPMI, simple 'best-fit' straight line analysis yields a value of  $27 \text{ mg cm}^{-2} \text{ y}^{-1}$  for the rate of sediment accumulation in comparison to  $22 \text{ mg cm}^{-2} \text{ y}^{-1}$  from weighted linear regression analysis. The programme also estimates the error on the regression coefficient.

### 3.2 Eastern Mediterranean

Tables 19, 20 detail some of the basic information on the Cilicia Basin core. Table 21 presents the results of the analytical investigations, the corresponding total  $^{210}\text{Pb}$  and  $^{226}\text{Ra}$  profiles are shown in fig. 24, and that for porosity in fig. 25a.

The  $^{210}\text{Pb}$  profile is contained in the upper few centimetres of the core (fig. 24) and exhibits a very rapid decline from a surface activity of slightly less than  $6 \text{ dpm.g}^{-1}$ , to a 'constant' value of around  $1.3 \text{ dpm.g}^{-1}$  at depths below 8 cm.  $^{226}\text{Ra}$  measurements on four sections of the core range from  $0.9 \text{ dpm.g}^{-1}$  to  $1.4 \text{ dpm.g}^{-1}$ , with a mean of  $1.2 \pm 0.2 \text{ dpm.g}^{-1}$ , which is the value used as a measure of supported  $^{210}\text{Pb}$  in determination of the sedimentation rate. Fig. 26 shows the semi-log plot of excess  $^{210}\text{Pb}$  versus depth ( $\text{mg.cm}^{-2}$ ) on this basis. Weighted linear regression analysis yields a sedimentation rate of  $16 \pm 3 \text{ mg.cm}^{-2}\text{y}^{-1}$ , corresponding to a  $0.34 \text{ mm.y}^{-1}$  mean rate of sediment accumulation in the upper 10 cms of the deposit. As the porosity shows very little decrease with depth (fig. 25a) this value is also a good measure of the rate of sediment growth at the sediment/water interface. The derived surface activity of excess  $^{210}\text{Pb}$  is  $5.4 \text{ dpm.g}^{-1}$  from which an annual flux of excess  $^{210}\text{Pb}$  to the sediment surface of around  $0.09 \text{ dpm.cm}^{-2}$  is computed. No  $^{137}\text{Cs}$  activity is observed, even in the surface layer of the deposit.

The core was recovered from off the southern Turkish coast between Turkey and Cyprus (fig 27). The sampling site, adjacent to the Goksu delta, is thought to receive a substantial input of detrital material from this source (extensive geochemical and mineralogical investigations have confirmed that the

sediments in the area comprise material characteristic of the adjacent landmasses (Shaw and Bush, 1978)). However, in the absence of an alternative direct estimate of the rate of sediment accumulation in the basin, it is difficult to comment on the feasibility of the observed value.

The estimated sedimentation rate could be greater than the 'true' rate for one or a combination of the following reasons:

- (1) if the upper layers of the deposit are subject to biological reworking or to any marked degree of physical disturbance by bottom currents, the net effect would be to transport surface material of high  $^{210}\text{Pb}_{\text{excess}}$  activity to depth in the core giving rise to an erroneously high estimate of the sedimentation rate,
- (2) Partial mixing of the upper layers of the deposit due to physical disturbance during the process of coring could also lead to the observed profile.

If option (1) is taken to extreme and the true sedimentation rate assumed negligible with respect to the half-life of  $^{210}\text{Pb}$  (e.g.  $<0.01 \text{ mm.y}^{-1}$  or 1 mm in five half-lives of  $^{210}\text{Pb}$ ), in the absence of biological reworking all of the excess  $^{210}\text{Pb}$  would be concentrated in the upper 1 mm of the sample. By assuming that the observed exponential profile of  $^{210}\text{Pb}_{\text{excess}}$  results from biological mixing, a biological mixing coefficient can be derived using equation 5.

$$\frac{dA}{dt} = \frac{d(K_b \frac{dA}{dz})}{dz} - \frac{s dA}{dz} - \lambda A$$

Under steady state conditions and assuming  $K_b$  to be constant over the mixing depth and  $s$  to be negligible, the equation

reduces to

$$K_b \frac{d^2 A}{dz^2} - \lambda A = 0 \quad \text{for which a solution is}$$

$$A = A_0 e^{-\left(\frac{\lambda}{K_b}\right)^{\frac{1}{2}} z}$$

Solving this equation for core 188 yields a value for  $K_b$  of  $8.5 \times 10^{-2} \text{ cm}^2 \text{ y}^{-1}$ , which is in good agreement with biological mixing coefficients evaluated in deep-sea deposits using microtektite, plutonium isotope and  $^{210}\text{Pb}$  excess distributions in the surface layers of deposits (Nozaki et al., 1977; Guinasso and Schink, 1975). Biological mixing coefficients quoted for near-shore sediments are, however, normally around two orders of magnitude greater than those for deep-sea sediments. The discrepancy would seem to rule out biological mixing as a reason for the observed  $^{210}\text{Pb}$  distribution. Further evidence which indicates that biological reworking is not responsible for the profile arises from X-radiographs of the core which show almost featureless fine grained sediments in the top 30 cms. with no apparent bioturbation or breaks in sedimentation (Shaw, personal communication). Furthermore, the sediments are very low in organic carbon, with average values of  $\sim 0.3\%$  and it is unlikely that this would be sufficient to support a substantial animal community.

The absence of any measurable concentration of  $^{137}\text{Cs}$  could have several explanations:

- (1) Loss of the uppermost layers of the deposit during sampling. Even with a sedimentation rate as high as  $16 \text{ mg. cm}^{-2} \text{ y}^{-1}$ ,  $^{137}\text{Cs}$  accumulation from bomb fallout would be confined to the upper  $1\frac{1}{2}$  cm. of the column. Loss of these layers and disturbance of the topmost sediment recovered (even in relatively low porosity

sediments such as this) are not uncommon in gravity coring (this phenomenon will be discussed more fully when considering results obtained for Clyde sea-loch sediments);

- (2) Levels of radiocaesium in the sediment may have been so diluted by mixing that they lie below the limits of detection of the analytical equipment;
- (3) Total  $^{137}\text{Cs}$  carried down to the sediment, may without mixing, be below the limit of detection.  $^{137}\text{Cs}$  is to a good first approximation non-reactive in sea-water (Brewer, 1975 quotes an oceanic residence time of  $6 \times 10^5$  y for stable caesium); hence in marine systems not experiencing high material fluxes (from biological sources or continental run-off) little caesium is likely to be concentrated on settling particulates. For example, the estimated total concentration of  $^{137}\text{Cs}$  in Clyde Sea Area sediments is <1% of the total  $^{137}\text{Cs}$  which has passed through the area yet particulate concentrations are considerably higher there than in the Cilicia basin (MacKenzie, 1977; McKinlay, 1978).

There is, however, some evidence from three independent sources to suggest that the topmost layers of the deposit have been lost from the core. Noshkin and Bowen (1973), in examination of a core from a site between Italy and Sardinia in the Mediterranean, observed a concentration of  $^{137}\text{Cs}$  in the upper layer of around 3.5% of the total inventory of  $^{137}\text{Cs}$  delivered to the area from atmospheric fallout for which they used a value of  $106 \pm 22 \text{ mCi km}^{-2}$  ( $23.3 \text{ dpm.cm}^{-2}$ ) (based on latitudinal inventories of fallout deposition). Noshkin

and Bowen also derived a residence time of only 300 years for radiocaesium in this marine environment, three orders of magnitude lower than the estimate of Brewer for stable caesium in the deep-sea. Assuming a similar value for  $^{137}\text{Cs}$  fallout at the Cilicia station, a similar percentage removal to the sediment and the sedimentation rate derived above, on the basis of no mixing, the generated  $^{137}\text{Cs}$  profile would be confined to the upper  $1\frac{1}{2}$  cm as indicated above and would have a concentration of around  $3 \text{ dpm.g}^{-1}$ . This activity would be easily measured. Under the particular conditions operating at time of analysis, the lower limit of detection was  $<1.5 \text{ dpm.g}^{-1}$  (McKinley, pers. comm.). Consequently if uniform fallout is assumed for the area, it seems most likely that the top layers of deposit have been lost during sampling.

Further justification for loss of surface material is inferred from consideration of the estimated flux of excess  $^{210}\text{Pb}$  to the deposit. It is well established that the atmospheric flux of  $^{210}\text{Pb}$  varies with latitude (Nozaki and Tsunogai, 1973) and is dependent on a number of factors including proximity to continental landmass, amount of rainfall and direction of prevailing winds. For example the atmospheric flux of  $^{210}\text{Pb}$  to Antarctic glaciers is  $0.005 \text{ dpm.cm}^{-2}\text{y}^{-1}$  (Windom, 1969), that to Germany ranges from 0.45 to  $1.0 \text{ dpm.cm}^{-2}\text{y}^{-1}$  (Jacobi and Andre, 1963) while Fukunda and Tsunogai (1972) determined a value of around  $2.0 \text{ dpm.cm}^{-2}\text{y}^{-1}$  for Japan near the Asian continent (table 22). The estimated flux of  $\sim 0.1 \text{ dpm.cm}^{-2}\text{y}^{-1}$  for the Cilicia Basin is therefore considerably less than the 'average' estimate of global  $^{210}\text{Pb}$  fallout of  $0.5 \text{ dpm.cm}^{-2}\text{y}^{-1}$ . (Rama et al., 1961; Goldberg, 1963). Furthermore, the

contribution from in-situ production of  $^{210}\text{Pb}$  from decay of  $^{226}\text{Ra}$  in the overlying water column must be considered. Koczy (1958) found uniform values of  $^{226}\text{Ra}$  in the Mediterranean, and derived a mean value of around  $0.7 \times 10^{-13} \text{g.l}^{-1}$  or  $0.15 \text{dpm.l}^{-1}$  of  $^{226}\text{Ra}$ . Using this estimate, the standing crop of  $^{226}\text{Ra}$  in a 570 metre water column is  $\sim 8.6 \text{dpm.cm}^{-2}$ , from which  $\sim 0.26 \text{dpm.cm}^{-2}\text{y}^{-1}$  of  $^{210}\text{Pb}$  would be generated. Assuming this  $^{210}\text{Pb}$  to be rapidly incorporated into the sediments, the activity of  $^{210}\text{Pb}$  estimated to be produced from in-situ decay of  $^{226}\text{Ra}$  alone is greater than the derived total flux of  $^{210}\text{Pb}$  to the sediment.

Finally, the surface sediments of the Mediterranean are known to be extensively contaminated by anthropogenic wastes. It would therefore be expected that if the uppermost layers of the deposit were recovered during coring some evidence of pollution would be present, e.g. high levels of pollutant trace metals. Although trace metal analyses were not available for Core 188, profiles of trace metal concentration in a core (core 1092, table 23) sampled from a nearby station showed no variability of trace metal levels with depth. This therefore provides indirect evidence that the topmost layers of sediment were not recovered efficiently during coring.

From the foregoing discussion, it is clear that the bulk of the evidence, i.e. the absence of (1) any increase in porosity near the core top; (2) pollutant trace metals; and (3) measurable concentrations of  $^{137}\text{Cs}$ , combined with the unrealistically low estimate of  $^{210}\text{Pb}$  flux to the sediment/water interface, strongly suggests that loss of surface material occurred during coring. Consequently, the estimate of  $16 \text{mg.cm}^{-2}\text{y}^{-1}$  is best regarded as a lower limit estimate of

the rate of sediment accumulation in the Cilicia Basin since the uncollected surface sediments would be expected (1) to have higher water content and (2) to contain anthropogenic inputs. Both factors would imply increased rates of sediment accumulation close to the sediment/water interface.



TABLE 20                      CHEMICAL AND MINERALOGICAL ANALYSES  
OF GRAB SAMPLES FROM STATION 188

<u>Chemical Analyses</u>				<u>Mineralogical Analyses</u>	
	%		ppm		%
CaCO <sub>3</sub>	30.9	Sr	431	Clay minerals	50
Ca	12.6	Mn	3080	Calcite	20
Mg	3.30	Zn	81	Quartz	15
Fe	4.28	Cu	41	Mg, calcite	5
		Ni	202	Dolomite	5
		Cr	310	Feldspar	< 5
		Ti	3350		

TABLE 21

## CILICIA BASIN GRAVITY CORE 188 : RESULTS OF ANALYTICAL INVESTIGATIONS

Section (cm)	Wet Wt. (g)	Dry Wt. (g)	Porosity <sup>1</sup> (%)	$^{210}\text{Pb} + 1\sigma$ (dpm.g <sup>-1</sup> )	$^{226}\text{Ra} + 1\sigma$ (dpm.g <sup>-1</sup> )	$^{210}\text{Pb}_{\text{xs}} + 1\sigma^2$ (dpm.g <sup>-1</sup> )	$^{137}\text{Cs}$
0 - 1	8.17	5.07	59.9	5.82 ± 0.21	0.92 ± 0.07	4.6 ± 0.3	B.D. <sup>3</sup>
1 - 2	14.58	8.97	60.4	3.29 ± 0.15		2.1 ± 0.3	
2 - 3	17.59	10.84	60.3	2.13 ± 0.14	1.35 ± 0.07	0.9 ± 0.2	
3 - 4	15.96	9.95	59.6	1.71 ± 0.11		0.5 ± 0.2	
4 - 5	19.38	12.10	59.5				
5 - 6	19.46	12.16	59.4				
6 - 7	17.51	10.88	59.8	1.42 ± 0.11	1.41 ± 0.10	0.2 ± 0.2	
7 - 8	15.56	9.72	59.4				
8 - 9	18.69	11.55	60.2				
9 - 10	20.08	12.78	58.2	1.35 ± 0.12	1.07 ± 0.08		
15 - 16	24.01	<del>25.14</del>	60.3	1.13 ± 0.11			
25 - 26	22.13	<del>24.04</del>	58.7	1.32 ± 0.11			

1. Porosity evaluated using assumed sediment density of 2.5 g.cm<sup>-3</sup>

2. Excess  $^{210}\text{Pb}$  evaluated using supported  $^{210}\text{Pb} = 1.2 \pm 0.2$  dpm.g<sup>-1</sup> (mean value of  $^{226}\text{Ra}$ )

3. B.D. = below detection limit (see text)

for the Eastern Mediterranean core

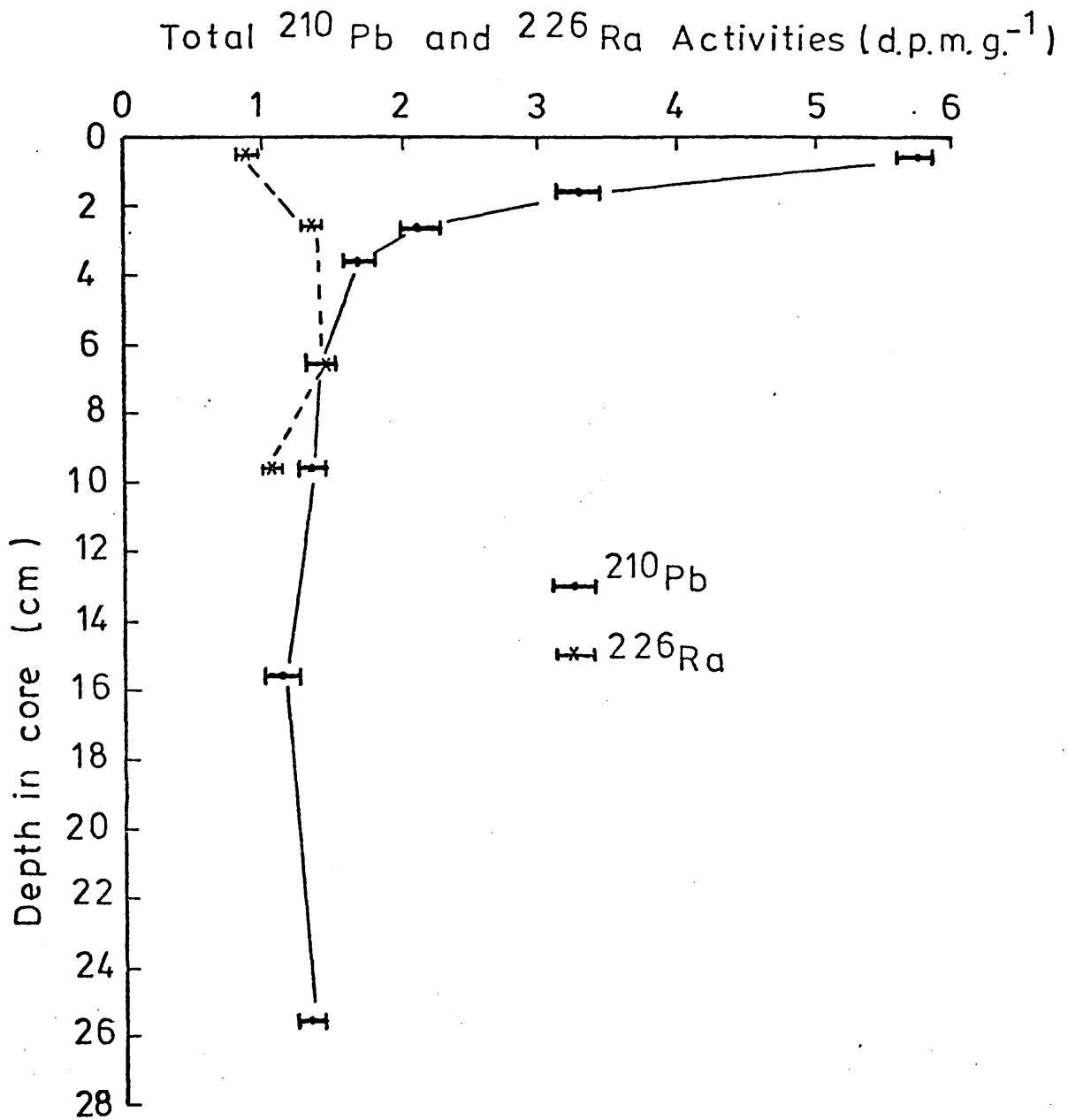


FIGURE 25a Porosity profile for the

Eastern Mediterranean core

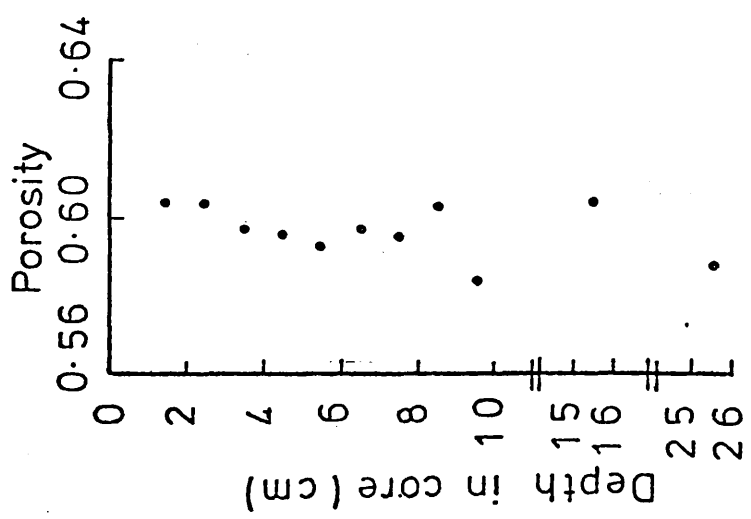


FIGURE 25b Curve of age (calendar date) against

depth for the Eastern Mediterranean core

Calendar date

(no mixing)

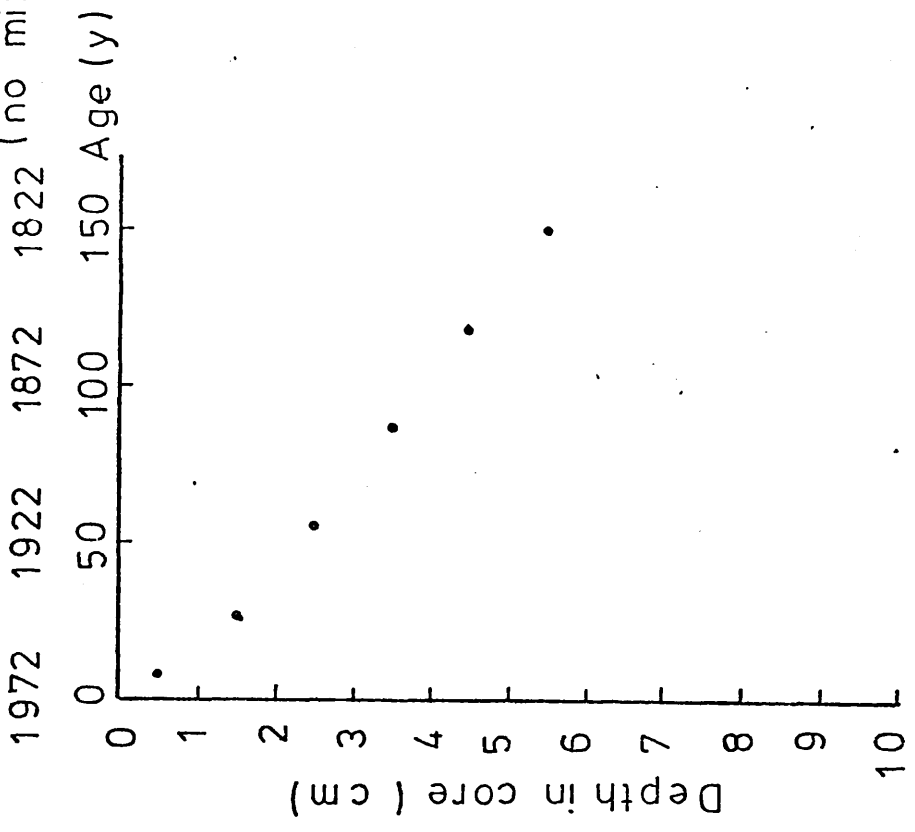


FIGURE 26    Depth profile of excess  $^{210}\text{Pb}$  for the  
Eastern Mediterranean core

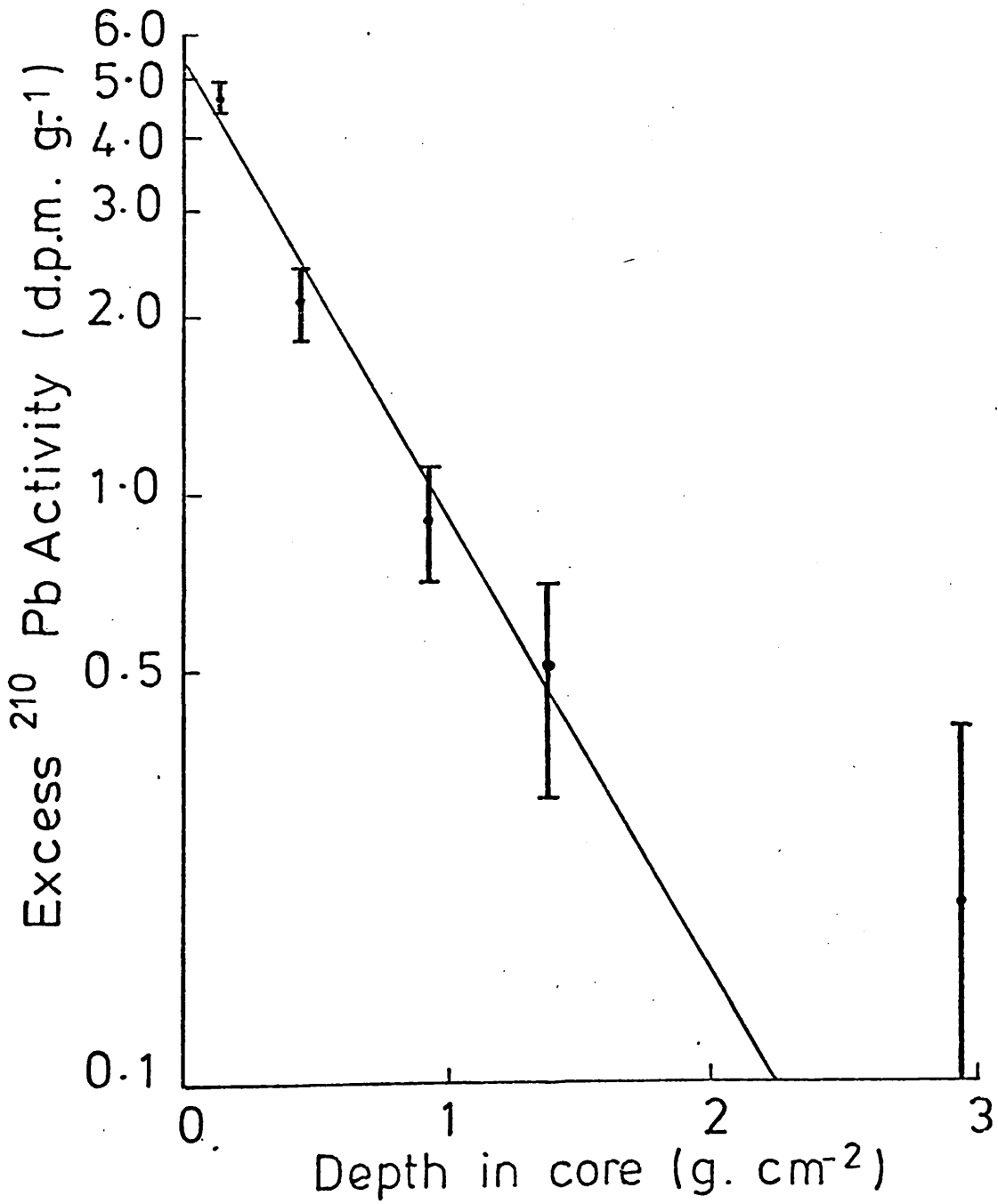


FIGURE 27      Cilicia Basin sampling station

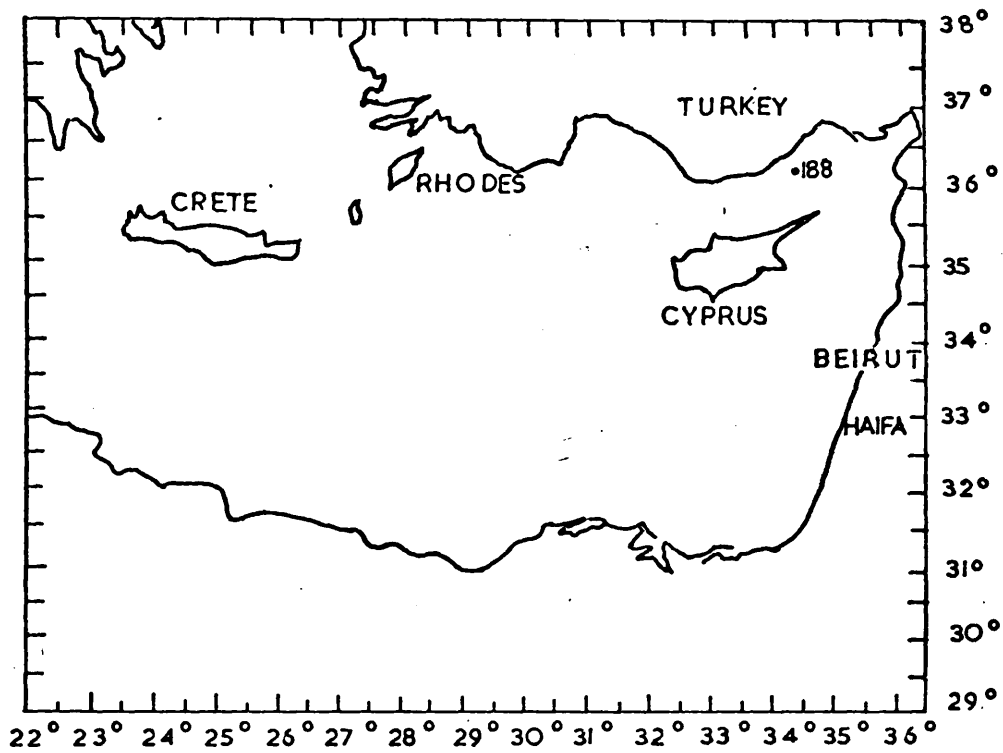


TABLE 22                    MEAN ANNUAL FLUXES OF  $^{210}\text{Pb}$  IN  
PRECIPITATION AT VARIOUS GEO-  
GRAPHICAL LOCATIONS.

<u><math>^{210}\text{Pb}</math> Activity</u> <u>dpm cm<sup>-2</sup> y<sup>-1</sup></u>	<u>Geographical</u> <u>Area</u>	<u>Reference</u>
0.005	Antarctica glaciers	Windom, 1969
0.11	Greenland glaciers	Windom, 1969
2.0	Japan	Fukuda and Tsunogai, 1972
0.38	England (Harwell)	Burton and Stewart, 1960
0.53	France	Lambert and Nezami, 1965
0.44 to 1.0	Germany	Jacobi and Andre, 1963
0.18	U.S.A.	Ter Haar et al., 1967

TABLE 23 CHEMICAL ANALYSIS ON CILICIA BASIN CORE 1092 (SHAW, 1975)

Sample	% Ca	% Mg	% Fe	Sr (ppm)	Mn (ppm)	Cu (ppm)	Zn (ppm)	Ni (ppm)	Cr (ppm)	% CaCO <sub>3</sub>
1092										
0-2 cms	12.52	2.88	3.90	296	1380	30	80	200	440	32.3
2-5 cms	12.52	2.88	4.00	282	700	30	90	210	410	
5-10 cms	12.30	2.88	3.90	282	720	30	80	210	410	
45-50 cms	12.18	3.03	3.90	282	624	30	80	210	440	31.6
80-85 cms	12.30	2.94	4.00	282	646	30	80	210	440	
115-118	12.30	2.88	3.90	282	628	30	90	210	410	
143-148	12.26	2.88	3.80	303	618	30	80	220	500	
178-183	12.18	3.03	4.00	275	586	30	80	210	450	30.9
232-237	12.10	2.96	3.90	282	620	30	80	210	430	
277-281	12.26	2.96	4.00	260	614	30	90	210	340	
321-326	12.16	2.94	3.80	268	628	30	80	220	370	
361-366	12.10	2.88	4.00	268	620	30	80	210	430	30.5
401-406	12.20	2.88	4.00	268	610	30	80	210	340	
441-446	12.10	2.99	3.70	290	610	30	90	220	440	
466-471	12.10	3.00	3.80	275	604	30	90	210	410	30.7

### 3.3 Loch Lomond

Table 24 presents basic information on the Loch Lomond mini-Mackereth core, LLRPM1, while table 25 presents the results of the analytical investigations. Fig. 28 indicates the Loch Lomond sampling station and profiles of total  $^{210}\text{Pb}$  and  $^{226}\text{Ra}$ ,  $^{137}\text{Cs}$  and porosity are shown in figs. 29,30,31 respectively.

The profile of total  $^{210}\text{Pb}$  activity versus depth (fig 29) exhibits the classical exponential decrease from the sediment surface, where an activity of around  $22 \text{ dpm.g}^{-1}$  is observed, to a constant value of  $\sim 1.7 \text{ dpm.g}^{-1}$  at depths greater than 15 cms. Similarly,  $^{226}\text{Ra}$  concentrations show a steady decline from the sediment/water interface, where a maximum  $^{226}\text{Ra}$  concentration of greater than  $3.0 \text{ dpm.g}^{-1}$  is recorded, to depth, where a mean activity of around  $1.8 \text{ dpm.g}^{-1}$  occurs.

In estimating a value for supported  $^{210}\text{Pb}$  the three alternatives outlined in section 3.1 may be applied. Sedimentation rates have been derived for each of the initial assumptions (a) (b) and (c) and weighted linear regression analysis yields values of  $21.3 \pm 1.7 \text{ mg.cm}^{-2}\text{y}^{-1}$ ,  $22.1 \pm 2.1 \text{ mg.cm}^{-2}\text{y}^{-1}$  and  $21.7 \pm 1.8 \text{ mg.cm}^{-2}\text{y}^{-1}$  respectively. In this instance because the total  $^{210}\text{Pb}$  activity is high and both the absolute value of  $^{226}\text{Ra}$  and its variation with depth are by comparison small, the difference in the derived sedimentation rates is insignificant. Fig. 32 shows the logarithmic plot of excess  $^{210}\text{Pb}$  versus depth based on the results of the iterative approach. Using a value of  $22 \text{ mg.cm}^{-2}\text{y}^{-1}$  for the sedimentation rate an age/depth curve for this core is developed (fig 33) and an estimate of  $\sim 1.2 \text{ mm.y}^{-1}$  derived for the thickness of sediment representing one year's increment at the sediment surface. From the sedimentation rate of  $22 \text{ mg.cm}^{-2}\text{y}^{-1}$  and the

derived surface activity of  $^{210}\text{Pb}$  of  $24.6 \text{ dpm.g}^{-1}$ , an estimate of  $0.54 \text{ dpm.cm}^{-2}\text{y}^{-1}$  is obtained for the flux of excess  $^{210}\text{Pb}$  to the sediment/water interface. This compares reasonably favourably with the estimate of  $\sim 0.38 \text{ dpm.cm}^{-2}\text{y}^{-1}$  for atmospheric  $^{210}\text{Pb}$  fallout obtained by Burton and Stewart (1960) from rainfall measurements at Harwell. An indication of the contribution of  $^{210}\text{Pb}$  arising from in-situ decay of  $^{226}\text{Ra}$  can be obtained from the data of Conlan et al (1969) who found a mean concentration of  $\sim 0.06 \text{ dpm.l}^{-1}$  for  $^{226}\text{Ra}$  in Loch Lomond surface waters. Based on a 26 metre water column, this  $^{226}\text{Ra}$  concentration implies a  $^{210}\text{Pb}$  flux from this source of  $< 0.01 \text{ dpm.cm}^{-2}\text{y}^{-1}$ , clearly insignificant relative either to atmospheric input or to the amount shown to be accumulating in the sediment. The small difference between these latter values may be produced by input from the catchment of eroded material containing sorbed  $^{210}\text{Pb}$ .

$^{137}\text{Cs}$  determined in this fresh-water core is entirely that due to atmospheric fallout; therefore the maximum depth at which it is found in an undisturbed deposit should be equivalent to an age of around 20 years. The depth distribution of  $^{137}\text{Cs}$  in core LLRPM1 is shown in fig. 30. Radiocaesium is confined largely to the upper 2 to 3 cms. of the deposit, and decreases exponentially below this level with an elongated 'tail' extending to a depth of some 7 cms. The profile is therefore consistent with a  $^{210}\text{Pb}$  age of around 20 years, or a calendar date of ca. 1957, for the 2 cm. level. The tail observed for  $^{137}\text{Cs}$  suggests some degree of downward diffusion or mixing, and indeed this could also be inferred from the slight flattening of the  $^{210}\text{Pb}$  profile in the upper 2 cms. of the deposit. Similar  $^{137}\text{Cs}$  tails have been reported by other workers (e.g. Pennington

et al., 1973; 1975). Any mixing effect is probably due to bottom currents or slight disturbance during coring since Loch Lomond does not support a large population of benthic fauna and as powerful subsurface currents are indeed common in the loch. As discussed previously, the net effects of surface mixing are to increase the apparent sedimentation rate and to generate erroneously young ages for specific layers. If the process giving rise to the  $^{137}\text{Cs}$  tail is operating with equal efficiency for  $^{210}\text{Pb}$  (not necessarily a valid assumption) then  $^{210}\text{Pb}$  ages may be artificially young. However, the magnitude of the downward displacement of radiocaesium on a percentage activity basis is extremely small so that any effect on  $^{210}\text{Pb}$  activities would also be minimal; hence the estimated sedimentation rate and derived ages should be accurate. Furthermore,  $^{137}\text{Cs}$  by its presence provides good evidence that the surficial layers of sediment have been successfully recovered during coring; indeed the total inventory of  $^{137}\text{Cs}$  in the column is consistent with that expected from atmospheric input. Pennington et al (1973) estimated the total deposition of  $^{137}\text{Cs}$  via rainfall on several lakes of the English Lake District, based on cumulative measured deposition at Millford Haven. Their mean value of  $\sim 44 \text{ dpm.cm}^{-2}$  compares with a total integrated activity of  $\sim 42 \text{ dpm.cm}^{-2}$  estimated for the Loch Lomond core. This agreement is remarkable, even although it must be remembered that the contribution of fallout over the catchment has not been included in the calculation. The latter input might be expected to contribute a significant activity due to  $^{137}\text{Cs}$  sorbed on incoming material. Balancing this to some extent, radio-caesium removal from water, even in a freshwater environment, is unlikely to reach an efficiency of 100%. There is therefore

strong evidence to suggest that the surface of the sediment was recovered in relatively undisturbed condition. Further circumstantial evidence supporting this belief is the observation of a distinct colour change between sections 1 and 2 in the core; the relatively light surficial material may be indicative of a thin surface oxidised zone overlying sediment of a more reduced nature.

A third time parameter, albeit of a less rigorous nature, is introduced to this study in the form of palaeomagnetic data. Profiles of intensity, declination and inclination are shown in fig. 34 (Thompson and Turner, 1976). The most recent westerly declination swing occurred ~155 years ago or around AD 1820, and this can be used to estimate modern sedimentation rates assuming uniform deposition between this horizon and the mud surface. However, if there is a time-lag between sedimentation and stabilisation of the magnetic remanence, the true 155 B.P. horizon would be observed at relatively greater depth in the sediment. On this basis, the turning point A (fig 34) corresponding to a depth of 25 cms. in the core is assigned a calendar age of around AD 1800 (Turner and Thompson, personal communication). If the  $^{210}\text{Pb}$  time-scale estimated for the upper layers of the deposit is extrapolated back to 25 cms., an age of around 460 years is obtained for this horizon, in marked disagreement to that based on palaeomagnetic evidence. For these time-scales to be brought into harmony, a substantial increase in sedimentation rate would have to be postulated for this core, between the depths (time period) containing the  $^{210}\text{Pb}$  profile and the palaeomagnetically-dated horizon. Some evidence for such an occurrence can be derived from the  $^{210}\text{Pb}$  data between 8 cms. and 15 cms., which, taken at face value,

show a marked shallowing of the profile (figs.29,32). In fact, a best fit straight line through the last four data points (fig.32) yields a sedimentation rate of  $63 \pm 13 \text{ mg.cm}^{-2}\text{y}^{-1}$ . By combining the sedimentation rate of  $22 \text{ mg.cm}^{-2}\text{y}^{-1}$  for the upper 8 cms with the larger value for deeper sediment, the 25 cm. section assumes an age of 200 years, i.e. around AD 1775 in better agreement with the palaeomagnetic result. This interpretation is however clearly speculative, since (a) it is 'dangerous' to extrapolate an estimated sedimentation rate beyond the applicable range of any dating technique and (b) the  $^{210}\text{Pb}$  radiometric evidence of a change in sedimentation rate is slender, being derived from data whose associated errors are very large.

However, there is some additional evidence that the natural processes of sedimentation in the south basin of Loch Lomond may have been substantially disrupted at some time in the recent past. Fig. 35 shows the results of  $^{14}\text{C}$  dating of a 5m Mackereth core recovered from a nearby location in the south basin of Loch Lomond. Drndarski (1977) estimated a natural sedimentation rate of  $\sim 0.3 \text{ mm.y}^{-1}$  on the basis of linear  $^{14}\text{C}$  dates at depth, but observed considerable apparent disturbance to the deposit in the upper 2 metres of the core. Erroneously 'old'  $^{14}\text{C}$  ages are commonly found in the upper layers of sediment columns, attributable to introduction of fossil or aged soil carbon to the sediments in recent years. However, in this particular case, an apparently young  $^{14}\text{C}$  age was derived at  $\sim 90$  cm depth, between layers apparently contaminated with old carbon. Furthermore, an anomalous variation in the concentration of aluminium and manganese also occurs at this depth (MacKenzie, 1978, personal communication), indicating that a major change in the composition of the sediments depositing at the site

may have occurred. The nature of the disturbance remains undefined at present, but may be compatible with a sudden input of a considerable quantity of material by slumping or a similar process. Interestingly, if the sedimentation rate of  $22 \text{ mg.cm}^{-2}\text{y}^{-1}$  derived for core LLRPM1 is used to estimate a value for the rate of accumulation at infinite compaction, using the equation

$$s = \frac{\omega}{\rho_s} \left( \frac{1}{1-\sigma} \right) \quad (\text{Berner, 1971})$$

and assuming a value of 0.76 for the porosity of the sediment at infinite compaction (fig. 31) (in fact, there is an indication from the porosity profile of this core at depths below 60 cms. that a marked change in sediment composition has occurred, with the introduction of material capable of retaining a relatively higher % water content, possibly organic) a sedimentation rate of  $\sim 0.36 \text{ mm.y}^{-1}$  is obtained in remarkably good agreement with that estimated by Drndarski from  $^{14}\text{C}$  ages. In view of the above it is tempting to suggest that the natural processes of sedimentation in the south basin of the loch which gave rise to a sedimentation rate of  $\sim 0.3 \text{ mm.y}^{-1}$  have been considerably disrupted at some time in the recent past. Conditions of sedimentation have since stabilised and returned to a more usual pattern during the last century. Furthermore, on  $^{210}\text{Pb}$  evidence, the modern rate of sediment accumulation may not be greatly different to that pertaining over the last 5000 years.

On the basis of the above arguments, the rate of sediment accumulation appears well-defined, at least over the last 100 years, from  $^{210}\text{Pb}$  dating and  $^{137}\text{Cs}$  radiometric evidence.

However, if the palaeomagnetic date of around AD 1800 for the 25 cm. horizon is accepted as correct and assuming a constant rate of sediment accumulation from this depth to the sediment/water interface, a value of  $57 \text{ mg.cm}^{-2}\text{y}^{-1}$  is derived for the sedimentation rate from the cumulative weight of sediment deposited since the 1800 horizon. A timescale based on this sedimentation rate would, however, require the bulk of the radiocaesium contained in the upper 2 cms. to have been deposited in the 8 years prior to sampling, i.e. from ~1969 onwards, a clearly unacceptable postulate. Only if the upper few centimetres of deposit were completely lost during sampling would the radiocaesium timescale become largely consistent with the palaeomagnetically dated horizon. From the palaeomagnetic evidence alone, a surface sedimentation rate of around  $3 \text{ mm.y}^{-1}$  is indicated. Hence loss of only 2 to 3 cms. of sediment would be sufficient to bring the palaeomagnetic and radiocaesium chronologies into agreement. The difference to the total estimated accumulation of  $^{137}\text{Cs}$  would of course be minimal since proportionately very little fallout  $^{137}\text{Cs}$  occurred in these latter years. Alternatively, it must be postulated that a time-lag of around five years has occurred between maximum atmospheric fallout of  $^{137}\text{Cs}$  and its incorporation in the loch deposit and this in turn would infer that most of the  $^{137}\text{Cs}$  falling directly on the loch and carried initially to the loch from the catchment escaped removal to the underlying sediment - i.e. the bulk of  $^{137}\text{Cs}$  observed in the deposit now is that initially adsorbed on soil in the catchment and only later eroded and transported to the loch. This conclusion is however in contradiction to the results of Pennington et al (1973; 1975) who observed the atmospheric fallout pattern of  $^{137}\text{Cs}$  to be well-preserved in

the sediments of several English lakes. They concluded that even if  $^{137}\text{Cs}$  sorbed on soil particles in the catchment were contributing to  $^{137}\text{Cs}$  levels in the sediment, the delay between adsorption of  $^{137}\text{Cs}$  by these particles and incorporation into the deposit must be short. Furthermore, these cores were also collected by a 1m Mackereth corer similar to that used in recovery of the Loch Lomond sample and no loss of surface sediment was inferred in their study.

Fig.36 presents the lead profile for this core (Farmer, 1978). It is typical of coastal marine and loch sediments adjacent to heavily industrialised regions, with the considerably higher levels of lead concentration observed at the surface attributable to cultural mobilisation. Taking surface concentrations as  $\sim 150$  ppm, a 15-fold increase in lead input to the sediment is indicated. Based on the  $^{210}\text{Pb}$  derived sedimentation rate of  $22 \text{ mg.cm}^{-2}\text{y}^{-1}$  a present anthropogenic flux of around  $3 \text{ }\mu\text{g.cm}^{-2}\text{y}^{-1}$  is estimated; while that based on palaeomagnetism would be considerably higher at  $\sim 8 \text{ }\mu\text{g.cm}^{-2}\text{y}^{-1}$ . Commencement of significant industrial activity in the area can be traced back to  $\sim$ AD 1750 with introduction of the woollen and dye industries to the Leven valley. Rising lead concentrations in sediments younger than this are therefore reasonable so that the trace metal results are compatible with either of the chronologies outlined previously.

In conclusion then,  $^{210}\text{Pb}$  and  $^{137}\text{Cs}$  distributions lead to entirely self-consistent timescales over the last century, and a steady state of sediment accumulation of  $\sim 22 \text{ mg.cm}^{-2}\text{y}^{-1}$  is implied; furthermore, on this basis, the Mackereth corer appears to retain surface sediments intact, the purpose for which it was specially designed. There is considerable

circumstantial evidence from a wide range of independent parameters, including  $^{14}\text{C}$ , metals,  $^{210}\text{Pb}$ , and porosity, that some disturbance to the natural processes of sediment accumulation occurred in the region between 100 and 200 years ago. If this is so, and under these circumstances the palaeomagnetic record has survived intact despite disturbance to the sediment, the AD 1800 horizon is in fact in reasonable agreement with the radiometric evidence.



TABLE 25 LOCH LOHOND MINI-MACKERETH CORE LLRPM1 ; RESULTS OF ANALYTICAL INVESTIGATIONS

Section (cm)	Wet Wt. (g)	Dry Wt. (g)	Porosity <sup>1</sup> (%)	CaCO <sub>3</sub> <sup>2</sup> (%)	Microanalysis (%) <sup>2</sup>		
					C	H	T or N <sup>3</sup>
0 - 1	27.38	4.33	93.0	0.91	4.94	1.89	T or N <sup>3</sup>
1 - 2	27.95	5.51	91.1	0.39	6.21	1.69	"
2 - 3	26.92	5.53	90.7	0.38	6.00	1.62	"
3 - 4	28.61	6.27	89.9	0.34	3.95	1.32	"
4 - 5	27.37	6.18	89.5	0.39	3.29	1.13	"
5 - 6	30.53	7.02	89.2		3.36	1.46	"
6 - 7	30.79	7.30	88.9	0.38			
7 - 8	25.81	6.19	88.8	0.58	3.10	1.09	"
8 - 9	28.57	7.03	88.5	0.29			
9 - 10	28.71	7.87	86.9	0.30	2.49	1.17	"
10 - 11	29.66	8.22	86.7				
11 - 12	30.41	9.97	83.7				
12 - 13	30.61	9.49	84.8				
13 - 14	31.79	10.59	83.4				
14 - 15	30.71	10.01	83.8	0.27	2.42	0.94	"
15 - 16	33.62	11.53	82.7				
16 - 17	31.72	10.91	82.7				
17 - 18	32.70	11.54	82.1				
18 - 19	32.04	11.41	81.9				

TABLE 25 (cont'd) LOCH LOMOND MINI-MACKERETH CORE LLRPM1 : RESULTS OF ANALYTICAL INVESTIGATIONS

Section (cm)	Wet Wt. (g)	Dry Wt. (g)	Porosity <sup>1</sup> (%)	CaCO <sub>3</sub> <sup>2</sup> (%)	Microanalysis (%) <sup>2</sup> C H N	T or N <sup>3</sup>
19 - 20	31.67	11.34	81.8	0.29	2.79	1.10 T or N <sup>3</sup>
20 - 22	63.09	24.10	80.2			
22 - 24	60.32	22.68	80.6			
24 - 26	60.17	24.37	78.6	0.17	2.66	0.98 "
26 - 28	61.87	24.25	79.5			
28 - 30	62.73	25.41	78.6	0.26		

1. Porosity evaluated using mean measured particle density of  $2.5 \pm 0.1 \text{ g.cm}^{-3}$

2. Percent CaCO<sub>3</sub>/microanalytical results on dry weight basis.

3. T = trace: N = nil

Section (cm)	$^{210}\text{Pb}_{\text{TOT}} \pm 1\sigma$ (dpm.g <sup>-1</sup> )	$^{226}\text{Ra} \pm 1\sigma$ (dpm.g <sup>-1</sup> )	$^{210}\text{Pb}_{\text{XS}} \pm 1\sigma^1$ (dpm.g <sup>-1</sup> )	$^{137}\text{Cs}$ (dpm.g <sup>-1</sup> )
0 - 1	21.9 ± 0.5	3.28 ± 0.24	20.1 ± 0.5	73 ± 4
1 - 2	19.2 ± 0.4	3.01 ± 0.22	17.4 ± 0.5	66 ± 3
2 - 3	13.9 ± 0.3	2.78 ± 0.21	12.1 ± 0.4	25 ± 2
3 - 4	9.29 ± 0.28	2.74 ± 0.20	7.5 ± 0.3	8 ± 1
4 - 5				5.0 ± 0.4
5 - 6	4.10 ± 0.14	2.49 ± 0.18	2.3 ± 0.2	
6 - 7				3.0 ± 0.4

TABLE 25 (cont'd) LOCH LOMOND MINI-MACKERETH CORE LLBPM1; RESULTS OF ANALYTICAL INVESTIGATIONS

Section (cm)	$^{210}\text{Pb}_{\text{TOT}} \pm 1\sigma$ (dpm.g <sup>-1</sup> )	$^{226}\text{Ra} \pm 1\sigma$ (dpm.g <sup>-1</sup> )	$^{210}\text{Pb}_{\text{XS}} \pm 1\sigma$ (dpm.g <sup>-1</sup> )	$^{137}\text{Cs}$ (dpm.g <sup>-1</sup> )
7 - 8	2.54 ± 0.09	1.98 ± 0.15	0.7 ± 0.2	
8 - 9				
9 - 10	2.25 ± 0.07	2.10 ± 0.16	0.5 ± 0.2	
10 - 11				
11 - 12	2.16 ± 0.08	2.00 ± 0.15	0.4 ± 0.2	
12 - 13				
13 - 14				
14 - 15	1.95 ± 0.07	1.96 ± 0.15	0.1 ± 0.2	
15 - 16.				
16 - 17				
18 - 19				
19 - 20	1.67 ± 0.06	1.54 ± 0.11	-	
20 - 22				
22 - 24				
24 - 26				
26 - 28				
28 - 30	1.66 ± 0.05	1.94 ± 0.14	-	

1. Excess  $^{210}\text{Pb}$  evaluated using supported  $^{210}\text{Pb} = 1.8 \pm 0.2 \text{ dpm.g}^{-1}$   
(mean of  $^{226}\text{Ra}$  determinations in sections 15, 20, 30)

River Falloch

FIGURE 28 Loch Lomond sampling station

+ Sampling Site  
(Ross Priory)

Loch Lomond

Endrick

Ross Priory

Blane W.

Balloch

River Leven

River Clyde

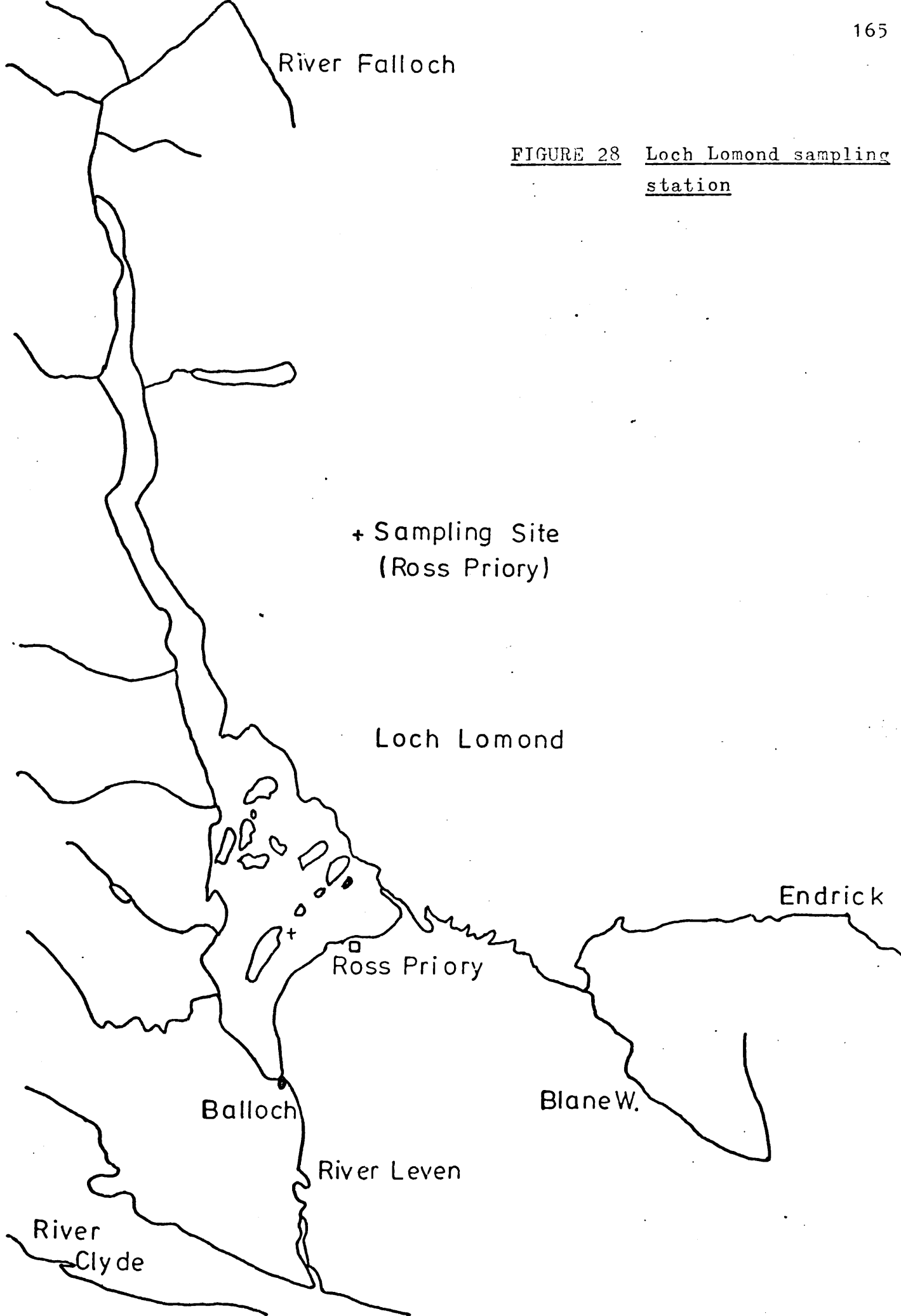


FIGURE 29 Depth profiles of total  $^{210}\text{Pb}$  and  $^{226}\text{Ra}$   
for Loch Lomond mini-Mackereth core LLRPM1

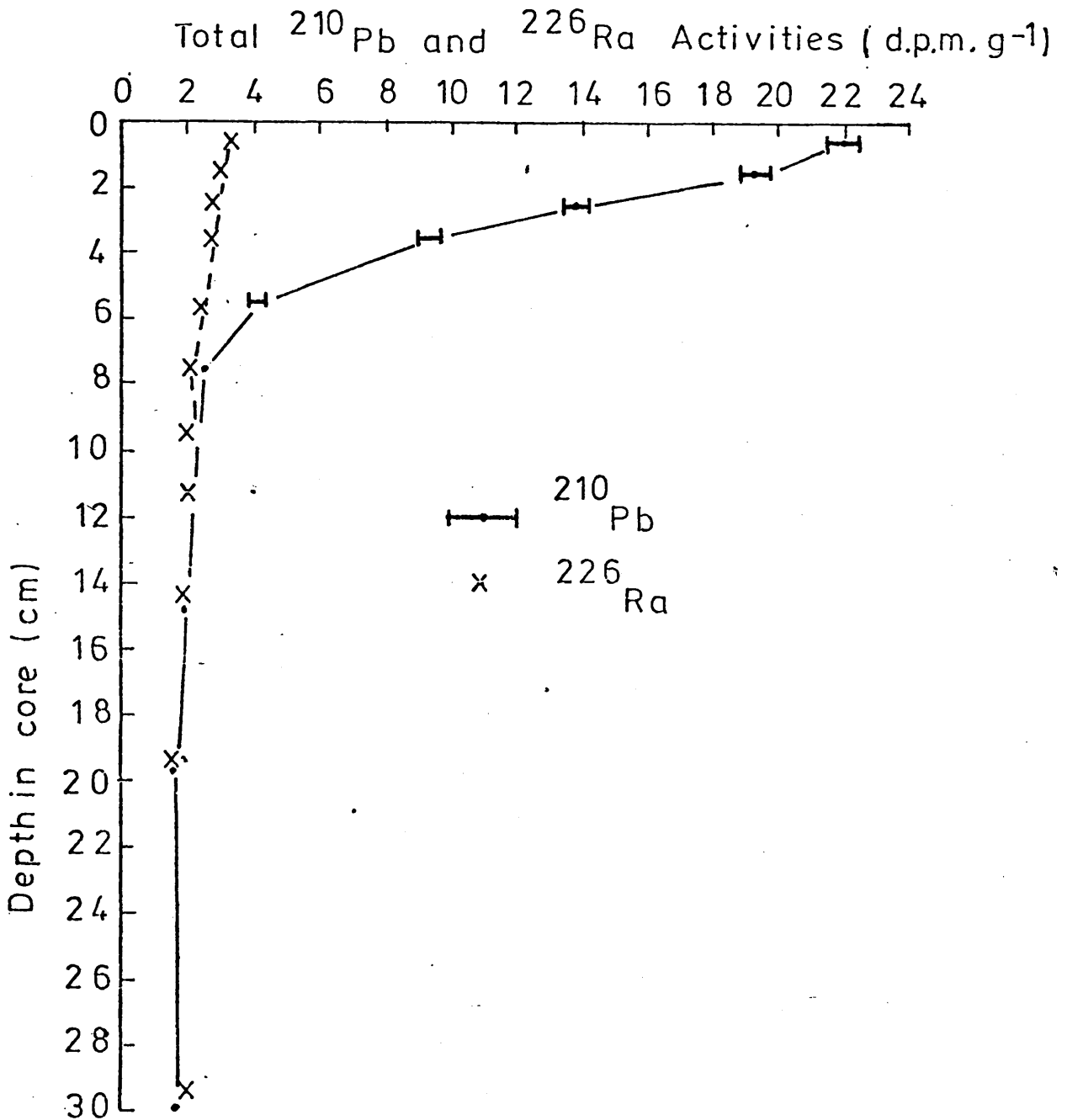
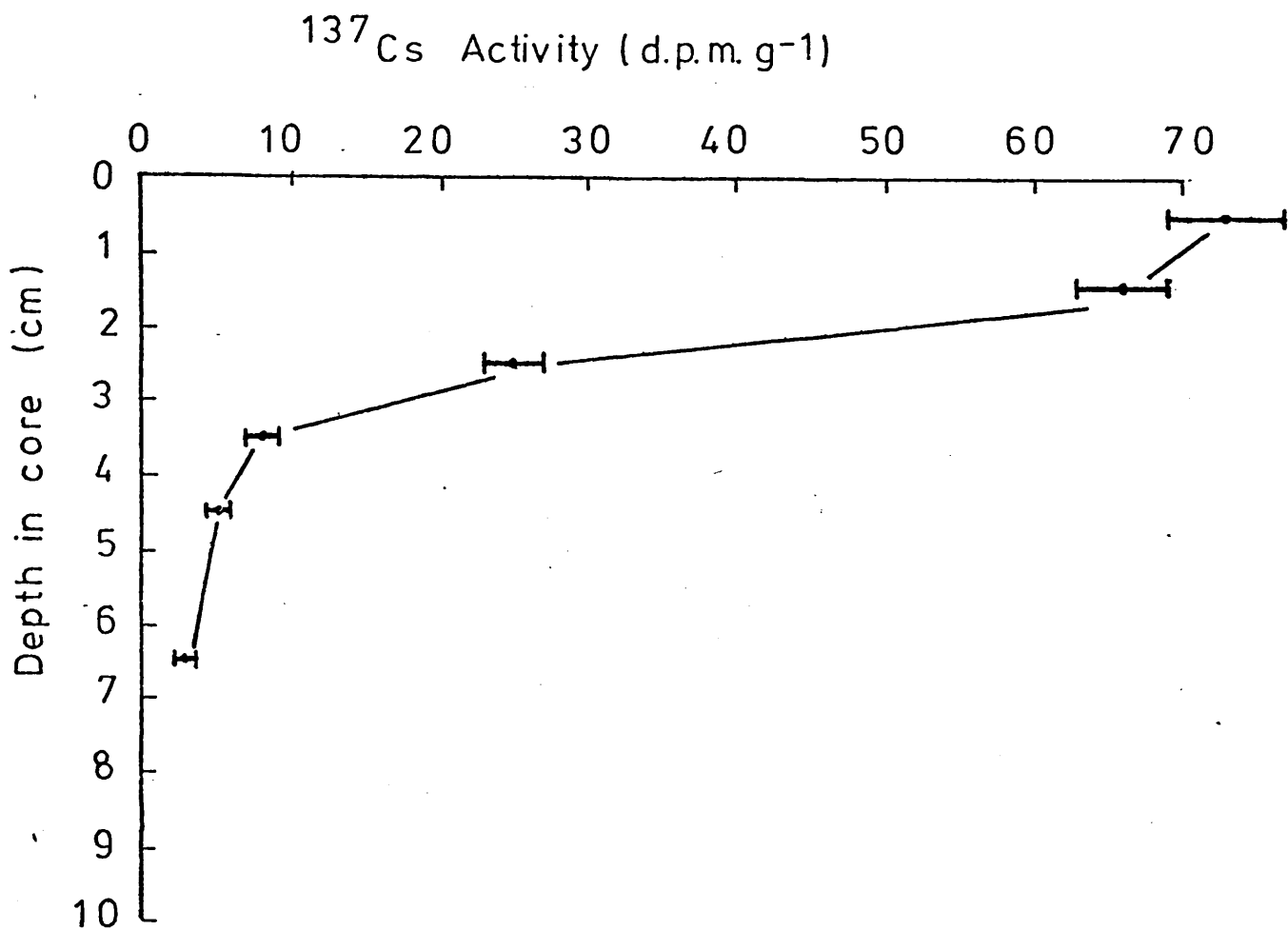


FIGURE 30  $^{137}\text{Cs}$  profile for Loch Lomond mini-Mackereth  
core LLRPM1



mini-Mackereth core LLRPM1

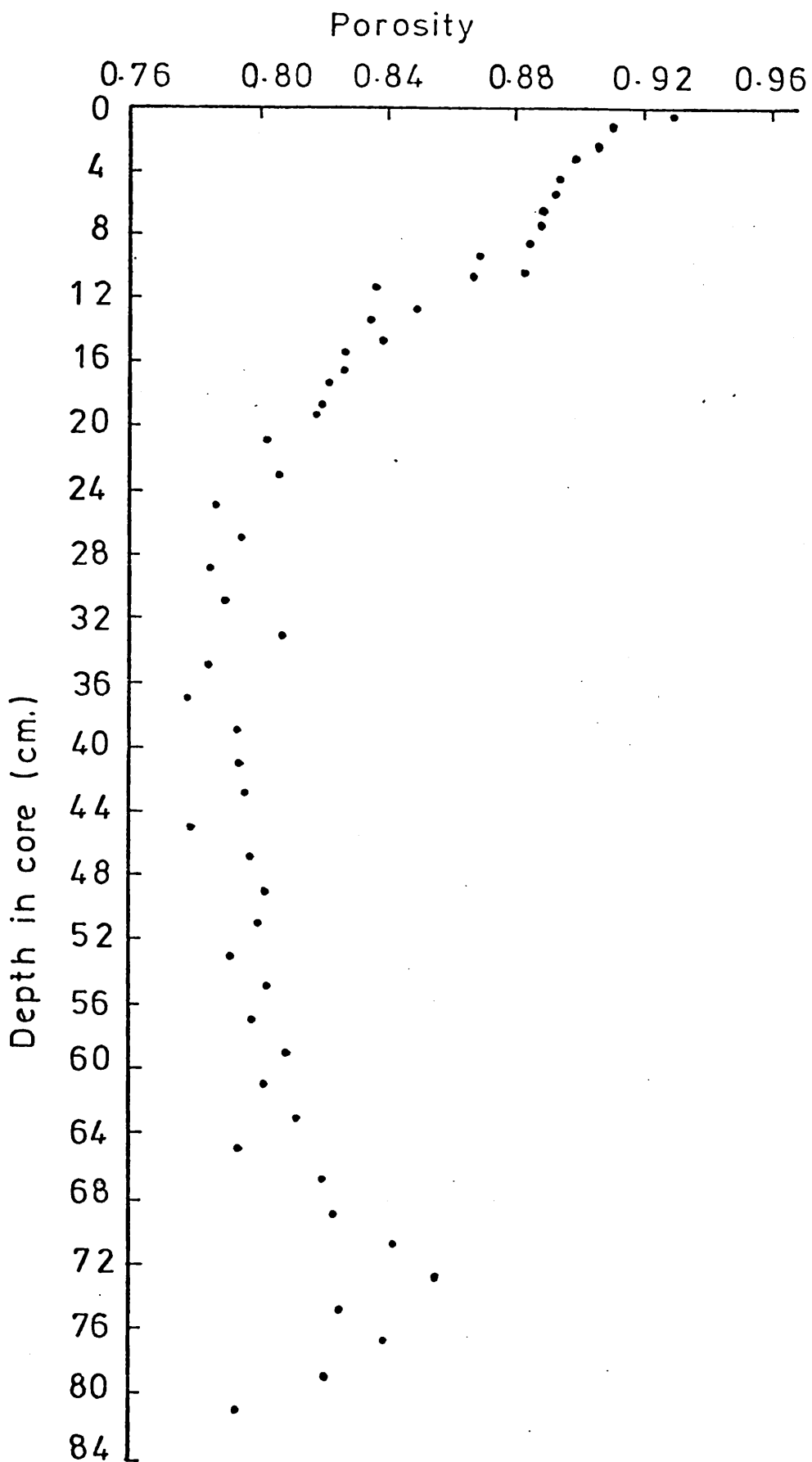


FIGURE 32 Depth profile of excess  $^{210}\text{Pb}$  for  
Loch Lomond mini-Mackereth core LLRPM1

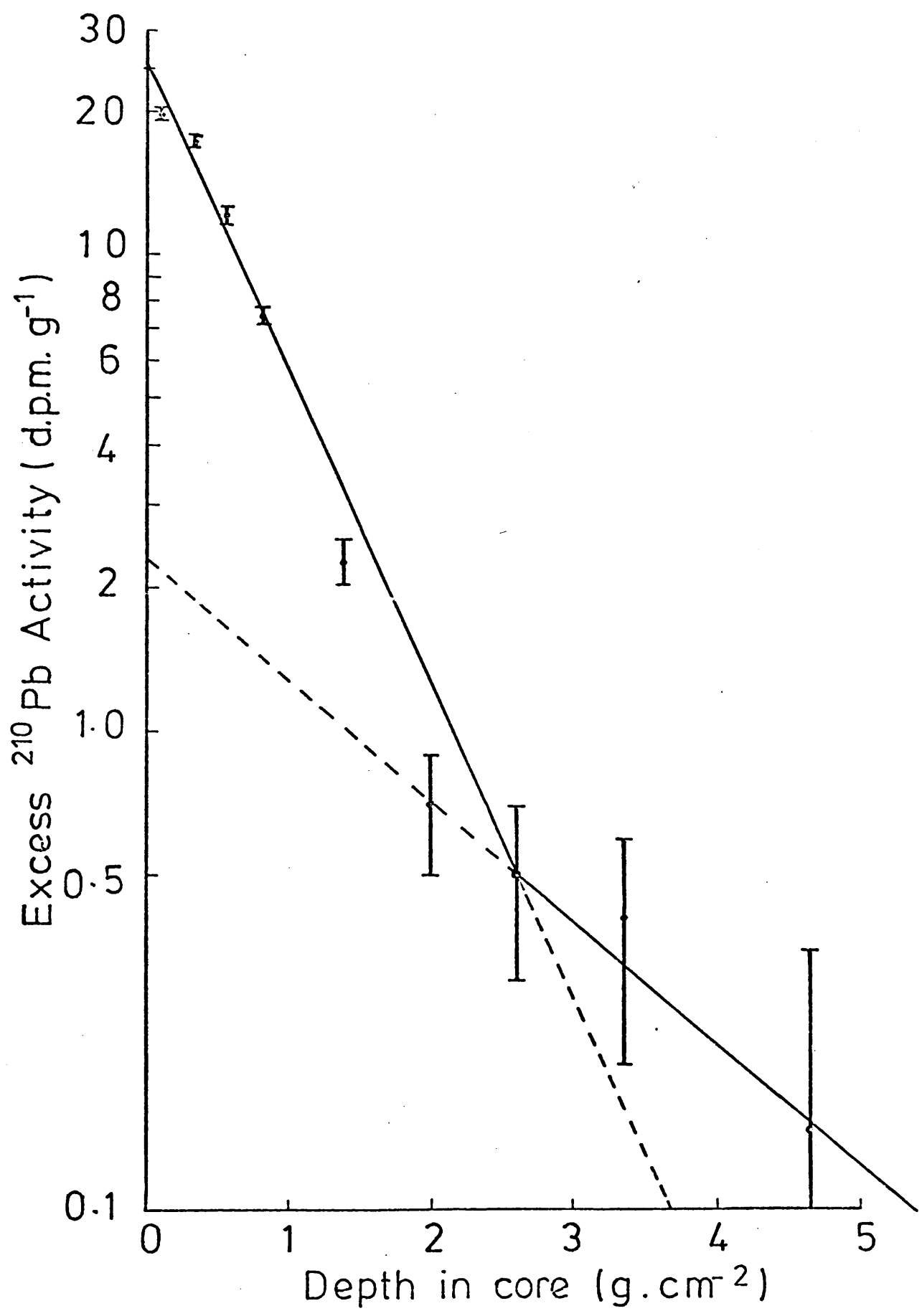


FIGURE 33 Curve of age (calendar date) against depth  
for Loch Lomond core LLRPM1 based on sediment-  
ation rate of  $22 \text{ mg cm}^{-2} \text{ y}^{-1}$

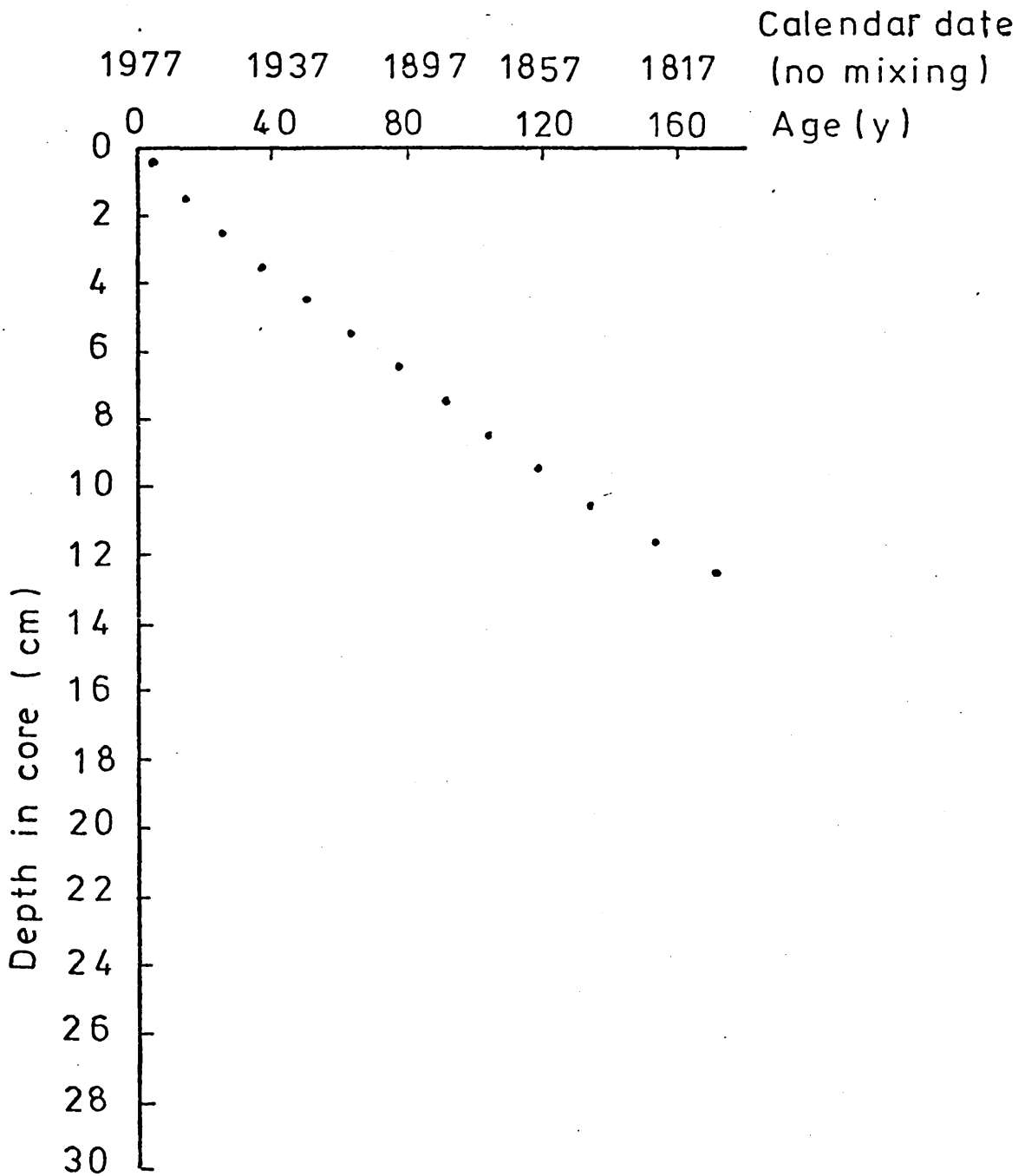


FIGURE 34 Magnetic measurements on Loch Lomond

mini-Mackereth core LLRPM1. (After Thompson and Turner, 1978, pers. comm.). The spacing of susceptibility readings is 2.6 cms, while that of intensity and declination is 5 cms.

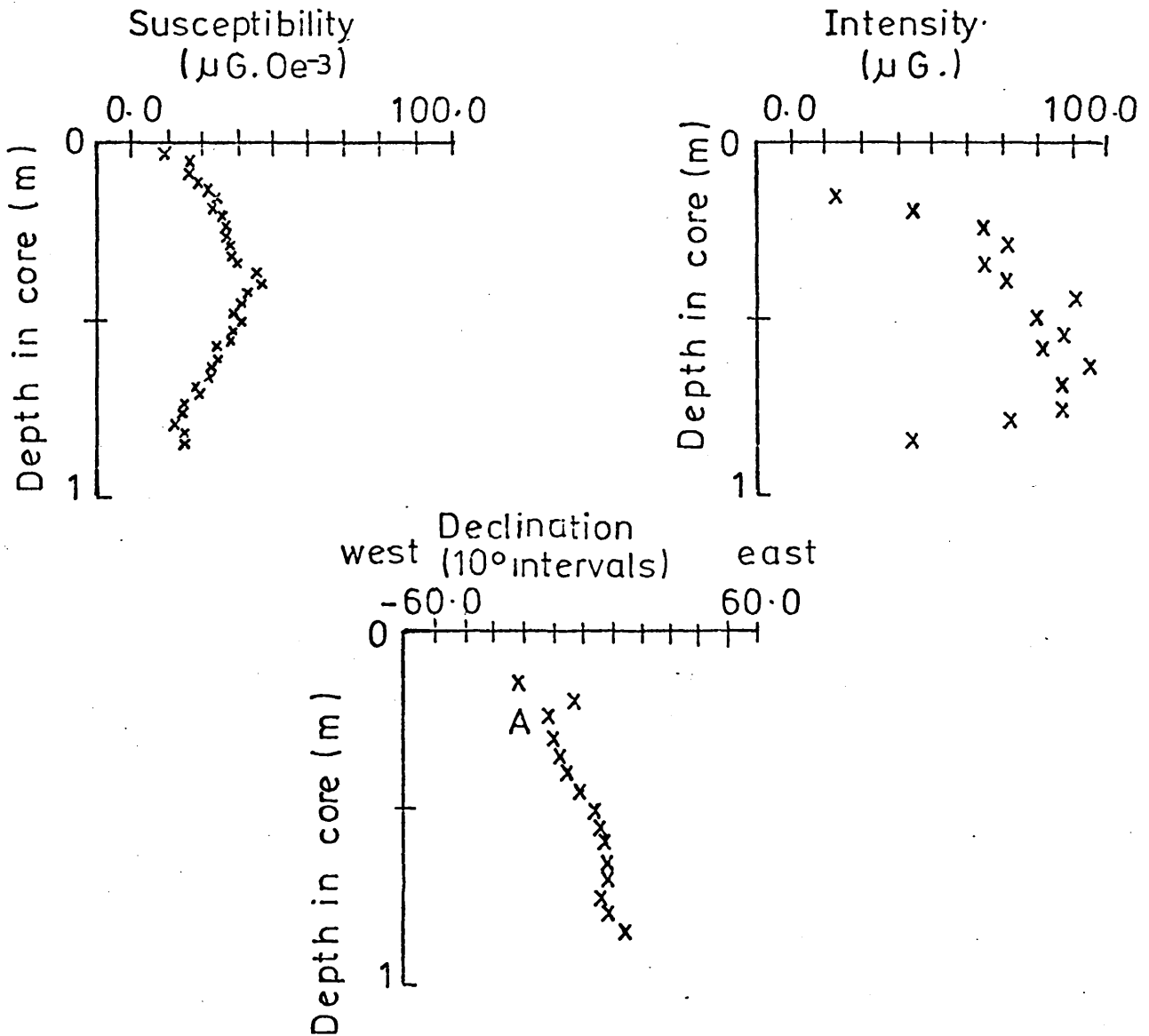


FIGURE 34a Curve of age (calendar date) against  
depth for Loch Lomond core LLRPM1 based  
on sedimentation rates of  $22 \text{ mg.cm}^{-2} \text{ y}^{-1}$   
to a depth of 8 cms. and  $63 \text{ mg.cm}^{-2} \text{ y}^{-1}$   
at greater depths.

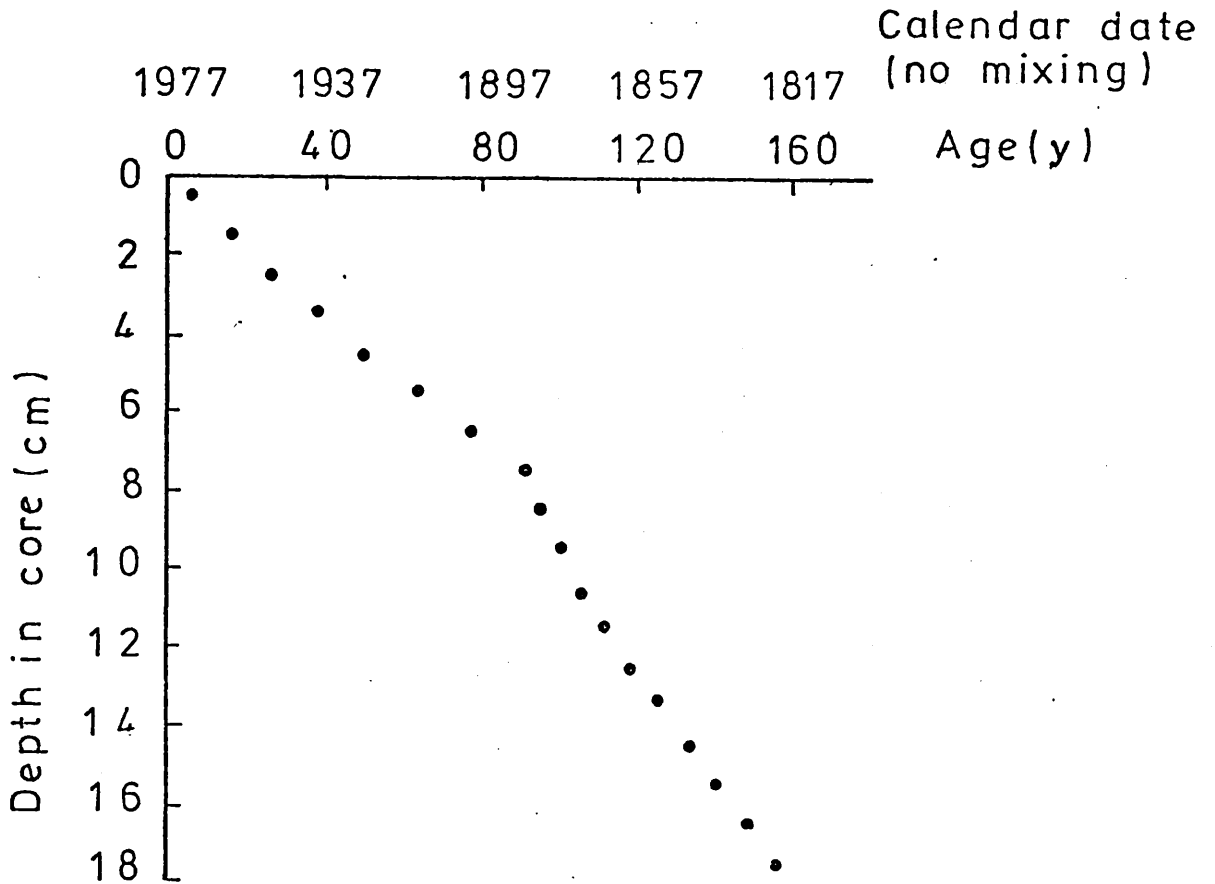


FIGURE 35 Radiocarbon Age, Calendar Age and Palaeomagnetic Age versus Depth

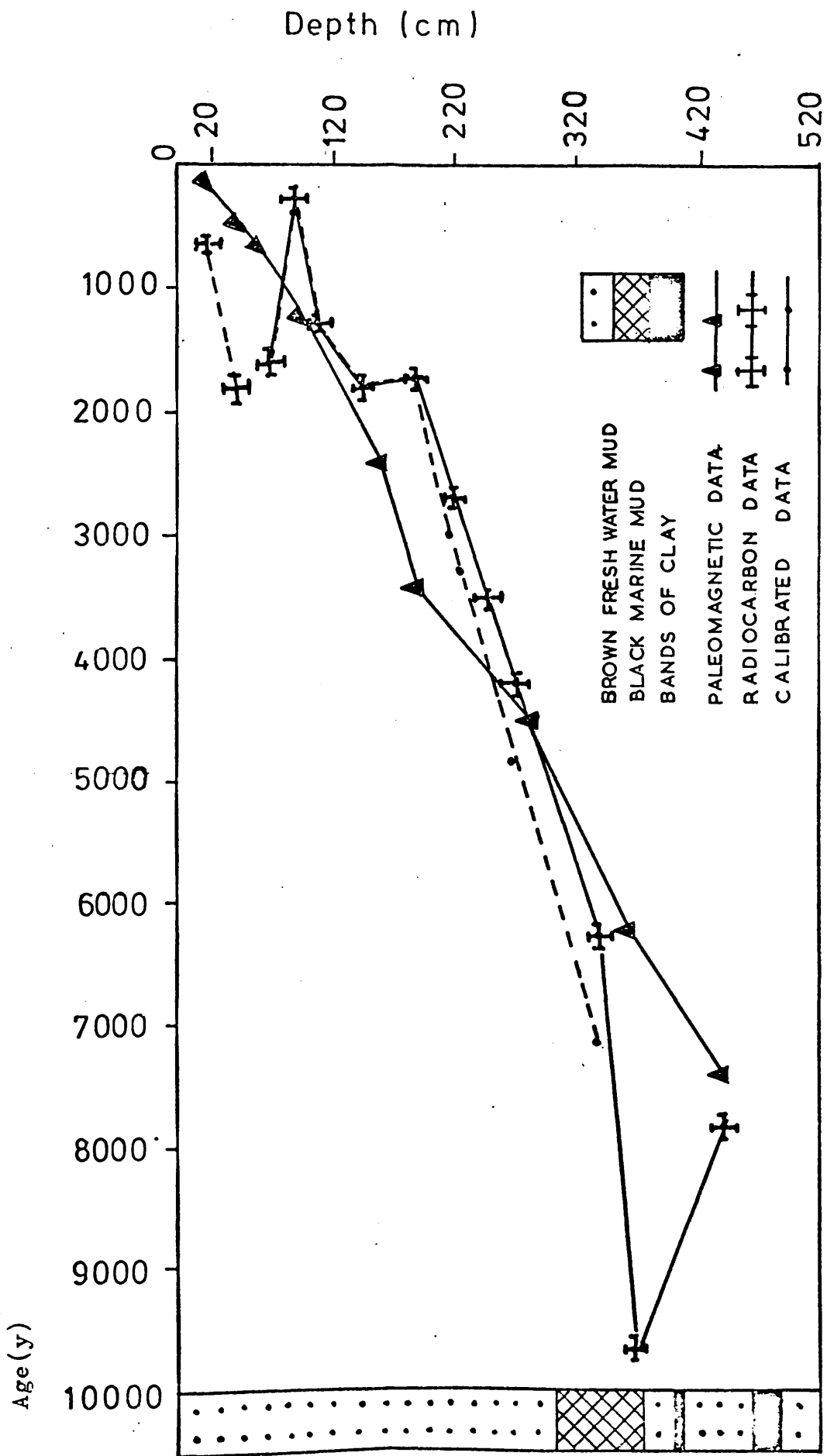
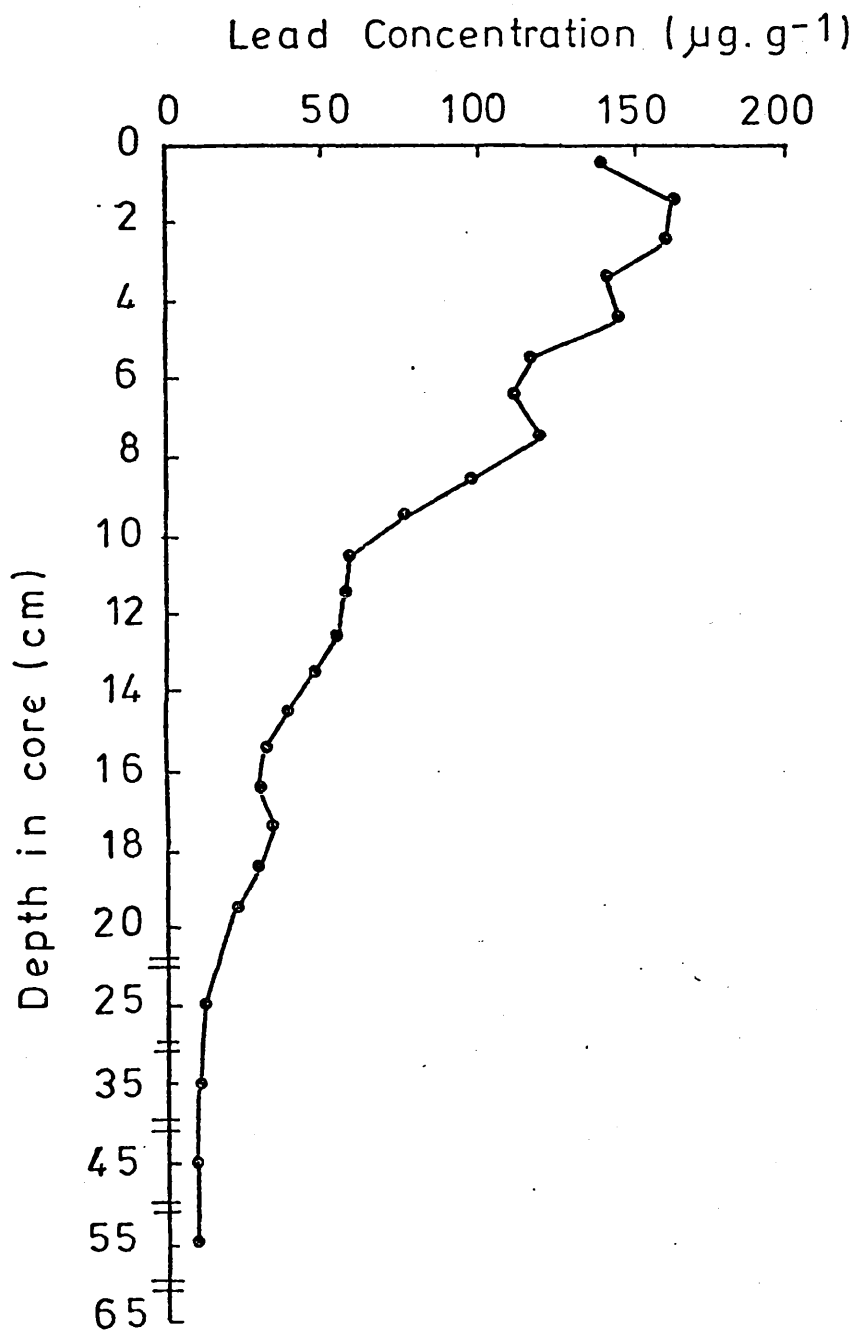


FIGURE 36    Depth profile of stable lead for  
Loch Lomond mini-Mackereth core LLRPM1



### 3.4 Clyde Sea-Loch Sediments : Gareloch and Loch Goil

In section 2.1 of Chapter 2 it was indicated that cores of sediment were recovered from the Clyde Sea Area using both gravity and Craib corers, the latter specifically designed to obtain undisturbed samples of surface sediment. By overlap of the results of Craib and gravity cores from individual sites it was the intention to obtain a complete profile of the distribution of  $^{210}\text{Pb}$  from the sediment/water interface to considerable depth. While there is good evidence to support the belief that the Craib corer fulfilled its specialised role and did indeed recover undisturbed material, there is also some evidence to suggest that the gravity corer was less efficient than had been anticipated in collecting representative sediment samples.

#### Gareloch

The sampling location for Gareloch is shown on page 183 (fig. 37) and the results of the analyses of a gravity and Craib core from this station are presented in the tables and figures of pages 184 to 203. These cores were collected during the same survey.

The total  $^{210}\text{Pb}$  distribution in gravity core GLG2 (fig 38) shows constant  $^{210}\text{Pb}$  activity in the upper 4 cms of the deposit consistent with a zone of biologically or physically mixed sediment. Beneath this mixed zone,  $^{210}\text{Pb}$  decreases exponentially towards a constant value of around  $1.8 \text{ dpm.g}^{-1}$  in sections deeper than 18 cms.  $^{226}\text{Ra}$  concentrations range from ca.  $1.6 \text{ dpm.g}^{-1}$  to  $1.9 \text{ dpm.g}^{-1}$  with the exception of section 1 where significantly higher activity of  $2.7 \text{ dpm.g}^{-1}$  is recorded. In estimating a sedimentation rate from excess  $^{210}\text{Pb}$  below the mixed zone,

supported  $^{210}\text{Pb}$  has been equated to the mean  $^{226}\text{Ra}$  concentration of  $1.7 \pm 0.1 \text{ dpm.g}^{-1}$ . Weighted linear regression analysis (fig. 42) yields a sedimentation rate of  $73 \pm 8 \text{ mg.cm}^{-2}\text{y}^{-1}$  ( $\sim 1.5 \text{ mm.y}^{-1}$ ), from which the age/depth curve of fig. 43 is derived; from this plot it can be seen that the thickness of sediment in the mixed zone corresponds to accumulation over a period equivalent to about 20 years. Assuming the upper 4 cms. of deposit to be homogeneous with respect to  $^{210}\text{Pb}$ , with a mean value of  $4.9 \pm 0.3 \text{ dpm.g}^{-1}$ , an estimate of the activity of unsupported  $^{210}\text{Pb}$  added to the sediment surface can be obtained using equation 3.

$$A_m = A_s / (1 + \frac{\lambda d}{w})$$

Thus  $A_s = 8.0 \pm 0.5 \text{ dpm.g}^{-1}$ , and a value of  $0.6 \text{ dpm.cm}^{-2}$  is derived for the annual flux of excess  $^{210}\text{Pb}$  to the sediment. Assuming a mean value for dissolved  $^{226}\text{Ra}$  of  $0.12 \text{ dpm.l}^{-1}$  (MacKenzie, 1977) and a water column of depth 48m, the contribution to this  $^{210}\text{Pb}$  flux from in-situ decay of  $^{226}\text{Ra}$  is estimated at around  $0.02 \text{ dpm.cm}^{-2}\text{y}^{-1}$  and is therefore insignificant. The value of  $0.6 \text{ dpm.cm}^{-2}\text{y}^{-1}$ , about  $1\frac{1}{2}$  times that estimated for the atmospheric flux of  $^{210}\text{Pb}$  ( $\sim 0.38 \text{ dpm.cm}^{-2}\text{y}^{-1}$ ) in this area, suggests that a sizeable proportion of excess  $^{210}\text{Pb}$  to the deposit arises from  $^{210}\text{Pb}$  associated with particulates entering the loch.

The  $^{210}\text{Pb}$  distribution for Craib core GLC3 is presented in fig. 44 and clearly shows little resemblance to that of the gravity core discussed above. Indeed, the  $^{210}\text{Pb}$  activity is relatively constant throughout the entire length of the core, decreasing by less than  $2 \text{ dpm.g}^{-1}$  from values of around  $8.4 \text{ dpm.g}^{-1}$  near the surface to about  $6.8 \text{ dpm.g}^{-1}$  at a depth of 15 cms.  $^{226}\text{Ra}$  concentrations are similar to those of the

gravity core and therefore typical of inshore marine sediments, with values ranging from 1 to 2 dpm.g<sup>-1</sup>.

A sedimentation rate of  $543 \pm 130 \text{ mg.cm}^{-2}\text{y}^{-1}$  is derived from weighted linear regression analysis (fig.47)(applying the same estimate of supported <sup>210</sup>Pb as used for GLG2), i.e. a sedimentation rate almost x8 greater than that estimated for the gravity core. This is equivalent to a surface sedimentation rate of  $\sim 2.5 \text{ cm.y}^{-1}$  or a mean rate of sediment accumulation over the core length of  $\sim 1.5 \text{ cm.y}^{-1}$ . An age/depth curve is presented in fig 49. From this sedimentation rate, a value of 6.6 dpm.g<sup>-1</sup> is obtained for excess <sup>210</sup>Pb depositing at the sediment/water interface, implying an estimated annual flux of unsupported <sup>210</sup>Pb to the sediment of  $3.6 \text{ dpm.cm}^{-2}$ . On this basis, by far the major input of excess <sup>210</sup>Pb is that brought to the sediment already adsorbed on particulate material entering the Gareloch, direct atmospheric fallout contributing a relatively minor amount.

Although these cores were collected virtually simultaneously from an 'identical' sampling location, there are clearly considerable differences between their respective <sup>210</sup>Pb profiles, perhaps the most striking of which is the observation of a higher specific <sup>210</sup>Pb activity in each section of the Craib core relative to even the top sections of the gravity core. The differences cannot therefore be explained in terms of gravity core compression; indeed, the cumulative total <sup>210</sup>Pb activity in the bottom 4 cms. of the Craib core ( $\sim 10.5 \text{ dpm.cm}^{-2}$ ) is very similar to that present in the upper 4 cms. of the gravity core ( $\sim 10.4 \text{ dpm.cm}^{-2}$ ). This is in fact the only respect in which the profiles are at all similar, the surface activity of <sup>210</sup>Pb in the mixed zone of the gravity core

(mean  $\sim 6.6$  dpm,  $g^{-1}$ ) being only slightly lower than that observed in the lower 6 cms. of the Craib core (mean  $\sim 6.9$  dpm,  $g^{-1}$ ). Therefore, if these cores represent sediment recovered from an equivalent site, considerable loss of surface material must have occurred during gravity coring; furthermore, the top of the gravity core may consist of material underlying that at the base of the Craib core, in which case more than 15 cms. of sediment appear to have been lost.

Consideration of the respective radiocaesium profiles (figs. 39, 45) confirms the differences apparent in the  $^{210}\text{Pb}$  data. In the Craib core, activities of  $^{137}\text{Cs}$  steadily decrease from the surface consistent with the increasing levels of the nuclide present in Clyde Sea Area waters through its rising discharge from Windscale since  $\sim 1952$ ;  $^{134}\text{Cs}$  concentrations show a similar trend. In contrast,  $^{137}\text{Cs}$  concentrations in the upper few cms. of the gravity core exhibit considerable variation and furthermore, the maximum observed activity is very much lower than that found in the Craib core. Below 4 cms.,  $^{137}\text{Cs}$  activities are less than those at the bottom of the Craib core and are decreasing. Moreover, no  $^{134}\text{Cs}$  is observed. The erratic distribution of  $^{137}\text{Cs}$  in the upper few cms. of the gravity core and the notable absence of  $^{134}\text{Cs}$  suggests that these layers of the recovered core are not undisturbed. Indeed the conclusion reached from comparison of the  $^{210}\text{Pb}$  profiles is generally supported, i.e. that around 15-20 cms. of the deposit have been lost during sampling. In addition, the radiocaesium results suggest that the upper 4 cms. of the gravity core represent the residue of both a substantial mixing effect and a loss of material. Such a combination is also consistent with  $^{210}\text{Pb}$  results.

Several additional points of interest arise from the radiocaesium profile of GLC3.

- (1) the profiles as observed are compatible with the increasing discharge of radiocaesium isotopes from Windscale, i.e. a postulate of physical/biological disturbance is not necessary to explain the profiles.
- (2) if the profiles represent the steady accumulation of undisturbed sediment, then the appearance of  $^{134}\text{Cs}$  (with a half-life of only 2.1y) in detectable amounts at a depth of 13 cms. indicates a very high rate of sediment accumulation (cf.  $^{210}\text{Pb}$ ). In fact, if the observation of  $^{134}\text{Cs}$  at 13 cms. is equated to its first release in significant quantities from Windscale (in 1968), then a sedimentation rate of around  $650 \text{ mg.cm}^{-2}\text{y}^{-1}$  is derived, in reasonable agreement to that based on  $^{210}\text{Pb}$  data. (On the assumption of no physical/biological disturbance and no caesium migration, this value would set a lower limit, since the 1968 to analysis period corresponds to  $\sim 3\frac{1}{2}$   $^{134}\text{Cs}$  half-lives. The concentration of the isotope accumulated in the sediment in 1968 would almost certainly have decayed below the limits of detection).
- (3) Although both the  $^{210}\text{Pb}$  and  $^{134}\text{Cs}$  profiles could be explained on the basis of a relatively slow rate of sediment accumulation (e.g. as derived from the  $^{210}\text{Pb}$  data of the gravity core) combined with sediment mixing, the  $^{137}\text{Cs}$  ( $t_{\frac{1}{2}} = 30\text{y}$ ) distribution does not lend itself to such an interpretation. For example, using the  $^{210}\text{Pb}$  sedimentation rate of  $73 \text{ mg.cm}^{-2}\text{y}^{-1}$ , all of the  $^{137}\text{Cs}$  would, in the absence of (biological) mixing,

be contained in the upper 4 cms. of the core. The mixing process would then be required to operate much more effectively with respect to redistribution of  $^{210}\text{Pb}$  (to produce an approximately constant profile of  $^{210}\text{Pb}$  activity throughout the 15 cms. of the core) relative to  $^{137}\text{Cs}$  which exhibits exponential decrease.

From the foregoing discussion of the radiochemical data it is therefore apparent that a substantial depth of surface sediment has been lost during gravity coring in these high porosity sediments. On the other hand, there is convincing evidence from  $^{210}\text{Pb}$  and radiocaesium data that the Craib corer has recovered relatively undisturbed cores of surface sediment. Consequently considerably more confidence can be placed in results obtained from cores recovered with this sampler.

With this in mind, the present picture of sedimentation in Gareloch from both  $^{210}\text{Pb}$  and radiocaesium data in Craib core GLC3 is that of a basin experiencing a very high rate of sediment accumulation, of the order of  $2 \text{ cm.y}^{-1}$ . Such a high rate of sedimentation is not inconsistent with expectations. The Gareloch is itself an arm of the Clyde Estuary which is, as indicated in the introduction, continually dredged. A large flux of resuspended particulates resulting from this operation could therefore be swept into the loch (a strong tidal current of  $\sim 5$  knots flows over the sill at the narrow entrance to the loch) to settle in this relatively deep trough; in other words, the Gareloch may act as a settling tank for sediments inwashed from the estuary. Interestingly, in 1892, Mill, in discussing the Gareloch described it as "in all parts thickly covered by sewage laden mud, carried in by tides from the estuary". Furthermore, the radionuclide data show no evidence to suggest intensive biological or physical reworking of these deposits; for example, although biological mixing or slumping would be consistent with the observed  $^{210}\text{Pb}$  profile, such alternatives

are not readily compatible with the evidence of the radio-caesium profiles since a more homogeneous radiocaesium distribution would be expected.

The stable lead profile for gravity core GLG2 is shown in fig.41, and that for GLC2, a further companion Craib core to GLC3, in fig. 50. Very high lead levels are observed throughout the 34 cms. of the gravity core, increasing sharply towards a maximum at a depth of ca. 4 to 7 cms. and then decreasing towards the sediment surface. In contrast, lead levels in core GLC2 are of similar magnitude at the core top to those observed at depth in GLG2, but increase linearly down the core. The stable lead profile is therefore also intriguing in itself.

On the basis of the general conclusions reached from interpretation of the radionuclide data, the concentration of any species in the upper few cms of the gravity core, as residual of a mixing/loss process, should reflect the concentration of that species in the overlying sediment (i.e. the Craib core); the concentration of lead ( $\sim 750$  ppm) observed in this zone is similar to concentrations found in the lower half of the Craib core and is therefore compatible with this interpretation. The observation of higher lead levels near the surface of GLG2 must reflect input of a significantly higher lead concentration to the sediment at some past time, presumably with a subsequent return to previous lower levels. Now, for the sake of argument, if the  $^{210}\text{Pb}$  sedimentation rate estimated from GLG2 is extrapolated to the full length of the gravity core, the age/depth curve of fig. 43 results. From this it follows either that levels of lead pollution were considerable in this loch even in the early 1700's or that natural levels are unusually high, up to x 60 those observed

in sediments of other areas (e.g. Loch Goil, where 'background' levels of lead are  $\sim 10$  ppm). Alternatively, if the sedimentation rate is indeed closer to the  $540 \text{ mg.cm}^{-2}\text{y}^{-1}$  value derived from Craib core GLC3 and established as being more acceptable, then the 34 cm horizon in the gravity core would correspond to an age of  $\sim 32$  y (this does not however take account of any sediment loss) and the profile might be explained in terms of recent cultural effects. Since there is no known local geological reason to expect such high natural lead levels (Leatherland, 1978, pers. comm.) and since the concentrations observed (600 to 800 ppm in the Craib core and up to  $\sim 950$  ppm in the Gravity core) are consistent with material derived from the estuary where levels reach  $\sim 1000$  ppm (Leatherland, 1978, pers. comm.), the latter explanation would seem more reasonable, although the absence of time-markers for the lead record in the area renders almost any interpretation possible. Further sampling and analysis are obviously required before unambiguous interpretation of these stable lead results is possible. Nonetheless, based on the "best estimate" sedimentation rate derived from the Craib core, the present annual flux of lead to the surface sediments of Gareloch appears to be  $\sim 340 \text{ } \mu\text{g.cm}^{-2}\text{y}^{-1}$ .

### Loch Goil

Sampling locations for Loch Goil are shown on page 221 (fig. 51). The results of the analyses of two Craib cores and one gravity core from station 1 are presented in the tables and figures on pages 222 to 246; those for a Craib core from station 2 are shown on pages 247 to 255.

4° 50' W

4° 45' W

56° 05' N

56° 0' N

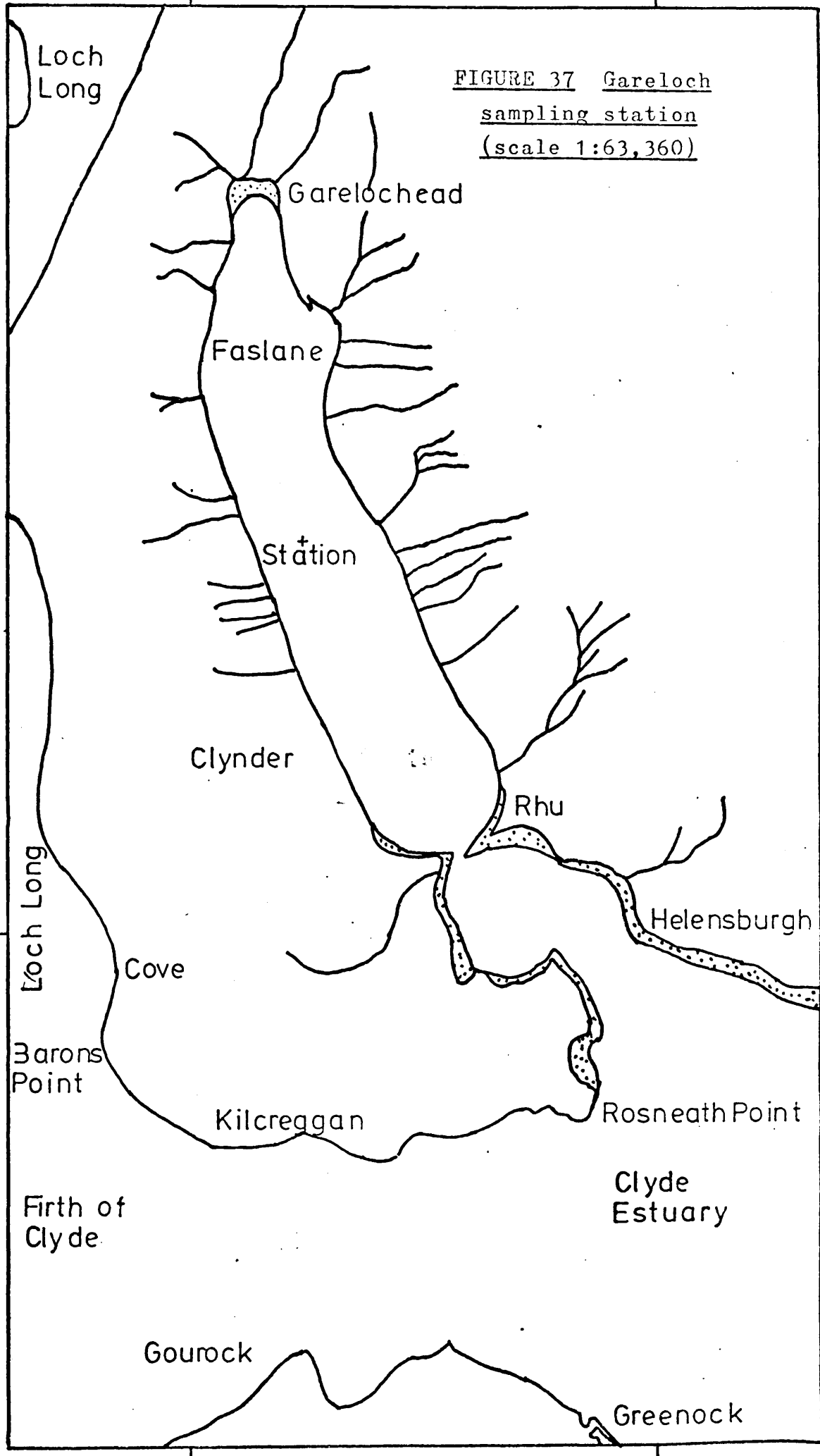


FIGURE 37 Gareloch  
sampling station  
(scale 1:63,360)

Loch Long

Garelohead

Faslane

Station

Clynder

Rhu

Helensburgh

Cove

Barons Point

Kilcreggan

Rosneath Point

Firth of Clyde

Clyde Estuary

Gourock

Greenock

Loch Long

TABLE 26BACKGROUND INFORMATION FOR  
GARELOCH GRAVITY CORE GLG2

CORE DESIGNATION: GARELOCH GRAVITY CORE  
CORE GLG2

SAMPLING DATE: 7-11-75

LOCATION: LAT, 56° 02' 42" N  
LONG, 04° 49' 36" W

WATER DEPTH: 48 m

TOTAL CORE LENGTH: 36 cm.

GENERAL DESCRIPTION OF SEDIMENTS:

homogeneous light/mid brown clay

TABLE 27      GARELOCH GRAVITY CORE GLG2 : RESULTS OF ANALYTICAL INVESTIGATIONS

<u>Section (cm)</u>	<u>Wet Wt. (g)</u>	<u>Dry Wt. (g)</u>	<u>Porosity %<sup>1</sup></u>
0 - 1	33.8	9.3	86
1 - 2	37.4	10.8	85
2 - 3	38.1	11.6	84
3 - 4	36.5	10.7	84
4 - 5	38.7	12.3	83
5 - 6	37.0	12.7	81
6 - 7	38.9	12.6	82
7 - 8	38.6	13.8	80
8 - 9	38.0	14.5	78
9 - 10	35.5	13.3	79
10 - 11	38.6	13.7	80
11 - 12	39.8	15.3	78
12 - 13	32.2	11.9	79
13 - 14	38.2	14.3	79
14 - 15	41.3	16.1	78
15 - 16	39.9	15.4	78
16 - 17	40.7	16.6	76
17 - 18	40.7	16.8	76
18 - 19	39.9	17.8	74
19 - 20	40.0	16.5	76
20 - 21	42.4	17.6	76

TABLE 27 (cont'd) GARELOCH GRAVITY CORE GLG2 : RESULTS OF ANALYTICAL INVESTIGATIONS

<u>Section (cm)</u>	<u>Wet Wt. (g)</u>	<u>Dry Wt. (g)</u>	<u>Porosity %<sup>1</sup></u>
21 - 22	41.5	16.6	77
22 - 23	39.8	15.9	77
23 - 24	38.8	16.1	76
24 - 25	43.0	17.6	76
25 - 26	38.9	16.0	76
26 - 27	45.7	20.7	73
27 - 28	37.1	15.2	76
28 - 29	44.9	18.9	76
29 - 30	37.3	15.5	76
30 - 31	41.8	17.6	76
31 - 32	45.1	19.1	73
32 - 33	44.9	20.4	73

1. Porosity evaluated using mean measured particle density of  $2.3 \pm 0.1 \text{ g.cm}^{-3}$

TABLE 27 (cont'd) GARELOCH GRAVITY CORE GLG2 : RESULTS OF ANALYTICAL INVESTIGATIONS

Section (cm)	$^{210}\text{Pb}_{\text{TOT}} \pm 1\sigma$ (dpm.g <sup>-1</sup> )	$^{226}\text{Ra} \pm 1\sigma$ (dpm.g <sup>-1</sup> )	$^{210}\text{Pb}_{\text{XS}} \pm 1\sigma^1$ (dpm.g <sup>-1</sup> )	$^{137}\text{Cs} \pm 1\sigma$ (dpm.g <sup>-1</sup> )	$^{134}\text{Cs} \pm 1\sigma$ (dpm.g <sup>-1</sup> )
0 - 1	6.79 ± 0.30	2.70 ± 0.20	5.1 ± 0.3	1.6 ± 2	B.D.
1 - 2	6.44 ± 0.25	1.76 ± 0.13	4.7 ± 0.3	2.7 ± 3	"
2 - 3	6.64 ± 0.35		4.9 ± 0.4		
3 - 4	6.36 ± 0.22		4.7 ± 0.3	8.1 ± 1.6	"
4 - 5	5.57 ± 0.25		3.9 ± 0.3		
5 - 6	5.33 ± 0.24	1.79 ± 0.14	3.6 ± 0.3	2.8 ± 0.6	"
6 - 7	4.81 ± 0.26		3.1 ± 0.3		
7 - 8					
8 - 9	3.76 ± 0.14	1.67 ± 0.13	2.1 ± 0.2	1.1 ± 0.2	"
9 - 10					
10 - 11	3.10 ± 0.17		1.4 ± 0.2		
11 - 12					
12 - 13					
13 - 14	2.37 ± 0.09	1.54 ± 0.12	0.7 ± 0.2		
14 - 15					
15 - 16					
16 - 17	1.85 ± 0.18		0.2 ± 0.2		
17 - 18					
18 - 19					
19 - 20	1.88 ± 0.12				

TABLE 27 (cont'd) GARELOCH GRAVITY CORE GLG2 : RESULTS OF ANALYTICAL INVESTIGATIONS

<u>Section</u> <u>(cm)</u>	$^{210}\text{Pb}_{\text{TOT}} \pm 1\sigma$ <u>(dpm.g<sup>-1</sup>)</u>	$^{226}\text{Ra} \pm 1\sigma$ <u>(dpm.g<sup>-1</sup>)</u>	$^{210}\text{Pb}_{\text{XS}} \pm 1\sigma$ <u>(dpm.g<sup>-1</sup>)</u>	$^{137}\text{Cs} \pm 1\sigma$ <u>(dpm.g<sup>-1</sup>)</u>	$^{134}\text{Cs} \pm 1\sigma$ <u>(dpm.g<sup>-1</sup>)</u>
22 - 23	1.78 ± 0.14				
26 - 27	1.74 ± 0.15	1.87 ± 0.14			
32 - 33	1.77 ± 0.13	1.62 ± 0.13			

1. Excess  $^{210}\text{Pb}$  evaluated with supported  $^{210}\text{Pb} = 1.7 \pm 0.1 \text{ dpm.g}^{-1}$   
(mean of  $^{226}\text{Ra}$  determinations)

FIGURE 38 Depth profiles of total  $^{210}\text{Pb}$  and  $^{226}\text{Ra}$   
for Gareloch gravity core GLG2

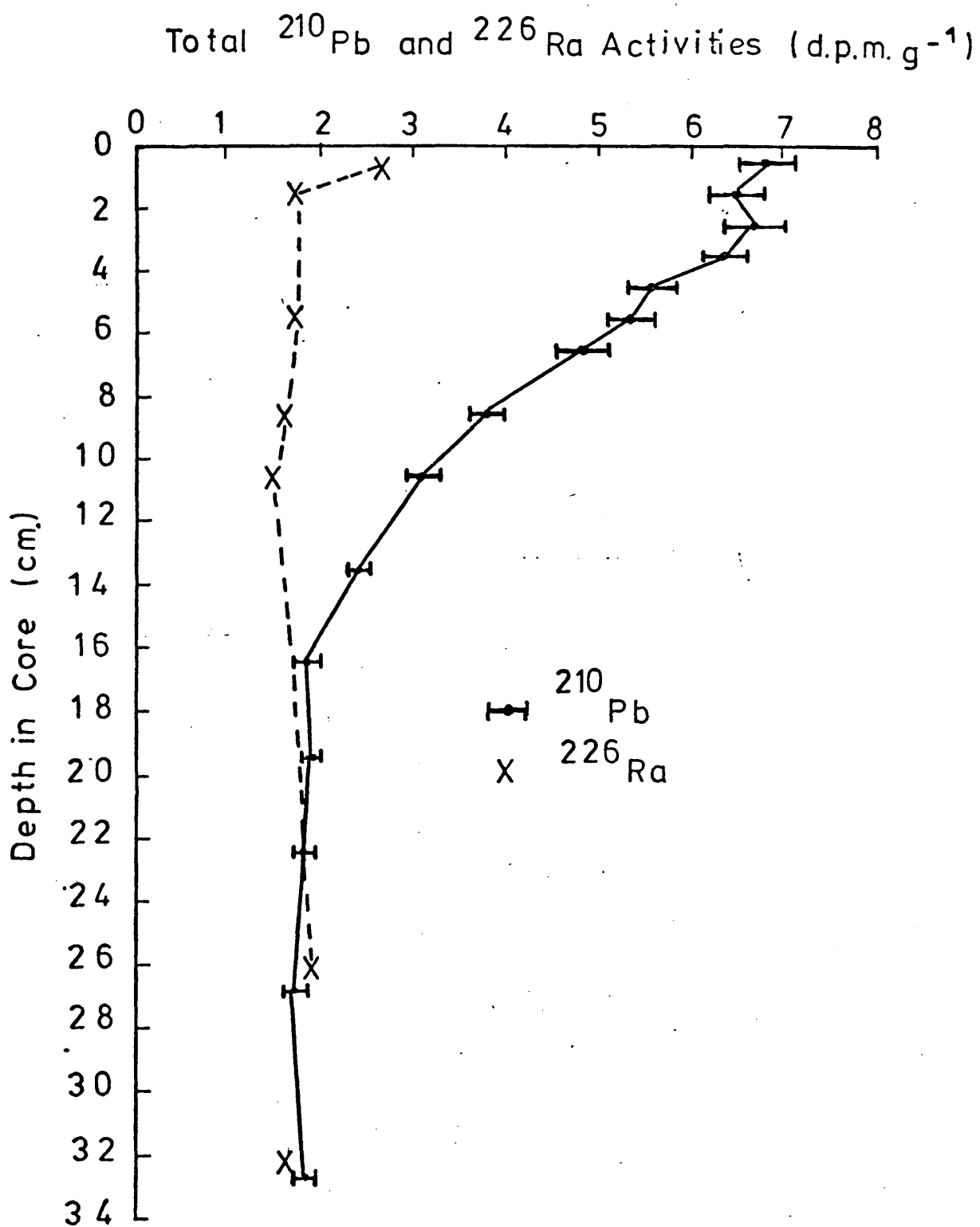


FIGURE 39    Radiocaesium profile for Gareloch  
gravity core GLG2

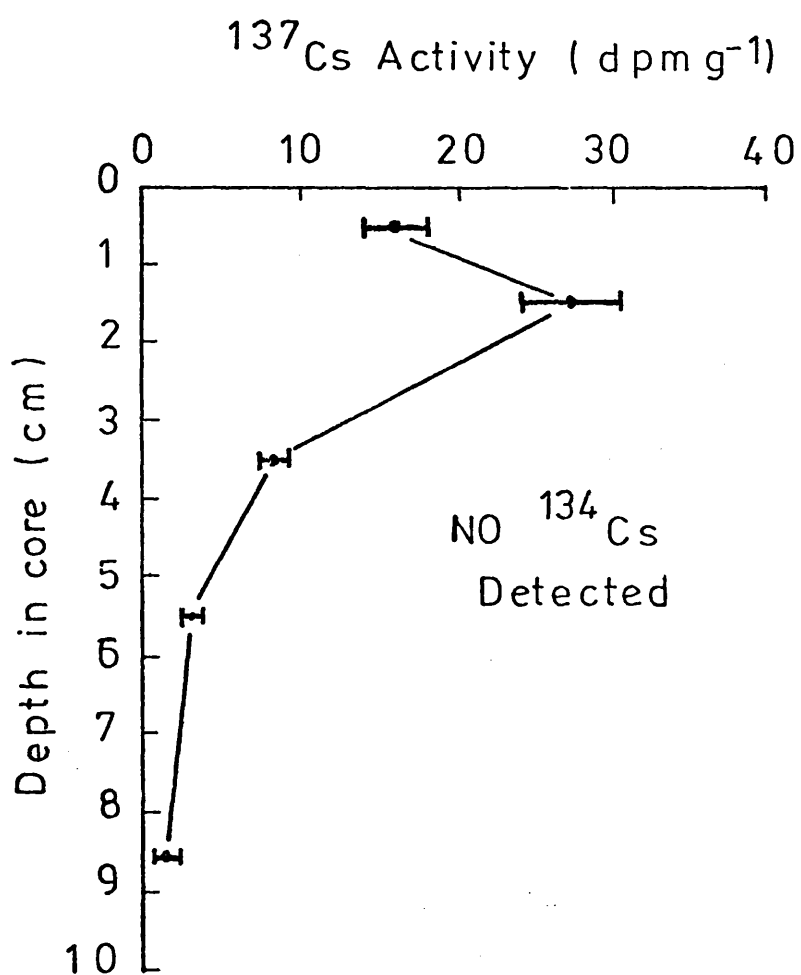


FIGURE 40 Porosity profile for Gareloch  
gravity core GLG2

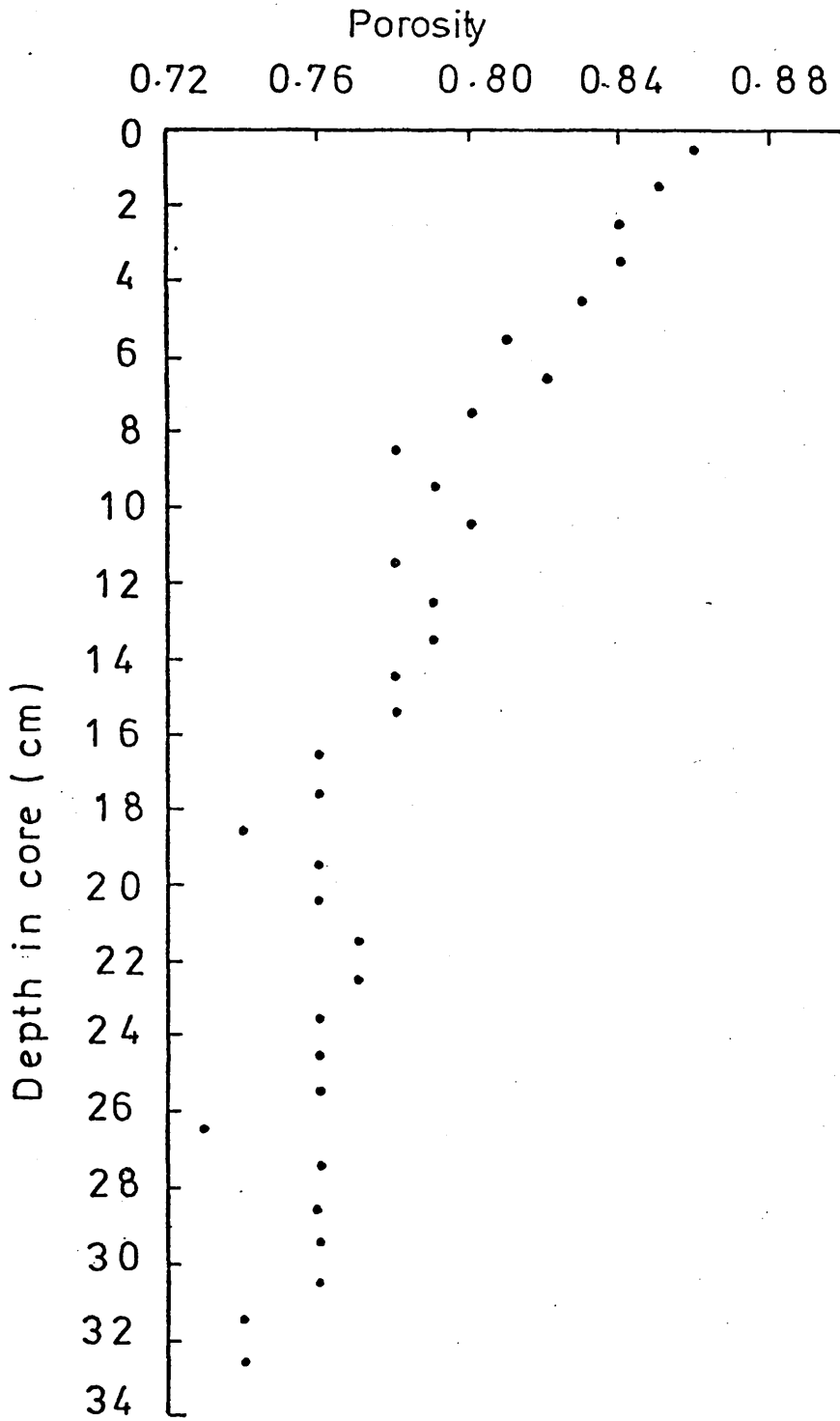
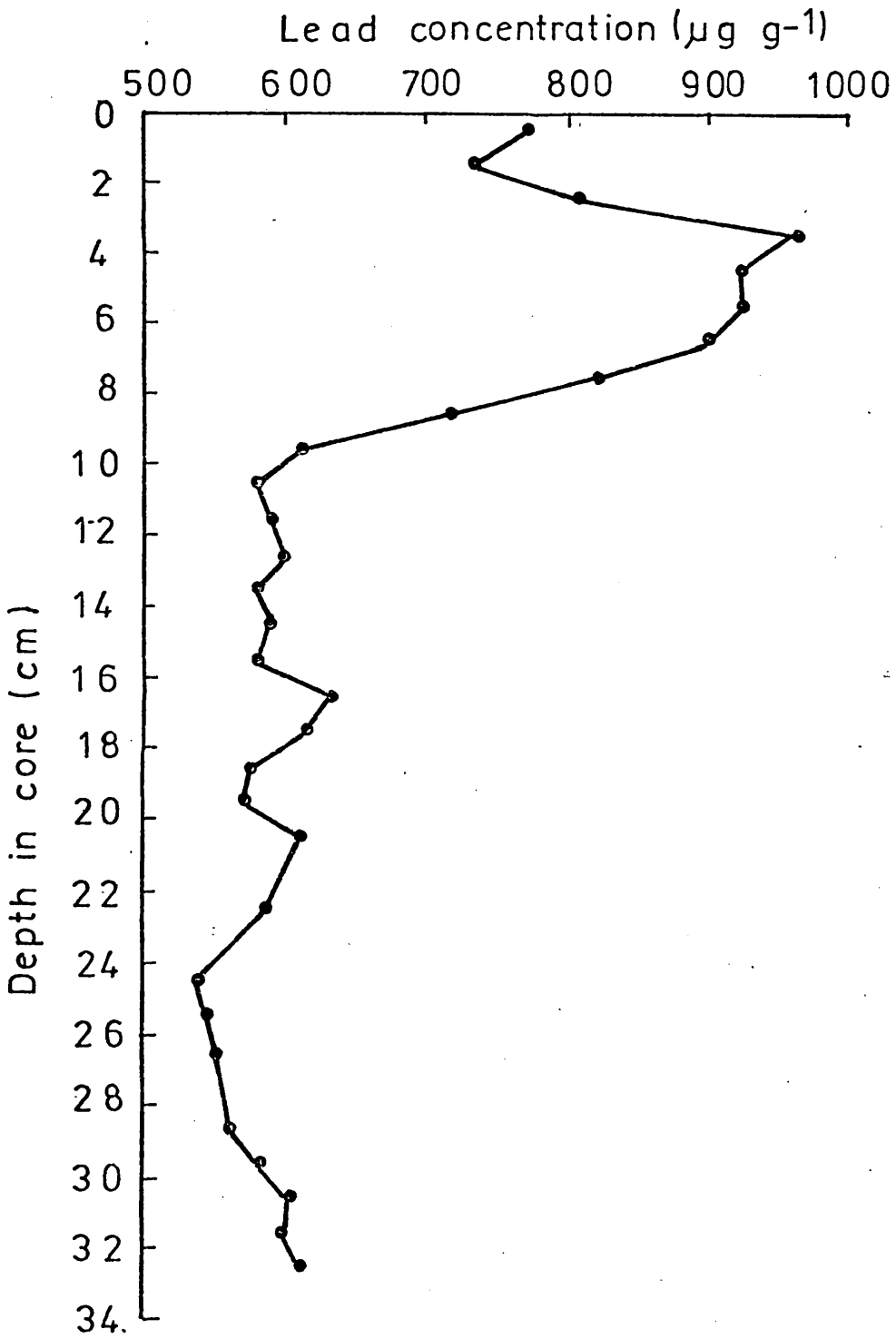


FIGURE 41    Lead profile for Gareloch gravity  
core GLG2



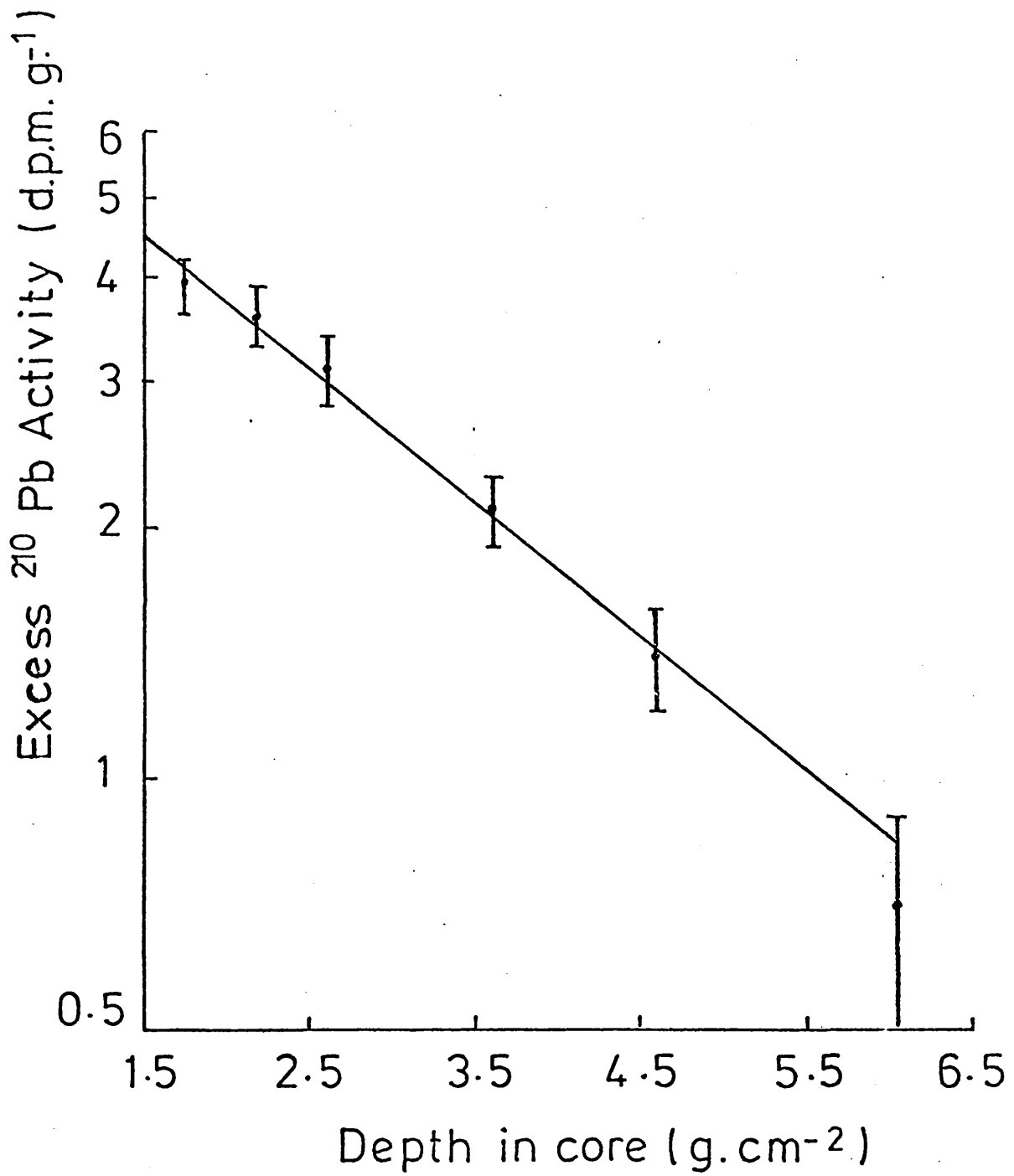
Gareloch gravity core GLG2

FIGURE 43 Curve of age (calendar date) against depth  
for Gareloch gravity core GLG2

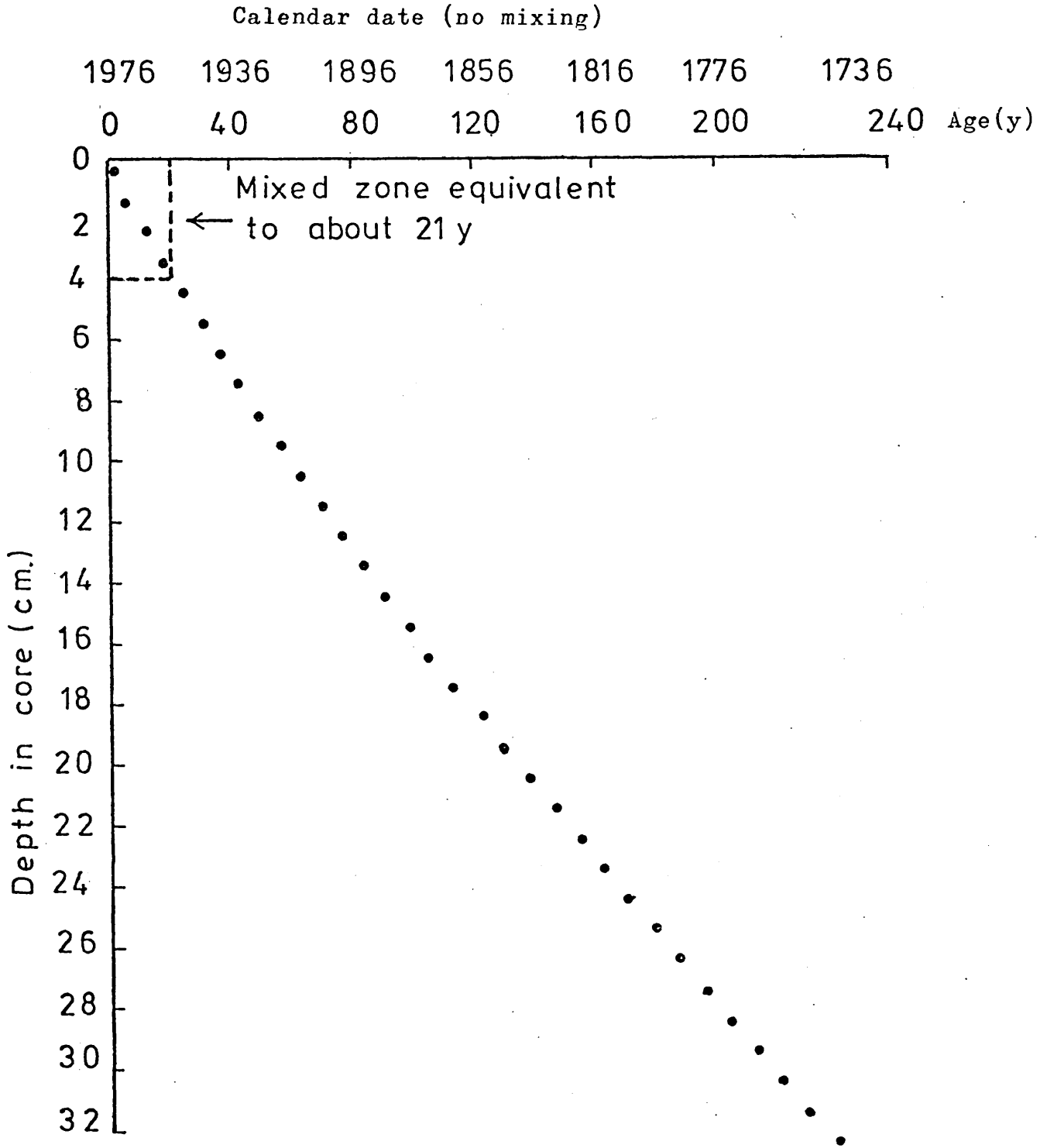


TABLE 28                    BACKGROUND INFORMATION FOR  
GARELOCH CRAIB CORE GLC3

CORE DESIGNATION:            GARELOCH CRAIB CORE  
   CORE GLC3

SAMPLING DATE:                7·11·75

LOCATION:                        LAT.    56° 02' 42" N  
   LONG.  04° 49' 36" W

WATER DEPTH:                  48 m.

TOTAL CORE LENGTH:          15 cm.

GENERAL DESCRIPTION OF SEDIMENTS:

homogeneous light/mid brown clay

TABLE 29 GABELOCH CRAIB CORE GLC3 : RESULTS OF ANALYTICAL INVESTIGATIONS

Section (cm)	Wet Wt. (g)	Dry Wt. (g)	Porosity <sup>1</sup> (%)	CaCO <sub>3</sub> <sup>2</sup> (%)	Microanalysis (%) <sup>2</sup> C H N
0 - 1	29.66	3.65	94.1	3.25	6.23 1.48 0.51
1 - 2	28.68	7.28	86.8	4.00	6.16 1.48 0.59
2 - 3	30.56	8.30	85.7	3.92	6.58 1.55 0.79
3 - 4	32.44	9.61	84.2	2.95	6.24 1.46 0.57
4 - 5	33.37	10.19	83.6	2.48	5.91 1.42 0.44
5 - 6	33.04	10.61	82.6	2.68	5.77 1.33 0.38
6 - 7	33.08	10.64	82.6		
7 - 8	33.56	10.48	83.2	2.48	5.62 1.36 0.41
8 - 9	33.30	10.53	82.9		
9 - 10	32.19	10.16	83.0	2.25	5.78 1.33 0.41
10 - 11	33.64	10.20	83.8		
11 - 12	31.14	10.25	82.1	2.16	5.70 1.93 0.40
12 - 13	31.75	10.54	81.9		
13 - 14	30.68	10.60	81.0	2.47	6.07 1.38 0.40
14 - 15	16.19	5.59	81.0		

1. Porosity evaluated using mean measured particle density of  $2.3 \pm 0.1 \text{ g.cm}^{-3}$

2. Percent CaCO<sub>3</sub>/microanalytical results expressed on dry weight basis.

TABLE 29 (cont'd) GARELOCH CRAIB CORE GLC3 : RESULTS OF ANALYTICAL INVESTIGATIONS

Section (cm)	$^{210}\text{Pb}_{\text{TOT}} \pm 1\sigma$ (dpm.g <sup>-1</sup> )	$^{226}\text{Ra} \pm 1\sigma$ (dpm.g <sup>-1</sup> )	$^{210}\text{Pb}_{\text{XS}} \pm 1\sigma$ (dpm.g <sup>-1</sup> )	$^{137}\text{Cs} \pm 1\sigma$ (dpm.g <sup>-1</sup> )	$^{134}\text{Cs} \pm 1\sigma$ (dpm.g <sup>-1</sup> )
0 - 1	8.08 ± 0.25		6.4 ± 0.3	75 ± 6	14 ± 1
1 - 2	8.36 ± 0.25		6.7 ± 0.3	60 ± 5	10.1 ± 0.7
2 - 3	8.53 ± 0.30	1.39 ± 0.10	6.8 ± 0.3	41 ± 3	5.6 ± 0.4
3 - 4	7.57 ± 0.29		5.9 ± 0.3	43 ± 3	8.5 ± 0.6
4 - 5	7.66 ± 0.25		6.0 ± 0.3	31 ± 3	4.4 ± 0.3
5 - 6	8.71 ± 0.23	1.66 ± 0.13	7.0 ± 0.2	26 ± 2	4.4 ± 0.3
6 - 7				26 ± 2	3.1 ± 0.2
7 - 8	8.02 ± 0.25		6.3 ± 0.3	22 ± 2	2.9 ± 0.2
8 - 9	6.69 ± 0.28	1.77 ± 0.13	5.0 ± 0.3	17 ± 1	2.3 ± 0.2
9 - 10	7.03 ± 0.28		5.3 ± 0.3	16 ± 1	1.9 ± 0.1
10 - 11	6.70 ± 0.33		5.0 ± 0.3	14 ± 1	3.9 ± 0.3
11 - 12	7.03 ± 0.28		5.3 ± 0.3	11 ± 1	1.6 ± 0.1
12 - 13				10 ± 1	B.D.
13 - 14	6.65 ± 0.25		5.0 ± 0.3		
14 - 15	6.97 ± 0.27	1.32 ± 0.10	5.3 ± 0.3		

1. Excess  $^{210}\text{Pb}$  evaluated with supported  $^{210}\text{Pb} = 1.7 \pm 0.1$  dpm.g<sup>-1</sup>  
(mean of  $^{226}\text{Ra}$  determinations in gravity core GLG2)

FIGURE 44 Depth profiles of total  $^{210}\text{Pb}$  and  $^{226}\text{Ra}$   
for Gareloch Craib core GLC3

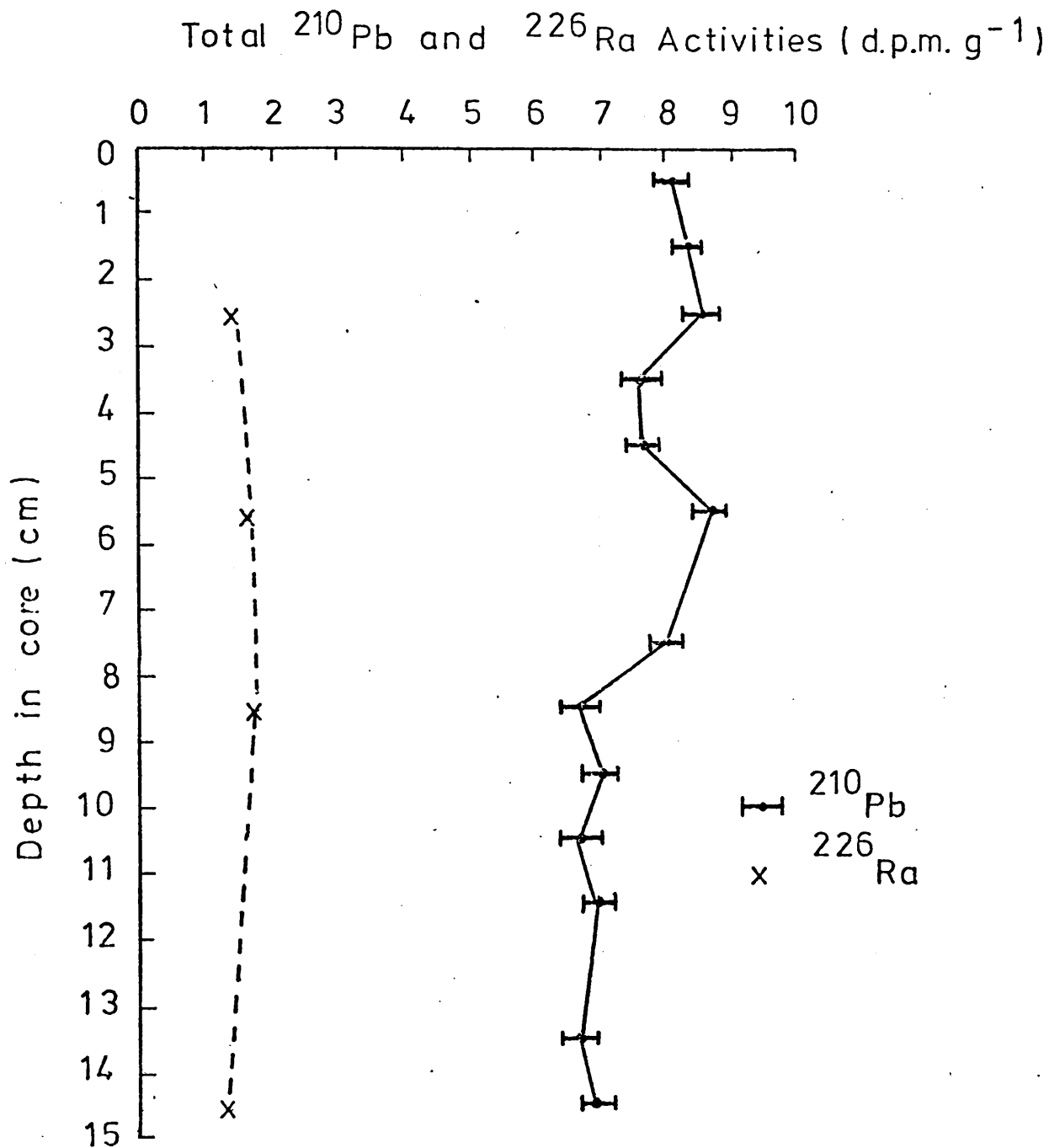


FIGURE 45 Radiocaesium profile for Gareloch  
Craib core GLC3

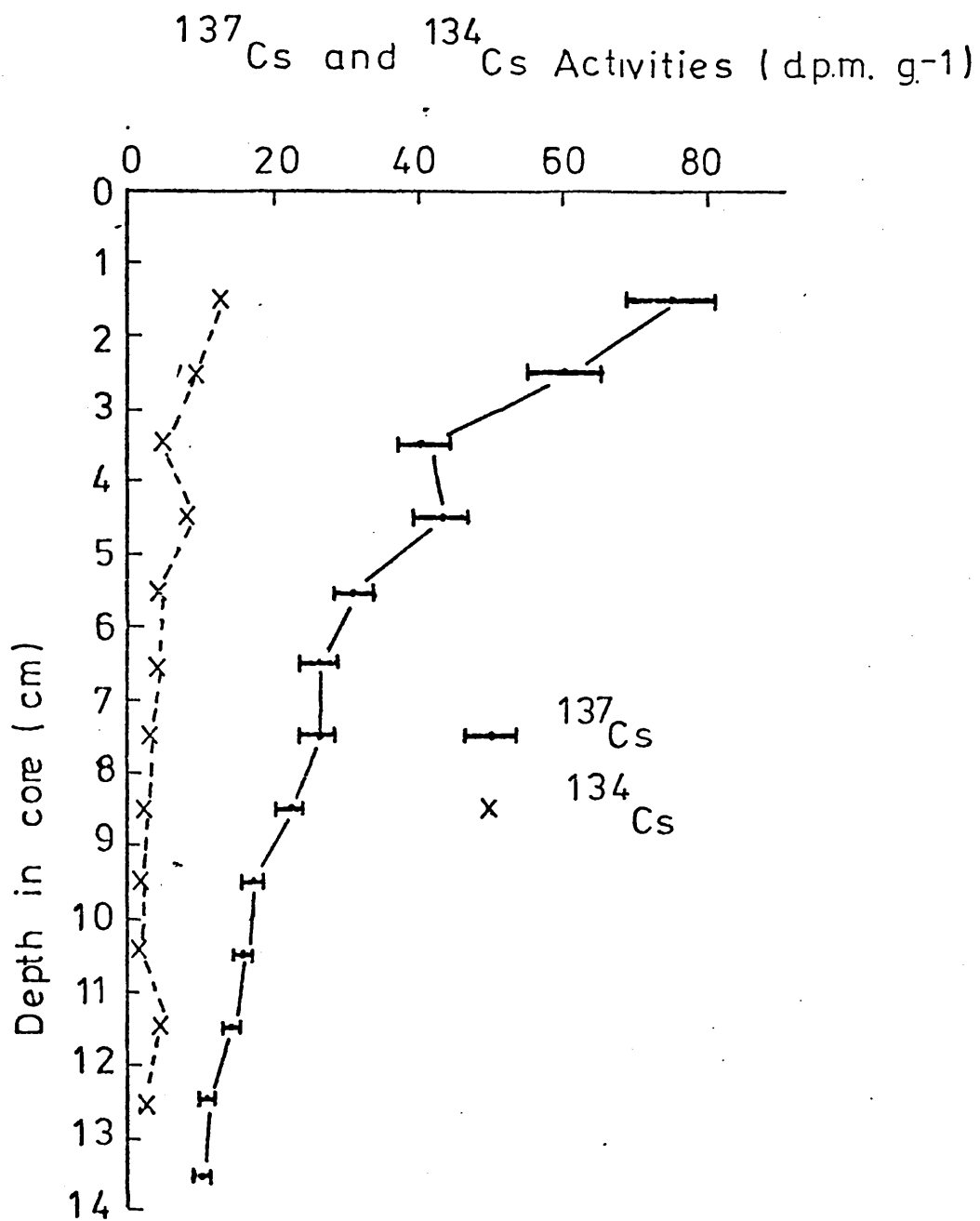


FIGURE 46 Porosity profile for Gareloch  
Craib core GLC3

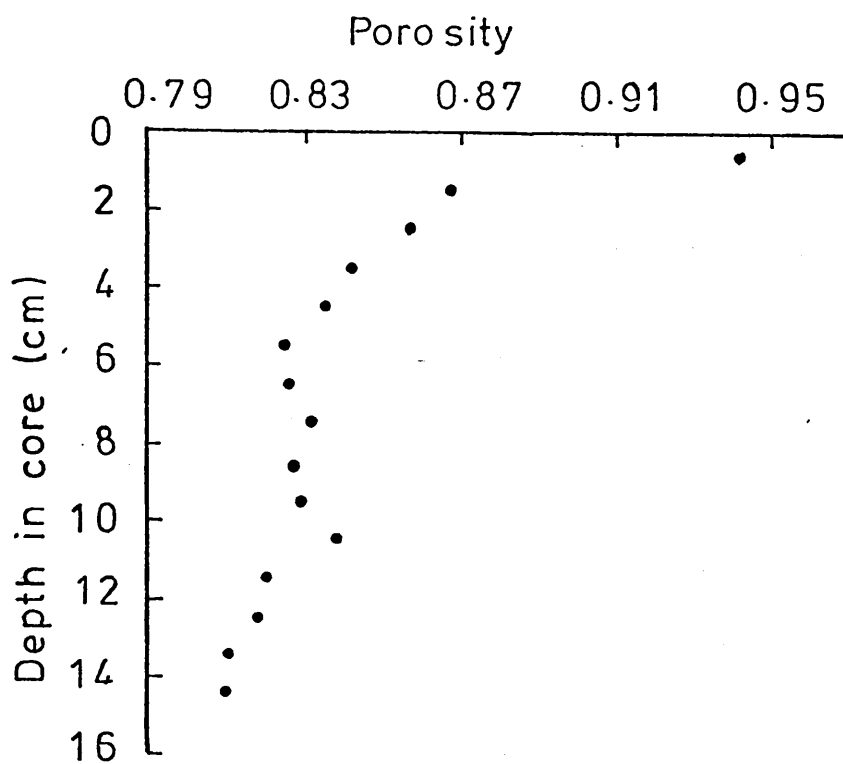


FIGURE 48 Porosity profile for Gareloch Craib core GLC2

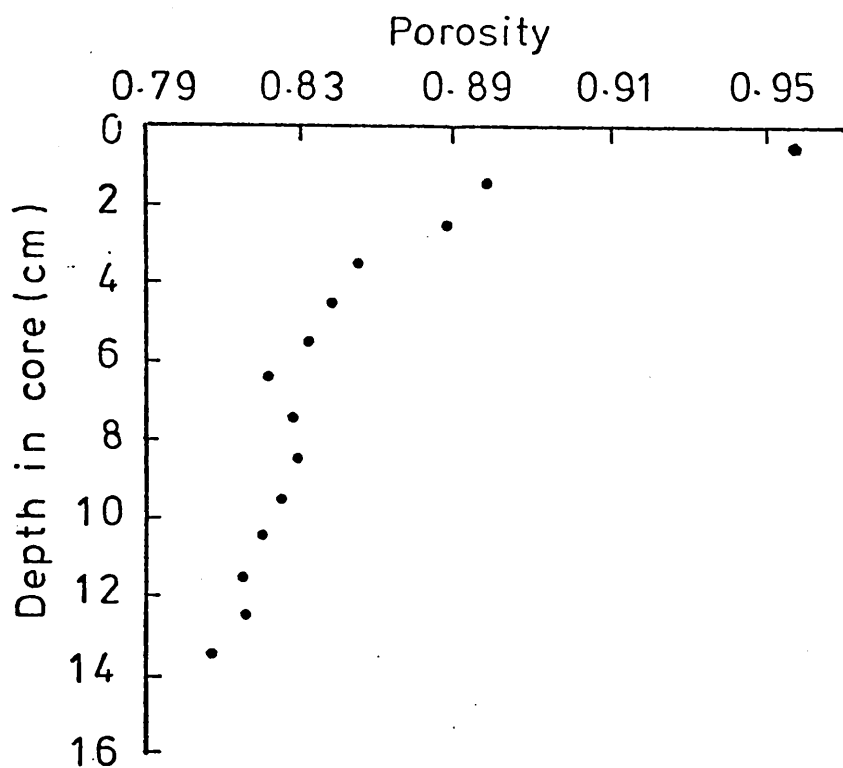


FIGURE 47    Depth profile of excess  $^{210}\text{Pb}$  for Gareloch  
Craib core GLC3

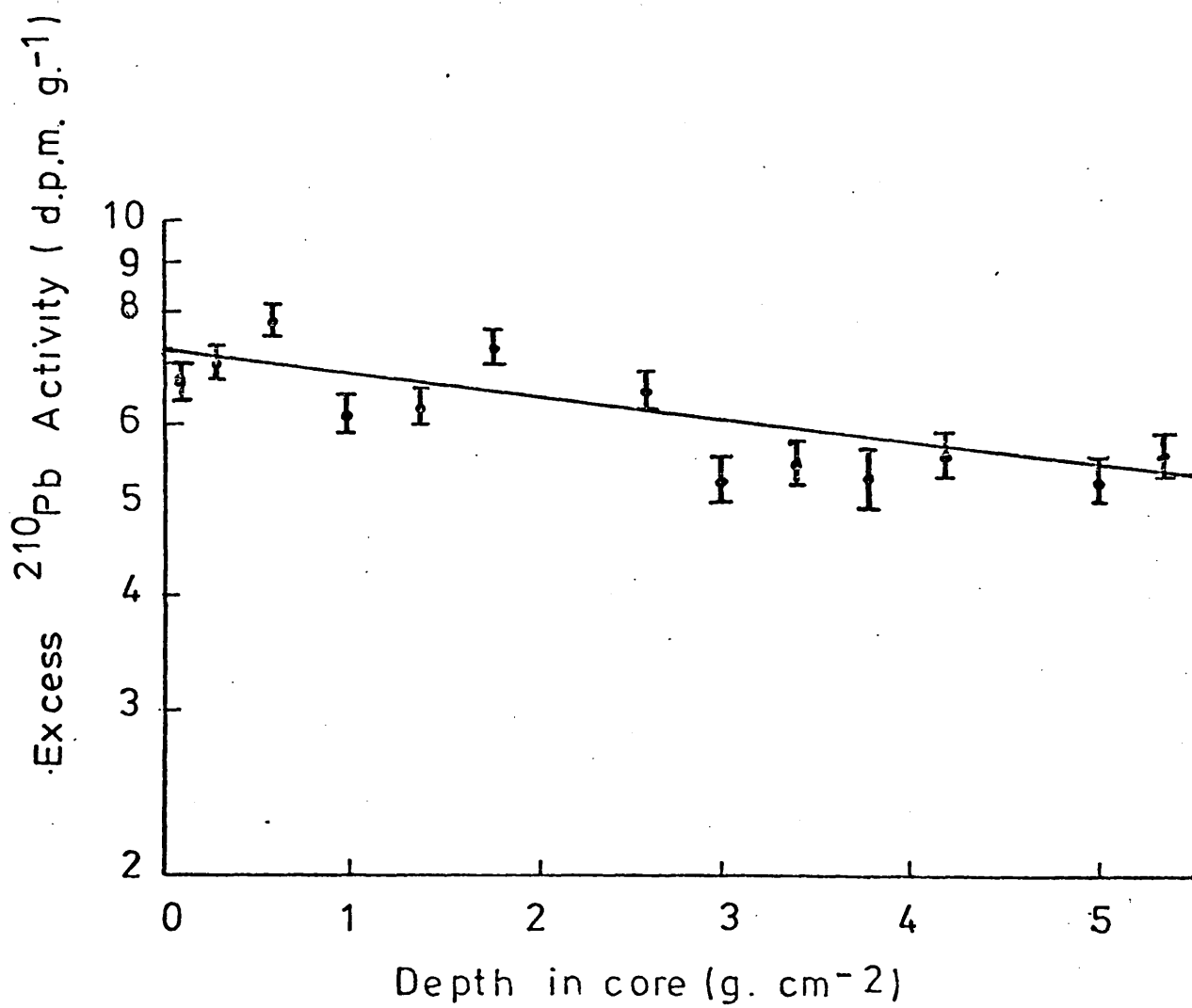
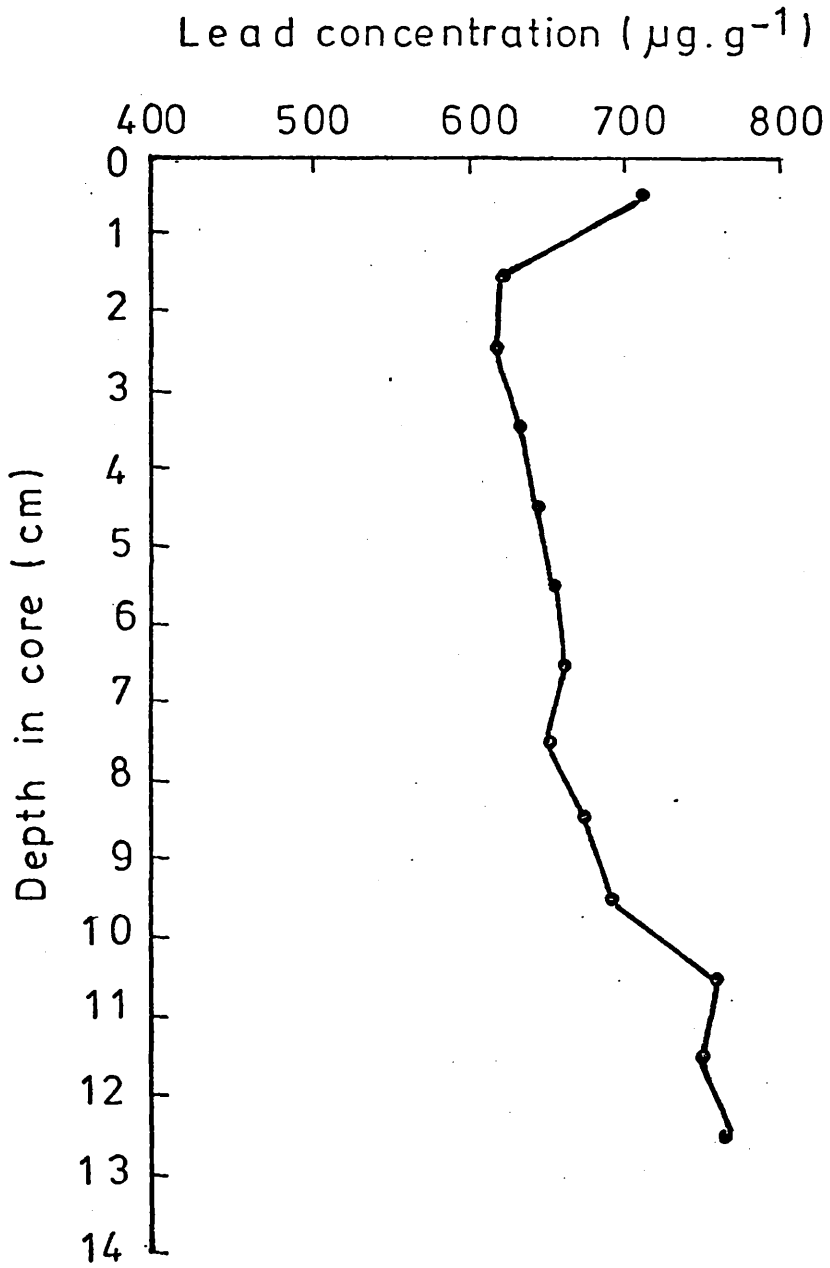




FIGURE 50      Lead profile for Gareloch Craib core GLC2



### Station 1

Total  $^{210}\text{Pb}$  and  $^{226}\text{Ra}$  distributions for Loch Goil gravity core LGG5 are plotted in fig. 52. Particularly interesting is the unusual profile observed for  $^{226}\text{Ra}$ , concentrations increasing from a typical inshore marine value of  $\sim 1.7 \text{ dpm.g}^{-1}$  at depth through a maximum of  $\sim 5.6 \text{ dpm.g}^{-1}$  at 3 cms. below the mud surface; activities in the upper 2 cms. of the core are relatively depressed. Similarly, the  $^{210}\text{Pb}$  profile exhibits reduced activities in the upper 2 cms of the core, passes through a maximum at a depth of 3 cms. and then declines exponentially to 10 cms., below which equilibrium between  $^{226}\text{Ra}$  and  $^{210}\text{Pb}$  is observed.

Using excess  $^{210}\text{Pb}$  data from 3 cms. to 10 cms. an estimate of the sediment accumulation rate can be obtained. However, since the  $^{226}\text{Ra}$  concentration shows a rapid decline with depth in this region and the degree of equilibrium between  $^{226}\text{Ra}$  and  $^{210}\text{Pb}$  is unknown, alternative estimates are derived as described before. Weighted linear regression analysis yields values of (a)  $45 \pm 2 \text{ mg.cm}^{-2}\text{y}^{-1}$ ; (b)  $40 \pm 2 \text{ mg.cm}^{-2}\text{y}^{-1}$ ; and (c)  $35 \pm 2 \text{ mg.cm}^{-2}\text{y}^{-1}$  for supported  $^{210}\text{Pb}$  equivalent to (a) measured  $^{226}\text{Ra}$ ; (b) mean total  $^{210}\text{Pb}$  at depth; and (c)  $^{210}\text{Pb}$  estimated iteratively. Confidence in the result of the iterative approach, however, is in this case, limited since the extent of loss of surface sediment (and therefore the 'true' age of the upper strata containing the  $^{210}\text{Pb}$  and 'anomalous'  $^{226}\text{Ra}$  profiles) is as yet undefined. For this reason and for reasons which will become apparent, the difference between the estimates of sedimentation rate is minor and therefore a mean value of  $40 \text{ mg.cm}^{-2}\text{y}^{-1}$  (fig. 55) (equivalent to a mean sedimentation rate of  $\sim 1.2 \text{ mm.y}^{-1}$ ) is used to evaluate the age/depth curve of fig. 56. With an extra-

polated value of unsupported  $^{210}\text{Pb}$  at the 'sediment/water' interface of  $12.6 \text{ dpm.g}^{-1}$  an estimate of the flux of excess  $^{210}\text{Pb}$  to the mud-surface of  $0.5 \text{ dpm.cm}^{-2}\text{y}^{-1}$  is calculated, in close agreement with the estimated atmospheric flux of  $\sim 0.38 \text{ dpm.cm}^{-2}$  for the region. On this basis the main source of excess  $^{210}\text{Pb}$  in the sediments is apparently that due to direct atmospheric rainout on to the loch surface. The contribution of excess  $^{210}\text{Pb}$  from in-situ decay of  $^{226}\text{Ra}$  in the water column is estimated at  $0.03 \text{ dpm.cm}^{-2}\text{y}^{-1}$  (based on a mean  $^{226}\text{Ra}$  concentration in the water of  $0.13 \text{ dpm.l}^{-1}$  and a water column depth of 80 metres) and is therefore insignificant.

The stable lead profile for core LGG5 presented in fig 57 is classical in form, lead concentrations increasing exponentially from depth to the core top where considerably higher values are recorded. Assuming a surface concentration of  $500 \mu\text{g.g}^{-1}$ , a modern flux of lead to the sediment of  $20 \mu\text{g.cm}^{-2}\text{y}^{-1}$  is estimated, corresponding to an increase of x50 over pre-industrial levels; this assumes that values of  $\sim 10 \mu\text{g.g}^{-1}$  observed at the base of the core represent natural concentrations and that the sedimentation rate has remained unchanged. If the sedimentation rate was in fact lower in the pre-industrial era then the increased input may be substantially greater than this value. Assuming the first significant rise in lead levels to occur at a depth of  $\sim 20 \text{ cms.}$  in the core, an age of  $\sim 180$  years is estimated for this horizon (i.e.  $\sim \text{AD } 1790$ ) which is not incompatible with the known onset of cultural change and industrial activity in the region. It is worth pointing out then, that considered independently, the radionuclide and metal data for this

gravity core are apparently sensible and in some ways follow classical trends. The interesting fact however is that these results will be shown to be almost totally erroneous.

Fig. 58 presents the total  $^{210}\text{Pb}$  and  $^{226}\text{Ra}$  distributions for Craib core LGC2 recovered from the same location as gravity core LGG5. Again, the most remarkable feature of the profile is the unusual distribution of the natural series nuclides, particularly that of  $^{226}\text{Ra}$  which exhibits a well-defined maximum at  $\sim 4$  cms. below the sediment/water interface. The total  $^{210}\text{Pb}$  profile shows some evidence of a maximum at a depth equivalent to that of the  $^{226}\text{Ra}$  maximum, with a gradual trend to decreasing concentrations below this level. However, in view of the  $^{226}\text{Ra}$  anomaly and of the short core length no estimate of sedimentation rate is possible. Moreover, from these results, there is no obvious point of overlap between the Craib and gravity cores.

To study the  $^{226}\text{Ra}$  anomaly further, to investigate the distribution of  $^{210}\text{Pb}$  below 10 cms, and to determine a possible point of overlap between Craib and gravity cores a substantially longer Craib core, LGC9, was recovered from the same location approximately 14 months later. Comparison of the total  $^{210}\text{Pb}$  and  $^{226}\text{Ra}$  distributions in this latter core (fig. 60) with those of LGC2, shows good agreement, the distinct maximum in  $^{226}\text{Ra}$  again being observed a few centimetres below the sediment surface. Furthermore, the cumulative total  $^{210}\text{Pb}$  and  $^{226}\text{Ra}$  concentrations in the upper 10 cms. of LGC9 compare favourably with those in LGC2 ( $35.1 \text{ dpm.cm}^{-2}$  and  $34.8 \text{ dpm.cm}^{-2}$  for  $^{210}\text{Pb}$  and  $17.9 \text{ dpm.cm}^{-2}$  and  $19.1 \text{ dpm.cm}^{-2}$  for  $^{226}\text{Ra}$  respectively). This agreement constitutes good evidence of the reproducibility with which the Craib corer recovers

undisturbed sediment. Moreover, the radiocaesium profiles for these cores (figs. 59, 61 ) reveal a considerably higher concentration of  $^{137}\text{Cs}$  in the topmost section of core LGC9 sampled 14 months after LGC2, consistent with the increasing output of  $^{137}\text{Cs}$  in waste from Windscale over this time period and implying that the superficial layer of sediment has been recovered undisturbed by the Craib corer. Craib cores, then, are essentially self-consistent, and profiles observed in the longer LGC9 confirm

(1) that the  $^{226}\text{Ra}$  anomaly is confined to the upper 8 cms. of the deposit, and

(2) that  $^{210}\text{Pb}$  concentrations decline gradually with depth below the level of the  $^{226}\text{Ra}$  maximum.

However, a considerable activity of excess  $^{210}\text{Pb}$  remains at a depth of 17 cms.

Although, in this instance, a similar general trend is observed in the distribution of the natural series nuclides in both the gravity and Craib cores, there nonetheless exist considerable and significant differences between the respective profiles in the two core types. For example, both the  $^{226}\text{Ra}$  and total  $^{210}\text{Pb}$  concentrations in the upper 6 cms. of the Craib core are considerably greater than the maximum activities observed in the gravity core, implying that at least this thickness of sediment has been lost from the gravity core during sampling. In addition, there is no point of overlap between Craib (below 6 cms.) and gravity (below 2 cms.) cores where an acceptable and simultaneous degree of correspondence occurs between  $^{210}\text{Pb}$  and  $^{226}\text{Ra}$  activities for an individual section. Furthermore, if the  $^{226}\text{Ra}$  activities are ignored,

and the cores matched solely on the basis of  $^{210}\text{Pb}$  activities (e.g. 3 cms. in the gravity core corresponding to 8 to 9 cms. in the Craib core) then the profile of  $^{210}\text{Pb}$  below these depths should show similar trends; clearly this is not the case. Furthermore, the total cumulative activity of  $^{210}\text{Pb}$  from 3 cms. to 10 cms. in the gravity core is  $\sim 15.5 \text{ dpm.cm}^{-2}$ , markedly lower than that from 9 cms to 16 cms. in the Craib core of  $\sim 21.4 \text{ dpm.cm}^{-2}$ . The inescapable conclusion from the radionuclide data is therefore that not only has a considerable quantity of surface sediment been lost during gravity core sampling but also that the distributions of  $^{210}\text{Pb}$  and  $^{226}\text{Ra}$  observed in the gravity core are not in fact indicative of the natural sediment conditions but are an artefact of coring and represent the 'remains' of a fairly large-scale mixing/loss process.

The general conclusions drawn from the natural series profiles are largely confirmed by the radiocaesium data for these cores. Figs. 59, 61 present the  $^{134}\text{Cs}$  and  $^{137}\text{Cs}$  profiles for cores LGC2 and LGC9 respectively while that for gravity core LGG5 is shown in fig. 53.

$^{137}\text{Cs}$  profiles in both Craib cores exhibit increasing concentrations from depth towards the sediment/water interface (cf Gareloch) consistent with the increasing concentration of these nuclides in waste released from Windscale. Furthermore, the activity of  $^{137}\text{Cs}$  in the upper few cms. of the Craib cores is around  $30 \text{ dpm.g}^{-1}$  and is greater than ca  $10 \text{ dpm.g}^{-1}$  to a depth of 8 cms. In contrast the maximum  $^{137}\text{Cs}$  activity observed in the gravity core is less than  $10 \text{ dpm.g}^{-1}$ , confirming that at least 8 cms. of surface sediment have been lost. While the total absence of  $^{134}\text{Cs}$  in the gravity core and the observed depth distribution of  $^{137}\text{Cs}$  could be compatible

with sediment below 8 cms. in the Craib core, when taken in conjunction with the natural series radionuclide data, the more internally consistent interpretation is that described above, i.e. complete loss of a substantial quantity of surface sediment, the upper 10 cm. of the gravity core comprising residual mixed sediment.

If the above interpretation is correct, then the implication is that only the data recorded at considerable depth in the gravity core may be reliable. For example, 10 ppm concentrations of lead in the sediment, based on observed levels in the lower 10 cms. of the gravity core, are probably valid indicators of natural values.

It is apparent then that any meaningful interpretation of sedimentary processes in Loch Goil will primarily derive from study of Craib core profiles. Since the  $^{226}\text{Ra}$  concentration is reasonably stable below a depth of 10 cms. in core LGC9 and exhibits a concentration typical of these deposits, it is possible to estimate a mean value for the supported  $^{210}\text{Pb}$  over the depth interval 10 cms. to 17 cms. and hence to derive a value for the sedimentation rate. Using a mean supported  $^{210}\text{Pb}$  activity of  $2.2 \pm 0.2 \text{ dpm.g}^{-1}$  (based on the last three measurements of  $^{226}\text{Ra}$ ), weighted linear regression analysis yields a value of  $200 \pm 73 \text{ mg.cm}^{-2}\text{y}^{-1}$  for the rate of sediment accumulation (fig.63) (equivalent to a mean sedimentation rate of  $6 \text{ mm.y}^{-1}$  and a surface rate of  $1 \text{ cm.y}^{-1}$ ). The corresponding age/depth curve for LGC9 is shown in fig 64. Although theoretically it would be possible to adopt an iterative approach to the excess  $^{226}\text{Ra}$  observed in the upper 10 cms. of the core, and thereby to include more data points in determining the sedimentation rate, in practice this would be unrealistic

since such a large error is already associated with the derived value. Confirmatory evidence of a relatively high rate of sediment accumulation for this location comes from the radiocaesium profile in LGC9, after allowing for a biological mixing depth of 4 cms. for these deposits, the evidence for which is outlined below.

X-radiographs of several cores from this location have indicated the presence of worm-holes to a depth of  $\sim 4$  cms. in the deposit; that for core LGC9 is shown in plate 1. This depth of biological reworking is consistent with the observed  $^{210}\text{Pb}$  distribution in this core, relatively constant  $^{210}\text{Pb}$  activities being observed in the upper 4 cms. of the deposit (fig. 60), and is also largely consistent with the  $^{137}\text{Cs}$  profile (fig. 61), which below the topmost section of the deposit exhibits constant activity to a depth of 4 cms. The observation of a much increased  $^{137}\text{Cs}$  activity in the upper 1 cm. section of the core suggests that biological reworking is not continuous, but follows a seasonal pattern or at least is intermittent in nature with a time-span of several months. (The  $^{210}\text{Pb}$  sedimentation rate indicates an 'age' of 6 to 12 months for the upper 1 cm. of deposit). The  $^{226}\text{Ra}$  profile is not immediately consistent with homogeneous particle redistribution in the upper 4 cms., but a possible explanation is presented later. Assuming a mixed zone of 4 cms., and equating the observation of  $^{137}\text{Cs}$  at 17 cms. to input around 1953 (based upon the first significant output of  $^{137}\text{Cs}$  from Windscale occurring in 1952 and one year delay in  $^{137}\text{Cs}$  incorporation into Clyde Sea Area sediments) a value of  $180 \text{ mg.cm}^{-2}\text{y}^{-1}$  is derived for the rate of sediment accumulation;

PLATE 1

X-radiograph of Craib core LGC9 from Loch Goil station 1

PLATE 1

X-radiograph of Craib core LGC9 from Loch Goil station 1



this sedimentation rate represents a minimum since  $^{137}\text{Cs}$  may in fact extend to greater depths than 17 cms. Furthermore, if the deepest observation of  $^{134}\text{Cs}$  at 9 cms. in the deposit is regarded, to a first approximation, as corresponding to input around 1968, a sedimentation rate of  $198 \text{ mg.cm}^{-2}\text{y}^{-1}$  is derived. Despite the obvious approximations involved, these estimates are in good agreement with the  $200 \text{ mg.cm}^{-2}\text{y}^{-1}$  value based on  $^{210}\text{Pb}$ , implying that little or no significant radio-caesium migration is occurring in these rapidly accumulating sediments.

Guinasso and Schink (1975) have shown that an estimate of the minimum biological mixing coefficient  $K_b$  ( $\text{cm}^2\text{y}^{-1}$ ) required to produce complete homogenisation of a deposit experiencing a sedimentation rate  $w$  ( $\text{cm.y}^{-1}$ ) and a mixing depth  $s$ (cm) is given by

$$K_b \geq 10 w.s. \quad (10)$$

Thus, if the constant  $^{210}\text{Pb}$  activity in the upper 4 cms. of this deposit is attributed to biological reworking, a lower limit estimate for  $K_b$  of  $31 \text{ cm}^2\text{y}^{-1}$  is obtained. This value is typical of estimates of  $K_b$ , ranging from 1 to  $10^3 \text{ cm}^2\text{y}^{-1}$ , for nearshore sediments.

An estimate of the flux of excess  $^{210}\text{Pb}$  to the sediment/water interface, although complicated by the presence of the  $^{226}\text{Ra}$  anomaly, can be obtained via the following assumptions;

- (1) that the  $^{210}\text{Pb}$  sedimentation rate derived over the depth interval 10 cms. to 17 cms. is applicable in the 'anomalous' upper 10 cms. of the deposit,
- (2) that the initial concentration of  $^{226}\text{Ra}$ -supported  $^{210}\text{Pb}$  depositing in each layer of sediment is

equivalent to that at depth (i.e.  $\sim 2.2 \text{ dpm.g}^{-1}$ );  
 the difference between this value of  $^{226}\text{Ra}$  and  
 measured  $^{226}\text{Ra}$  concentrations being 'excess'  $^{226}\text{Ra}$ ,

(3) that a mixed zone of 4 cms. exists at the  
 sediment surface.

Thus an estimate of the mean total  $^{226}\text{Ra}$  activity ( $\text{dpm.g}^{-1}$ )  
 in the mixed zone is obtained by summing the total  $^{226}\text{Ra}$   
 activity in each section (measured activity x section weight)  
 and dividing by the total weight of sediment in the mixed  
 zone. A value of  $9.7 \text{ dpm.g}^{-1}$  is calculated. Similarly,  
 the mean total  $^{210}\text{Pb}$  activity in the mixed zone is calculated  
 to be  $13.9 \text{ dpm.g}^{-1}$ . Assuming a mean  $^{226}\text{Ra}$ -supported  $^{210}\text{Pb}$   
 activity of  $2.2 \text{ dpm.g}^{-1}$ , the mean excess  $^{226}\text{Ra}$  activity in  
 the mixed zone is estimated at  $7.5 \text{ dpm.g}^{-1}$ . From the  $^{210}\text{Pb}$ -  
 derived sedimentation rate, the age of the 4 cm. horizon is  
 $5.2 \text{ y}$ , corresponding to the mean lifetime of a particle in  
 the mixed zone. The growth of  $^{210}\text{Pb}$  from excess  $^{226}\text{Ra}$  is  
 obtained from solution of the equation.

$$A_D = A_P (1 - e^{-\lambda_D t}) \quad \text{with } t = 5.2 \text{ y.}$$

from which, a value of  $1.1 \text{ dpm.g}^{-1}$  is obtained. Therefore  
 the mean total supported  $^{210}\text{Pb}$  activity in the mixed zone is  
 $3.3 \text{ dpm.g}^{-1}$  ( $2.2 \text{ dpm.g}^{-1}$  as the natural component +  $1.1 \text{ dpm.g}^{-1}$   
 growth from 'excess'  $^{226}\text{Ra}$ ). Hence the mean excess  $^{210}\text{Pb}$   
 activity in the mixed zone is  $10.6 \text{ dpm.g}^{-1}$  and an activity of  
 excess  $^{210}\text{Pb}$  depositing at the mud surface of  $12.3 \text{ dpm.g}^{-1}$   
 is derived from equation 3

$$A_m = \frac{A_s}{\left(1 + \frac{\lambda d}{w}\right)}$$

Combining this specific activity with the sedimentation rate of  $200 \text{ mg.cm}^{-2}\text{y}^{-1}$  a flux of excess  $^{210}\text{Pb}$  to the sediment surface of  $2.5 \text{ dpm.cm}^{-2}\text{y}^{-1}$  is derived. This is considerably higher than the estimated atmospheric input of  $0.38 \text{ dpm.cm}^{-2}\text{y}^{-1}$  and implies that particulates depositing at this location must carry considerable quantities of  $^{210}\text{Pb}$  sorbed in the catchment.

The stable lead profile for core LGC9 is shown in fig. 65. Lead concentrations increase from 400 ppm at the bottom of the core, to pass through a broad maximum of  $\sim 550$  ppm between 10 cms. and 5 cms. depth before declining steadily towards the sediment surface where a value of around 400 ppm is again recorded. Comparison of this profile with that of the gravity core LGG5 (fig. 57) indicates that in general the observed distributions are consistent with the interpretation of a mixing/loss process for the gravity core; that is

- (1) stable lead concentrations near the top of the gravity core are similar to those recorded in the lower half of the Craib core, and
- (2) the observed decrease in stable lead concentrations below 10 cms. in the Craib core is more gradual than that observed in the gravity core, i.e. similar to the trend observed for  $^{210}\text{Pb}$ . The apparent lack of homogeneity in the upper 4 cms. of the deposit with respect to stable lead is however unexplained. Apparently there has been a decreased input of lead to the sediment in recent years. Based on the  $^{210}\text{Pb}$  sedimentation rate of  $200 \text{ mg.cm}^{-2}\text{y}^{-1}$  and a surface concentration of  $400 \text{ }\mu\text{g.g}^{-1}$ , the modern flux of lead to the sediment is  $\sim 80 \text{ }\mu\text{g.cm}^{-2}\text{y}^{-1}$  which compares with a natural flux, estimated from the

gravity core, of  $\sim 2 \mu\text{g} \cdot \text{cm}^{-2} \cdot \text{y}^{-1}$ , assuming a similar rate of sediment accumulation in the pre-industrial era; however this apparent 40-fold increase in lead input probably represents a minimum estimate, as the sedimentation rate might reasonably be expected to have been lower in pre-settlement times.

In summary then, there is good evidence from Craib core radionuclide and X-radiographic evidence that the sediments of station 1 in Loch Goil are subject to bioturbation to a depth of  $\sim 4$  cms. The depth distribution of  $^{210}\text{Pb}$  infers a relatively high rate of sediment accumulation of  $200 \text{ mg} \cdot \text{cm}^{-2} \cdot \text{y}^{-1}$  ( $0.6 \text{ cm} \cdot \text{y}^{-1}$ ). The derived annual flux of  $^{210}\text{Pb}$  to the sediment surface is about 6 times that expected on the basis of direct atmospheric fallout alone. The flux of stable lead to the sediment is calculated to be around  $80 \mu\text{g} \cdot \text{cm}^{-2} \cdot \text{y}^{-1}$ . A particularly interesting feature of these deposits is the presence of a considerably higher concentration of  $^{226}\text{Ra}$  in the upper layers of the deposit, levels being roughly 5 times greater than those observed in deeper sediments.

### Loch Goil

#### Station 2

Fig. 66 presents the profile of total  $^{210}\text{Pb}$  and  $^{226}\text{Ra}$  for Craib core LGC4, recovered from Loch Goil station 2.  $^{210}\text{Pb}$  is relatively constant in the upper 6 cms. of the core with a mean activity of  $6.6 \text{ dpm} \cdot \text{g}^{-1}$ . Below 8 cms.  $^{210}\text{Pb}$  decreases slowly with depth, a minimum value of  $3.0 \text{ dpm} \cdot \text{g}^{-1}$  being observed in the bottom section of the core, at a depth of 16 cms.  $^{226}\text{Ra}$  shows evidence of a surface maximum, but of considerably reduced magnitude relative to that observed at station 1. Concentrations

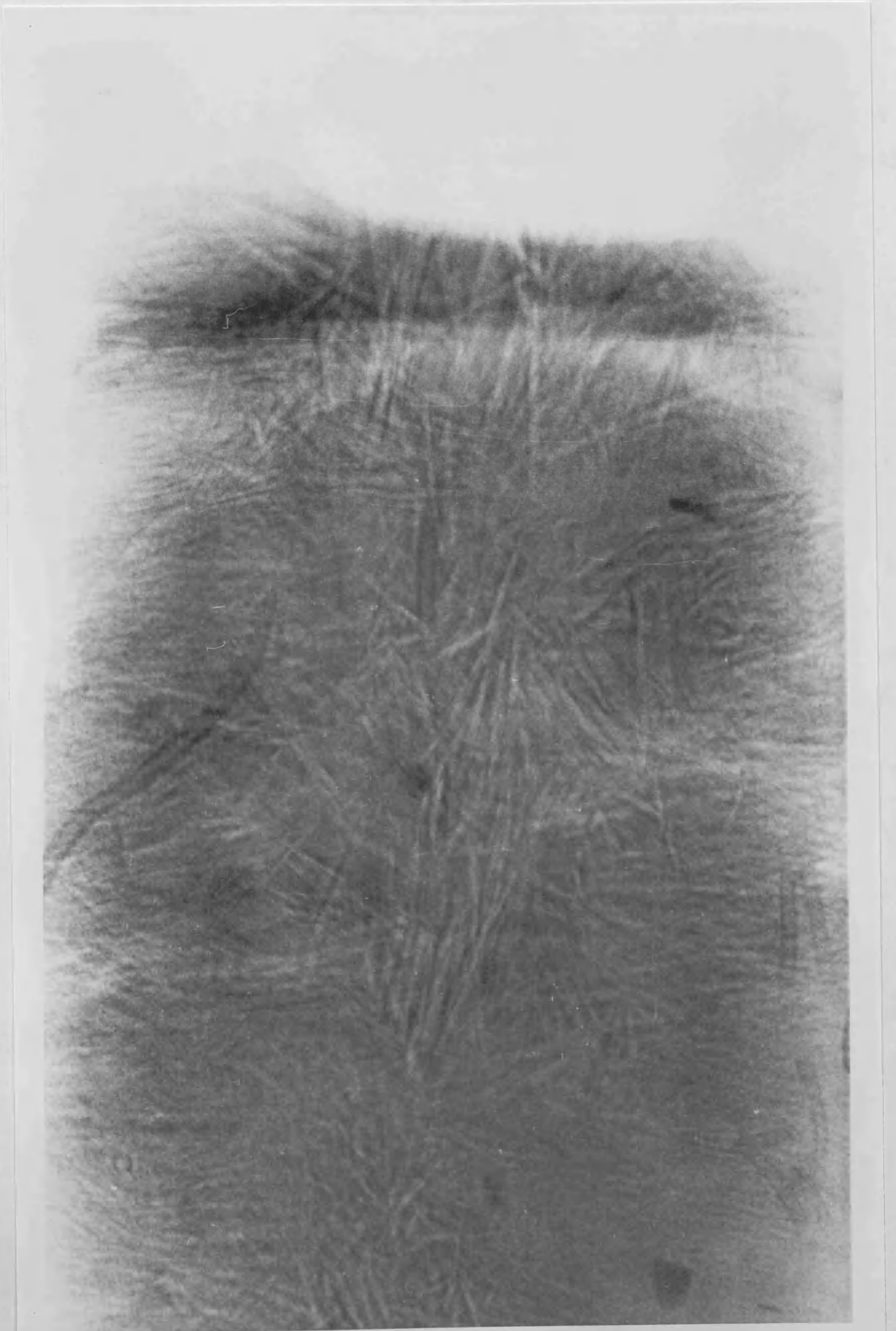
in the upper 4 cms. of the core have a mean of  $\sim 2.9 \text{ dpm.g}^{-1}$ , roughly 2 times that observed below this horizon, where 6 measurements of  $^{226}\text{Ra}$  yield a mean of  $1.5 \text{ dpm.g}^{-1}$ .

Using this estimate for supported  $^{210}\text{Pb}$ , weighted linear regression analysis yields a value of  $123 \pm 18 \text{ mg.cm}^{-2}\text{y}^{-1}$  (fig.69) for the sedimentation rate based on the decreasing concentration of excess  $^{210}\text{Pb}$  with depth in the lower half of the Craib core. This is equivalent to a mean sedimentation rate of  $3.5 \text{ mm.y}^{-1}$  over the length of the core, and a surface accumulation rate of  $7 \text{ mm.y}^{-1}$ .

X-radiographs of Craib cores from this site show evidence of worm tracks to depths slightly greater than 4 cms. Plate 2 shows an X-ray photograph of the upper 6 cms. of a companion Craib core to that of LGC4. Assuming homogenisation of the deposit to 6 cms. through bioturbation, consistent with  $^{210}\text{Pb}$  data and X-radiographic evidence, and using equation 10 after Guinasso and Schink (1975), a minimum estimate for  $K_b$  of  $26 \text{ cm}^2\text{y}^{-1}$  is derived for this location, in close agreement with that calculated previously for station 1. Also on the basis of this assumption, an estimate of excess  $^{210}\text{Pb}$  in the mixed zone can be made and hence a value obtained for the flux of excess  $^{210}\text{Pb}$  to the sediment/water interface, in a manner similar to that described for core LGC9. Thus the mean total  $^{226}\text{Ra}$  activity in the upper 6 cms. of the deposit is  $2.5 \text{ dpm.g}^{-1}$ , of which the detrital component giving rise to supported  $^{210}\text{Pb}$  is  $1.5 \text{ dpm.g}^{-1}$ ; excess  $^{226}\text{Ra}$  in the mixed zone is therefore  $1.0 \text{ dpm.g}^{-1}$ . From the sedimentation rate of  $123 \text{ mg.cm}^{-2}\text{y}^{-1}$  an age of  $\sim 15 \text{ y}$  is calculated for the base of the mixed zone and a value of  $0.4 \text{ dpm.g}^{-1}$  obtained for the growth of  $^{210}\text{Pb}$  from

PLATE 2

X-radiograph of a Craib core from Loch Goil station 2



excess  $^{226}\text{Ra}$ . Therefore the estimated total supported  $^{210}\text{Pb}$  in the mixed zone is  $1.9 \text{ dpm.g}^{-1}$ . Since the mean total  $^{210}\text{Pb}$  in the upper 6 cms. of the deposit is  $6.6 \text{ dpm.g}^{-1}$ , the estimated  $^{210}\text{Pb}$  excess in the mixed zone is  $4.7 \text{ dpm.g}^{-1}$ . Using equation 3 a value of  $6.8 \text{ dpm.g}^{-1}$  is obtained for the activity of excess  $^{210}\text{Pb}$  depositing at the sediment/water interface, implying a flux of excess  $^{210}\text{Pb}$  to the sediment of  $0.8 \text{ dpm.cm}^{-2}\text{y}^{-1}$ . This  $^{210}\text{Pb}$  flux is again considerably higher than that expected from atmospheric fallout alone.

The radiocaesium profile for core LGC4 is shown in fig. 68 and as before the trend of increasing concentrations of  $^{134}\text{Cs}$  and  $^{137}\text{Cs}$  towards the mud surface is consistent with that expected on the basis of radiocaesium discharge from Windscale. The interpretation of a mixed zone of 6 cms. is consistent with the profile, with the exception of section 2 where  $^{137}\text{Cs}$  shows a surprisingly high concentration. If the low  $^{137}\text{Cs}$  concentration at the base of the core (17 cms.) is equated to incorporation of  $^{137}\text{Cs}$  into the sediments in 1953, as discussed for core LGC9, and correction made for the mixing depth of 6 cms., the estimated rate of sediment accumulation is  $110 \text{ mg.cm}^{-2}\text{y}^{-1}$ , in good agreement to that based on  $^{210}\text{Pb}$  results. Again this sedimentation rate based on  $^{137}\text{Cs}$  represents a minimum, since  $^{137}\text{Cs}$  may be present below 17 cms.

The stable lead profile for core LGC4 is shown in fig. 71. Lead levels are constant in the top 10 to 12 cms. but follow a decreasing trend below this depth. The profile is therefore consistent with a surface mixed zone of 6 cms. Interestingly, there is no indication of a reduced concentration of lead in the upper few cms. of this core relative to deeper sections, as was found in LGC9, (fig. 65). Combining the surface

concentration of stable lead ( $300 \mu\text{g.g}^{-1}$ ) with the  $^{210}\text{Pb}$ -derived sedimentation rate ( $123 \text{mg.cm}^{-2}\text{y}^{-1}$ ) yields an estimate of  $37 \mu\text{g cm}^{-2}\text{y}^{-1}$  for the modern flux of lead to this location.

Both from the analyses performed in this study on Craib cores LGC9 and LGC4, and from the following additional information, it is apparent that there are major and interesting differences between the sediments depositing at stations 1 and 2 in Loch Goil.

Firstly, in Deegens' (1974) study of the superficial deposits of the Clyde Sea Area, the bottom sediments at these two stations are shown to be quite different in texture (fig.7). While those of station 1 are described as muds, indicating composition largely of very fine materials, i.e. silt and clay, the sediments of station 2 are classified as a mixture of mud, sand and gravel, suggesting the presence of a substantially greater proportion of coarse-grained particles. This classification is in accord with (a) comparison of the porosity profiles for the two stations (tables 35, 37).

which indicate a considerably higher % water content for station 1, consistent with a greater proportion of fine-grained material, and (b) the results of Lennie (1978) who, as discussed later, performed a preliminary investigation of the particle size distribution of the sediments from this site.

Secondly, the rate of sediment accumulation at station 1, at the deepest part of the loch, has been shown in this study to be greater than  $1\frac{1}{2}$  times that occurring at station 2. Presumably, therefore, this relatively deep basin is acting as a low-energy trough into which particulates from overlying waters are preferentially settling either directly, or more likely, through resuspension and lateral gravitational

transport following deposition elsewhere in higher energy environments. Such a process would tend to operate in favour of lighter, smaller materials and could therefore account for the high proportion of fines of which this deposit is composed. This model is in accord with that proposed by Davis et al (1973) to explain factor of three differences in rates of sediment accumulation found in Michigan lakes. Pennington et al (1975), however, who found considerable variation in sediment accumulation rates at different locations in Blelham Tarn, regard the process as more akin to down-slope flow of a semi-fluid (in such high porosity sediments). The net result in either case is the same, i.e. transport and preferential settling of fine-grained materials in deep basins.

Thirdly, and of particular interest, is the substantial difference in basic chemical composition of the sediments between these locations. For example, the mean  $\text{CaCO}_3$  content of the upper few centimetres of sediment at station 1 is 6%, while that at station 2 is only 2.4%. Similarly, the mean total carbon concentration at station 1 is about 6%, higher than the value of 4.7% for station 2. Together these results indicate a greater concentration of biogenic debris in the muds of the deep site. This postulate forms the basis of the tentative explanation presented later for the  $^{226}\text{Ra}$  anomaly which is conspicuous by its magnitude at this location. Moreover, it is interesting to note here the decrease in percentage  $\text{CaCO}_3$  with depth apparent in these sediments. This gradient may give rise to a further dilution of  $^{210}\text{Pb}$  in the surface layers of the deposit (cf. salt) and may therefore be a further contributory factor to the observation by some

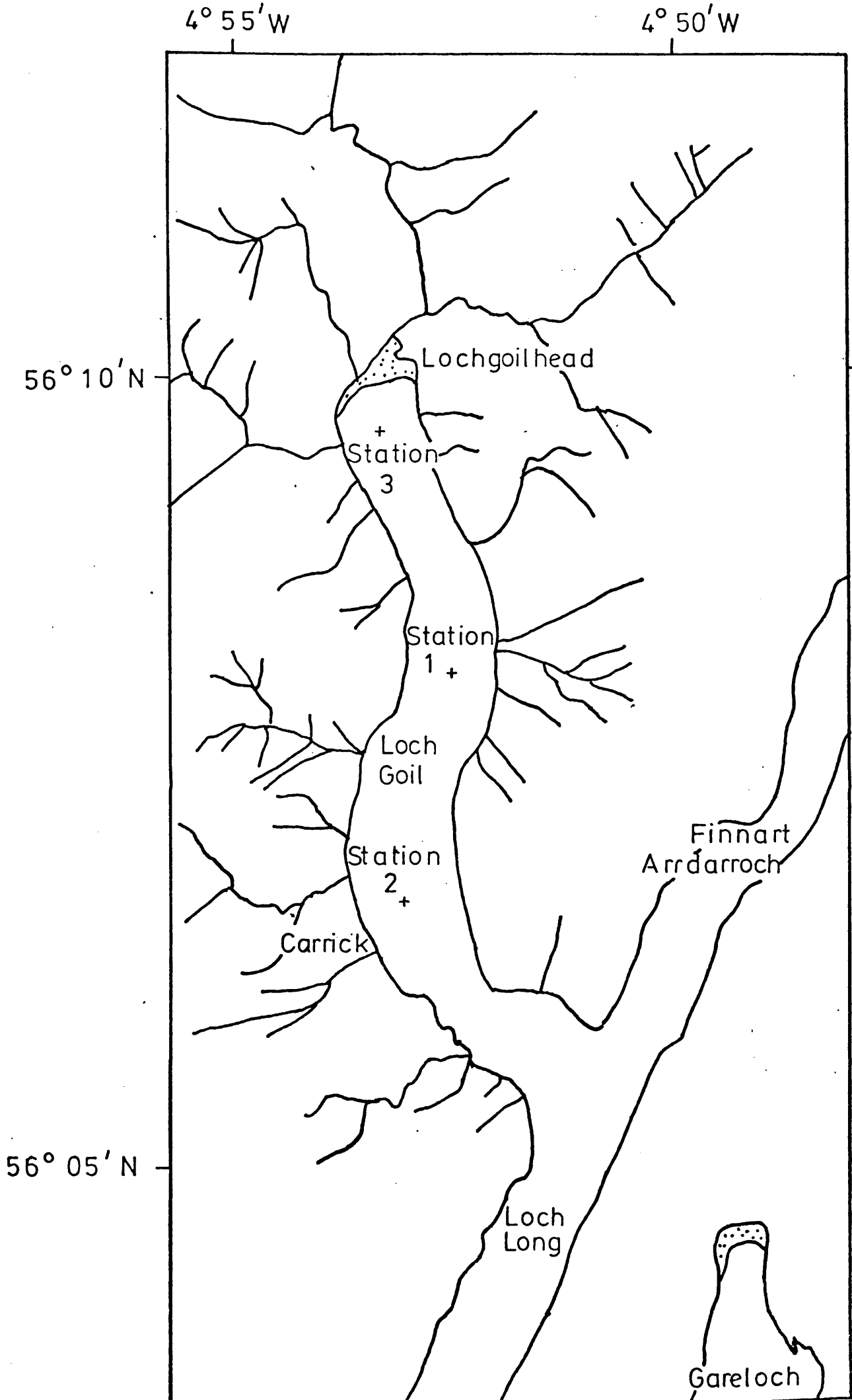




TABLE 31 LOCH GOIL GRAVITY CORE LGG5 : RESULTS OF ANALYTICAL INVESTIGATIONS

Section (cm)	Wet Wt. (g)	Dry Wt. (g)	<sup>1</sup> Porosity (%)	Microanalysis (%)		
				C	H	N
0 - 1	24.71	3.10	94.0	6.77	1.89	T or N <sup>2</sup>
1 - 2	31.78	6.78	89.2	8.42	2.16	0.54
2 - 3	34.30	7.63	88.7	7.74	1.64	T or N
3 - 4	35.12	8.01	88.4	7.29	1.61	0.29
4 - 5	36.68	8.77	87.7			
5 - 6	37.19	8.98	87.6			
6 - 7	39.49	10.13	86.7			
7 - 8	39.40	10.55	86.0			
8 - 9	41.20	11.57	85.3			
9 - 10	41.86	12.38	84.2	7.23	1.91	T or N
10 - 11	38.31	11.89	83.3			
11 - 12	38.05	12.21	82.6			
12 - 13	42.60	14.01	81.5			
13 - 14	44.16	14.96	81.4			
14 - 15	44.26	15.20	81.1	4.25	1.59	"
15 - 16	43.96	14.87	81.4			
16 - 17	41.78	14.06	81.6			
17 - 18	39.08	13.23	81.4			
18 - 19	41.38	13.89	81.6			

TABLE 31 (cont'd) LOCH GOIL GRAVITY CORE LGG5 : RESULTS OF ANALYTICAL INVESTIGATIONS

Section (cm)	Wet Wt. (g)	Dry Wt. (g)	<sup>1</sup> Porosity (%)	Microanalysis (%)		
				C	H	N
19 - 20	42.74	14.26	81.7	5.71	1.49	T or N
21 - 22	43.18	14.63	81.4			
23 - 24	45.40	16.09	80.3			
25 - 26	46.11	16.48	80.1	3.90	1.49	"
27 - 28	46.04	16.30	80.4			
29 - 30	47.72	17.42	79.6	4.16	1.35	"
31 - 32	45.85	16.72	79.6			
33 - 34	42.62	15.21	80.2			
35 - 36	47.54	18.43	78.0	3.29	1.23	"
37 - 38	43.77	16.17	79.3			
38 - 39	43.11	16.07	79.1	4.10	1.28	"

1. Porosity evaluated using mean measured particle density of  $2.3 \pm 0.1 \text{ g.cm}^{-3}$

2. T = trace; N = nil.

TABLE 31 (cont'd) LOCH GOIL GRAVITY CORE LGG5 : RESULTS OF ANALYTICAL INVESTIGATIONS

Section (cm)	$^{210}\text{Pb} \pm 1\sigma$ (dpm.g <sup>-1</sup> )	$^{226}\text{Ra} \pm 1\sigma$ (dpm.g <sup>-1</sup> )	$^{210}\text{Pb}_{\text{XS}} \pm 1\sigma^1$ (dpm.g <sup>-1</sup> )	$^{137}\text{Cs} \pm 1\sigma$ (dpm.g <sup>-1</sup> )	$^{134}\text{Cs} \pm 1\sigma$ (dpm.g <sup>-1</sup> )
0 - 1	7.18 ± 0.38	4.28 ± 0.32		6.6 ± 0.7	B.D.
1 - 2	9.41 ± 0.39	4.67 ± 0.35		9.1 ± 0.9	"
2 - 3	9.98 ± 0.29	5.56 ± 0.41	8.28 ± 0.31	7.4 ± 0.7	"
3 - 4	9.18 ± 0.40	4.88 ± 0.36	7.48 ± 0.43	8.0 ± 0.8	"
4 - 5	7.03 ± 0.27	4.06 ± 0.30	5.33 ± 0.29		
5 - 6	6.13 ± 0.33	3.47 ± 0.26	4.43 ± 0.35		
6 - 7	4.70 ± 0.26	3.01 ± 0.22	3.00 ± 0.29		
7 - 8	4.18 ± 0.20	2.82 ± 0.21	2.43 ± 0.23	1.9 ± 0.4	"
8 - 9					
9 - 10	3.04 ± 0.18	2.74 ± 0.20	1.34 ± 0.22		
10 - 11					
11 - 12					
12 - 13	2.39 ± 0.16	2.07 ± 0.20			
13 - 14					
14 - 15					
15 - 16	2.22 ± 0.14	2.21 ± 0.19			
16 - 17					
17 - 18					
18 - 19					
19 - 20	2.17 ± 0.15				

TABLE 31 (cont'd) LOCH GOIL GRAVITY CORE LGG5 : RESULTS OF ANALYTICAL INVESTIGATIONS

Section (cm)	$^{210}\text{Pb} \pm 1\sigma$ ( $\text{dpm}\cdot\text{g}^{-1}$ )	$^{226}\text{Ra} \pm 1\sigma$ ( $\text{dpm}\cdot\text{g}^{-1}$ )	$^{210}\text{Pb}_{\text{XS}} \pm 1\sigma$ ( $\text{dpm}\cdot\text{g}^{-1}$ )	$^{137}\text{Cs} \pm 1\sigma$ ( $\text{dpm}\cdot\text{g}^{-1}$ )	$^{134}\text{Cs} \pm 1\sigma$ ( $\text{dpm}\cdot\text{g}^{-1}$ )
21 - 22					
23 - 24					
25 - 26	$1.90 \pm 0.13$	$2.29 \pm 0.17$			
27 - 28					
29 - 30	$1.75 \pm 0.13$	$1.82 \pm 0.14$			
31 - 32					
33 - 34					
34 - 35	$1.65 \pm 0.14$	$1.67 \pm 0.12$			
37 - 38					
38 - 39	$1.70 \pm 0.13$	$1.71 \pm 0.12$			

1. Excess  $^{210}\text{Pb}$  evaluated with supported  $^{210}\text{Pb} = 1.7 \pm 0.1 \text{ dpm}\cdot\text{g}^{-1}$   
(mean of deepest three  $^{226}\text{Ra}$  determinations)

for Loch Goil gravity core LGG5

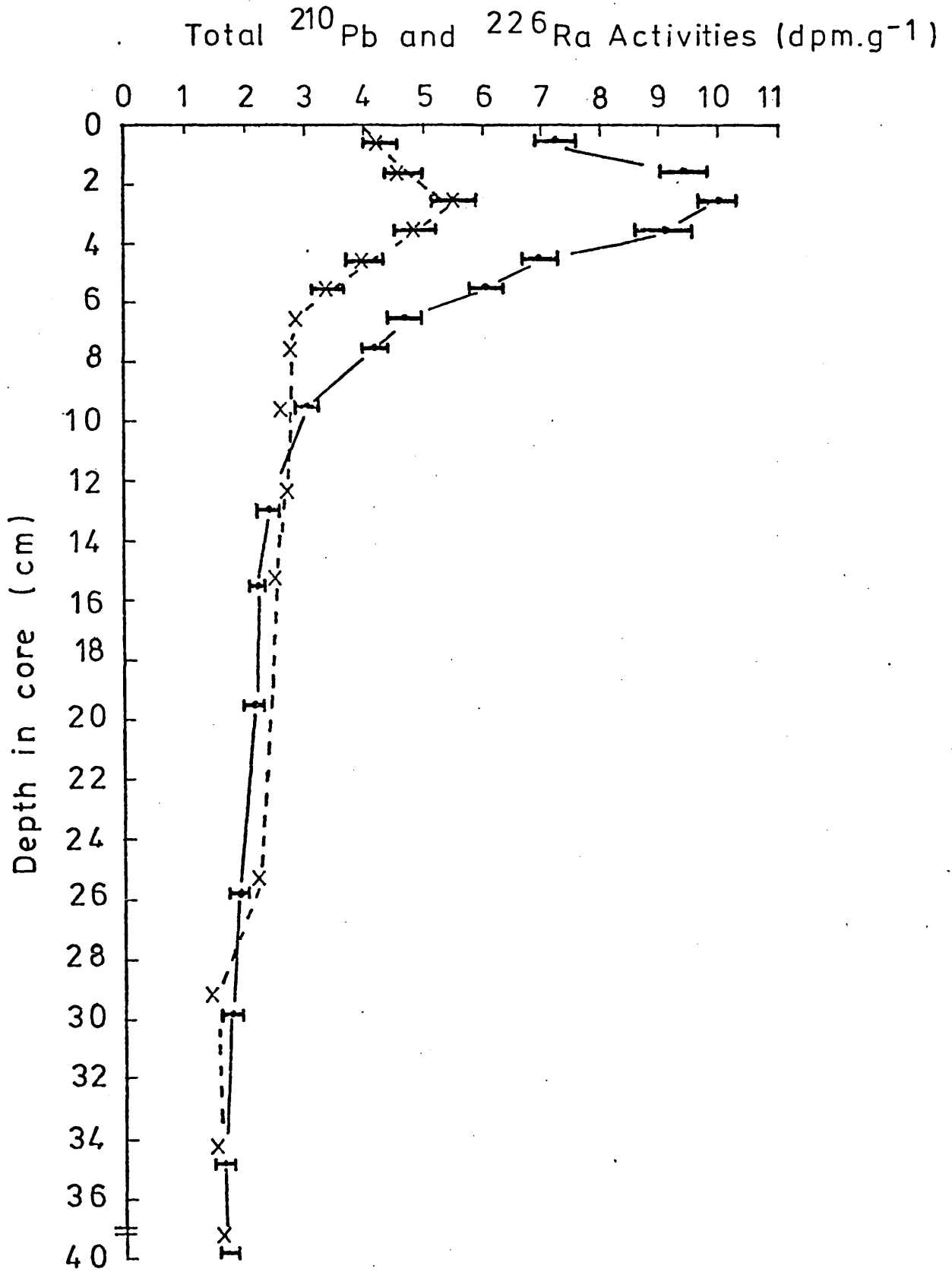


FIGURE 53 Radiocaesium profile for Loch Goil  
gravity core LGG5

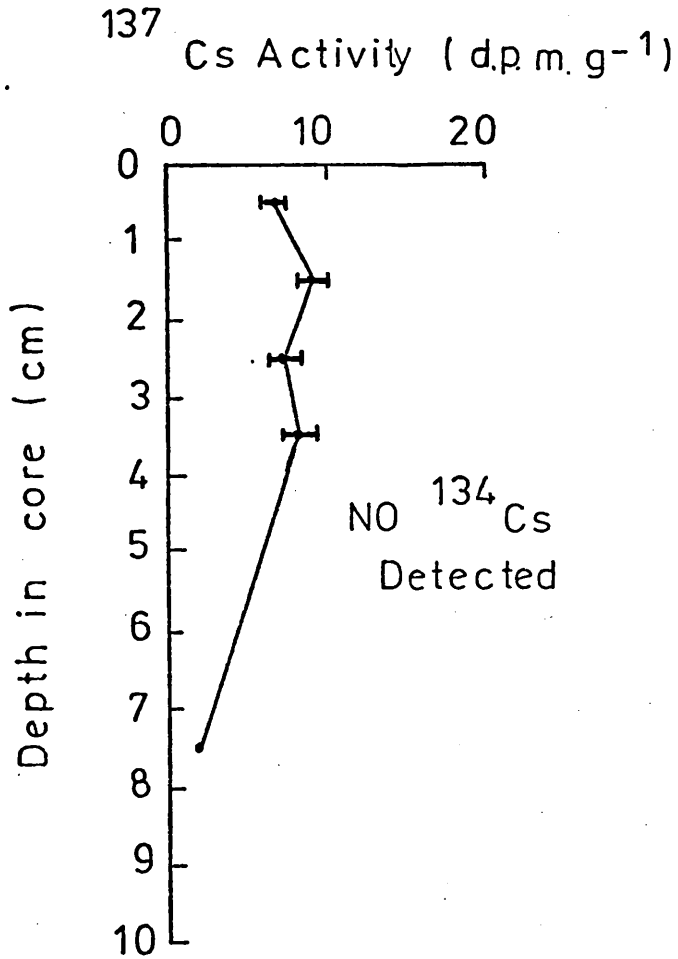


FIGURE 54 Porosity profile for Loch Goil gravity core LGG5

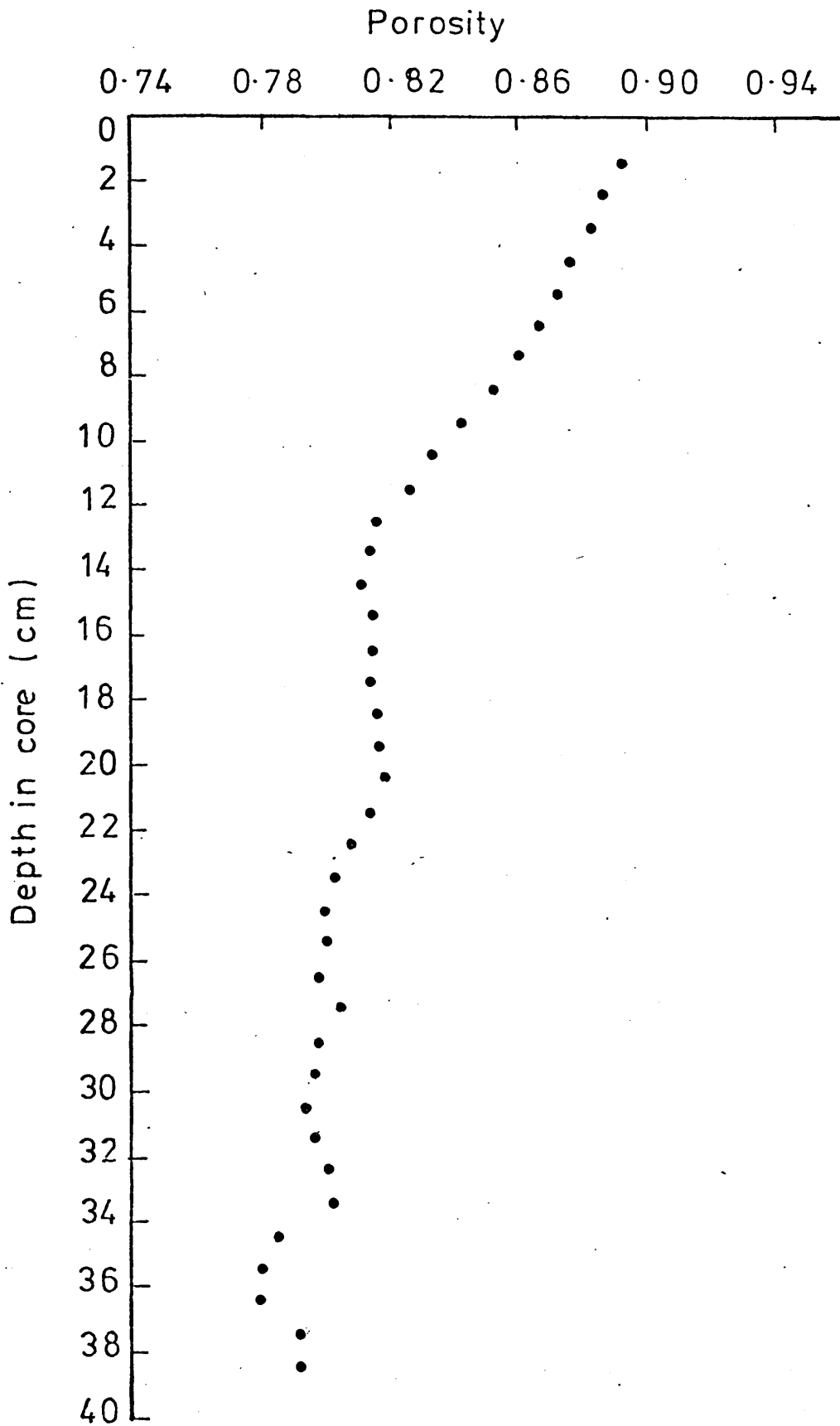


FIGURE 55      Depth profile of excess  $^{210}\text{Pb}$  for  
Loch Goil gravity core LGG5

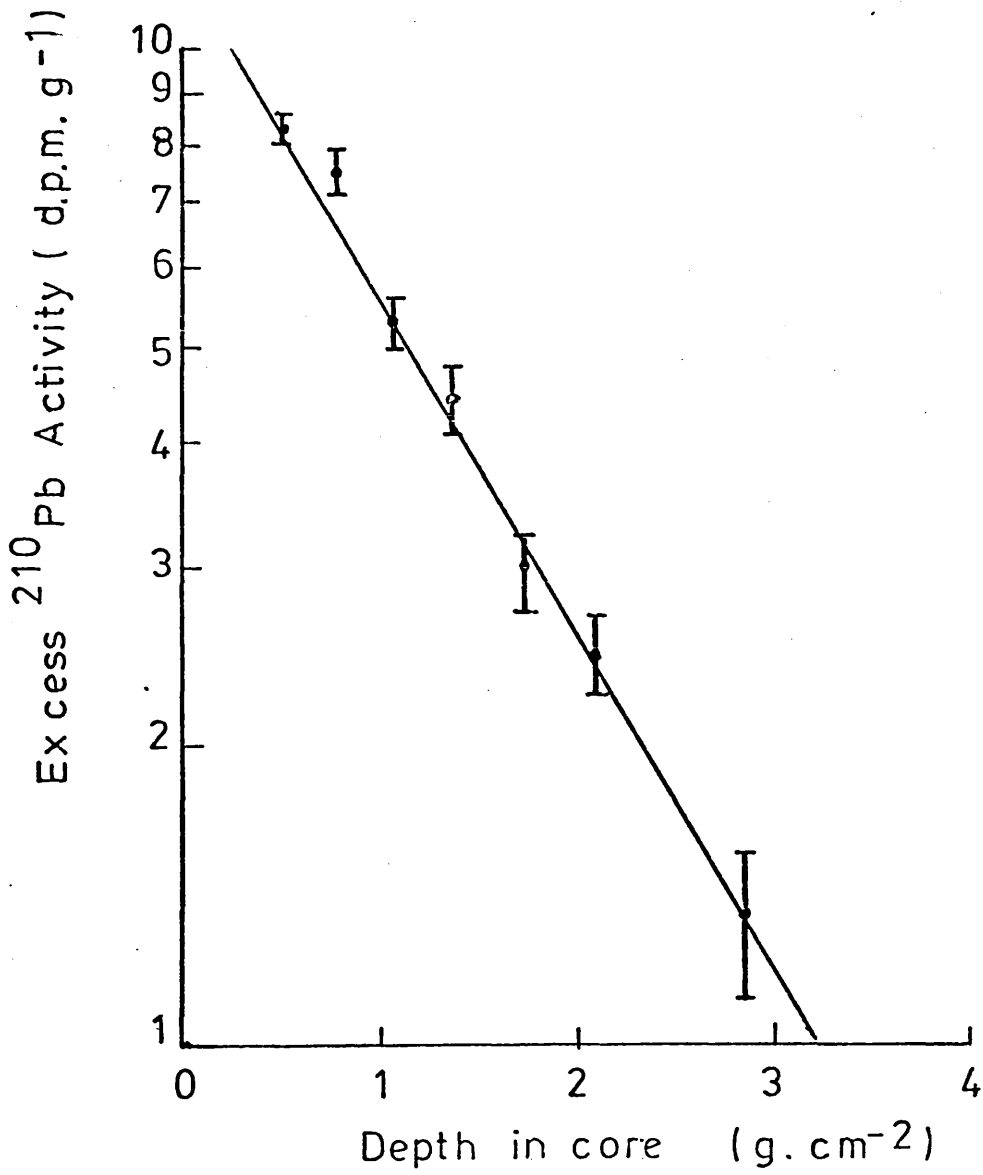


FIGURE 56

Curve of age (calendar date) against depth for  
Loch Goil gravity core L G G 5

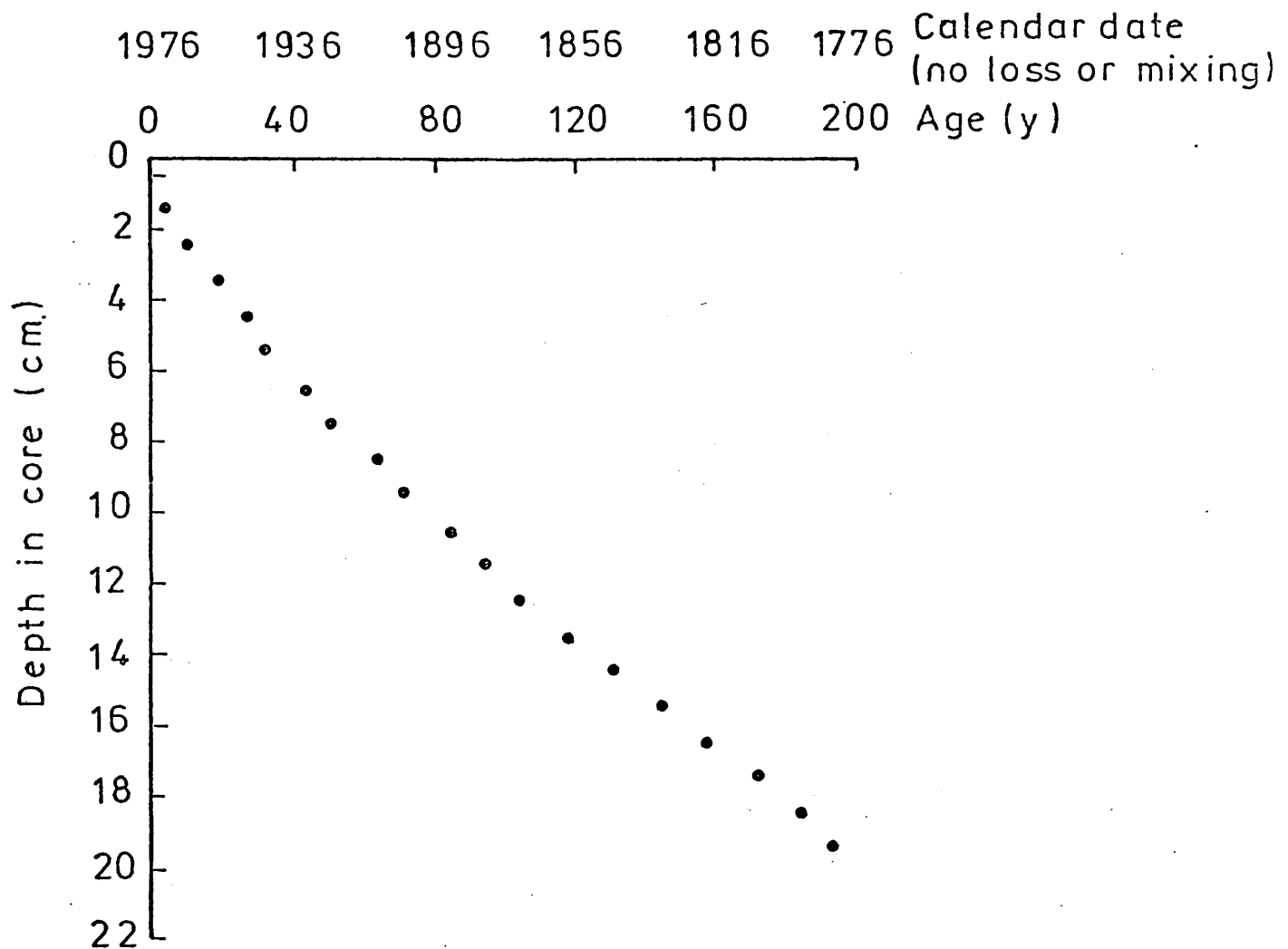


FIGURE 57 Lead profile for Loch Goil  
gravity core LGG5

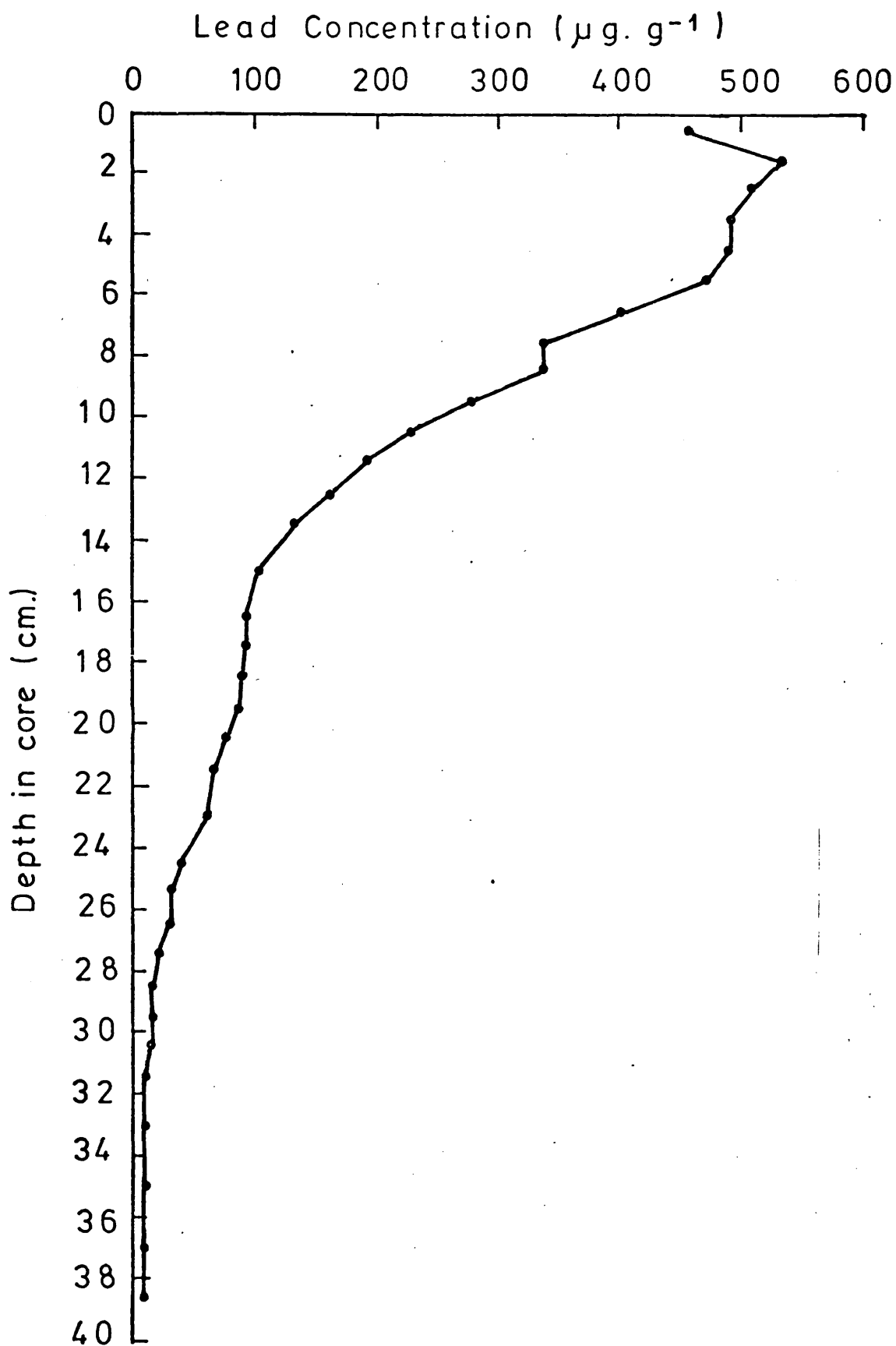


TABLE 32BACKGROUND INFORMATION FORLOCH GOIL CRAIB CORE LGC2

CORE DESIGNATION: LOCH GOIL CRAIB CORE  
CORE LGC2

SAMPLING DATE: 8.4.75

LOCATION: LAT. 56° 08' 20" N STATION 1  
LONG. 04° 53' 21" W

WATER DEPTH: 81 m

TOTAL CORE LENGTH: 10 cm

GENERAL DESCRIPTION OF SEDIMENTS:  
homogeneous very dark brown/black very fine mud

TABLE 33 LOCH GOIL CRAIB CORE LGC2 : RESULTS OF ANALYTICAL INVESTIGATIONS

Section (cm)	Wet Wt. (g)	Dry Wt. (g)	<sup>1</sup> Porosity %	Microanalysis (%)		
				C	H	N
0 - 1	24.50	3.48	93.1	6.05	1.32	T or N <sup>2</sup>
1 - 2	28.40	8.06	85.0	6.13	1.30	"
2 - 3	29.17	8.07	85.4	6.03	1.35	"
3 - 4	28.45	6.91	87.5	6.06	1.23	"
4 - 5	28.66	7.14	87.1	6.00	2.00	0.19
5 - 6	29.86	7.61	86.8	6.03	1.18	T or N
6 - 7	28.42	7.93	85.3	5.86	1.07	"
7 - 8	28.26	8.34	84.3			
8 - 9	27.36	8.13	84.1			
9 - 10	33.91	10.14	84.0	5.94	1.14	"

1. Porosity evaluated using mean measured particle density of  $2.3 \pm 0.1 \text{ g.cm}^{-3}$

2. T = trace; N = nil.

TABLE 33 (cont'd) LOCH GOIL CRAIB CORE LGC2 : RESULTS OF ANALYTICAL INVESTIGATIONS

Section (cm)	$^{210}\text{Pb}_{\text{TOT}} \pm 1\sigma$ (dpm.g <sup>-1</sup> )	$^{226}\text{Ra} \pm 1\sigma$ (dpm.g <sup>-1</sup> )	$^{137}\text{Cs} \pm 1\sigma$ (dpm.g <sup>-1</sup> )	$^{134}\text{Cs} \pm 1\sigma$ (dpm.g <sup>-1</sup> )
0 - 1	12.80 ± 0.62	7.0 ± 0.5	30.8 ± 0.8	4.0 ± 0.3
1 - 2	11.75 ± 0.55	9.3 ± 0.5	25.4 ± 0.6	3.6 ± 0.3
2 - 3	12.03 ± 0.56	10.0 ± 0.7	22.5 ± 0.6	1.5 ± 0.3
3 - 4	14.79 ± 0.72	12.2 ± 0.8	21.8 ± 0.5	2.2 ± 0.3
4 - 5	13.39 ± 0.52	11.6 ± 0.7	16.6 ± 0.4	0.0
5 - 6	12.09 ± 0.46	6.1 ± 0.3	15.2 ± 0.4	0.0
6 - 7	11.80 ± 0.37	4.0 ± 0.2	9.6 ± 0.2	0.0
7 - 8	12.21 ± 0.34	2.9 ± 0.2	10.6 ± 0.3	0.0
8 - 9	10.37 ± 0.26	2.7 ± 0.2	7.2 ± 0.2	0.0
9 - 10	9.20 ± 0.30	1.4 ± 0.1	7.2 ± 0.2	0.0

1. Error quoted is ± 1σ count only

FIGURE 58    Depth profiles of total  $^{210}\text{Pb}$  and  $^{226}\text{Ra}$   
for Loch Goil Craib core LGC2

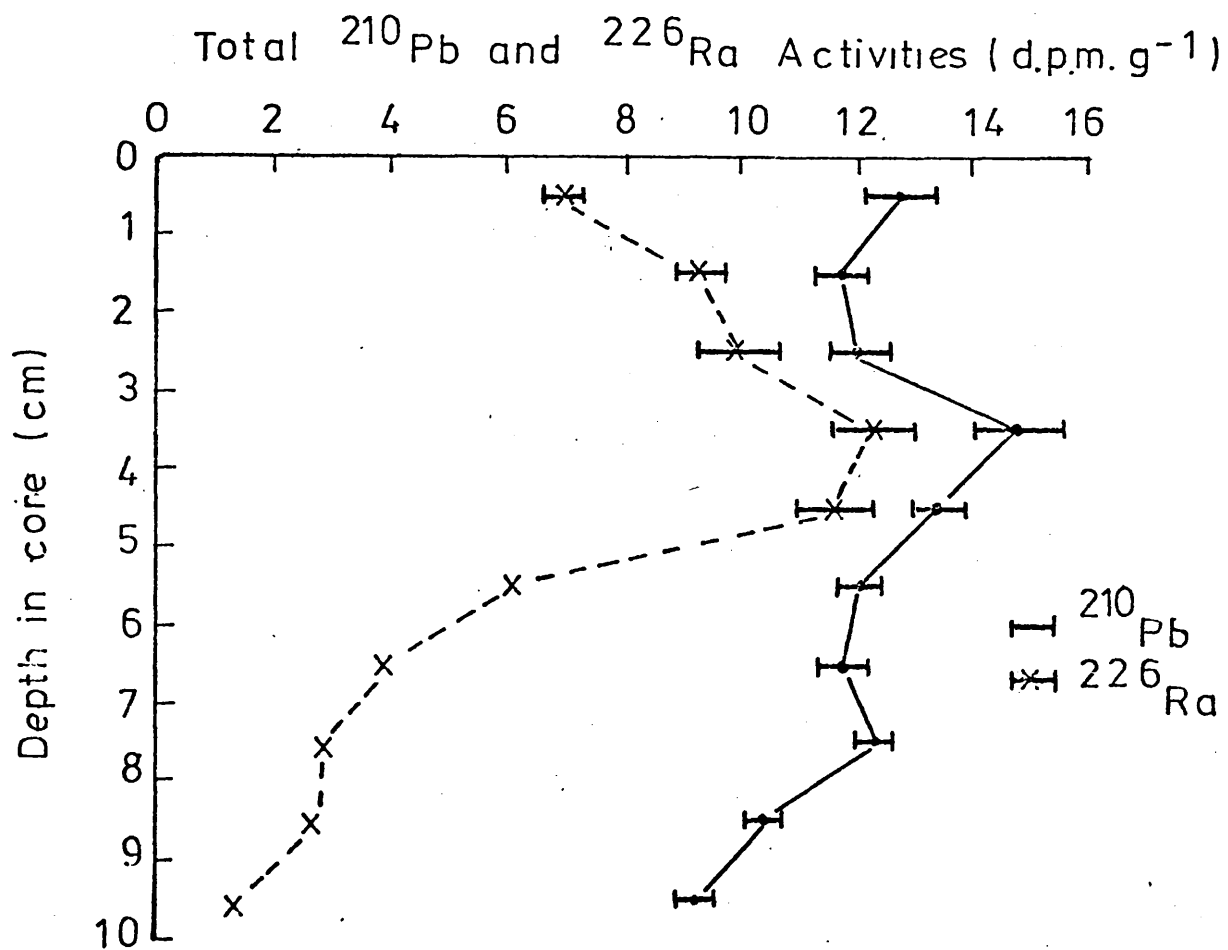


FIGURE 59      Radiocaesium profile for Loch Goil  
Craib core LGC2

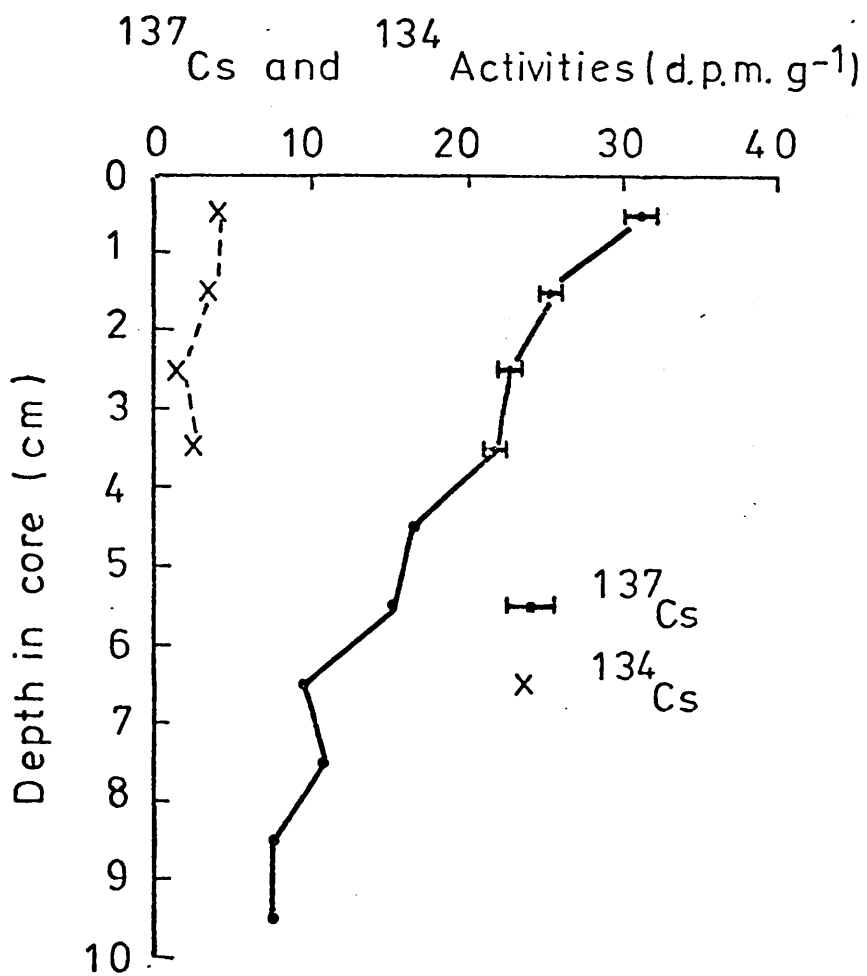


TABLE 34                    BACKGROUND INFORMATION FOR  
LOCH GOIL CRAIB CORE LGC9

CORE DESIGNATION:            LOCH GOIL CRAIB CORE  
   CORE LGC9

SAMPLING DATE:                10.8.76

LOCATION:                        LAT.    56°08'20"N                    STATION 1  
   LONG.   04°53'21"W

WATER DEPTH:                    81 m

TOTAL CORE LENGTH:            18 cm.

GENERAL DESCRIPTION OF SEDIMENTS:

homogeneous dark brown/black very fine mud

TABLE 35 LOCH GOIL CRAIB CORE LGC9 : RESULTS OF ANALYTICAL INVESTIGATIONS

Section (cm)	Wet Wt. (g)	Dry Wt. (g)	<sup>1</sup> Porosity (%)	<sup>2</sup> CaCO <sub>3</sub> (%)			<sup>2</sup> Microanalysis (%)		
				C	H	N	C	H	N
0 - 1	27.44	5.68	89.6	6.61	1.87	T or N	5.94	1.87	T or N
1 - 2	28.25	5.74	89.8	6.32	1.45	"	5.99	1.45	"
2 - 3	30.54	7.58	87.2	5.64	1.90	"	6.23	1.90	"
3 - 4	32.45	7.78	87.7	4.70	1.46	0.59	6.16	1.46	0.59
4 - 5	27.04	7.40	85.6	3.65	1.92	0.64	6.50	1.92	0.64
5 - 6	30.97	7.29	87.9	3.28	2.03	0.56	6.10	2.03	0.56
6 - 7	31.87	8.83	85.4						
7 - 8	31.87	8.01	87.0						
8 - 9	33.23	10.00	83.9	3.95	1.93	T or N	6.10	1.93	T or N
9 - 10	32.01	8.62	85.9						
10 - 11	31.43	9.85	83.1						
11 - 12	30.39	7.63	87.0	7.01	1.23	0.55	5.98	1.23	0.55
12 - 13	29.78	8.77	84.3						
13 - 14	33.64	8.31	87.2						
14 - 15	34.03	9.29	85.7	2.94	2.04	0.62	5.81	2.04	0.62
15 - 16	32.60	8.08	87.2						
16 - 17	44.16	12.66	84.8	5.36	1.17		5.53	1.17	

1. Porosity evaluated using mean measured particle density of  $2.3 \pm 0.1 \text{ g.cm}^{-3}$ .

2. Percent CaCO<sub>3</sub>/microanalytical results expressed on dry weight basis.

TABLE 35 (cont'd) LOCH GOIL CRAIB CORE LGC9 : RESULTS OF ANALYTICAL INVESTIGATIONS

Section (cm)	$^{210}\text{Pb}_{\text{TOT}} \pm 1\sigma$ (dpm.g <sup>-1</sup> )	$^{226}\text{Ra} \pm 1\sigma$ (dpm.g <sup>-1</sup> )	1 $^{210}\text{Pb}_{\text{XS}} \pm 1\sigma$ (dpm.g <sup>-1</sup> )	$^{137}\text{Cs} \pm 1\sigma$ (dpm.g <sup>-1</sup> )	$^{134}\text{Cs} \pm 1\sigma$ (dpm.g <sup>-1</sup> )
0 - 1	13.01 ± 0.28	8.01 ± 0.60		55.2 ± 4.6	6.1 ± 1.2
1 - 2	14.24 ± 0.30	11.08 ± 0.83		33.6 ± 2.9	4.5 ± 1.1
2 - 3	13.46 ± 0.26	12.50 ± 0.93		32.0 ± 2.6	2.9 ± 0.6
3 - 4	14.68 ± 0.29	7.21 ± 0.54		31.1 ± 2.6	2.4 ± 0.6
4 - 5	12.82 ± 0.27	6.34 ± 0.47		23.5 ± 2.0	2.3 ± 0.6
5 - 6	11.54 ± 0.24	5.18 ± 0.39		19.0 ± 1.7	2.0 ± 0.6
6 - 7	11.09 ± 0.23	4.07 ± 0.30		16.0 ± 1.4	1.2 ± 0.5
7 - 8	10.46 ± 0.22	3.55 ± 0.26		13.6 ± 1.2	1.4 ± 0.5
8 - 9	9.21 ± 0.27	2.71 ± 0.20		7.3 ± 0.6	1.4 ± 0.4
9 - 10	8.77 ± 0.21			4.7 ± 0.6	B.D.
10 - 11	8.62 ± 0.21	2.32 ± 0.17	6.42 ± 0.29	5.0 ± 0.6	"
11 - 12	7.50 ± 0.20		5.30 ± 0.29	4.6 ± 0.6	"
12 - 13	6.49 ± 0.18		4.29 ± 0.28	2.5 ± 0.5	"
13 - 14	7.02 ± 0.16	2.29 ± 0.17	4.82 ± 0.27	3.3 ± 0.6	"
14 - 15	7.38 ± 0.20		5.18 ± 0.29	3.1 ± 0.6	"
15 - 16	6.81 ± 0.25		4.61 ± 0.34	3.3 ± 0.6	"
16 - 17	6.26 ± 0.19	1.97 ± 0.14	4.06 ± 0.29	2.6 ± 0.5	"

1. Excess  $^{210}\text{Pb}$  evaluated with supported  $^{210}\text{Pb} = 2.2 \pm 0.2$  dpm.g<sup>-1</sup>  
(Mean of three deepest  $^{226}\text{Ra}$  determinations)

FIGURE 60 Depth profiles of total  $^{210}\text{Pb}$  and  $^{226}\text{Ra}$   
for Loch Goil Craib core LGC9

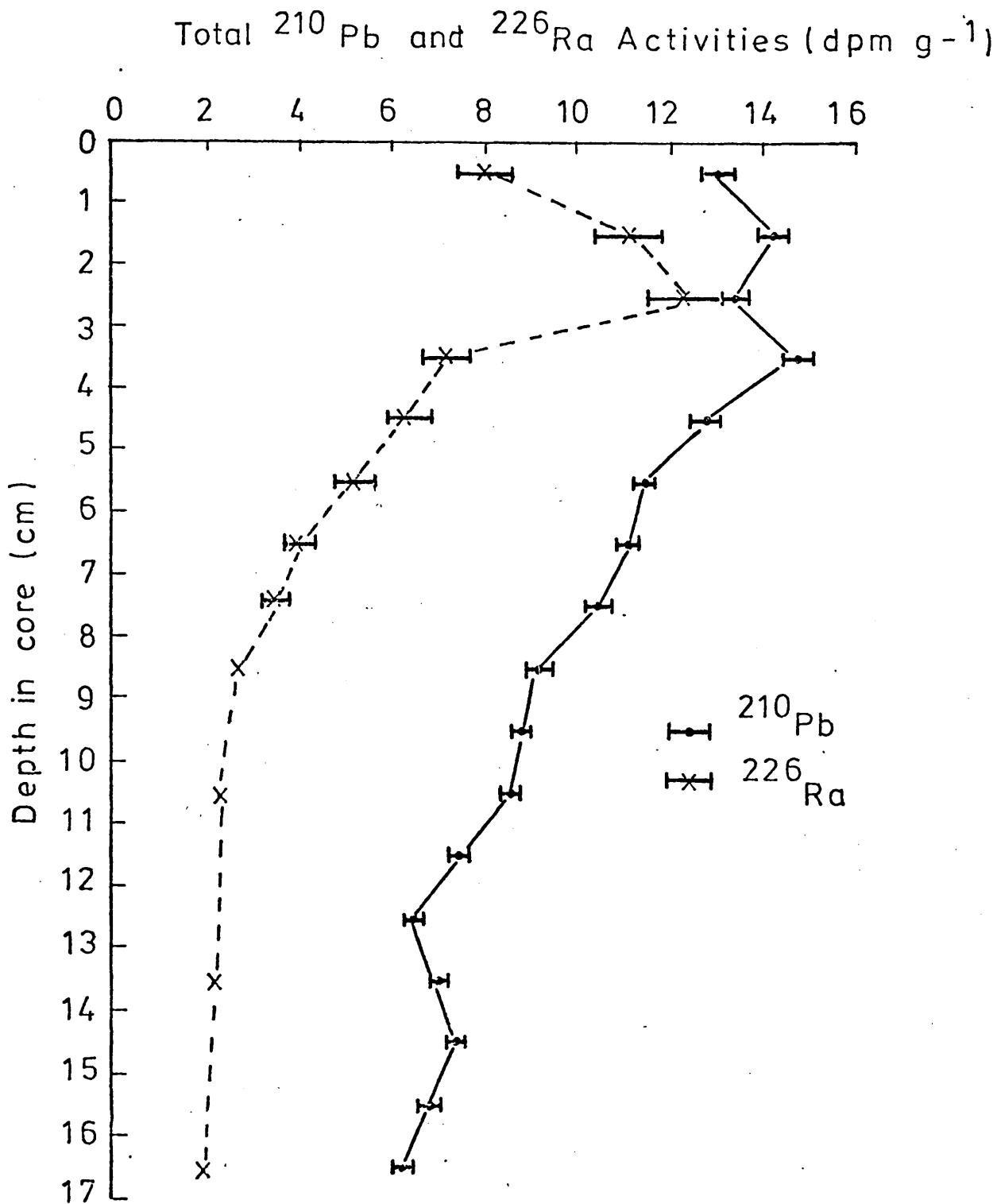


FIGURE 61    Radiocaesium profile for Loch Goil Craib  
core LGC9

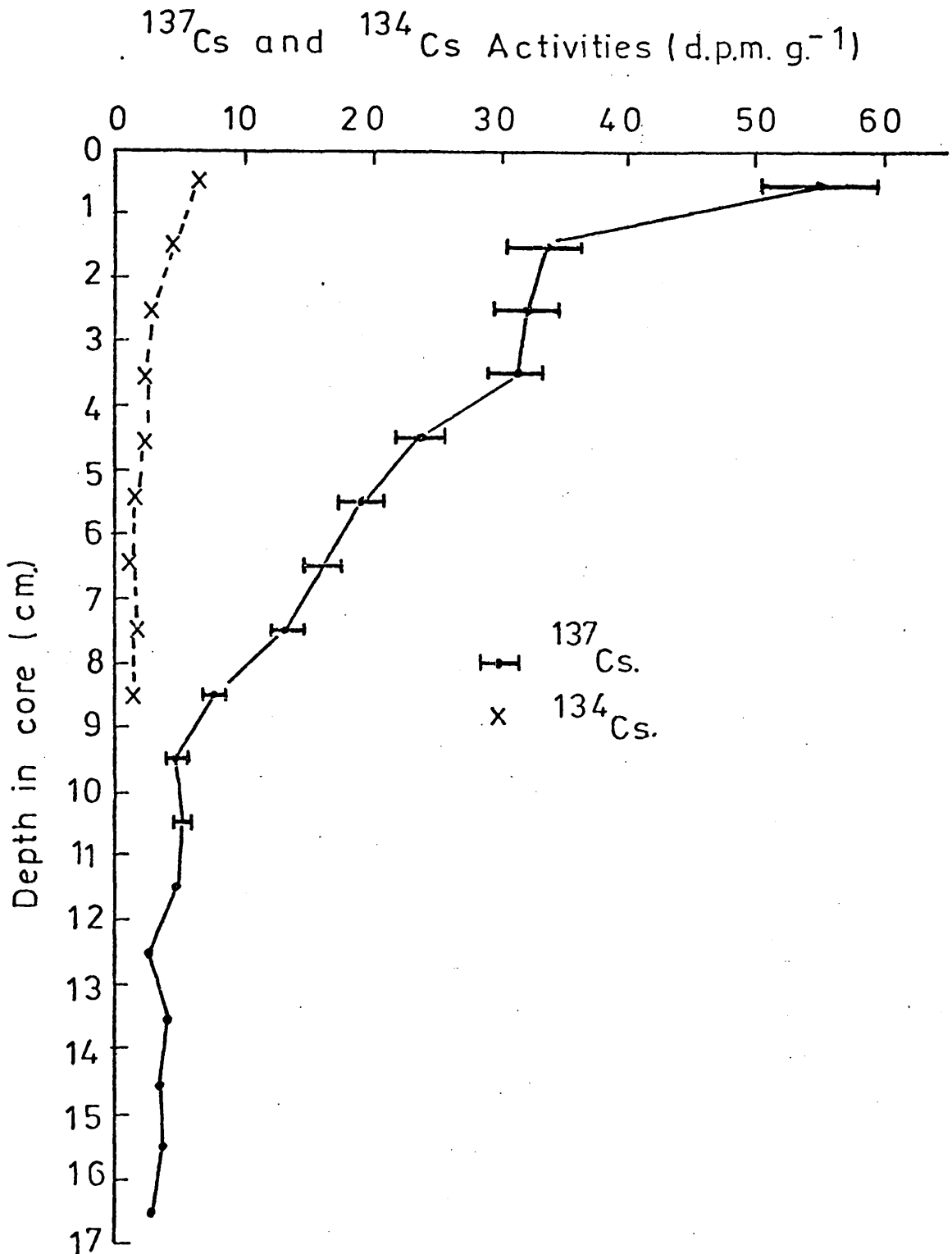


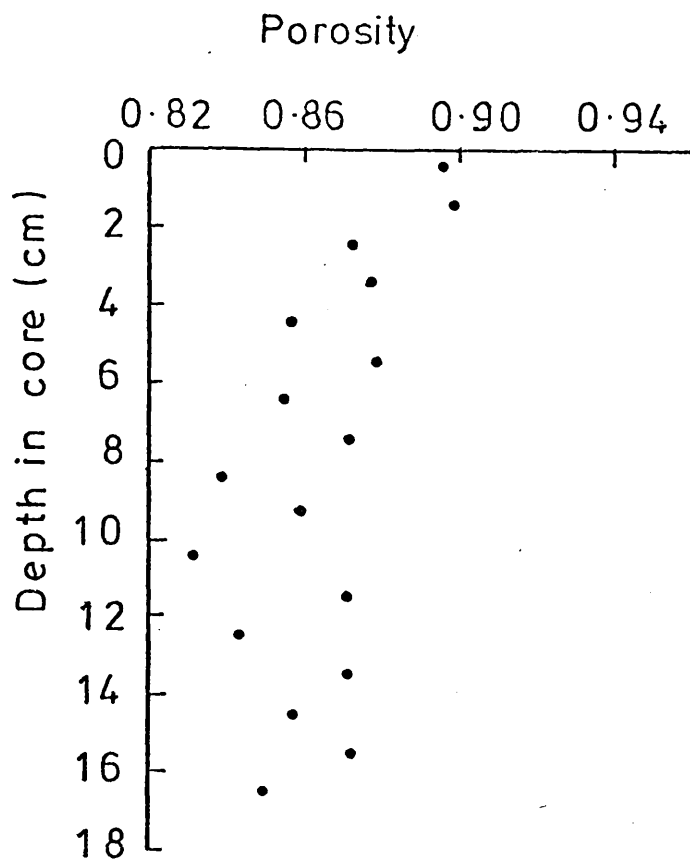
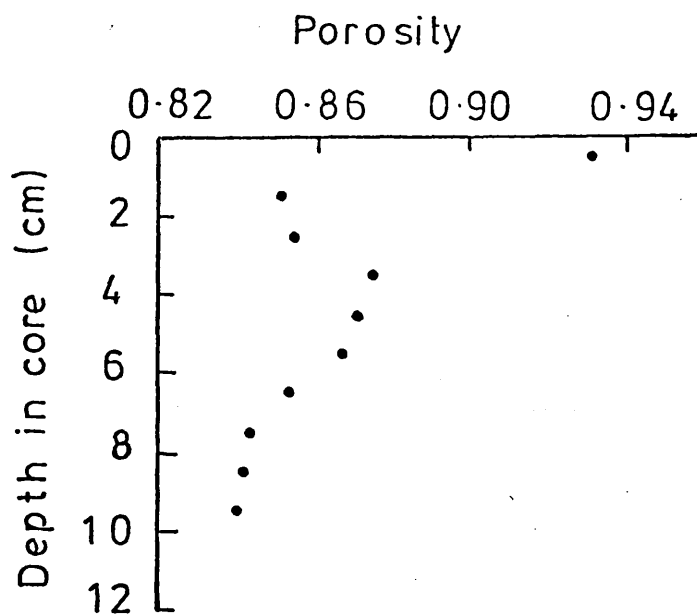
FIGURE 62a Porosity profile for Loch GoilCraib core LGC9FIGURE 62b Porosity profile for Loch GoilCraib core LGC2

FIGURE 63 Depth profile of excess  $^{210}\text{Pb}$  for Loch Goil  
Craib core LGC9

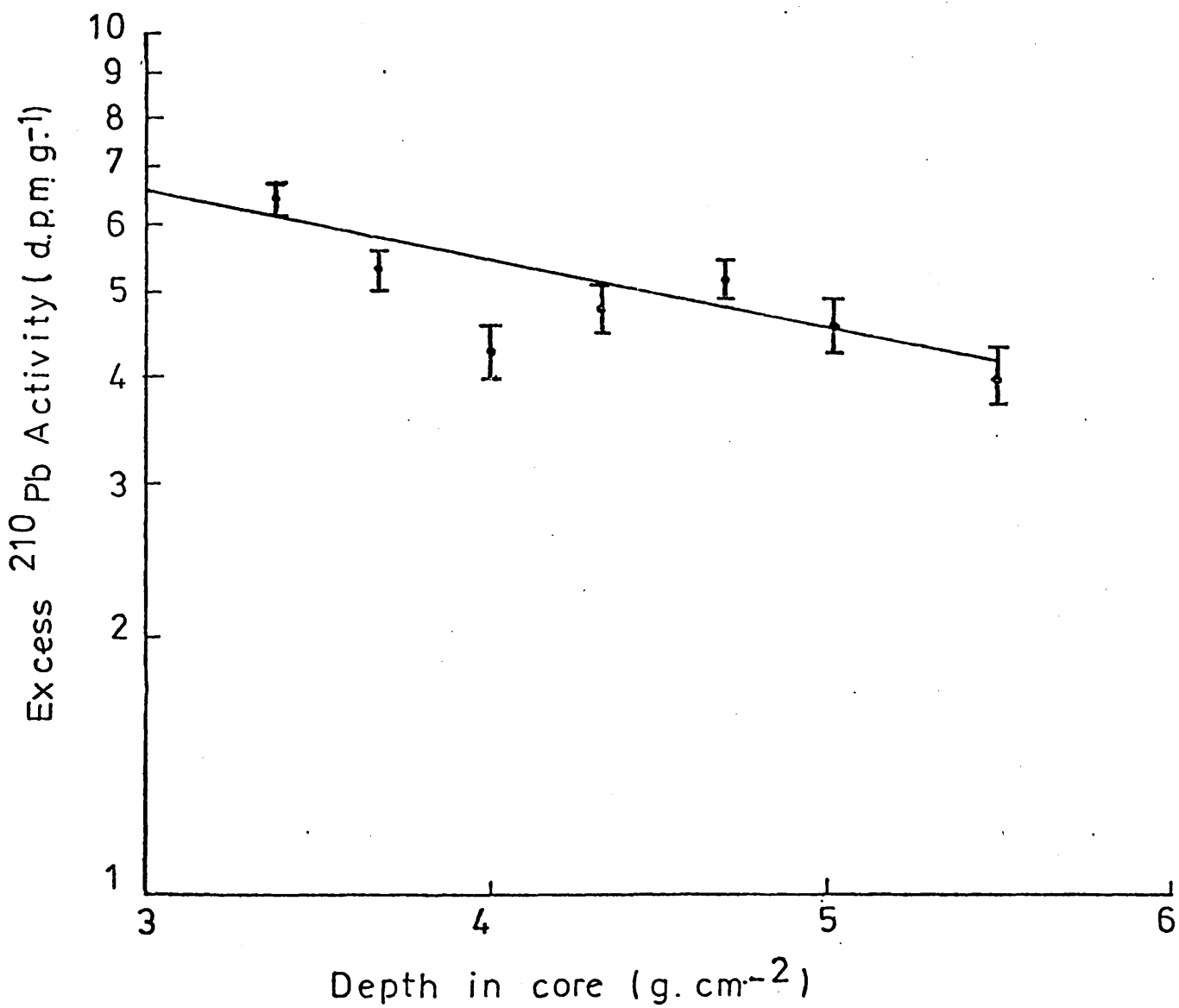


FIGURE 64      Curve of age (calendar date) against depth  
for Loch Goil Craib core LGC9

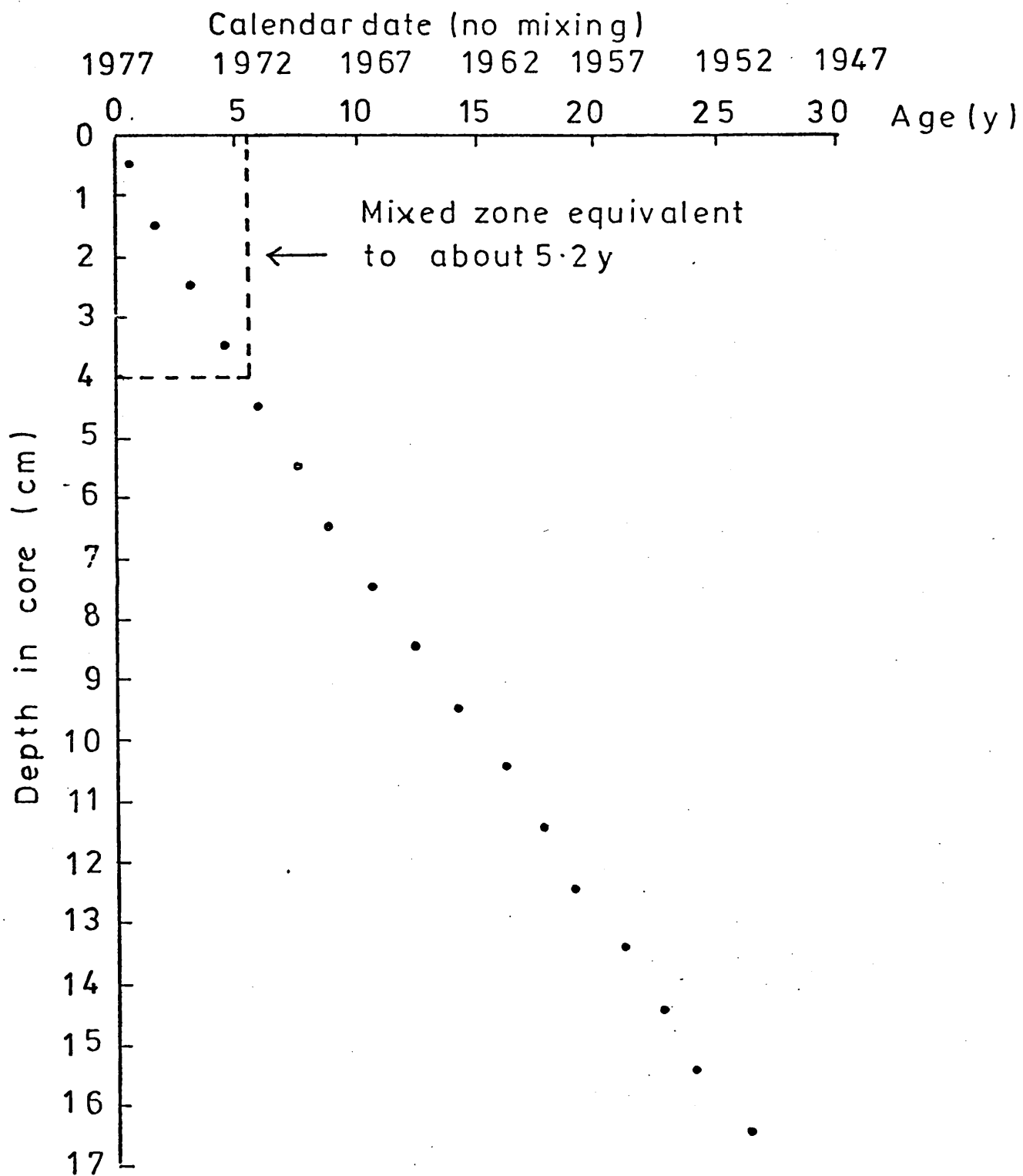


FIGURE 65 Lead profile for Loch Goil Craib core LGC9

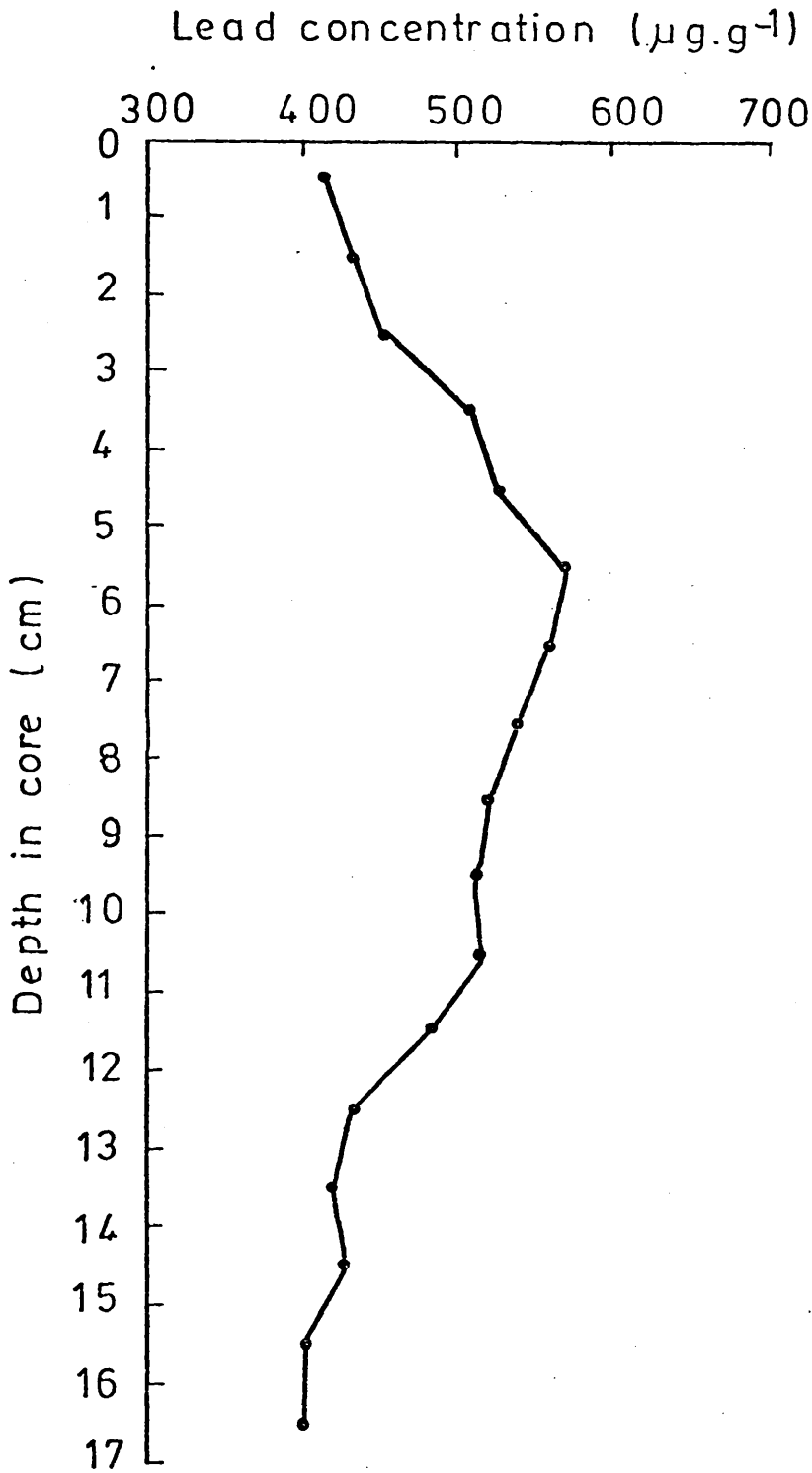




TABLE 37

## LOCH GOIL CRAIB CORE LGC4 : RESULTS OF ANALYTICAL INVESTIGATIONS

Section (cm)	Wet Wt. (g)	Dry Wt. (g)	<sup>1</sup> Porosity (%)	<sup>2</sup> CaCO <sub>3</sub> (%)	<sup>2</sup> Microanalysis (%)		
					C	H	N
0 - 1	22.39	5.07	88.5	2.96	4.19	1.82	T or N <sup>3</sup>
1 - 2	24.67	7.07	84.8	2.47	5.87	1.79	"
2 - 3	25.72	7.74	83.9		4.69	1.51	"
3 - 4	25.71	7.96	88.3	2.30	4.10	1.10	"
4 - 5	23.25	7.44	82.7	2.34	4.15	1.36	"
5 - 6	28.56	9.57	81.7	2.05	5.30	1.64	"
6 - 7	28.36	9.67	81.3	1.88			
7 - 8	28.10	9.71	81.0	1.89			
8 - 9	28.02	9.96	80.3	1.87	5.09	1.55	"
9 - 10	25.80	9.35	79.8	1.84			
10 - 11	26.34	9.54	79.8	1.81			
11 - 12	26.10	9.44	79.8	1.69	4.03	1.42	"
12 - 13	27.02	9.91	79.5	1.98			
13 - 14	26.59	9.71	79.6	1.70			
14 - 15	25.92	10.03	78.1	1.66	3.60	1.29	"
15 - 16	25.73	10.56	76.3	1.47			
16 - 17	21.24	8.60	76.8	1.54	5.79	1.40	"

1. Porosity evaluated using mean measured particle density of  $2.3 \pm 0.1 \text{ g.cm}^{-3}$

2. Percent CaCO<sub>3</sub>/microanalytical results expressed on dry weight basis.

3. T = trace; N = nil

TABLE 37 (cont'd) LOCH GOIL CRAIB CORE LGC4 : RESULTS OF ANALYTICAL INVESTIGATIONS

Section (cm)	$^{210}\text{Pb}_{\text{TOT}} \pm 1\sigma$ (dpm.g <sup>-1</sup> )	$^{226}\text{Ra} \pm 1\sigma$ (dpm.g <sup>-1</sup> )	$^{210}\text{Pb}_{\text{XS}} \pm 1\sigma$ (dpm.g <sup>-1</sup> )	$^{137}\text{Cs} \pm 1\sigma$ (dpm.g <sup>-1</sup> )	$^{134}\text{Cs} \pm 1\sigma$ (dpm.g <sup>-1</sup> )
0 - 1	6.51 ± 0.20	2.76 ± 0.20		36.3 ± 3.0	6.3 ± 1.1
1 - 2	6.20 ± 0.18	2.83 ± 0.21		54.2 ± 4.4	7.6 ± 1.1
2 - 3	6.92 ± 0.18	2.73 ± 0.20		39.1 ± 3.2	5.3 ± 1.0
3 - 4	7.01 ± 0.19	3.12 ± 0.24		36.6 ± 3.0	5.8 ± 0.9
4 - 5				34.7 ± 2.9	4.9 ± 0.9
5 - 6	6.26 ± 0.16	1.51 ± 0.12		32.4 ± 2.7	4.6 ± 0.9
6 - 7				25.5 ± 2.2	3.0 ± 0.8
7 - 8	5.81 ± 0.19	1.41 ± 0.11		18.6 ± 1.6	2.2 ± 0.8
8 - 9	5.16 ± 0.18		3.7 ± 0.3	14.5 ± 1.3	B.D.
9 - 10	4.66 ± 0.14	1.25 ± 0.10	3.2 ± 0.3	9.9 ± 0.9	"
10 - 11	4.89 ± 0.16		3.4 ± 0.3	10.2 ± 0.9	"
11 - 12	4.61 ± 0.16	1.23 ± 0.13	3.1 ± 0.3	9.9 ± 0.9	"
12 - 13	4.06 ± 0.16		2.6 ± 0.3	10.5 ± 0.9	"
13 - 14	3.89 ± 0.16	1.86 ± 0.14	2.4 ± 0.3	11.4 ± 1.0	"
14 - 15	3.70 ± 0.13		2.3 ± 0.3	7.0 ± 0.7	"
15 - 16	3.02 ± 0.12	1.44 ± 0.10	1.5 ± 0.3	3.4 ± 0.5	"

1. Excess  $^{210}\text{Pb}$  estimated with supported  $^{210}\text{Pb} = 1.5 \pm 0.2$  dpm.g<sup>-1</sup>.  
(mean of four deepest  $^{226}\text{Ra}$  determinations).

FIGURE 66 Depth profile of total  $^{210}\text{Pb}$  and  $^{226}\text{Ra}$   
for Loch Goil Craib core LGC4

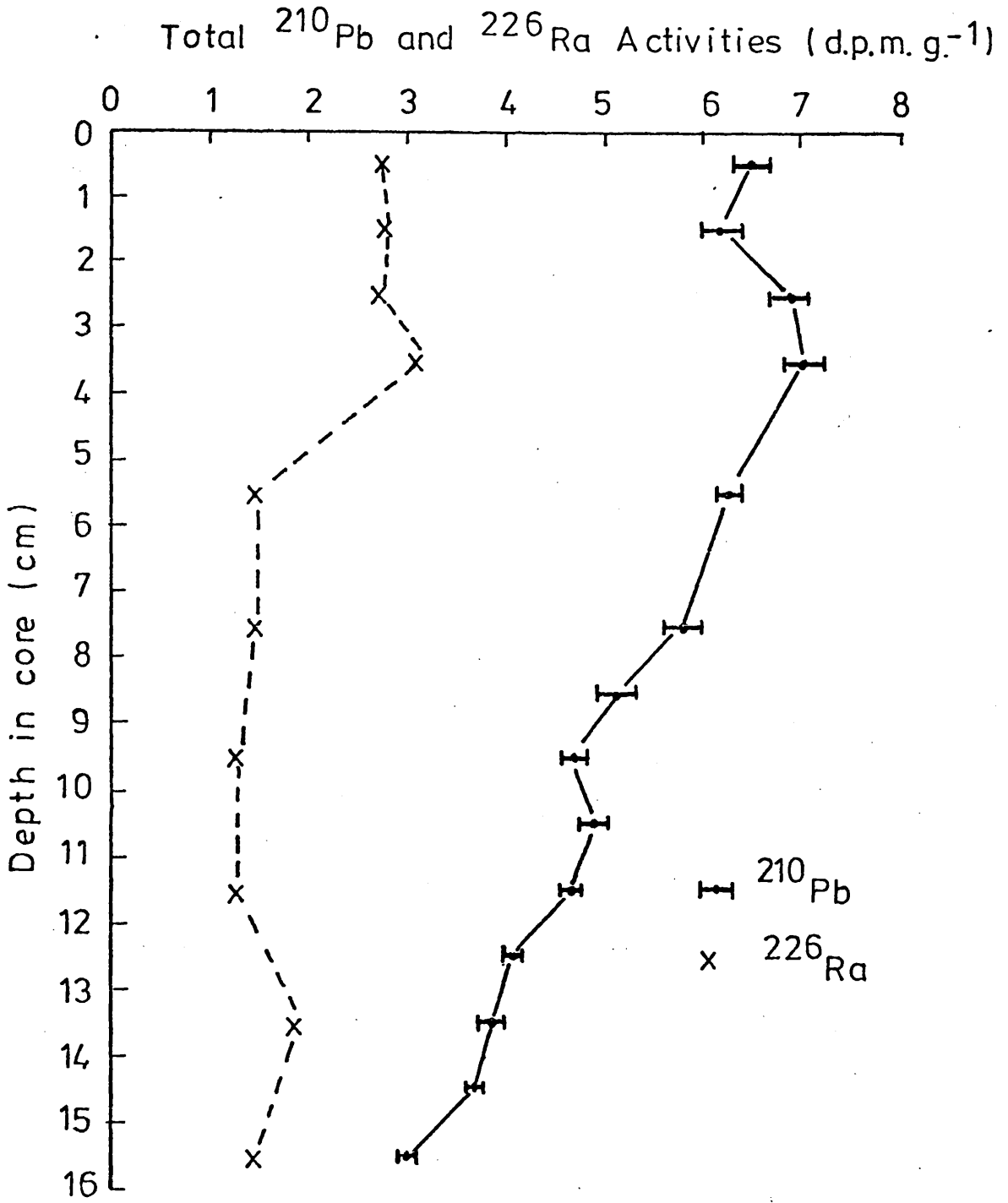


FIGURE 67    Porosity profile for Loch Gail  
Craib core LGC4

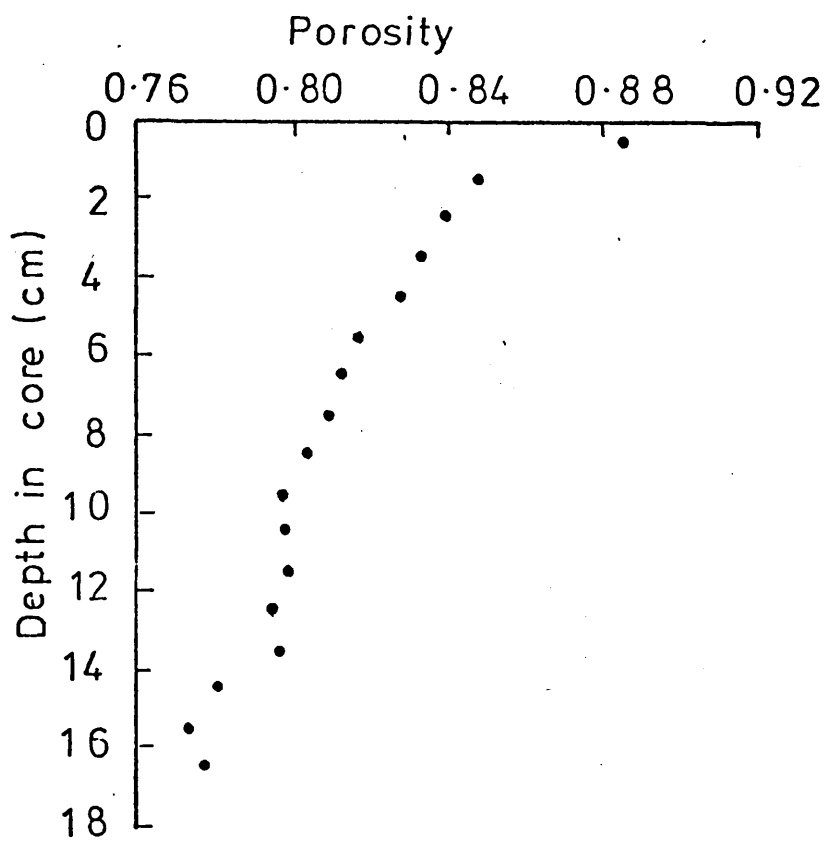


FIGURE 68 Radiocaesium profile for Loch Goil Craib  
core LGC4

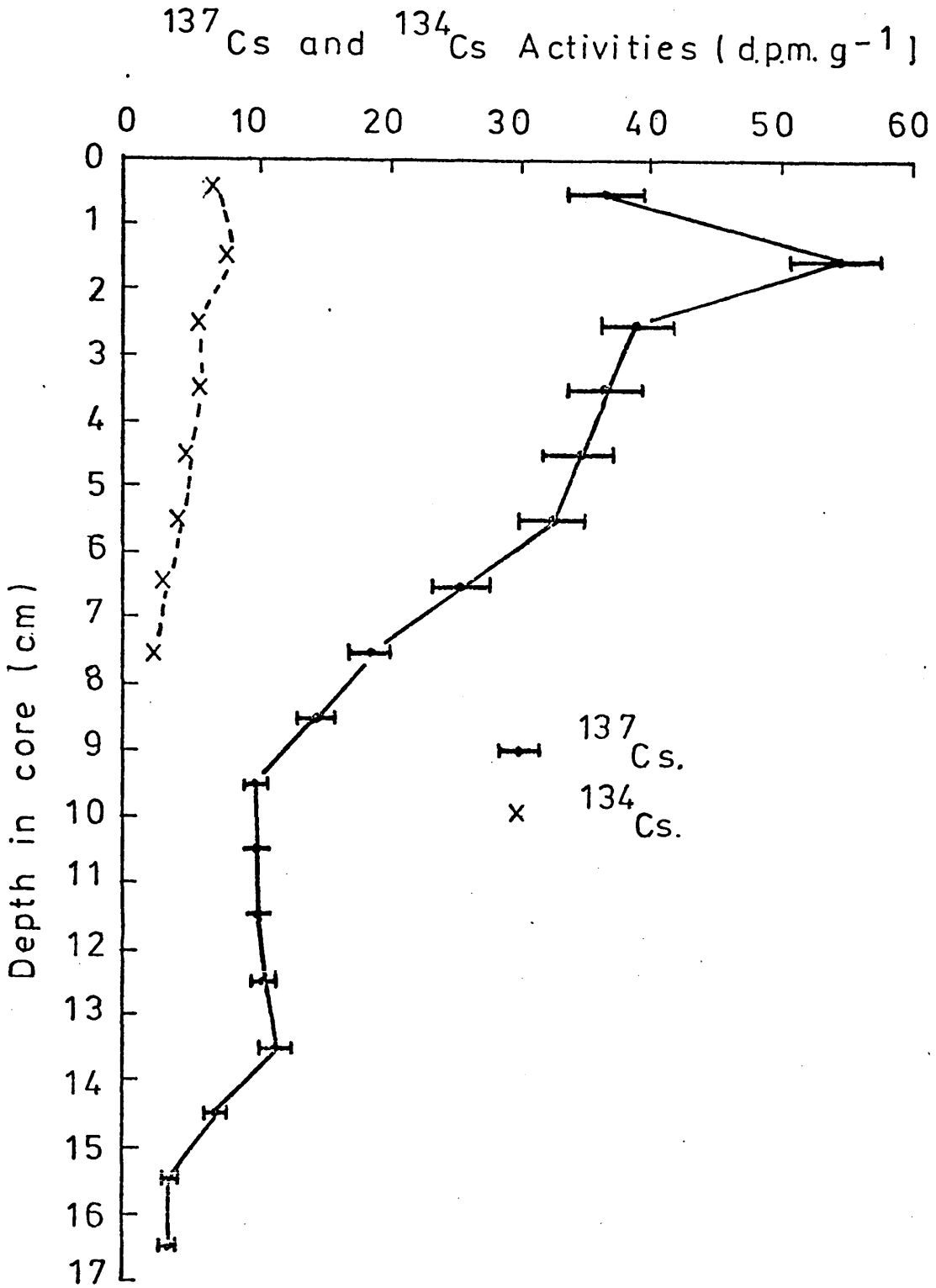


FIGURE 69 Depth profile of excess  $^{210}\text{Pb}$  for  
Loch Goil Craib core LGC4

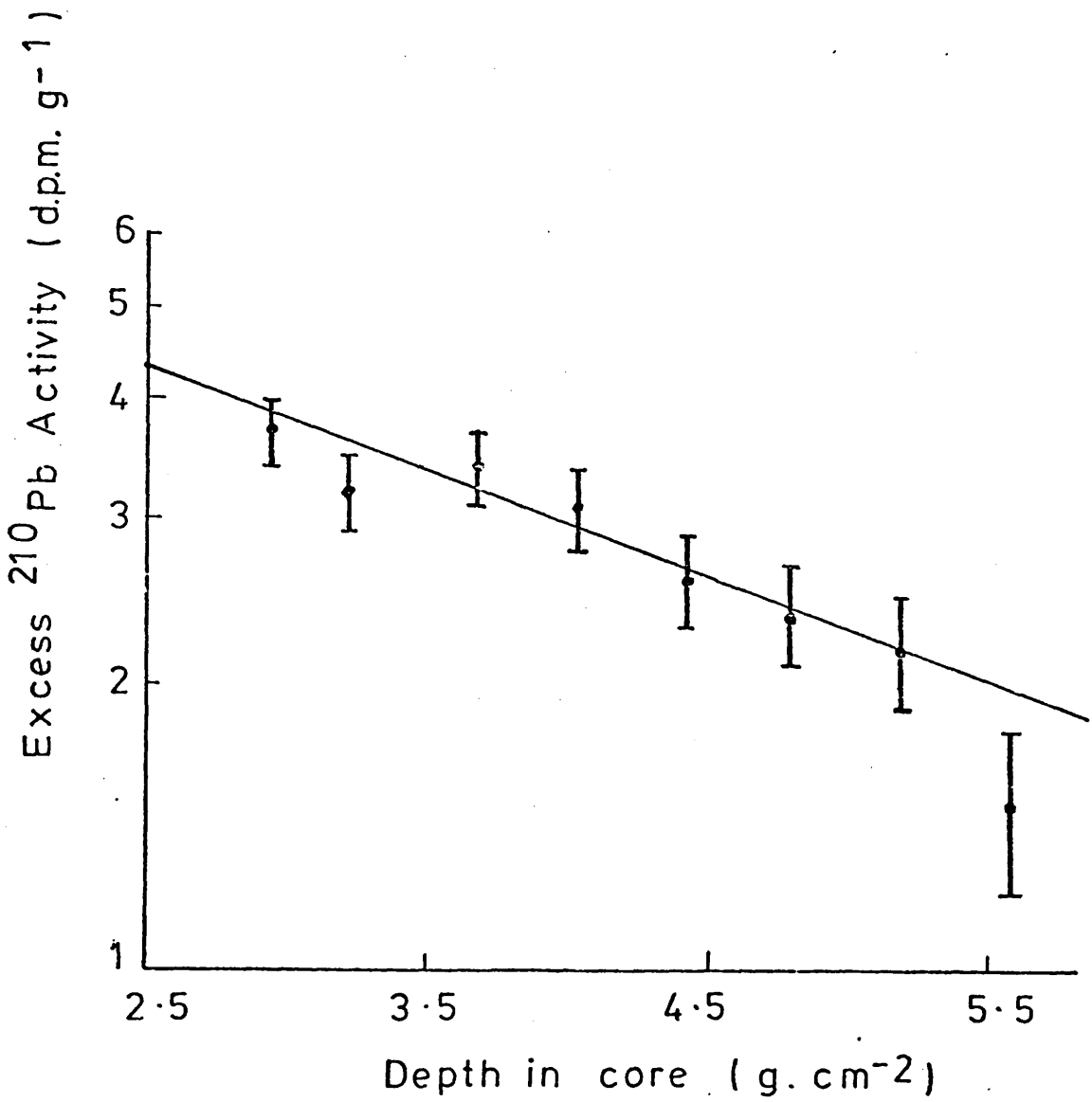


FIGURE 70 Curve of age (calendar date) against depth  
for Loch Goil Craib core LGC4

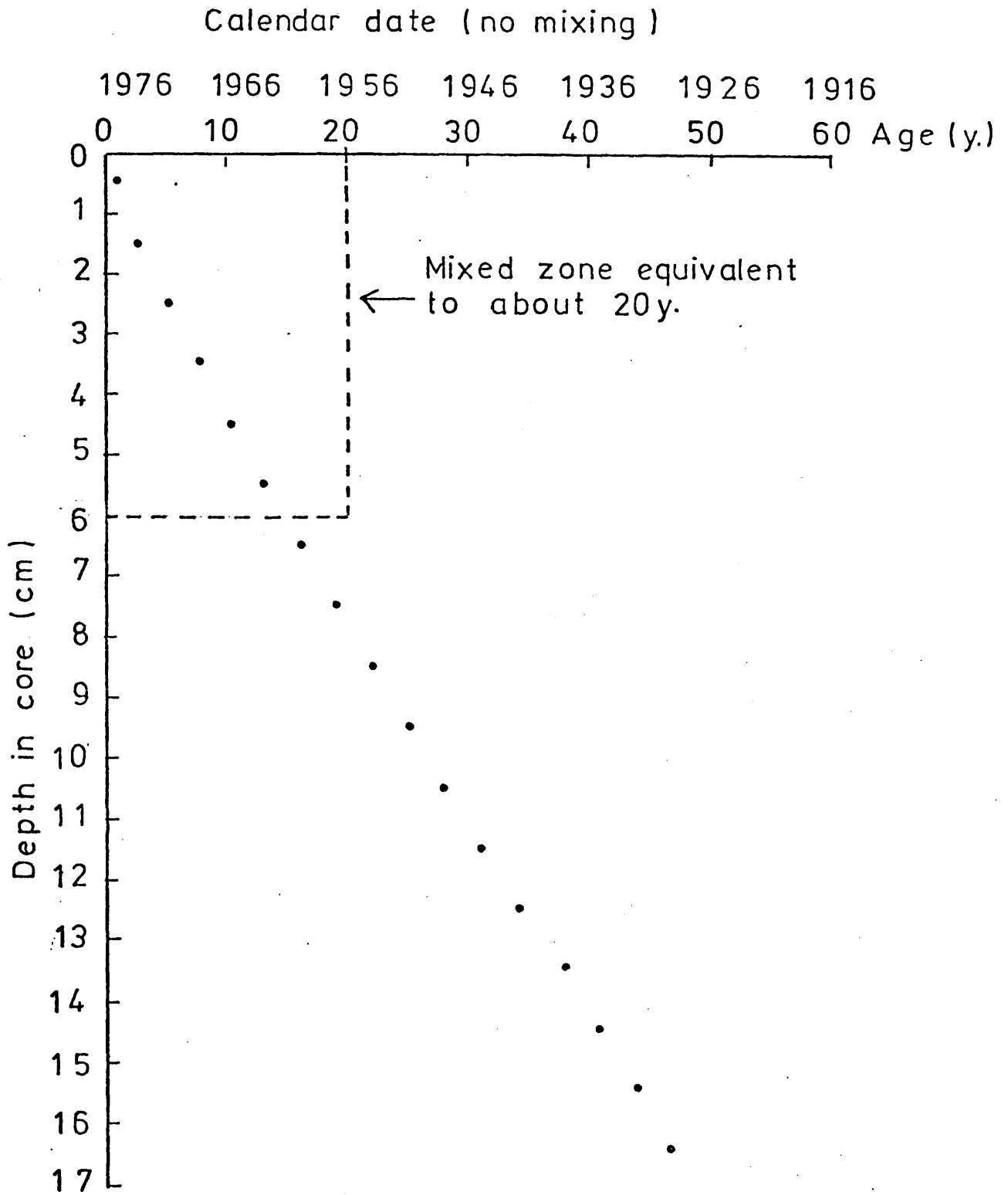
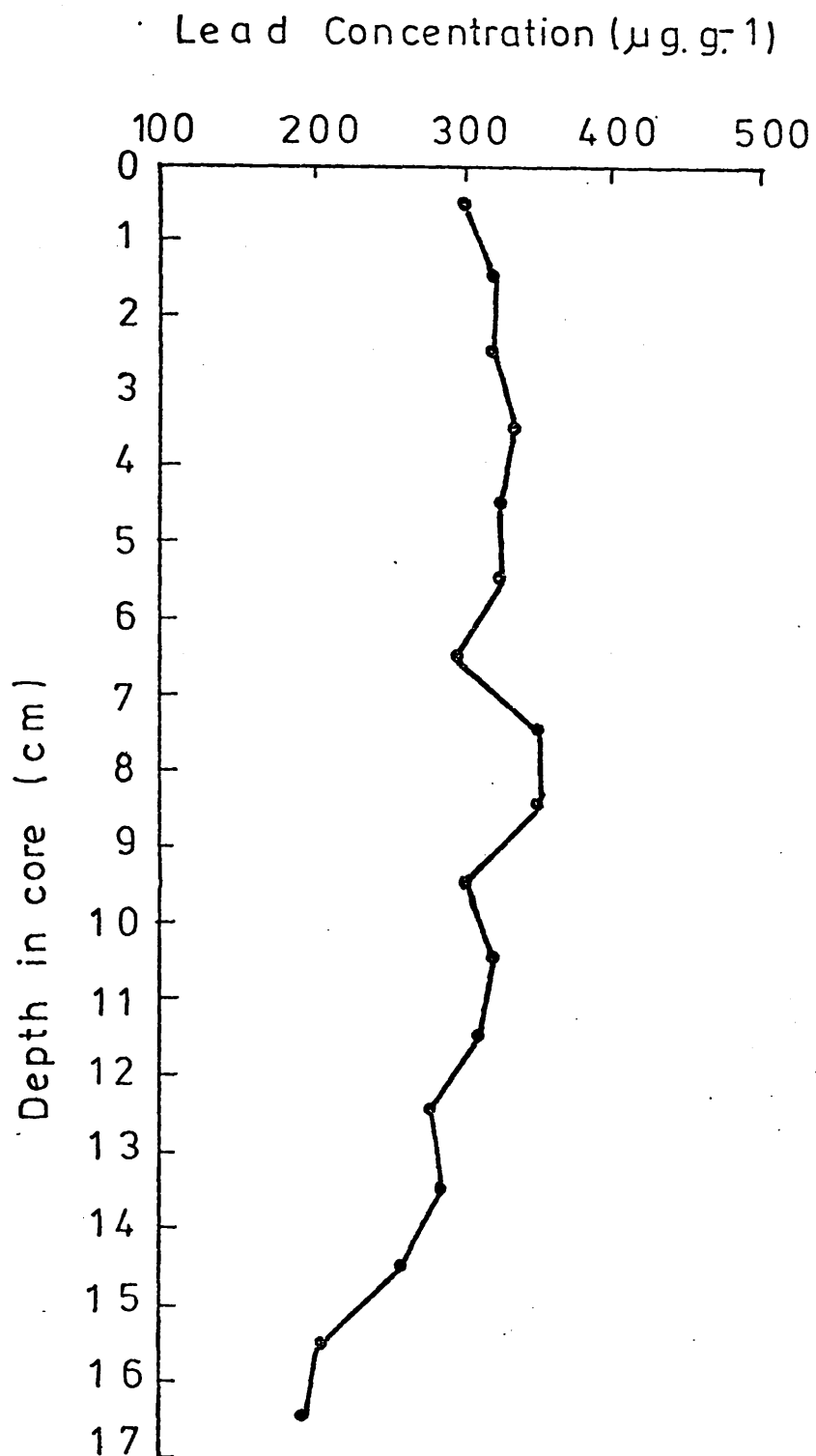


FIGURE 71    Lead profile for Loch Goil Craib core LGC4



workers of depressed levels of  $^{210}\text{Pb}$  at sediment surfaces. The decreasing concentration with depth presumably reflects either diagenetic change resulting in decomposition of the  $\text{CO}_3^{2-}$  phase on burial, or resistance to burial through selective particle redistribution. Comparison of  $^{210}\text{Pb}$  activities ( $13.9 : 6.6 \text{ dpm.g}^{-1}$ ) and of stable lead concentrations ( $400/550 : 300 \mu\text{g.g}^{-1}$ ) in the mixed zones of these deposits also indicates a higher specific concentration of each species at station 1. A similar variation is also observed for  $^{226}\text{Ra}$  ( $9.7 : 2.5 \text{ dpm.g}^{-1}$ ) and for manganese ( $3\% : 1.1\%$ ) (Farmer, 1978, personal communication). The three major phases which are normally associated with efficient scavenging of heavy metals to sediments are clay minerals, Fe/Mn oxides and organic substances; since there is evidence that all three phases are present in greater amounts at station 1, it is not surprising that higher concentrations of reactive chemical species are also found there. However, it is impossible without analysis of the distribution of these elements in the various fractions of the sediment to define which particular phase is primarily responsible for the effect. Certainly, the phases responsible for high lead levels will differ from those giving rise to high radium levels. For example, Leland et al (1972), in comparing the relative efficiencies of organic, clay, and Fe/Mn oxide phases in scavenging lead, found a stronger correlation for this metal with organics and Fe/Mn oxides. (Recent literature (e.g. Yen, 1977) has further emphasised the importance of organic materials in such processes). Radium enrichment from water on the other hand, appears to be dominated by scavenging by biological silicate.

The exception to this general trend in elemental distribution between sites appears to be that of radiocaesium,  $^{137}\text{Cs}$  showing similar specific activities at both stations, Unlike lead and other heavy metals which are particularly reactive in the hydrosphere and can apparently be readily scavenged from solution by various phases, caesium shows a much higher degree of specificity in its adsorption properties. Removal of caesium has been shown to result primarily from ion-exchange on to clay minerals, and in particular on to layered alumino-silicate minerals, which have a C-crystallographic-axis-spacing of  $10\text{\AA}$  e.g. illite, micas. (Tamura and Jacobs (1960); Pickering et al (1966)). If caesium adsorption is as specific as suggested then presumably there are similar concentrations of the clay mineral responsible for its uptake at both stations in Loch Goil. This would require that at station 2, dilution of this phase by assumed non-reactive sands and gravels is equivalent to dilution by other clay minerals/organics/Fe/Mn oxides (which are relatively non-reactive to caesium) at station 1. Clearly an interesting future study could involve determination and comparison of the particular materials responsible for preferential removal of these chemically quite different elements at each location.

One of the most unexpected features of this study has been the observation of a considerably higher concentration of  $^{226}\text{Ra}$  in the upper few cms. of the sediments of station 1 in Loch Goil relative either to those observed at depth or to literature values for normal coastal deposits. During the course of the work a number of possible explanations for this effect have been considered and these are outlined below.

One such alternative, an interpretation in terms of upward diffusion of  $^{226}\text{Ra}$  from depth in the sediment, is unlikely for the following reason. Although upward diffusion of inorganic radium has been reported in deep-sea cores (e.g. Goldberg and Koide, 1963), rates of sediment accumulation in such deposits are many orders of magnitude lower than those recorded in nearshore sediments; in addition, diffusion is known to be a very slow process for most radionuclides (see for example Duursma and Gross (1971) and Koczy and Bourrett (1958) who report a value of  $10^{-8}\text{ cm}^2\text{ s}^{-1}$  for the diffusion coefficient of  $^{226}\text{Ra}$ ). Explanation of the present anomaly in terms of upward migration of  $^{226}\text{Ra}$  followed by 'trapping' in the topmost layers of the deposit, shown to be accumulating at  $6\text{ mm.y}^{-1}$ , therefore seems highly improbable. For this reason, explanation of the higher  $^{226}\text{Ra}$  levels in surface sediment through increased input at the sediment/water interface is preferred. Clearly, since the sedimentation rate is high and as mixing occurs to  $\sim 4\text{ cms}$ . (to which depth the  $^{226}\text{Ra}$  anomaly is largely confined), the cause must be a recent one. An obvious possible explanation is recent change either in the nature of the material depositing at the site or in the proportion of that material responsible for the introduction of  $^{226}\text{Ra}$  to the sediment. Recent cultural change in the catchment was therefore investigated, particularly forestry activity during development of the local Argyle Forest since this could reasonably be expected to increase soil erosion. Subsequent investigation, however, showed that insufficient afforestation/deforestation had occurred in recent years. A second line of investigation followed the discovery that a factory in Balloch had extracted, processed and distributed radium isotopes in production of medical radiation

sources, luminous paints, etc. The factory was closed in the mid 1920's; however, the soil underlying the premises was later found to be contaminated with radioactivity and the site was therefore excavated to a depth of six feet. Further investigation, however, has shown that this soil, which contained an estimated 0.2 Ci of  $^{226}\text{Ra}$ , was disposed of in 1963 at the Garroch Head dumping ground (Stott, 1976). Clearly, for the following reasons, this disposal event cannot explain the anomaly;

- (1) it has been well established by the Clyde River Purification Board from studies of trace metal distributions that solid wastes dumped at the spoil ground remain confined to a localised area of  $20 \text{ km}^2$ .
- (2) if dispersion had occurred, some observation of an equivalent anomaly in Gareloch would be expected, and
- (3) the total activity of radioactivity involved is so low that, if distributed over a wide area, it would produce an immeasurable increase in  $^{226}\text{Ra}$  content.

To obtain some basic information on the textural composition of the sediments at this site and in particular to examine the possibility that the  $^{226}\text{Ra}$  anomaly might be associated with, for example, a change in mineral composition in the upper layers of the deposit, a further core was recovered from this station and particle size and clay mineral analyses performed throughout the length of the core by Lennie (1978). The results of this investigation are presented in tables 38 and 39. From table 38 it is apparent that

TABLE 38            LOCH GOIL CRAIB CORE LGCS; STATION 1 :  
PARTICLE SIZE DISTRIBUTION (%)

<u>SECTION</u>	<u>SIZE FRACTION (%)</u>			
	<u>Coarse</u> <u>&gt;50 <math>\mu</math>m</u>	<u>Silt</u> <u>50-20 <math>\mu</math>m</u>	<u>Fine Silt</u> <u>20-1.4 <math>\mu</math>m</u>	<u>Clay</u> <u><math>\leq</math>1.4 <math>\mu</math>m</u>
0 - 2	8	66	4	22
2 - 4	1	59	7	33
4 - 6	2	42	40	18
6 - 8	3	32	45	20
8 - 10	8	6	60	25
10 - 12	3	9	71	18
12 - 14	2	39	25	34
14 - 16	1	20	46	33
16 - 18	3	34	38	25

TABLE 39            LOCH GOIL CRAIB CORE LGCS; STATION 1 :  
CLAY MINERAL COMPOSITION (%) BY X-RAY  
DIFFRACTOMETRY

<u>Section</u>	<u>Illites</u>	<u>Kaolin and Chlorite</u>	<u>Montmorillonite</u>
0 - 2	40	59	0
2 - 4	51	49	0
4 - 6	40	49	11
6 - 8	22	67	11
8 - 10	38	47	15
10 - 12	41	58	0
12 - 14	36	64	0
14 - 16	39	55	6
16 - 18	35	50	15

- (1) coarse-grained material ( $>50 \mu\text{m}$ ) forms a relatively minor component of the sediment;
- (2) the largest proportion comprises a combination of fine silts ( $1.4 \mu\text{m}$  to  $20 \mu\text{m}$ ) and silts ( $20 \mu\text{m}$  to  $50 \mu\text{m}$ ), although the relative abundance of these fractions is highly variable, and
- (3) the clay size fraction ( $<1.4 \mu\text{m}$ ) represents a significant proportion of the sediment, with a mean value of about 25%.

This distribution is therefore in good general agreement with Deegens' classification of sediments from this location and with the porosity data of this study. The distribution of size fractions within the sediment is, however, seen to be quite variable and no obvious correlation of size fraction with  $^{226}\text{Ra}$  anomaly is possible. Composition of the coarse fraction of this sediment (examined under a high-power microscope) was generally uniform, consisting largely of muscovite, mica, quartz, chlorite, ferric oxide and shell fragments, all of extremely small grain size (Lennie, personal communication). Table 39 indicates that the dominant clay minerals in the  $<1.4 \mu\text{m}$  fraction are illites, with a mean of  $\sim 38\%$ , and kaolinites and chlorites, which have a slightly higher mean of  $\sim 55\%$ . The remainder is composed of montmorillonite which ranges apparently randomly from zero to a maximum of 15%. Again no direct correlation of clay mineral composition with  $^{226}\text{Ra}$  anomaly is established. Organic contents, estimated in this study by treatment of sediment with  $\text{H}_2\text{O}_2$ , have a mean value of 11%, although two high values of 21% and 19% were recorded; this finding is in general agreement with the results of %  $\text{CaCO}_3$

and % total carbon determinations (by microanalytical methods) which indicated a relatively high organic content for the deposit.

Clearly, however, there is no clue to interpretation of the  $^{226}\text{Ra}$  distribution either from the results of investigation of possible artificial influences or from detailed comparison of the composition of the sediment in the anomalous zone with that at depth.

In the absence of a definitive explanation, the most convincing interpretation at present relates to the well-established 'natural' involvement of  $^{226}\text{Ra}$  in biological processes. Thus, Shannon and Cherry (1971) found very high concentrations of  $^{226}\text{Ra}$  in some species of marine phytoplankton from coastal waters of South Africa. Enrichment factors were observed to be considerably greater for phytoplankton than for zooplankton with average values of 7,300 and 860 respectively, relative to sea-water. Additional evidence of significant uptake of radium by planktonic species is inferred from similarities between the chemistries of radium and barium. For example, high values of barium were found in microplankton collected from the coasts of Oregon and Hawaii by Martin and Knauer (1973). Moreover, Ku et al (1970) and Edmond (1970) have noted a strong interdependence of  $^{226}\text{Ra}$ , barium and silicate concentrations in studies of the scavenging of  $^{226}\text{Ra}$  by carbonate and silicate phases and concluded that silica was the major scavenger of  $^{226}\text{Ra}$ . There is therefore substantial evidence to suggest that  $^{226}\text{Ra}$  is enriched in plankton and clearly this could result in transfer of considerable quantities of  $^{226}\text{Ra}$  to sediments, particularly in biologically productive inshore marine and loch environments.

Indeed MacKenzie (1977) has recently found a strong correlation between the total inventories of silicate and  $^{226}\text{Ra}$  in Loch Goil and has concluded that the distributions of  $^{226}\text{Ra}$  and silicate are interlinked and are dominantly influenced by common processes, namely the intermittent blooms and subsequent death, sinking and decay of siliceous plankton. MacKenzie further derived an estimated radium enrichment factor of x 6200, in good agreement to that observed by Shannon and Cherry.

It is therefore tempting to suggest that the high concentrations of  $^{226}\text{Ra}$  in the topmost layers of sediment at this station in Loch Goil result from annual input of high levels of  $^{226}\text{Ra}$  associated with seasonal delivery of skeletal remains of siliceous organisms to the sediments.  $^{226}\text{Ra}$  arriving at the sediment/water interface from this source is subsequently redistributed by biological reworking throughout the mixed zone of 4 cms.; continued decay and dissolution of silicate remains release the  $^{226}\text{Ra}$ , which, in soluble form, is free to migrate to the sediment/water interface (aided by biological disturbance) and hence to escape in to overlying waters. This hypothesis is consistent with the observation by MacKenzie of increased concentrations of  $^{226}\text{Ra}$  in the bottom waters of Loch Goil. The decreasing concentration of  $^{226}\text{Ra}$  from the base of the mixed zone to the mud surface therefore relates to enhanced exchange of components dissolved in interstitial waters near the sediment/water interface. The exponential decrease in  $^{226}\text{Ra}$  concentrations observed below the mixed zone is attributed to an exponential decline in silica remains below this level; supporting evidence for this postulate from other sources is outlined below. Perhaps the

major uncertainty in the above argument is the apparently high rate of silica dissolution which would be required, since from  $^{210}\text{Pb}$  dating, the age of the mixed zone corresponds to  $\sim 5.2$  y. However, Robbins et al (1975), who investigated the distribution of diatom frustules in a  $^{210}\text{Pb}$ -dated core from Southern Lake Michigan, found that abundances decreased exponentially over the upper 10 cms. of the deposit, with values at the sediment/water interface two orders of magnitude higher than those at depth. This distribution was attributed to a combination of dissolution of frustules on burial and a preferential sorting of sediment grains which operated to maintain diatom frustule remains near the mud surface; this phenomenon produced constant  $^{210}\text{Pb}$  (and other heavy metal) concentrations in a mixed zone of 2.5 cms., where diatom frustule concentrations exhibited rapid decline. The sedimentation rate estimated for the Michigan core was  $46 \text{ mg.cm}^{-2}\text{y}^{-1}$ , of similar magnitude to that derived for Loch Goil and implying that a rapid rate of silica dissolution is not unacceptable for the latter. Furthermore, Parker et al (1977) measured the concentration of diatom frustules in the water column, in sediment traps at various depths, and in a sediment core from Lake Michigan. They concluded that the major portion of amorphous silicon produced annually as diatom frustules is decomposed before incorporation into the permanent sediment.

The above tentative explanation appears to be consistent with the observed results and the known marine chemistry of  $^{226}\text{Ra}$ . Unfortunately no data are as yet available on the distribution of planktonic remains in these Clyde sediments. The relatively reduced  $^{226}\text{Ra}$  anomaly observed at station 2 in Loch Goil is consistent with the above explanation on the

basis of preferential accumulation of fine materials at station 1, or indeed on the basis of the 'patchy' production and distribution of plankton in sea-lochs (Grantham et al., 1978, Solorzano and Grantham, 1975). The increased levels of  $^{226}\text{Ra}$  apparent in the surface sediments of Loch Lomond clearly may have a similar explanation. The complete absence of the effect in Gareloch, however, is initially surprising but may have one or a combination of the following reasons; (a) the known lower biological productivity in this loch resulting from riverborne pollutant inputs; (b) reduced  $^{226}\text{Ra}$  uptake by the specific planktonic species present; (c) increased dilution of any  $^{226}\text{Ra}$ -rich skeletal remains by greater amounts of detrital material (cf. sedimentation rate  $\sim x2\frac{1}{2}$  that for station 1 Loch Goil) and (d) a 'patchy' distribution of planktonic activity.

A key assumption in the above argument is that the 'anomalous' levels of  $^{226}\text{Ra}$  in these deposits are not supported by an equivalent concentration of parent  $^{230}\text{Th}$ . If future analyses prove that this is not the case, then an alternative explanation for the observed change in distribution will be required. Koide et al (1976), however, also found high levels ( $\sim 9 \text{ dpm.g}^{-1}$ ), of unsupported  $^{226}\text{Ra}$  in marine sediments off the coast of Southern California and attributed these to enrichment in phytoplankton. Moreover, they compiled data for the  $^{230}\text{Th}$  and  $^{226}\text{Ra}$  activities of surface sediments from various locations and found excess and unsupported  $^{226}\text{Ra}$  present in a number of loch and coastal marine deposits. Interestingly, Koide et al made further use of the depth distribution of excess  $^{226}\text{Ra}$  to derive a chronology for the deposits on the assumption that no migration of  $^{226}\text{Ra}$  had

occurred after burial. Sedimentation rates thus derived were in reasonable agreement (within a factor of x2) with those based on independent methods ( $^{14}\text{C}$ ,  $^{230}\text{Th}/^{232}\text{Th}$ ). Clearly therefore silica dissolution (and therefore possible  $^{226}\text{Ra}$  migration) is complex and must depend on the form of silica of which particular skeleta are composed and on the particular chemical environment of the sampling location.

Comparison of the results for Loch Goil and Gareloch highlights some interesting differences between the sedimentation processes and chemical compositions of the deposits in the two lochs. Thus while there is conclusive proof of biological mixing to a depth of 4 to 6 centimetres in Loch Goil sediments there is no firm evidence of this in the radionuclide results from Gareloch. Furthermore, a considerably higher rate of sediment accumulation is apparent in Gareloch, around  $\times 2\frac{1}{2}$  that observed at the deep site in Loch Goil; this difference is consistent with the higher mean particulate concentration in Gareloch of  $\sim 3.2 \text{ mg.l}^{-1}$  relative to  $\sim 1.4 \text{ mg.l}^{-1}$  in Loch Goil (Leatherland, 1976, pers. comm.). Similarly higher levels of lead are observed in Gareloch sediments (600 ppm to 800 ppm in the Craib core and  $>900$  ppm in the gravity core, for which the levels are accurate although the 'depth' is uncertain) compared to maximum levels in Loch Goil of  $\sim 550$  ppm. That Gareloch is therefore experiencing a considerably higher total flux of lead is consistent with its geographical position near the heart of the Clydeside Industrial conurbation. Furthermore both the high sedimentation rate and the enhanced lead levels are confirmative that the main source of sediment to the Gareloch derives from influx from the estuary rather than from direct runoff from the

immediate catchment. Loch Goil, on the other hand, probably derives most of its sediments from particulates originating in its own drainage basin. Interestingly, surface concentrations of radiocaesium at this station in Gareloch are x2 higher than those in Loch Goil. MacKenzie (1977) has observed concentration factors of x685 and x320 for radiocaesium in Gareloch and Loch Goil sediments respectively. This difference again presumably reflects the greater proportion of clay minerals introduced into Gareloch deposits.

### 3.5 Summary and General Conclusions

Radioanalytical separation techniques appropriate to  $^{210}\text{Pb}$  dating in sediments have been established.  $^{210}\text{Pb}$  is measured indirectly via  $\alpha$ -spectrometric determination of its  $\alpha$ -emitting grand-daughter  $^{210}\text{Po}$ ;  $^{208}\text{Po}$  spike is added as chemical yield tracer.  $^{226}\text{Ra}$  is measured indirectly via separation and gas phase  $\alpha$ -scintillation counting of its radioactive daughter,  $^{222}\text{Rn}$ . Sediment cores recovered from the Cilicia Basin in the Eastern Mediterranean, Loch Lomond, a freshwater loch in west central Scotland, and Loch Goil and Gareloch, two fjord-like sea-lochs of the Clyde Sea Area, have been examined for their  $^{210}\text{Pb}$  and  $^{226}\text{Ra}$  distributions and where appropriate a  $^{210}\text{Pb}$  chronology covering the last 100 to 150 y. has been developed. Major complementary studies include radiocaesium assay, which is particularly useful in providing acceptable evidence of recovery of undisturbed surface sediment and as an additional chronometer, and lead analysis, as indicator of recent anthropogenic influences.

In developing  $^{210}\text{Pb}$  chronologies, the importance of correcting for a number of sediment properties has been emphasised. Thus the discovery of systematic variation in the depth distribution of  $^{226}\text{Ra}$  in several cores has stressed the need to measure  $^{226}\text{Ra}$  concentrations throughout the length of cores before making correction for the supported  $^{210}\text{Pb}$  contribution in  $^{210}\text{Pb}$  excess dating. Often, in studies elsewhere,  $^{226}\text{Ra}$ -supported  $^{210}\text{Pb}$  is simply taken either as that observed at depths where all excess  $^{210}\text{Pb}$  is assumed to have decayed, or from direct measurement of  $^{226}\text{Ra}$  activities in only a few random sections of core. In addition, the

significance of correcting for sediment variables including water content and in the case of marine sediments, salt-residues from interstitial waters, is indicated. Such corrections are also often omitted, with the result that sedimentation rates and age/depth curves must be erroneous.

The results of analysis of the Cilicia Basin core, recovered by a conventional small diameter gravity corer, indicate exponential decrease of  $^{210}\text{Pb}$  with depth consistent with a sedimentation rate of  $16 \text{ mg.cm}^{-2}\text{y}^{-1}$  ( $0.34 \text{ mm.y}^{-1}$ ). The flux of excess  $^{210}\text{Pb}$  to the sediments is estimated at only  $0.09 \text{ dpm.cm}^{-2}\text{y}^{-1}$ , which is lower even than the estimated flux of excess  $^{210}\text{Pb}$  expected from in-situ production of  $^{210}\text{Pb}$  from decay of  $^{226}\text{Ra}$  in overlying waters. This fact, taken in conjunction with the absence of (1) detectable concentrations of  $^{137}\text{Cs}$ , (2) significant levels of culturally derived heavy metals, and (3) increasing porosity towards the surface of the core, indicate that an undefined depth of surface sediment has been lost during sampling. It is further shown that the  $^{210}\text{Pb}$  profile is unlikely to arise from biological mixing since a biological mixing coefficient of  $8.5 \times 10^{-2} \text{ cm}^2\text{y}^{-1}$  is calculated, approximately two orders of magnitude lower than that expected for a coastal deposit. If the sediments from which the  $^{210}\text{Pb}$  sedimentation rate is derived are undisturbed, then the estimated sedimentation rate is a minimum value.

The Loch Lomond core was collected by mini-Mackereth corer, a sampler specifically designed to recover cores up to 1 metre in length, with minimal disturbance to the superficial layers of deposit. The  $^{210}\text{Pb}$  profile, contained in the upper 12 to 15 cms. of the 82 cm. core, exhibited exponential decline

with depth. A slight flattening of the profile in the upper 2 cms. is consistent with either slight disturbance during coring or a very limited degree of physical or biological mixing. A sediment accumulation rate of  $22 \text{ mg.cm}^{-2}\text{y}^{-1}$  ( $\sim 1 \text{ mm.y}^{-1}$ ) is derived from the excess  $^{210}\text{Pb}$  profile, and the estimated flux of  $^{210}\text{Pb}$  to the deposit is about  $0.54 \text{ dpm.cm}^{-2}\text{y}^{-1}$ . This is greater than the estimated atmospheric flux of  $^{210}\text{Pb}$  in the area ( $\sim 0.38 \text{ dpm.cm}^{-2}\text{y}^{-1}$ ) and since the estimated flux of  $^{210}\text{Pb}$  due to in-situ production of  $^{210}\text{Pb}$  from decay of  $^{226}\text{Ra}$  in the overlying waters is insignificant at  $< 0.01 \text{ dpm.cm}^{-2}\text{y}^{-1}$ , some excess  $^{210}\text{Pb}$  depositing in the sediments must arise from  $^{210}\text{Pb}$  adsorbed on particulates in the catchment.

Radiocaesium in this core is due entirely to bomb fallout. The  $^{137}\text{Cs}$  profile is contained essentially in the upper 2 to 3 cms. of the deposit and is consistent both with the  $^{210}\text{Pb}$  observed sedimentation rate and the expected time-integrated flux of  $^{137}\text{Cs}$  from atmospheric fallout. Therefore the sediment surface has probably been recovered during sampling. An elongated 'tail' of  $^{137}\text{Cs}$  extends to a depth of about 7 cms. indicative of some small degree of downward mixing or possibly radiocaesium migration.

Some indication of a change in slope is apparent in the excess  $^{210}\text{Pb}$  profile below  $\sim 8$  cms. in the core, possibly indicative of a change in sedimentation pattern. This would be consistent with evidence derived from  $^{14}\text{C}$ , and metal (Al and Mn) anomalies in a 5 metre core recovered from a nearby sampling station in the south basin. A tentative explanation involving recent major disturbance to the natural processes of sedimentation is postulated. If so, then a palaeomagnetic 'date' of  $\sim 1800 \text{ A.D.}$  for the 20 - 25 cm. horizon in this core becomes

compatible with an extrapolated  $^{210}\text{Pb}$  time-scale. The estimated rate of sediment accumulation at final compaction from  $^{210}\text{Pb}$  results is  $0.4 \text{ mm.y}^{-1}$ , in good agreement with a  $^{14}\text{C}$ -based sedimentation rate for this basin of  $0.3 \text{ mm.y}^{-1}$ . This suggests that, outwith a possible 'slump-event', the modern rate of sediment accumulation may not be significantly different from the post-glacial rate.  $^{226}\text{Ra}$  concentrations show an interesting increasing trend from typical inshore marine and loch sediment values of  $1.8 \text{ dpm.g}^{-1}$  from about 15 cms depth to a maximum of  $3.3 \text{ dpm.g}^{-1}$  at the sediment/water interface. A similar effect is observed, though to a much more marked degree, in the sediments of Loch Goil.

Stable lead shows a typical profile with levels increasing from depth towards the mud surface. Natural levels are around 10 ppm (equivalent to a flux of  $0.22 \text{ } \mu\text{g.cm}^{-2}\text{y}^{-1}$ ), approximately x15 lower than modern inputs of 150 ppm ( $3.3 \text{ } \mu\text{g.cm}^{-2}\text{y}^{-1}$ ). Levels of lead contamination in Loch Lomond are considerably lower than those experienced by the Clyde sea-lochs, Gareloch and Loch Goil; this is generally consistent with its greater distance and physical isolation from major industrial centres and the Clyde estuary respectively. Loch Goil, virtually as far removed from such influences as Loch Lomond, may receive additional input of lead pollution from shipping and local oil-pollution sources.

The major aim of this project has been to examine the applicability of the  $^{210}\text{Pb}$  dating technique in investigations of the patterns and rates of recent sediment accumulation in the sea-lochs of the Clyde Sea Area. Determination of the concentration of  $^{210}\text{Pb}$  in cores from Loch Goil and Gareloch

has shown  $^{210}\text{Pb}$  to be present in sufficient excess, over that required for radioactive equilibrium with  $^{226}\text{Ra}$ , for use in such studies. The value of accompanying measurements of radiocaesium,  $^{137}\text{Cs}$  and  $^{134}\text{Cs}$ , distributions in these sediments is apparent. Sediment profiles of radiocaesium mirror increasing discharge of these nuclides from Windscale since 1952 and are therefore invaluable in establishing that undisturbed surface sediment has been recovered and, in conjunction with X-radiographic evidence and  $^{210}\text{Pb}$  results, in indicating to what depth sediment mixing occurs.

This project through the concomittant use of a conventional (and still generally used) small-diameter gravity corer and a hydraulically damped Craib corer, specially designed to recover undisturbed surface sediments has provided an excellent opportunity to compare the effectiveness of these different samplers in retrieving sediment from high porosity deposits; indeed this has proved a particularly enlightening aspect of the study. Clearly, in sediment studies of any kind which involve investigation of the vertical distributions of variables in the sediment column, the collection of representative material, i.e. cores in which the vertical integrity of the sediments is maintained, is of paramount importance. No matter how carefully subsequent storage, pretreatment and chemical analysis is performed, if the original sample has been disturbed in collection, then the environmental relevance of the results is at the very least reduced. Comparison of the distributions of  $^{210}\text{Pb}$ ,  $^{226}\text{Ra}$ , and  $^{134}\text{Cs}/^{137}\text{Cs}$  in these cores has indicated conclusively that a substantial amount of surface sediment has been lost during gravity core sampling

and the extent of loss appears to be considerable, as much as 15 - 20 cms. Furthermore, there is strong evidence to suggest that a considerable depth of the 'surface' material recovered in gravity cores does not in fact represent undisturbed sediment but is material which results from a substantial mixing/loss process. In addition, and perhaps of most significance, comparison of gravity core profiles shows not only good internal consistency but profiles which exhibit 'classical' forms (e.g. exponential decrease of excess  $^{210}\text{Pb}$ ). In other words, examined by themselves, the results from these gravity cores would have been accepted as good evidence of a constant rate of sediment accumulation, a sedimentation rate would have been derived and an apparently quite erroneous chronology developed for the sediments; only in the light of comparison of results with those from Craib cores are the inadequacies of the use of small-diameter gravity corers to such deposits noticed. The 6 cm. diameter U.H.E.L. gravity corer used was of conventional design and standard coring procedures were adopted in recovery of these cores; in addition the crew of the C.R.P.B. survey vessel, Endrick II, are highly experienced in their mode of collection. Thus, if, as seems likely, the conclusions reached from this study are generally applicable, then the wide literature, which is based on data from sediments collected by such corers, must be treated with caution. Although, increasingly, sediment studies are conducted using specially designed 'soft-landing' samplers, there are few if any instances of direct comparison of results obtained using such corers with those previously obtained from gravity cores. Clearly in the light of the evidence gathered in this study, such a comparison could be quite revealing.

Valid conclusions concerning the patterns and rates of recent sediment accumulation in Loch Goil and Gareloch are consequently restricted to interpretation of results derived from Craib core analysis:

In general, sediments examined are homogeneous in appearance with no obvious visible signs of stratigraphic markers or laminations. X-radiographic evidence shows animal burrows to a depth of ~4 cms. and ~6 cms. in Loch Goil sediments, dependent upon location, indicating active bioturbation to these depths. This conclusion is generally consistent with radionuclide profiles which exhibit relatively constant activity over such depth intervals; furthermore radiocaesium evidence suggests that reworking may be intermittent, with a time period of several months to a year. In contrast, there is no conclusive evidence from radionuclide data of biological reworking in Gareloch sediments.

Sedimentation rates have been estimated from depth profiles of excess  $^{210}\text{Pb}$  for each station. In Loch Goil, rates are derived from the excess  $^{210}\text{Pb}$  distribution at depths beneath the zone of active mixing. Values of  $200 \text{ mg.cm}^{-2}\text{y}^{-1}$  ( $6 \text{ mm.y}^{-1}$ ) and  $123 \text{ mg.cm}^{-2}\text{y}^{-1}$  ( $3.5 \text{ mm.y}^{-1}$ ) have been found for stations 1 and 2, respectively. The corresponding ages of the mixed zones are just over 5 y. and 15 y. respectively; the maximum resolution which can be achieved in age-determination of a specific horizon is therefore limited by this mixing zone. Gareloch experiences a significantly higher rate of sediment accumulation of  $540 \text{ mg.cm}^{-2}\text{y}^{-1}$  (or  $1.5 \text{ cm.y}^{-1}$ ), consistent with its considerably greater influx of particulates from the adjacent Clyde estuary. Estimated fluxes of  $^{210}\text{Pb}$  to the

sediments range from 0.8 to 2.5  $\text{dpm}\cdot\text{cm}^{-2}\cdot\text{y}^{-1}$  in Loch Goil to 3.6  $\text{dpm}\cdot\text{cm}^{-2}\cdot\text{y}^{-1}$  in Gareloch and are therefore considerably higher than the estimated atmospheric flux for the area of 0.33  $\text{dpm}\cdot\text{cm}^{-2}\cdot\text{y}^{-1}$ . The contribution to this from in-situ production of  $^{210}\text{Pb}$  from  $^{226}\text{Ra}$  in the overlying waters is shown to be totally insignificant (0.03  $\text{dpm}\cdot\text{cm}^{-2}\cdot\text{y}^{-1}$ ). Therefore the major source of excess  $^{210}\text{Pb}$  to these deposits appears to be associated with river and stream particulates.  $^{210}\text{Pb}$ -derived sedimentation rates indicated above compare favourably with the only other estimates of 'natural' rates of sedimentation in the area, i.e. 5  $\text{mm}\cdot\text{y}^{-1}$  for Loch Riddon (Moore, 1931) and 5  $\text{mm}\cdot\text{y}^{-1}$  for Holy Loch quoted by Best (1970). Interestingly, Moore's estimate was based on sediment traps and on alternating light/dark bands observed in sediment cores, presumed due to annual diatom blooms; this stratification is therefore in marked contrast to Loch Goil/Gareloch sediments and infers that the bottom deposits of Loch Riddon are or were subject to less disturbance from faunal mixing. Furthermore, minimum rates of sedimentation derived from radiocaesium data, on the assumptions that no significant migration of caesium isotopes has occurred and that the first significant input of  $^{137}\text{Cs}$  and  $^{134}\text{Cs}$  to the sediments occurred in 1953 and 1968 respectively, are in good agreement - viz, 180  $\text{mg}\cdot\text{cm}^{-2}\cdot\text{y}^{-1}$ , 110  $\text{mg}\cdot\text{cm}^{-2}\cdot\text{y}^{-1}$  and 650  $\text{mg}\cdot\text{cm}^{-2}\cdot\text{y}^{-1}$  for Loch Goil stations 1 and 2 and Gareloch respectively.

Major differences in the concentrations of  $^{210}\text{Pb}$ ,  $^{226}\text{Ra}$  stable lead and manganese in the sediments of the two sampling locations in Loch Goil apparently reflect differences in physical and chemical composition of the sediments. Higher specific elemental concentrations are correlated with the finer

sediments of the deep-basin, station 1. Particularly interesting are the increased levels of  $^{226}\text{Ra}$  observed in the surface sediments at this location both relative to those at depth and at station 2. At present, this excess is attributed to enrichment of  $^{226}\text{Ra}$  in the remains of siliceous organisms, deposited in the sediment after death; their remains, undergoing rapid decay in the upper layers of the deposit release incorporated  $^{226}\text{Ra}$  which migrates back to the overlying waters. No equivalent  $^{226}\text{Ra}$  'anomaly' is apparent in the sediments of Gareloch, and this may be a consequence of its lower biological productivity.  $^{226}\text{Ra}$  concentrations, other than those regarded as 'excess' above are typical of coastal marine deposits with values ranging from 1 to 2  $\text{dpm.g}^{-1}$ .

Lead concentrations in Gareloch (600 to 800 ppm; corresponding flux 325 to 435  $\mu\text{g.cm}^{-2}\text{y}^{-1}$ ) are higher than those in Loch Goil (400 to 550 ppm; corresponding flux 80 to 110  $\mu\text{g.cm}^{-2}\text{y}^{-1}$ ), consistent with the closer proximity of Gareloch to the heavily industrialised and densely populated regions of the area.

In chapter 1 the highly variable nature of the sediment matrix was indicated; while from this study there is good evidence that the Craib corer consistently recovers relatively undisturbed sediment cores, nonetheless some differences in detail are still apparent between results from such cores collected at an 'identical' location (station 1, Loch Goil). As further example of this, Carpenter (1975) has described the use of a hydrostatically damped soft-landing multiple core sampler, which recovers four undisturbed cores simultaneously at the corners of a rectangular base-frame; even cores

collected in this way, with the guarantee of identical time and location to within a few square metres, showed up to 25% differences in  $^{210}\text{Pb}$ -derived sedimentation rates. Ideally, therefore, sediment studies should be conducted on the basis of multiple core analysis at each location, with conclusions drawn from resultant general trends in sedimentation patterns and sediment composition. Unfortunately, both temporal and financial restrictions are masters of this ideal.

Conclusions drawn from this preliminary sediment study have by necessity been derived from a limited number of cores; therefore they are best regarded (a) as initial indicators of the patterns and rates of sedimentation occurring in the regions studied, and (b) as a useful baseline from which future research can be more extensively conducted. Nevertheless the results do highlight the value of  $^{210}\text{Pb}$  geochronology while simultaneously emphasising the critical limitations which apply both in methodology and interpretation.



## APPENDIX 1

### Particle Size Analysis

The following general scheme was used in particle size analysis; the coarse fraction was estimated by wet sieving, fine silt and clay fractions by the pipette method, and coarse silt by difference. Organic matter was destroyed by oxidation with  $H_2O_2$ .

Prior to particle size separation, dispersion and deflocculation of sediment aggregates were achieved by treating ~15 g. sediment (weighed to three decimal places) with 50 mls. distilled water and 25 mls. of 50%  $NH_3$  solution; this mixture was agitated for 16 hours using a reciprocating shaker.

### Coarse Fraction Analysis

Following dispersion, the sediment was washed through a fine sieve (300 mesh; equivalent to 50  $\mu m$ ) into a 1000 ml. graduated cylinder. After air-drying at 30°C, material retained by the sieve was brushed into a crystallising dish. Organic material was subsequently destroyed by treatment with 10 mls. distilled  $H_2O$  and 3 mls. 30%  $H_2O_2$ . This mixture was heated on a hotplate till cessation of frothing, and the process repeated by further addition of small aliquots of  $H_2O_2$  until no further effervescence occurred. The suspension was then evaporated to dryness, weighed and the coarse fraction of the sediment calculated as a percentage of total weight.

### Fine Fraction Analysis : The Pipette Method

This technique is based upon the differing rates of

sedimentation of particles of different size; STOKES' LAW states that the rate of fall,  $V$ , of a particle of radius,  $r$ , in a liquid of viscosity,  $\eta$ , is given by

$$V = \frac{2}{9} \frac{gr^2}{\eta} (\rho_P - \rho_L)$$

where  $\rho_P$  and  $\rho_L$  are the densities of particle and liquid respectively and  $g$  is the acceleration of gravity  $9.81 \text{ m.s}^{-2}$ . All fractions having a settling velocity greater than that of the size fraction sought will settle below a certain depth in a column of liquid after time ' $t$ '. Particles of the size required can then be withdrawn from the solution above this level using a pipette.

In practice, the concentration of particles which fall for time ' $t$ ', through a certain depth of liquid at a specified temperature, is measured. (Temperature dependence is due to the variation of liquid viscosity with temperature). Tables relating time of settling to 'equivalent settling diameters' of  $<20 \mu\text{m}$  at a depth of 10 cms, and of  $<1.4 \mu\text{m}$  at a depth of 10 cms, over a wide range of temperatures are used (table 40).

#### Fine Silt Plus Clay Fractions (<20 $\mu\text{m}$ )

The suspension of fine material passing through the 50  $\mu\text{m}$  sieve was made up to the mark in the 1000 ml. cylinder and shaken well for 30 seconds. The suspension was then allowed to settle for an appropriate period of time. With roughly 20 seconds of this time remaining, the 10 ml. pipette was lowered to a depth of 10 cms. in the suspension and at the predetermined time, the suspension withdrawn. The 10 ml. suspension was placed in a crystallising dish, 3 mls. of 30%  $\text{H}_2\text{O}_2$  added and organic matter destroyed as before. The residual mixture was dried, weighed and the percentage fine silt plus clay calculated as follows,

TABLE 40 SETTLING TIMES FOR CLAY (EQUIVALENT SETTLING  
DIAMETER <1.4  $\mu\text{m}$  and <20  $\mu\text{m}$ ) AT 10 cms. DEPTH

<u>TEMP. °C</u>	<u>TIME</u>			
	<u>&lt;1.4 <math>\mu\text{m}</math></u>		<u>&lt;20 <math>\mu\text{m}</math></u>	
	<u>hours</u>	<u>mins.</u>	<u>mins.</u>	<u>secs.</u>
16	17	42	5	27
17	17	32	5	19
18	17	05	5	10
19	16	39	5	3
20	16	15	4	55
21	15	51	4	48
22	15	29	4	41

$$\% \text{ silt + clay} = \frac{\text{Wt. fraction}}{\text{Oven dry wt. sample}} \times \frac{\text{Vol. cylinder}}{\text{Vol. pipette}} \times 100$$

#### Clay Fraction (<1.4 $\mu\text{m}$ )

An identical procedure to that described above was employed but with a longer settling period.

$$\% \text{ clay} = \frac{\text{Wt. fraction}}{\text{Oven dry wt. sample}} \times \frac{\text{Vol. cylinder}}{\text{Vol. pipette}} \times 100$$

#### Clay Mineral Analysis

Clay mineral analysis was performed by X-ray diffractometry. In theory, when a monochromatic X-ray beam makes contact with the surface of a crystal, parallel planes of atoms interact with it and the beam is reflected. A maximum in the intensity of the reflected beam is observed if the component waves reflected from each plane of the crystal re-inforce, i.e. are in phase. The conditions necessary for this to occur are described by Bragg's Law,

$$\eta\lambda = 2d \sin \theta$$

where,  $\eta$  is an integer

$\lambda$  is the wavelength of the monochromatic radiation.

$d$  is the spacing of similar planes of atoms.

$\theta$  is the angle of incidence of the X-ray beam.

Clay minerals have very similar crystal structures; however, they can be distinguished from each other on a semi-quantitative basis by a combination of the differing d-spacing of planes along their C-crystallographic axes together with the characteristic intensities of the associated reflections.

In practice, a powdered specimen is mounted such that a monochromatic beam of X-rays reflects from it to a Geiger-

Müller counter which in turn transmits a signal to a chart recorder; this system produces a trace from which values of  $2\theta$  can be directly read, and hence d-spacings derived. Tables of d-spacings for various minerals are readily available (e.g. Fink, 1966) and from these the mineral composition of the specimen determined. Since the area under the peak corresponds to the intensity of reflection, a semi-quantitative picture can be obtained.

In this study, identification of clay minerals present in the  $<1.4 \mu\text{m}$  size fraction was performed using a Phillips wide-angle X-ray diffractometer with Geiger counter, utilising Ni filtered  $\text{CuK}_\alpha$  monochromatic radiation. The X-ray tube was operated at 35 KV with a current of 20 mA. All specimens were run at one degree per minute and a chart speed of  $5 \times 240 \text{ mm} \cdot \text{min}^{-1}$ . Randomly orientated specimens (necessary to minimise distortion to the 001 reflections which correspond to reflections along the C-crystallographic axes) were prepared by adding a few drops of clay suspension to a glass slide and leaving to dry, thereby allowing the clay minerals to orientate themselves during fall through the liquid. Standards of illite, kaolin and montmorillonite were analysed and compared to the clay fraction of the sediment.

APPENDIX 2

SAMPLE CALCULATIONS AND COMPUTER PROGRAMS

The methods used to calculate  $^{210}\text{Pb}$  and  $^{226}\text{Ra}$  activities in sediment samples are illustrated below. Uncertainties associated with the values due to counting statistics only, are determined by means of the formulae,

Error on a sum or difference;  $C=A\pm B$ ,

$$\sigma_c = \sqrt{\sigma_A^2 + \sigma_B^2}$$

Error on a product or quotient;  $c=A \times B$  or  $A/B$ ,

$$\sigma_c = c \sqrt{\left(\frac{\sigma_A}{A}\right)^2 + \left(\frac{\sigma_B}{B}\right)^2}$$

(1) Calculation of  $^{210}\text{Pb}$  activity in sediment

Let A = observed count rate for  $^{208}\text{Po}$  (cpm);  $\sigma_A$  = counting error (cpm).

Let B = observed count rate for  $^{210}\text{Po}$  (cpm);  $\sigma_B$  = counting error (cpm).

(count rates, A and B, have been corrected for partial peak overlap as described in section 2.4 (II)).

Let D = detector blank under  $^{208}\text{Po}$  peak (cpm);  $\sigma_D$  = counting error (cpm).

Let E = detector blank under  $^{210}\text{Po}$  peak (cpm);  $\sigma_E$  = counting error (cpm).

Let F = activity of  $^{208}\text{Po}$  tracer added (dpm).

Let G = weight of sediment dissolved (g).

(G and F have been corrected to the fraction of total dissolution removed for analysis).

Calculation of  $^{208}\text{Po}$  activity

$$\text{Activity of } ^{208}\text{Po} = A - D = H \text{ cpm.}$$

$$\text{Error on activity of } ^{208}\text{Po} = \sqrt{(\sigma_A)^2 + (\sigma_D)^2} = \sigma_H \text{ cpm.}$$

$$^{208}\text{Po activity} = H \pm \sigma_H \text{ cpm.}$$

Calculation of overall efficiency

$$\text{Overall efficiency} = \frac{H}{F} = I$$

$$\text{Error on overall efficiency} = \frac{\sigma_H}{F} = \sigma_I$$

$$\text{Overall efficiency} = I \pm \sigma_I$$

Calculation of  $^{210}\text{Po}$  activity

$$\text{Activity of } ^{210}\text{Po} = B - E = J \text{ cpm.}$$

$$\text{Error on activity of } ^{210}\text{Po} = \sqrt{(\sigma_B)^2 + (\sigma_E)^2} = \sigma_J \text{ cpm.}$$

$$^{210}\text{Po activity} = J \pm \sigma_J \text{ cpm.}$$

Calculation of  $^{210}\text{Po}$  activity in sediment

$$\text{Activity of } ^{210}\text{Po} = \frac{J}{I} = K \text{ dpm.}$$

$$\text{Error on activity of } ^{210}\text{Po} = \frac{J}{I} \sqrt{\left(\frac{\sigma_J}{J}\right)^2 + \left(\frac{\sigma_I}{I}\right)^2} = \sigma_K \text{ dpm.}$$

$$\text{Activity of } ^{210}\text{Po} \text{ in sediment} = \frac{K}{G} = L \text{ dpm/g.}$$

$$\text{Error on activity of } ^{210}\text{Po} \text{ in sediment} = \frac{\sigma_K}{G} = \sigma_L \text{ dpm/g.}$$

$$\text{Therefore activity of } ^{210}\text{Po} \text{ in sediment} = L \pm \sigma_L \text{ dpm/g.}$$

$$= \text{Activity of } ^{210}\text{Pb} \text{ in sediment.}$$

A computer program has been written in FORTRAN IV to perform the above  $^{210}\text{Pb}$  calculation.

TABLE 41      PROGRAMME IN FORTRAN IV FOR THE CALCULATION OF <sup>210</sup>Po ACTIVITY IN SEDIMENT

```

C   CALCULATION OF PO-210 ACTIVITY IN SEDIMENT
C   CALCULATION OF PO-208 ACTIVITY
    DIMENSION TITLE(4)
    WRITE(6,5)
    5  FORMAT(/' RESULTS'//' TITLE',7X,'OVERALL',12X,'PO-210 ACT
    SIVITY',12X,'ERROR ON PO-210 ACTIVITY'/'
    6,12X,'IN SEDIMENT',19X,'IN SEDIMENT')
    MIX=0
    READ(5,1)NUNRUM
    1  FORMAT(I3)
    999 NIX=NIX+1
    IF(NIX.GT NUMRUM) GO TO 1000
    READ(5,10)CNT1,CNT2,TIME,DETL1,DETL2,ERRBL1,ERRBL2,TRACER,SEDWT,
    7(TITLE(I),I=1,4)
    10 FORMAT(3F8.0,4F8.4,F8.3,F8.5,4A2)
    ACT1=CN1/TIME
    ERACT1=SQRT(CNT1)/TIME
    TACT1=ACT1-DETL1
    ERTAC1=SQRT(ERACT1**2+ERRBL1**2)
    CALCULATION OF OVERALL EFFICIENCY
    OVEFF=TACT1/TRACER
    EROEFF=TACT1/TRACER*ERTAC1/TACT1
    CALCULATION OF PO-210 ACTIVITY
    ACT2=CN2/TIME
    ERACT2=SQRT(CNT2)/TIME
    TACT2=ACT2-DETL2
    ERTAC2=SQRT(ERACT2**2+ERRBL2**2)
    CALCULATION OF PO-210 ACTIVITY IN SEDIMENT
    ACT3=TACT2/OVEFF
    ERACT3=ACT3*SQRT((ERTAC2/TACT2)**2+(EROEFF/OVEFF)**2)
    SACT4=ACT3/SEDWT
    ERSAC4=ERACT3/SEDWT
    WRITE(6,60)(TITLE(I),I=1,4),OVEFF,SACT4,ERSAC4
    60 FORMAT(/5X,4A2,4X,F5.4,19X,F5.2,22X,F3.2)
    GO TO 999
    1000 STOP
    END

```

(2) Calculation of  $^{226}\text{Ra}$  activity in sediment

Let A = the observed count rate (cpm) at time t (h);  $\sigma_A$  = counting error (cpm).

t(h) = the time elapsed between separation and counting (calculated by the method of Hoffmann and Van Camerik (1967) to allow a small correction for decay during counting).

Let B = the detector background count rate (cpm);  $\sigma_B$  = counting error (cpm).

Let C = the blank count rate (cpm) corrected to time zero;  $\sigma_C$  = counting error (cpm).

Let D = the detector efficiency (%) for collection and counting of  $^{222}\text{Rn}$  based on  $3\alpha$  emissions per  $^{222}\text{Rn}$  decay.

Let E = the equilibration time (% growth of  $^{222}\text{Rn}$  to secular equilibrium with  $^{226}\text{Ra}$  in the solution).

Let F = the equivalent weight of sediment in the solution analysed.

Background correction

$$G \text{ (cpm)} = A - B; \quad \sigma_G \text{ (cpm)} = \sqrt{\sigma_A^2 + \sigma_B^2}$$

Correct to time zero

$$H \text{ (cpm)} = G e^{\lambda^{222}\text{Rn} t(h)}; \quad \sigma_H \text{ (cpm)} = \sigma_G \times \frac{H}{G}$$

Blank correction

$$I \text{ (cpm)} = H - C; \quad \sigma_I \text{ (cpm)} = \sqrt{\sigma_H^2 + \sigma_C^2}$$

Efficiency correction

$$J \text{ (dpm)} = 100 \times \frac{I}{D}; \quad \sigma_J \text{ (dpm)} = \sigma_I \times 100 \times \frac{I}{D}$$

But this is based on  $3\alpha$  measurements for each  $^{222}\text{Rn}$  decay.

Therefore  $^{222}\text{Rn}$  activity =  $\frac{J^+ \sigma_J}{3} \text{ dpm} = K^+ \sigma_K \text{ dpm}$ .

Equilibration correction

$$L(\text{dpm}) = 100 \times \frac{K}{E}; \quad \sigma_L (\text{dpm}) = \sigma_K \times \frac{100K}{E}$$

Therefore  $^{222}\text{Rn}$  activity in sediment

$$M (\text{dpm/g}) = \frac{L}{F}; \quad \sigma_M (\text{dpm/g}) = \frac{\sigma_L}{F}$$

$$\begin{aligned} \text{Activity of } ^{222}\text{Rn in sediment} &= M^+ \sigma_M (\text{dpm/g}) \\ &= \text{Activity of } ^{226}\text{Ra in sediment.} \end{aligned}$$

A computer program has been written in FORTRAN IV to solve the above  $^{226}\text{Ra}$  calculation.

```

C   CALCULATION OF RA-226 ACTIVITY IN SEDIMENT
    DIMENSION TITLE(4)
    WRITE(6,5)
    5  FORMAT(/5X'RESULTS',/5X'TITLE',12X,'RA-226 ACTIVITY',12X,'ERROR ON
    1  RA-226 ACTIVITY'/26X'IN SEDIMENT(DPM/G)',9X,'IN SEDIMENT(DPM/G)')
    NIX=0
    READ(5,1)NUMRUM
    1  FORMAT(I3)
    999 NIX=NIX+1
    IF(NIX.GT.NUMRUM) GO TO 1000
    READ(5,10)ACT1,TIME,DETBGD,BLANK,DETEFF,EQTIME,SEDWT,ERACT1,ERDBGD
    2,ERBLNK,(TITLE(I),I=1,4)
    10  FORMAT(F7.3,F7.0,2F7.2,F7.1,F7.2,F7.4,F7.3,2F7.2,4A2)
    BACKGROUND CORRECTION
    ACT2=ACT1-DETBGD
    CORRECT TO TIME ZERO
    ACT3=ACT2*EXP(0.0001258*TIME)
    BLANK CORRECTION
    ACT4=ACT3-BLANK
    EFFICIENCY CORRECTION
    ACT5=ACT4*100/(DETEFF*3)
    EQUILIBRATION CORRECTION
    RAACT=ACT5*100/EQTIME
    RAACTS=RAACT/SEDWT
    CALCULATION OF ERROR ON RA-226 ACTIVITY IN SEDIMENT
    BACKGROUND CORRECTION
    ERACT2=SQRT(ERACT1**2+ERDBGD**2)
    CORRECT TO TIME ZERO
    ERACT3=ERACT2*ACT3/ACT2
    BLANK CORRECTION
    ERACT4=SQRT(ERACT3**2+ERBLNK**2)
    EFFICIENCY CORRECTION
    ERACT5=ERACT4*ACT5/ACT4
    EQUILIBRATION CORRECTION

```

TABLE 42 (cont'd) PROGRAMME IN FORTRAN IV FOR THE CALCULATION OF  $^{226}\text{Ra}$  ACTIVITY IN SEDIMENT

```
ERAECT=ERACT5*100/EQTIME
ERACTS=ERACT/SEDWT
WRITE(6,60)(TITLE(I), I=1,4),RAACTS,ERACTS
60  FORMAT(/5X,4A2,15X,F5.2,28X,F3.2)
GO TO 999
1000 STOP
END
```

REFERENCES

- Allen, J.A., 1960. "Manganese deposition on the shells of living molluscs"; *Nature*, 185, 336.
- Aller, R.C. and Cochran, J.K., 1976. " $^{234}\text{Th}/^{238}\text{U}$  disequilibrium in near shore sediment; particle reworking and diagenetic time scales"; *Earth and Planetary Sci. Letts.*, 29, 37.
- Appleby, P.G. and Oldfield, F., 1978. "The calculation of  $^{210}\text{Pb}$  dates assuming a constant rate of supply of unsupported  $^{210}\text{Pb}$  to the sediment"; Manuscript (In press in "Catena").
- Armentano, T.V. and Woodwell, G.M., 1975. "Sedimentation rates in a Long Island marsh determined by  $^{210}\text{Pb}$  dating"; *Limnol and Oceanog.*, 20, 3.
- Aston, S.R., Bruty, D., Chester, R. and Padgham, R.C., 1973. "Mercury in lake sediments; a possible indicator of technological growth"; *Nature*, 241, 450.
- Bagnall, K.W., 1957. "Chemistry of the rare radio-elements"; Butterworth's Scientific Pub., London.
- Batterbee, R.W., 1973. "Preliminary studies of L. Neagh sediments. II. Diatom analysis from the uppermost sediment". in "Quat. Plant Ecology". (eds. Birks, H.J. and West, R.G.), 279.

- Batterbee, R.W. and Digerfeldt, G., 1976. "Palaeoecological studies of the Recent development of lake Våxjösjön. I Introduction and chronology"; Arch. Hydrobiol., 77, 3, 330.
- Baxter, M.S. and Harkness, D.D., 1975. " $^{14}\text{C}/^{12}\text{C}$  ratios as tracers of urban pollution"; Proc. I.A.E.A. and F.A.O. Conf. "Isotope ratios as pollutant source and behaviour indicators", 135.
- Baxter, M.S., McKinley, I.G., MacKenzie, A.B. and Jack, W., 1978; Mar. Poll. Bull. (in press).
- Beasley, T.M., 1969. "Lead-210 production by nuclear devices, 1946-1958". Nature, 224, 573.
- Benninger, L.K., Lewis, D.M. and Turekian, K.K., 1975. "The use of  $^{210}\text{Pb}$  as a heavy metal tracer in the river estuarine system"; in "Marine Chemistry in the Coastal Environment", ed. Church, T.M., Am. Chem. Soc. Symp. Ser. 18, 202.
- Berger, W.H. and Heath, G.R., 1968. "Vertical mixing in pelagic sediments"; J. of Mar. Res., 26, 134.
- Berner, R.A., 1971. "Principles of Chemical Sedimentology". McGraw-Hill Inc.
- Best, G.A., 1970. "Radioactive particulate matter from pressurised water reactors and its discharge into the sea"; Ph.D. thesis, University of Liverpool.
- Blake, G.R., 1965. In "Methods of Soil Analysis. Part. 1", Eds. Black, C.A., Evans, D.D., White, J.L., Ensminger, L.E. and Clark, F.E., Am. Soc. of Agronomy.

- Blauer, H.M., 1976. Personal Communication.
- Bloom, A.L., 1966. "Peat accumulation and compaction in a Connecticut coastal marsh"; *J. Sed. Petrol.*, 34, 599.
- Bortleson, G.C. and Lee, G.F., 1972. "Recent sedimentary history of Lake Mendota, Wisconsin"; *Environ. Sci. Technol.*, 6, 799.
- Bradbury, J.P. and Waddington, J.C.B., 1973. "The impact of European settlement on Shagawa Lake, North-eastern Minnesota, U.S.A."; in "Quat. Plant. Ecology". Eds. Birks, H.J. and West, R.G., Blackwell Scientific Pub., Oxford, 289.
- Brewer, P.G., 1975. In "Chemical Oceanography", Vol. 1, Chapter 7. Eds. Riley, J.P. and Skirrow, G.
- Bricker, P.O. III., and Troup, B.N., 1975. "Sediment-water exchange in Chesapeake Bay"; in "Estuarine Research" Vol. 1. Ed. Cronin, L.E., Academic Press, London.
- Bruland, K.W., 1974. "<sup>210</sup>Pb Geochronology in the Coastal Marine Environment"; Ph.D. thesis, University of California, San Diego.
- Bruland, K.W., Koide, M., Bowser, C., Maher, L.J. and Goldberg, E.D., 1975. "Lead-210 and pollen geochronologies on Lake Superior sediments"; *Quat. Res.*, 5, 89.
- Buchanan, J.Y., 1891. "On the composition of oceanic and littoral manganese nodules"; *Trans. Roy. Soc. Ed.*, Vol. 36, 459.

- Burton, J.D. and Liss, P.S., 1976. Eds. Estuarine Chemistry. Academic Press.
- Burton, W.M. and Stewart, N.G., 1960. "Use of long-lived natural radioactivity as an atmospheric tracer"; Nature, 186, 584.
- Calvert, S.E. and Price, N.B., 1970. "Composition of manganese nodules and manganese carbonates from Loch Fyne, Sootland"; Contrib. Mineral. Petrol., 29, 215.
- Cambray, R.S., Jefferies, D.F. and Topping, G., 1975. "An estimate of the input of atmospheric trace elements into the North Sea and the Clyde Sea (1972-3). "U.K.A.E.A. Publ. A.E.R.E. - R7733, H.M.S.O.
- Carpenter, R., 1975. "Chemical and geochemical studies off the coast of Washington". Report of progress May 1974-May 1975. U.S.A.E.C. reference A75-56 RLO-2225-T24-18.
- Chapman, W.A., Rice, T.A. and Price, T.J., 1958. "Uptake and accumulation of radioactive zinc by marine plankton, fish and shellfish"; U.S. Fish Wild. Serv. Fish. Bull., 58, 279.
- Chow, T.J., Bruland, K.W. Bertine, K.K., Soutar, A., Koide, M., and Goldberg, E.D., 1973. "Lead pollution; records in southern California coastal sediments"; Science, 181, 551.
- Church, T.M., 1975. Editor "Marine Chemistry in the Coastal Environment"; Am. Chem. Soc. Symp. Se 18.
- Clyde River Purification Board, 1972, 17th Annual Report.
- Clyde River Purification Board, 1973, 18th Annual Report.

Clyde River Purification Board, 1974a, 19th Annual Report

Clyde River Purification Board, 1974b, "Pollution in the Clyde" in "The Clyde Estuary and Firth. An assessment of present knowledge compiled by members of the Clyde Study Group"; N.E.R.C. Pub. Ser. C., number 11, 24.

Collar, R.H.F., 1974. "The River Clyde Estuary. Current knowledge of water and sediment movement", in "The Clyde Estuary and Firth". N.E.R.C., 1974, Pub. Ser. C. number 11.

Conlan, B., Henderson, P. and Walton, A., 1969. "A simplified procedure for the assay of picocurie concentrations of Radium-226 and its application to a study of the natural radioactivity in surface water in Scotland"; Analyst, 94, 15.

Cox, A., 1969. Science, N.Y., 163, 237.

Craib, J.S., 1965. "A sampler for taking short undisturbed marine cores"; J. Cons. perm. int. Explor. Mer., 30, 1, 34.

Craig, R.E., 1959. "Hydrography of Scottish coastal waters"; Mar. Res., No. 2.

Crozaz, G., Picciotto, E. and DeBrueck, W., 1964. "Antarctic snow chronology with  $^{210}\text{Pb}$ "; Jour. of Geoph. Res., 69, 2597.

- Damon, P.E. and Hyde, H.I., 1952. "Scintillation tubes for the measurement of radioactive gases"; *Rev. Sci. Instr.* 23, 766.
- Davies, A.T. and Gorsline, D.S., 1976. "Oceanic sediments and sedimentary processes"; In "Chemical Oceanography," eds. Riley, J.P. and Chester, R., 2nd ed. Vol. 5, Chapter 1.
- Davis, M.B., 1968. "Pollen grains in lake sediments; redeposition caused by seasonal water circulation". *Science, N.Y.*, 162, 796.
- Davis, M.B., Brubaker, L.B. and Webb, T. III, 1973. "Calibration of absolute pollen influx"; in "Quat. Plant Ecology", Eds. Birks, M.J., and West, R.G., 9, Blackwell Scientific Pub., Oxford.
- Dearnley, G. and Northrup, D.C., 1966. "Semiconductor Counters for Nuclear Radiations". 2nd ed., Spon., London.
- Deegan, C.E., Kirby, R., Rae, I. and Floyd, R., 1973. "The superficial deposits of the Firth of Clyde and its sea-lochs"; Institute of Geological Sciences, report no. 73/9, H.M.S.O.
- Dickson, J.H., Stewart, D.A., Thompson, R., Turner, G., Baxter, M.S., Drndarski, N.D. and Rose, J., 1978. "Palynology, palaeomagnetism, and radiometric dating of Flandrian marine and freshwater sediments of Loch Lomond"; *Nature*, 274, 548.
- Dooley, H.D. and Steele, J.H., 1969. "Wind driven currents near a coast"; *Dt. Hydrogr. Z.*, 22, 213.

- Drndarski, N.D., 1977. "Studies in Radiocarbon Geochemistry";  
Ph.D. thesis, University of Glasgow.
- Duursma, E.K. and Bosch, C.J., 1970. "Theoretical, experimental  
and field studies concerning diffusion of radioisotopes  
in sediments and suspended solid particles of the sea.  
Part B. Methods and experiments". Neth. J. Sea Res.,  
4(4), 395.
- Duursma, E.K. and Gross, M.G., 1971. "Marine sediments and  
radioactivity"; in "Radioactivity in the Marine Environment",  
National Academy of Sciences.
- Eakins, J.D., 1977. Personal communication.
- Eakins, J.D. and Morrison, R.J., 1976. "A new procedure for  
the determination of Pb-210 in marine and lake sediments".  
A.E.R.E. - R8475.
- Edgington, D.N., and Robbins, J.A., 1976. "Records of lead  
pollution in Lake Michigan sediments since 1800";  
Environ. Sci. Technol., 10, No. 3, 266.
- Edgington, D.N. Wahlgren, M.A. and Marshall, J.S., 1975.  
"The behaviour of plutonium in aquatic ecosystems: A  
summary of studies on the Great Lakes"; in "Environmental  
Toxicity of Aquatic Radionuclides: models and mechanisms";  
Eds. Miller, W.M. and Stannard, J.N.; Ann. Arbor. Sci.  
Pub. Inc., Michigan.

- Edmond, J.M., 1970. "Comments on the paper by T.L. Ku, Y.H. Li, G.G. Mathieu and H.K. Wong" "Radium in the Indian-Antarctic Ocean south of Australia"; Jour. of Geophys. Res., 75, 6878.
- Elderfield, H. and Hepworth, A., 1975. "Diagenesis, Metals and Pollution in Estuaries"; Marine Pollution Bulletin, 6, No. 6, 85.
- Emery, K.O., 1960. "The Sea off Southern California"; John Wiley, N.Y., p.366.
- Ericson, D.B. and Wollin, G., 1968. "The Ever-changing Sea"; MacGibbon and Kee Ltd., London.
- Evans, G., 1971. "The Recent sedimentation of Turkey and the adjacent Mediterranean and Black Seas", a review in "Geology and History of Turkey", Ed. Campbell, A.J., Petrol. Expl. Soc. Libya, 385.
- Evans, D.W., Cutshall, N.H., Cross, F.A. and Wolfe, D.A., 1977. "Manganese cycling in the Newport River estuary, North Carolina"; Estuarine and Coastal Mar. Sci., to be published.
- Farmer, J.G., 1978. Personal communication.
- Farrington, J.W., Henrichs, S.M. and Anderson, R., 1977. "Fatty acids and  $^{210}\text{Pb}$  geochronology of a sediment core from Buzzards Bay, Massachusetts"; Geochim. et Cosmochim. Acta, 41, 289.

- Feely, H.W. and Seitz, H., 1970. "Use of lead-210 as a tracer of transport processes in the stratosphere". Jour. of Geoph. Res., 75, 2285.
- Ferrante, E.R., Gourski, E. and Boulenger, R.R., 1964. "Detector for radon-222 measurements at very low level"; in "The natural radiation environment", Eds. Adams, J.A.S. and Lowder, W.M.; Chicago Uni. Press, 353.
- Fink, I., 1966. "Fink Index to the Powder Diffraction file". Eds. Bigelow, W.C., and Smith, J.V. A.S.T.M. pub. P.D.I.S. -16-f.
- Fleming, G. 1969. "The Clyde Basin; Hydrology and sediment transport". Ph.D. thesis, University of Strathclyde.
- Flynn, W.W., 1968. "The determination of low-levels of polonium-210 in environmental materials"; Anal. Chim. Acta., 43, 221.
- Francis, C.W., Chesters, G. and Hawkins, L.A., 1970. "The determination of  $^{210}\text{Pb}$  mean residence times in the atmosphere"; Environ. Sci. Technol., 4, 586.
- Gäggeler, H., Von Gunten, H.R., and Nyffeler, U., 1976. "Determination of  $^{210}\text{Pb}$  in lake sediments and in air samples by direct  $\gamma$ -ray measurement"; Earth and Planetary Sci. Letts., 33, 3119.
- Gair, R., 1967. "Clyde sediments: Rheological properties and movement" Ph.D. thesis, University of Strathclyde.

- Gojkovic, S., Deleon, G. and Cervenjek, E., 1963.  
"Dating of some Uraninites from Yugoslav localities  
by the  $^{206}\text{Pb}/^{210}\text{Pb}$  method"; in "Radioactive Dating"  
Proc. Symp. Rad. Dating, I.A.E.A., Vienna, 105.
- Goldberg, E.D., 1963. "Geochronology with  $^{210}\text{Pb}$ " in  
"Radioactive Dating". Proc. Symp. Rad. Dating,  
I.A.E.A., Vienna, 121.
- Goldberg, E.D., 1971. "Atmospheric Transport"; in  
"Impingement of Man on the Oceans". Ed. Hood, D.W.,  
John Wiley and Sons Inc., 75.
- Goldberg, E.D. and Bruland, K.W., 1974. "Radioactive  
Geochronologies"; in "The Sea", Vol. 5, Ed. Goldberg, E.D.,  
John Wiley and Sons [see also Bruland, K.W., Bertine, K.,  
Koide, M. and Goldberg, E.D., 1974. "History of metal  
pollution in southern California Coastal Zone"; Environ.  
Sci. Technol., 8, 425.]
- Goldberg, E.D. and Koide, M., 1962. "Geochronological studies  
of deep-sea sediments by the  $\text{Ia}/\text{Th}$  method"; Geochim. et  
Cosmochim. Acta, 26, 417-450.
- Goldberg, E.D. and Koide, M., 1963. "Rates of sediment  
accumulation in the Indian Ocean"; Earth Sciences and  
Meteorites, 90.
- Goldberg, E.D., Gamble, E., Griffin, J.J. and Koide, M., 1977.  
"Pollution history of Narragansett Bay as recorded in its  
sediments"; Estuarine and Coastal Mar. Sci., 5, 549.
- Goulding, F.S. and Stone, Y., 1970. "Semiconductor Radiation  
Detectors"; Science, 170, 280.

- Grill, E.V., 1978. "The effect of sediment-water exchange on manganese deposition and nodule growth in Jervis Inlet, British Columbia"; *Geochim. et Cosmochim. Acta.*, 42, 485.
- Grantham, B., Tett, T.B. and Wood, B.J.B., 1978. "Phytoplankton distribution in relation to hydrography in sea-lochs"; *Proc. Roy. Soc. Ed.*, 76B, 144. (in press)
- Guinasso, N.L. and Schink, D.R., 1975. "Quantitative estimates of biological mixing rates in abyssal sediments"; *Jour. of Geophys. Res.*, 80, 21, 3032.
- Halcrow, W., Mackay, D.W. and Thornton, I., 1973. "The distribution of trace metals and fauna in the Firth of Clyde in relation to the disposal of sewage sludge"; *J. Mar. Biol. Ass. U.K.*, 53, 721.
- Harrison, C.G.A. and Funnell, B.M., 1964. "Relationship of Palaeomagnetic Reversals and Micropalaeontology in two late Cenozoic Cores from the Pacific Ocean"; *Nature*, London, 204, 566.
- Höhndorf, A., 1968. "Bestimmung der halbwertszeit von Pb-210"; *Z. Naturforschung*, 24A, 612.
- Hoffmann, B.W. and Van Camerik, S.B., 1967. "A table and method for determining the true time representing a count rate observed in radionuclear counting"; *Analytical Chemistry*, 39, 1198.
- Jaworowski, Z., 1969. *At. Energy Rev.*, 7, 3.

- Jaworowski, Z., 1970. "Sources of lead-210 in the environment".  
The Biology and Ecology of Polonium and Radiolead.  
(Proc., Meeting Sutton, 1970). Inst. Cancer Res., Sutton.
- Jacobi, W., and Andre', K., 1963. Jour. Geophys. Res., 68, 13,  
3799.
- Johnston, R., Adams, J.A. and Dooley, H.D., 1974. "Some  
observations on the hydrography, chemistry and plankton  
of the Firth of Clyde in relation to nitrate-rich  
effluents" in "The Clyde Estuary and Firth", N.E.R.C.  
pub. series C, number 11.
- Johnstone, G.S., Read, H.H. and MacGregor, A.G., 1966.  
"The Grampian Highlands" (3rd edition); Institute of  
Geological Sciences Handbook on the regional geology of  
Great Britain, H.M.S.O.
- Klein, D.A. and Goldberg, E.D., 1970. "Mercury in the marine  
environment"; Environ. Sci. Technol., 4, 765.
- Koczy, F.F., 1958. "Natural Radium as a tracer in the Oceans";  
Proc. 2nd United Nations int. Conf. "Peaceful Uses of  
Atomic Energy", 18, 351.
- Koczy, F.F. and Bourrett, R., 1958. "The distribution of  
radium in deep-sea sediments" Progr. Rep. Nat. Sci. Found.,  
Grant No. G3995, V.M. Acct. 8891.
- Koide, M., Soutar, A. and Goldberg, E.D., 1972. "Marine  
geochronology with  $^{210}\text{Pb}$ "; Earth and Planetary Sci. Letts.,  
14, 442.

- Koide, M., Bruland, K.W. and Goldberg, E.D., 1973. " $^{228}\text{Th}/^{232}\text{Th}$  and  $^{210}\text{Pb}$  geochronologies in marine and lake sediments"; *Geochim. et Cosmochim. Acta*, 37, 1171.
- Koide, M., Griffin, J.J. and Goldberg, E.D., 1975. "Records of plutonium fallout in marine and terrestrial samples"; *Jour. of Geophys. Res.*, 80, 30.
- Koide, M., Bruland, K.W. and Goldberg, E.D., 1976 " $^{226}\text{Ra}$  chronology of a coastal marine sediment"; *Earth and Planetary Sci. Letts.*, 31, 31.
- Krishnaswami, S., Lal, D., Martin, J.M. and Meybeck, M., 1971. "Geochronology of lake sediments"; *Earth and Planetary Sci. Letts.*, 11, 407.
- Krishnaswami, S., Lal, D., Amin, B.S. and Soutar, A., 1973. "Geochronological studies in Santa Barbara Basin;  $^{55}\text{Fe}$  as a unique tracer for particulate settling"; *Limnol. and Oceanog.*, 18 (5), 763.
- Ku, T.L., 1966. Ph.D. Thesis, Columbia University.
- Ku, T.L., Li, Y.J., Mathieu, G.G. and Wong, H.K., 1970. "Radium in the Indian-Antarctic Ocean south of Australia"; *Jour. of Geophys. Res.*, 75, 5286.
- Ku, T.L. and Glasby, G.P., 1972. "Radiometric evidence for the rapid growth rate of shallow-water, continental margin manganese nodules"; *Geochim. et Cosmochim. Acta*, 36, 699.
- Kulp, J.L., 1953. "Age determination of Uranium minerals by the  $^{210}\text{Pb}$  method"; *Nucleonics*, 11, 8, 19.

Leatherland, T.M., 1978, Personal Communication.

Lederer, C.M., Hollander, J.M. and Perlman, I., 1967.

"Table of Isotopes" (6th edition), Wiley, New York.

Leland, H.V. and Shukla, S.S., 1972. "Factors affecting the distribution of lead and other trace elements in sediments of southern Lake Michigan"; in "Trace metals and metal-organic interactions in natural waters" Ed. Singer, P.C., Ann. Arbor. Sci. Pub. Inc.

Lennie, D., 1978. B.Sc. thesis, Chemistry Dept., University of Glasgow.

Lennie, D., 1978. Personal communication.

Lerman, A. and Lietzke, T.A., 1975. "Uptake and migration of tracers in lake sediments"; Limnol. and Oceanog., 20, 4, 497.

Lietzke, T.A., Lerman, A. and Taniguchi, H., 1973. " $^{137}\text{Cs}$  and  $^{90}\text{Sr}$ ; similarities and differences between transport modes in sediments"; Trans. Am. Geophys. Un., 54, 341.

Livingston, H. and Bowen, V.T., 1975. "Americium in the marine environment - relationships to plutonium"; in "Environmental Toxicity of Aquatic Radionuclides; Models and Mechanisms", Eds., Miller, M.W. and Stannard, J.N., Ann. Arbor. Sci. Pub. Inc.

Lucas, H.F., 1957. "Improved low-level alpha-scintillation counter for radon"; Rev. Sci. Instr., 28, 680.

- MacGregor, M. and MacGregor, A.G., 1948. "The Midland Valley of Scotland" (2nd edition). Institute of Geological Sciences handbook on the regional geology of Great Britain, H.M.S.O.
- MacKay, D.W. and Topping, G., 1970. "Preliminary report on the effects of sludge disposal at sea"; Effluent and Water treatment Journal, 641.
- MacKay, D.W., Halcrow, W. and Thornton, I., 1972. "Sludge dumping in the Firth of Clyde"; Marine Pollution Bull., 3, (2), 7.
- MacKenzie, A.B., 1977. "A radionuclide study of the Clyde Sea Area". Ph.D. thesis, Chemistry Department, University of Glasgow.
- MacKenzie, A.B., Baxter, M.S., McKinley, I.G., Swan, D.S. and Jack, W., 1978. "The determination of  $^{134}\text{Cs}$ ,  $^{137}\text{Cs}$ ,  $^{210}\text{Pb}$ ,  $^{226}\text{Ra}$  and  $^{228}\text{Ra}$  concentrations in nearshore marine sediments and seawater"; Journal of Radioanalytical Chemistry; (in press).
- Mackereth, F.J.H., 1969. "A short core sampler for subaqueous deposits"; Limnol. and Oceanog., 14, 145.
- Mackereth, F.J.H., 1971. "On the variation in direction of the horizontal component of remanent magnetisation in lake sediments"; Earth and Planetary Sci. Letts., 12, 332.
- Martin, J.H. and Knauer, G.A., 1973. "The elemental composition of plankton"; Geochim. et Cosmochim. Acta, 37, 1639.

- Matsumoto, E., 1975. "<sup>210</sup>Pb geochronology of sediments from Lake Shinji"; *Geochemical Journal*, 9, 167.
- Matsumoto, E. and Wong, C.S., 1977. "Heavy metal sedimentation in Saanich Inlet measured with <sup>210</sup>Pb technique"; *Jour. of Geophys. Res.*, 82, 34, 5477.
- McDonald, J.G., 1974. "Geology" in "A Natural History of Loch Lomond", University of Glasgow Press.
- McKinley, I.G., 1978. "Tracer applications of radiocaesium in a coastal marine environment". Ph.D. thesis, Chemistry Department, University of Glasgow.
- Meade, R.H., 1973. In "Continental Shelf Sediment Transport"; eds. Swift, D.J.P., Duane, D.B. and Pilkey, O.H.; Dowden Hutchinson and Ross, Stroudsburg, Pennsylvania.
- Mill, H.R., 1892. "The Clyde Sea Area"; *Trans. of the Royal Soc. Ed.*, Vol. XXXVI, part III, No. 23, 640.
- Miller, W.M. and Stannard, J.N., 1975. Eds. "Environmental Toxicity of Aquatic Radionuclides"; Ann. Arbor. Sci. Pub. Inc., Michigan.
- Milne, P.H., 1974. "Physical characteristics and tides of the Clyde Sea Area"; in "The Clyde Estuary and Firth", N.E.R.C. pub. series C, number 11.
- Mitchell, N.T., 1975. "Radioactivity in surface and coastal waters of the British Isles 1972-73"; Ministry of Agriculture, Fisheries and Food, Fisheries Radiobiological Laboratory Technical Report, FRL 10.

- Moore, H.B., 1931. "The muds of the Clyde Sea Area III: Chemical and physical conditions, rate and nature of sedimentation and fauna"; Jour. Mar. Biol. Assoc., U.K., 17, 325.
- Moore, H.E., Poet, S.E. and Martell, E.A., 1973. " $^{222}\text{Rn}$ ,  $^{210}\text{Pb}$ ,  $^{210}\text{Bi}$  and  $^{210}\text{Po}$  profiles and aerosol residence times versus altitude"; Jour. of Geophys. Res., 78, 7065.
- Murray, I., 1976. Personal communication.
- Murray, J. and Irvine, R., 1894. "On the manganese oxides and manganese nodules in marine deposits"; Trans. Roy. Soc. Ed., Vol. 37, 721.
- National Academy of Sciences, 1961. "Radiochemistry of Polonium"; pub. no. N.S. 3037.
- National Academy of Sciences, 1971. "Radioactivity in the Marine Environment".
- Natural Environmental Research Council, 1974. "The Clyde Estuary and Firth"; N.E.R.C. publications series C, number 11.
- Noshkin, V.E., 1972. "Ecological aspects of plutonium dissemination in aquatic environments"; Health Physics, 22, 537.
- Noshkin, V.E. and Bowen, V.T., 1973. "Concentrations and distributions of long-lived fallout radionuclides in open ocean sediments"; International Atomic Energy Agency, S.M. - 158/45.

- Nozaki, Y. and Tsunogai, S., 1973. "Lead-210 in the North Pacific and the transport of terrestrial material through the atmosphere"; *Earth and Planetary Sci. Letts.*, 20, 88.
- Nozaki, Y., Cochran, J.K., Turekian, K.K. and Keller, G., 1977. "Radiocarbon and  $^{210}\text{Pb}$  distribution in submersible taken deep sea cores from project Famous"; *Earth and Planetary Sci. Letts.*, 34, 2, 167.
- Opdyke, N.D., Glass, B., Hays, J. and Foster, J., 1966. "Palaeomagnetic Study of Antarctic Deep-Sea Cores"; *Science, N.Y.*, 154, 349.
- Oldfield, F., Appleby, P.G. and Batterbee, P.W., 1978. "Alternative  $^{210}\text{Pb}$  dating; results from the New Guinea Highlands and Lough Erne"; *Nature*, 271, 339.
- Parker, J.I., Conway, H.L. and Yaguchi, E.M., 1977. "Dissolution of diatom frustules and recycling of Amorphous Silicon in Lake Michigan"; *Jour. Fish. Res. Board, Can.*, 34, 4, 545.
- Patterson, C., 1971. "Lead"; in "Impingement of Man on the Oceans", ed. Hood, D.W., John Wiley and Sons Inc., 245.
- Peirson, D.H., Cambray, R.S. and Spicer, G.S., 1966. "Lead-210 and Polonium-210 in the atmosphere"; *Tellus*, 18, 427-433.
- Pennington, W., 1973. "The recent sediments of Windermere"; *Freshwater Biology*, 3, 363.
- Pennington, W., Cambray, R.S. and Fisher, E.M., 1973. "Observations on lake sediments using fallout  $^{137}\text{Cs}$  as a tracer", *Nature*, 242, 324.

- Pennington, W., Cambray, R.S., Eakins, J.D. and Harkness, D.D., 1976. "Radionuclide dating of the recent sediments of Blelham Tarn"; *Freshwater Biology*, 6, 317.
- Petit, D., 1974. " $^{210}\text{Pb}$  et isotopes stables du plomb dans des sediments lacustres", *Earth and Planetary Sci. Letts.*, 23, 199.
- Pickering, R.J., Carrigan, P.H. Jr., Tamura, T., Abee, H.H., Beverage, J.W. and Andrew, R.W. Jr., 1966. "Radioactivity in bottom sediments of the Clinch and Tennessee Rivers"; in "Disposal of radioactive wastes into seas, oceans, and surface waters"; I.A.E.A. pub. SM 72/4.
- Poet, S.E., Moore, H.E. and Martell, E.A., 1972. "Lead-210, Bi-210 and Po-210 in the atmosphere: Accurate ratio measurement and application to aerosol residence time determination"; *Jour. of Geophys. Res.*, 77, 6515.
- Presley, B.J., Kolodny, Y., Nissenbaum, A. and Kaplan, I.R., 1972. "Early diagenesis in a reducing fjord, Saanich Inlet, British Columbia - I. Trace element distribution in interstitial water and sediment"; *Geochim. et Cosmochim. Acta*, 36, 1073.
- Preston, A., 1966. "The concentration of  $^{65}\text{Zn}$  in the flesh of oysters related to the discharge of cooling pond effluent from the C.E.G.B. nuclear power station at Bradwell on Sea, Essex"; in "Radioecological Conc. Proc." Eds. Aberg, B. and Hungate, F.P., 995-1004. Pergamon Press, New York.

- Rama, Koide, M. and Goldberg, E.D., 1961. "Lead-210 in natural waters"; *Science*, 134, 98.
- Riley, J.P. and Chester, R., 1976. "Chemical Oceanography" Vol. 6, 2nd edition. Academic Press.
- Ritchie, J.C., McHenry, J.R. and Gill, A.C., 1973. "Dating recent reservoir sediments". *Limnol. and Oceanog.*, 18, 254.
- Robbins, J.A. and Edgington, D.N., 1975. "Determination of recent sedimentation rates in Lake Michigan using  $^{210}\text{Pb}$  and  $^{137}\text{Cs}$ "; *Geochim. et Cosmochim. Acta*, 39, 285-304.
- Robbins, J.A., Edgington, D.A. and Parker, J.I., 1975. "Distribution of amorphous, diatom frustule, and dissolved silica in a lead-210 dated core from Southern Lake Michigan"; (manuscript).
- Robbins, J.A. Krezoski, J.R. and Mozley, S.C., 1977. "Radioactivity in sediments of the Great Lakes. Post-depositional redistribution by deposit-feeding organisms"; *Earth and Planetary Sci. Letts.*, 36, 325.
- Runwell, D.S., 1964. "Spartina salt marshes in Southern England; rate and seasonal pattern of sediment accretion"; *Jour. of Ecol.*, 52, 79.
- Sackett, W.M., 1965. "Deposition rates by the protactinium method". Third Annual Symposium on Marine Geochem., Univ. of Rhode Island Occasional Pub. No. 3., 29.
- Sadauskis, J., 1958. Argonne National Lab. (A.N.L.) - 5967.
- Sadauskis, J., 1960. Argonne National Lab. (A.N.L.) - 6186.

- Schell, W.R., 1977. "Concentrations, physico-chemical states and mean residence times of  $^{210}\text{Pb}$  and  $^{210}\text{Po}$  in marine and estuarine waters"; *Geochim. et Cosmochim. Acta*, 41, 1019.
- Shannon, L.V. and Cherry, R.D., 1971. "Radium-226 in marine phytoplankton"; *Earth and Planetary Sci. Letts.*, 11, 339.
- Shaw, H.F., 1978. "The clay mineralogy of the recent surface sediments from the Cilicia Basin, Northeastern Mediterranean"; *Marine Geology*, 26, M51.
- Shaw, H.F. and Bush, P.R., 1978. The mineralogy and geochemistry of the recent surface sediments of the Cilicia Basin, Northeast Mediterranean"; *Marine Geology*, 27, 115.
- Sill, C.W. and Olsen, D.G., 1970. "Sources and prevention of recoil contamination of solid-state alpha detectors"; *Analytical Chemistry*, 42, 13, 1596.
- Singer, P.C., 1972. Ed. "Trace metals and metal-organic interactions in natural waters". Ann. Arbor, Science Pubs. Inc., Michigan.
- Sissons, J.B., 1967. "The Evolution of Scotland's Scenery"; Oliver and Boyd Ltd., Edinburgh.
- Sissons, J.B., 1967. "Glacial stages and radiocarbon dates in Scotland"; *Scott. J. Geol.*, 3, 375.
- Smith, F.A., Della Rosa, R.J. and Casarett, L.J., 1955. *Amer. Rep., U.R.* - 305.

- Solórzano, L. and Grantham, B., 1975. "Surface nutrients chlorophylla, and phaeopigment in some Scottish sea-lochs"; *J. exp. mar. Biol. Ecol.*, 20, 63-76.
- Stewart, D., 1978. Personal communication.
- Stott, W., 1976. Personal communication.
- Talvitie, N.A., 1972. "Electrodeposition of actinides for alpha spectrometric determination"; *Analytical Chemistry*, 44, 2, 280.
- Tamura, T. and Jacobs, D.G., 1960. "Structural implications in caesium sorption"; *Health Physics*, 2, 391.
- Templeton, W.L. and Preston, A., 1966. "Transport and distribution of radioactive effluents in coastal and estuarine waters of the United Kingdom" in "Disposal of radioactive wastes into seas, oceans and surface waters". I.A.E.A., Vienna, SM - 72/16, 267.
- TerHaar, G.L. Holtzmann, R.B. and Lucas, H.F., 1967. "Lead and lead-210 in rainwater"; *Nature*, 216, 353.
- Thom, A.S., 1949. "Investigation of tidal phenomena in the Clyde Estuary using a scale model"; *J. Instr. civ. Engrs.*, 33, 100.
- Thompson, R., 1977. Personal communication.
- Thompson, R. and Turner, G., 1977. Personal communication.
- Thompson, A., 1969. "A hydraulic investigation of the Clyde"; Ph.D. thesis, University of Strathclyde.

- Thomson, J. and Walton, A., 1972. "Natural Radioactive decay series elements in the Oceans and Sediments"; Proc. Roy. Soc. Ed., 72/73, 15.
- Thomson, J., Turekian, K.K. and McCaffrey, R.J., 1975. "The accumulation of metals in and release from sediments of Long Island Sound"; in "Estuarine Research" Ed. Cronin, L.E. Vol. I, 28. Academic Press, London.
- Tippett, R., 1974. "A Natural History of Loch Lomond", Glasgow University Press.
- Tobailem, J., 1955. Ann. Phys., 10, 783.
- Topping, G. 1974. "The atmospheric input of some heavy metals to the Firth of Clyde and its relation to other inputs"; ICES CM 1974/E32.
- Turekian, K.K., 1956. "Rapid technique for determination of carbonate content of deep-sea cores"; Bull. Amer. Assoc., Petrol. Geologists, 40, 2507.
- Turekian, K.K., 1977. "The fate of metals in the oceans"; Geochim. et Cosmochim. Acta, 41, 1139.
- United Nations, 1972. "Ionizing Radiation; Levels and Effects; 1-Levels." United Nations Pub. E72, IX, 17.
- Windom, M., 1969. "Atmospheric dust records in permanent snowfields: Implications to marine sedimentation"; Geol. Soc. Amer. Bull., 80, 761.
- Wright, H.E., 1971. "Late quaternary vegetational history of North America" in "The Late Cenozoic Glacial Ages". Ed. Turekian, K.K. Yale Press, New Haven, 425.

Yaffe, L., 1962. "Preparation of thin films, sources and targets"; Ann. Rev. Nu. Sci., 12, 153.

Yen, J.F., 1977. Ed. "Marine Chemistry"; Ann. Arbor. Science Pub. Inc.